ResearchOnline@JCU

JAMES COOK UNIVERSITY AUSTRALIA

This file is part of the following work:

Enyi, Chinyere Chidimma (2024) ***Plant extracts as renewable resource for preparative photooxygenations.*** **PhD Thesis, James Cook University.**

Access to this file is available from:

https://doi.org/10.25903/0t5q%2Dcx76

Copyright © Chinyere Chidimma Enyi

The author has certified to JCU that they have made a reasonable effort to gain permission and acknowledge the owners of any third party copyright material included in this document. If you believe that this is not the case, please email researchonline@jcu.edu.au

PLANT EXTRACTS AS RENEWABLE RESOURCE FOR PREPARATIVE PHOTOOXYGENATIONS

Submitted by

Enyi, Chinyere Chidimma

In fulfilment of the requirements for the degree of

Doctor of Philosophy

College of Science and Engineering

James Cook University

September, 2024

Advisory Panel

Prof. Michael Oelgemöller

Dr. Mark Robertson

Prof. Mohan Jacob

Prof. Godswill Kuta Fekarurhobo

Dr. Gloria Ihuoma Ndukwe

ABSTRACT

This thesis investigated the photosensitizer potentials of some plant extracts in photooxygenation reactions. Photooxygenation reactions utilize dye photosensitizers and light to provide easy and green access to fragrances, flavours, and pharmaceuticals. However, some currently used conventional (synthetic) photosensitizers are toxic to the environment, expensive or are not easily recovered from the product mixture. Natural plant extracts thus represent cheap and green alternatives to synthetic dyes and have subsequently been used for photodynamic therapeutical applications. This study investigated *Hibiscus sabdariffa*, *Carpolobia lutea* and *Justicia secunda* extracts as novel sources of photosensitizers for industrially relevant photooxygenation reactions. Initially, the photooxygenation of α-terpinene and 1,5-dihydroxynaphthalene served as model reactions for the photoactivity screening of the plant dyes. Subsequently, the active plant dye was investigated concerning the photooxygenation of 1-naphthol, 1,6-dihydroxy naphthalene, α-pinene, and β-pinene. Photooxygenation of α-terpinene in a batch reactor using *Hibiscus sabdariffa*, *Carpolobia lutea* and *Justicia secunda* extracts yielded 3.1%, 62.8% and 5.5% of ascaridole by GC-FID, respectively, after 90 minutes. The composition of ascaridole product in *Carpolobia lutea* extract sensitized reaction mixture (62.8%) was slightly above that obtained with the synthetic rose iengal and methylene blue (60.5% and 61.7%, respectively) under the same irradiation conditions. The addition of 0.3 M 1,4-diazabicyclo[2.2.2]octane to the photoactive extract identified resulted in the decrease of ascaridole yield to 13.3% after 90 minutes of irradiation. This confirmed that the active plant extract operated more through a Type II (singlet oxygen generation) than a Type I (free radical generation) mechanism. Photooxygenation of 1,5-dihydroxynaphthalene, 1-naphthol, 1,6-dihydroxynaphthalene, α-pinene, and β-pinene using *Carpolobia lutea* extract gave comparable conversions to the commercial sensitizers. The three plant dyes showed absorption in the visible region of the electromagnetic spectrum. Photostability tests showed that the photoactive dye extract was somewhat stable in isopropanol but only partially stable for a few hours in acetonitrile. In dichloromethane, the dye showed photobleaching after just two hours of irradiation. The photoactive *Carpolobia lutea* was further fractionated by VLC to obtain 18 fractions, 10 of which gave > 40.0% ascaridole when its photoactivity was tested by α-terpinene photooxygenation. HPLC-MS analysis of the active fractions showed the presence of anthraquinones, dianthrones, flavonoids and chlorophyll which are natural photosensitizers found in plants. Some other compounds such as phenolics and triterpenes were also present. The results obtained show that natural dye extracts can be used as renewable sensitizers for preparative photooxygenations.

ACKNOWLEDGEMENTS

I wish to express my profound and unreserved gratitude to Prof. Godswill Kuta Fekarurhobo, my supervisor at Rivers State University. I have seen further in photochemistry, by standing on his shoulders. I am very grateful for his inspirational and phenomenal tutelage, from introducing me and making me fall in love with photochemistry during my undergraduate days, to thoroughly and robustly supervising my M Sc research and topping it up with this PhD supervision. The culture of hard work, scientific enthusiasm, logical and critical thinking in research which he taught me through our discussions, always cheering me on, will be unforgettable. I am sure a grounded researcher and a sound scientist, by his training. I deeply appreciate Dr. Gloria Ihuoma Ndukwe, my co-supervisor at Rivers State University for her exceptional support, commitment, motivation, mentorship and constant encouragement while insisting I pursue best-world-practices and standards in research. She also gave me comprehensive training in chromatographic techniques and guided me on the importance of instrumentation in chemistry research. I am most grateful to her for the important research skills she imparted to me which will be useful in my future researches.

Words cannot express my gratitude to my amazing primary advisor at James Cook University, Professor Michael Oelgemöller, for providing me with the opportunity to work in his multicultural, well-equipped, world-class photochemistry laboratory. The experience has positively changed the trajectory of my career and professional life. His meaningful contributions, detailed knowledge of organic synthesis, key suggestions and assistance at crucial stages of this research made all of the difference. Despite the distance and time difference during the supervision period, He created time to attend to my research needs and had regular meetings with me, teaching me academic conscientiousness and professional commitment. I am most grateful. I also wish to thank my secondary advisor at JCU, Dr Mark Robertson, for providing all possible assistance, making available all reagents, solvents, apparatus and equipment needed during my time at JCU and introducing me to the analytical equipment I used. Thanks also to Southern Cross University, Analytical Research Laboratory, for helping out with the HPLC-MS analysis.

I wish to thank members of the organic chemistry research team at Rivers State University and other members of the Postgraduate laboratory during this study: Ogochukwu Udeh, Felix Obasi Okoronkwo, Tochukwu Ugboaja, Amarachi Oluah, Rachael Ekong, Angela Atata, Mathias Chukwuebuka Ekezie and others. Thank you for all the support and encouragement. I would also like to thank members of the Oelgemöeller group at JCU amongst whom are Lene Welter, Aiden Kemp, Akashnila Mele and especially Jayson Wau, for all the assistance rendered, the ideas we shared, for creating a friendly environment and giving me a memorable stay at JCU.

My gratitude goes to my head of department – Dr (Mrs) Grace Agbizu Cookey, postgraduate coordinator at RSU – Dr Gloria Ihuoma Ndukwe, Faculty of Science Postgraduate coordinator – Dr Holy Brown and the Dean of Science – Prof. Ndokiari Boisa all at Rivers State University. Thank you all for making this possible.

I thank the Vice Chancellor and Director Linkages (RSU), Nigeria and James Cook University, Australia for signing the co-tutelle agreement that allowed me to conduct this study. I additionally thank the Vice-Chancellor (RSU), Prof Nlerum Okogbule, for approving the travel support for the trip to JCU and I thank JCU for the 2022 College of Science and Engineering Competitive Research Grant.

I want to thank my dearest husband, Mr Progress Uzodhu Enyi, for his unequivocal support and understanding throughout this study. Thank you for believing in me and letting me pursue my dream. I will never forget. To my lovely kids, Prowess Enyi, Pamela Enyi and Palma Enyi, thank you for bearing with me during my 8-month study trip to JCU, and thank you for your patience throughout this study. To my parents, Victoria Nwanneka Mbadugha and Daniel Oseloka Mbadugha, I am grateful for your assistance during my study trip, and all the love and prayers since I was a kid, I will keep making you both proud. To my parents-in-law, thank you for all the love and support.

DEDICATION

This work is dedicated to God**.**

TABLE OF CONTENTS

Content	Page
ABSTRACT	i
ACKNOWLEDGEMENTS	ii
DEDICATION	iv
TABLE OF CONTENTS	v
LIST OF TABLES	xii
LIST OF FIGURES	xii
LIST OF SCHEMES	xviii
LIST OF PLATES	xix
LIST OF APPENDICES	xx
LIST OF ABBREVIATIONS	xxiv
CHAPTER 1 : INTRODUCTION	1
1.1 Background of Study	1
1.2 Photooxygenation Reactions	2
1.3 Photosensitizers	3
1.3.1 Properties of Good Photosensitizers	5
1.3.2 Classification of Photosensitizers	6
1.3.2.1 Organic Dyes	6
1.3.2.2 Porphyrins, Related Tetrapyrroles and Phthalocyanines	6
1.3.2.3 Transition Metal Complexes	7
1.3.2.4 Semiconductors	7
1.4 Absorbance Measurement and Photostability Testing of Photosensitizers	8
1.5 Immobilization of Photosensitizers	9
1.6 Applications of Photosensitizers	10
1.6.1 Wastewater Treatment	10
1.6.2 Dye-sensitized Solar Cells (DSSCs)	10
1.6.3 Photodynamic Therapy	11
1.6.3.1 Blood Sterilization	12
1.6.3.2 Herbicides	12
1.6.3.3 Insecticides	12

1.6.3.4 Cancer Therapy 12
1.6.4 Synthesis of Fine Chemicals 13
1.7 Plant Extracts as Photosensitizers 13
1.8 Use of Plant Extracts for Photochemical Synthesis 15
1.9 Photochemical Synthesis of Selected Chemicals 15
1.9.1 Ascaridole 15
1.9.1.1 Synthesis of Ascaridole 16
1.9.2 5-hydroxy-1,4-naphthaquinone 17
1.9.2.1 Synthesis of 5-hydroxy-1,4-naphthoquinone 18
1.9.3 1,4-Naphthaquinone 19
1.9.3.1 Synthesis of 1,4-Naphthoquinone 19
1.9.4 6-Hydroxy-1,4-naphthoquinone 20
1.9.4.1 Synthesis of 6-Hydroxy-1,4-naphthoquinone 20
1.9.5 Pinocarvone and Myrtenal 21
1.9.5.1 Synthesis of Pinocarvone and Myrtenal 21
1.10 Quantum Yield 23
1.11 Chemical Composition of Plant Extracts 24
1.11.1 *Hibiscus sabdariffa* (Zobo) 24
1.11.2 *Carpolobia lutea* (Cattle Stick) leaves 28
1.11.3 *Justicia secunda* Vahl (Bloodroot) Leaves 31
CHAPTER 2 : AIM AND OBJECTIVES 33
2.1 Aim 33
2.2 Objectives 33
The specific objectives of this research were to 33
CHAPTER 3 : MATERIALS AND METHOD 35
3.1 Materials 35
3.2 Equipment 38
3.3 Methods 39
3.3.1 NMR Method 39
3.3.2 Chromatographic Methods 39
3.3.3 TLC 39

3.3.4 GC 39
3.3.5 UV/Vis 40
3.3.6 HPLC-MS 40
3.3.7 Photoreactor 40
3.4 Sample Identification, Preparation and Extraction 42
3.4.1 *Hibiscus sabdariffa* Calyces (Zobo) 42
3.4.1.1 Sample Identification and Preparation 42
3.4.1.2 Extraction 44
3.4.2 *Carpolobia lutea* Leaves (Cattle Stick) 44
3.4.2.1 Sample Identification and Preparation 44
3.4.2.2 Extraction 46
3.4.3 *Justicia secunda* Vahl Leaves (Blood root) 46
3.4.3.1 Sample Identification and Preparation 46
3.4.3.2 Extraction 48
3.5 General Photooxygenation Reaction Method 48
3.6 Photooxygenation of α-Terpinene using Methylene Blue, Rose Bengal and the Plant Extracts as Photosensitizers 49
3.6.1 Photooxygenation of α-Terpinene with Anthraquinone Carboxylic Acid (ANT-COOH) 49
3.6.2 Photooxygenation α-Terpinene using *Carpolobia lutea* Extract in the presence of DABCO (1,4-diazabicyclo [2.2.2] octane) 50
3.7 Photooxygenation of 1,5-Dihydroxynaphthalene using Methylene Blue, Rose Bengal and the Plant Extracts as Photosensitizers 50
3.8 Photooxygenation of 1-Naphthol using Rose Bengal and *Carpolobia lutea* Extract as Photosensitizers 51
3.9 Photooxygenation of 1,6-Dihydroxynaphthalene using Rose Bengal and *Carpolobia lutea* Extract as Photosensitizers 51
3.10 Photooxygenation of α-Pinene using Tertraphenylporphyrin and *Carpolobia lutea* Extract as Photosensitizers 52
3.11 Photooxygenation of β-Pinene using Tetraphenylporphyrin and *Carpolobia lutea* Extract as Photosensitizers 53
3.12 Absorbance Measurements of the Dyes and Plant Extracts 53
3.13 Photostability Testing of Rose Bengal and *Carpolobia lutea* in Isopropyl Alchohol 54
3.14 Photostability Testing of Methylene Blue and *Carpolobia lutea* Extract in Acetonitrile 54

3.15 Photostability Testing of Tetraphenylporphyrin and *Carpolobia lutea* Extract In Dichloromethane 55

3.16 Fractionation of *Carpolobia lutea* Extract by Vacuum Liquid Chromatography 55

3.17 Photooxygenation of α-Terpinene using VLC Fractions of *C. lutea* Extract as Photosensitizer 57

3.18 Analysis of the Photoactive VLC Fractions by HPLC-MS 57

CHAPTER 4 : RESULTS 58

4.1 TLC Result of Preliminary Tests for Suitable Extraction Solvents 58

4.2 Yield and Physical Properties of Extracts 62

4.3 Photooxygenation of α –Terpinene 64

4.3.1 Photooxygenation of α-Terpinene using Rose Bengal and Methylene Blue as Photosensitizers. 66

4.3.2 Photooxygenation of α-Terpinene using *Hibiscus sabdariffa*, *Carpolobia lutea* and *Justicia secunda* Extracts as Photosensitizers 68

4.3.3 Summary of the Photooxygenation of α-Terpinene using Different Photosensitizers 68

4.3.4 Photooxygenation of α-Terpinene in the Presence of DABCO and ANT-COOH 71

4.3.5 α-Terpinene Photooxygenation Replicates Result Summary 75

4.4 Photooxygenation of 1,5-Dihydroxynaphthalene 78

4.4.1 Summary of the Photooxygenation of 1,5-Dihydroxynaphthalene 81

4.4.2 Percentage Isolated Yields of 5-hydroxy-1,4-naphthaquinone 83

4.4.3 1,5-Dihydroxynaphthalene Photooxygenation Replicate Result Summary 85

4.5 Photooxygenation of 1-Naphthol 87

4.5.1 1-Naphthol Photooxygenation Replicate Result Summary 92

4.6 Photooxygenation of 1,6-Dihydroxynaphthalene 94

4.6.1 1,6-Dihydroxynaphthalene Photooxygenation Replicate Result Summary 99

4.7 Photooxygenation of α-Pinene 101

4.7.1 α-Pinene Photooxygenation Replicate Result Summary 104

4.8 Photooxygenation of β-Pinene 106

4.8.1 β-pinene Photooxygenation Replicate Result Summary 109

4.9 Absorbance of the Dyes and Plant Extract 112

4.10 Photostability of Dyes 119

4.10.1 Photostability of Rose Bengal in Isopropanol 119

4.10.2 Photostability of *Carpolobia lutea* Extract in Isopropanol 121
4.10.3 Photostability of Methylene Blue in Acetonitrile 123
4.10.4 Photostability of *Carpolobia lutea* Extract in Acetonitrile 125
4.10.5 Photostability of Tetrraphenylporphyrin in Dichloromethane 127
4.10.6 Photostability of *C. lutea* Extract in Dichloromethane 129
4.11 Fractions from VLC of *Carpolobia lutea* Extract 131
4.11.1 Photooxygenation of α-Terpinene using VLC Fractions 133
4.11.2 Photoactivity of Methylene Blue and VLC Fractions of *Carpolobia lutea* Extract 133
4.12 HPLC-MS Result of *C. lutea* Extract VLC Fractions Active as Photosensitizers 135
CHAPTER 5 : DISCUSSION 140
5.1 Identification and Extraction of Plant Materials 140
5.2 α-Terpinene Photooxygenation 141
5.3 Rose Bengal and Methylene Blue Sensitized Photooxygenation of α-Terpinene 141
5.4 *Hibiscus sabdariffa* Extract, *Carpolobia lutea* Extract and *Justicia secunda* Extract Sensitized Photooxygenation of α-Terpinene 142
5.5 The Photooxygenation of α-Terpinene in the Presence of DABCO and ANT-COOH 144
5.6 1,5-Dihydroxynaphthalene Photooxygenation 146
5.7 1-Naphthol Photooxygenation 149
5.8 1,6-Dihidroxynaphthalene Photooxygenation 151
5.9 α-Pinene Photooxygenation 152
5.10 β-Pinene Photooxygenation 153
5.11 Absorbance of Dyes 155
5.12 Photostability of Rose Bengal in Isopropanol 159
5.13 Photostability of *Carpolobia lutea* Extract in Isopropanol 160
5.14 Photostability of Methylene Blue in Acetonitrile 161
5.15 Photostability of *Carpolobia lutea* Extract in Acetonitrile 162
5.16 Photostability of Tetrraphenylporphyrin in Dichloromethane 162
5.17 Photostability of *C. lutea* in Dichloromethane 164
5.18 Photoactivity of C*arpolobia lutea* VLC Fractions 165
5.19 Components of the Photoactive Fractions of *Carpolobia lutea* Extract 165
CHAPTER 6 : CONCLUSION AND RECOMMENDATION 173

6.1 Conclusion 173
6.2 Recommendations 174
6.3 Contribution To Knowledge 174
REFERENCES 176
APPENDICES 187

LIST OF TABLES

Table		Page
1.1	Summary of Selected Literature Report on *Hibiscus sabdariffa* Calyces' Extract	26
1.2	Summary of Selected Literature Report on *Carpolobia lutea* Leaves Extract	29
1.3	Summary of Selected Literature Report on *Justicia secunda* Vahl Leaves Extract	32
3.1	Reagents	36
3.2	Instrument and Equipment	38
4.1	Extraction Yield of Plant	63
4.2	Summary of Composition of the Photooxygenation of α-Terpinene Reaction Mixtures using Different Photosensitizers	70
4.3	Summary of the Photooxygenation of α-Terpinene with *C. lutea* Extract as Sensitizer in the Presence of DABCO and with ANT- COOH	74
4.4	α-Terpinene Photooxygenation Replicate Result Summary	76
4.5	1,5-Dihydroxynaphthalene Photooxygenation Replicate Result Summary	86
4.6	1-Naphthol Photooxygenation Replicate Result Summary	93
4.7	1,6-Dihydroxynaphthalene Photooxygenation Replicates Result Summary	100
4.8	α-Pinene Photooxygenation Replicates Result Summary	105
4.9	β-pinene Photooxygenation Replicates Result Summary	110
4.10	Weight of Fractions from VLC of *Carpolobia lutea* Extract	132
4.11	% Composition of Reaction Mixtures in the Photooxygenation of α-Terpinene using Methylene Blue and VLC fractions of *C. lutea* Extract as Photosensitizers	134
4.12	Summary of Fractions 2d, Fraction 3, Fraction 4 and Fraction 5 HPLC-MS Results	136
4.13	Summary of Fractions 6, Fraction 7, Fraction 8 and Fraction 9 LCMS Results	138

LIST OF FIGURES

Figure		Page
1.1	Photodynamic Therapy	11
4.1	Chromatogram of Autoxidation Reaction Mixture of α-Terpinene at 0 Minute	65
4.2	Chromatogram of Autoxidation Reaction Mixture of α-Terpinene at 90 Minutes	65
4.3	Chromatogram of Rose Bengal Sensitized Reaction Mixture of α-Terpinene at 0 Minute	67
4.4	Chromatogram of Rose Bengal Sensitized Reaction Mixture of α-Terpinene at 90 Minutes	67
4.5	Chromatogram of Methylene Blue Sensitized Reaction Mixture of α-Terpinene at 0 Minute	67
4.6	Chromatogram of Methylene Blue Sensitized Reaction Mixture of α-Terpinene at 90 Minutes	67
4.7	Chromatogram of *Hibiscus sabdariffa* Extract Sensitized Reaction Mixture of α-Terpinene at 0 Minute	69
4.8	Chromatogram of *Hibiscus sabdariffa* Extract Sensitized Reaction Mixture of α-Terpinene at 90 Minutes	69
4.9	Chromatogram of *Carpolobia lutea* Extract Sensitized Reaction Mixture of α-Terpinene at 0 Minute	69
4.10	Chromatogram of *Carpolobia lutea* Extract Sensitized Reaction Mixture of α-Terpinene at 90 Minutes	69
4.11	Chromatogram of *Justicia secunda* Extract Sensitized Reaction Mixture of α-Terpinene at 0 Minute	69
4.12	Chromatogram of *Justicia secunda* Extract Sensitized Reaction Mixture of α-Terpinene at 90 Minutes	69
4.13	GC-FID Chromatogram of Initial Reaction Mixture in the Photooxygenation of α-Terpinene with *C. lutea* Extract as Sensitizer in the Presence of 0.07 mmol DAB CO	72

4.14	GC-FID Chromatogram of Reaction Mixture in the Photooxygenation of α-Terpinene with *C. lutea* Extract as Sensitizer in the Presence of 0.3 mmol DAB CO After 90 Minute	72
4.15	GC-FID Chromatogram of Initial Reaction Mixture in the Photooxygenation of α-Terpinene with *C. lutea* Extract as Sensitizer in the Presence of 0.3mmol DAB CO	72
4.16	GC-FID Chromatogram of Reaction Mixture in the Photooxygenation of α-Terpinene with *C. lutea* Extract as Sensitizer in the Presence of 0.3 mmol DAB CO After 90 Minutes	72
4.17	GC-FID Chromatogram of Initial Reaction Mixture in the Photooxygenation of α-Terpinene with ANT-COOH as Sensitizer	72
4.18	GC-FID Chromatogram of Reaction Mixture in the Photooxygenation of α-Terpinene with ANT-COOH as Sensitizer	72
4.19	^{1}H NMR Spectrum of Synthesized Isolated Ascaridole Acquired in $CDCl_3$	79
4.20	Autoxidation 1,5-Dihydroxynaphthalene at 0 Hour Irradiation	79
4.21	Autoxidation of 1,5-Dihydroxynaphthalene at 5 Hours Irradiation	79
4.22	Rose Bengal Sensitized Photooxygenation of 1,5-DHN at 0 Hour Irradiation	79
4.23	Rose Bengal Sensitized Photooxygenation of 1,5-DHN at 5 Hours Irradiation	79
4.24	Methylene Blue Sensitized Photooxygenation of 1,5-DHN at 0 Hour Irradiation	79
4.25	Methylene Blue Sensitized Photooxygenation of 1,5-DHN at 5 Hours Irradiation	80
4.26	*H. sabdariffa* Extract Sensitized Photooxygenation of 1,5-DHN at 0 Hours Irradiation	80
4.27	*H. sabdariffa* Extract Sensitized Photooxygenation of 1,5-DHN at 5 hours Irradiation	80
4.28	*C. lutea* Extract Sensitized Photooxygenation of 1,5-DHN at 0 Hours Irradiation	80

4.29	*C. lutea* Exract Sensitized Photooxygenation of 1,5-DHN at 5 Hours Exposure	80
4.30	*J. secunda* Extract Sensitized Photooxygenation of 1,5-DHN at 0 Hours	80
4.31	*J. secunda* Extract Sensitized Photooxygenation of 1,5-DHN at 5 Hours	80
4.32	Summary of the Hourly Conversion of 1,5-Dihydroxynaphthalene to 5-hydroxy-1,4-naphthaquinone	82
4.33	Percentage Isolated Yields of 5-hydroxy-1,4-naphthaquinone after Column Chromatography	84
4.34	^{1}H NMR Spectrum of Pure Synthesized 5-Hydroxy-1,4-naphthoquinone (Juglone) Acquired in $(CD_3)_2CO$	88
4.35	Autoxidation of 1-Naphthol at 0 Hours	88
4.36	Autoxidation of 1-Naphthol at 12 Hours	88
4.37	Rose Bengal Sensitized Photooxygenation of 1-Naphthol at 0 Hours	88
4.38	Rose Bengal Sensitized Photooxygenation of 1-Naphthol at 2 Hours	88
4.39	Rose Bengal Sensitized Photooxygenation of 1-Naphthol at 3 Hours	88
4.40	1,4-Naphthaquinone Standard	89
4.41	*Carpolobia lutea* Extract Sensitized Photooxygenation of 1-Naphthol at 0 Hours	89
4.42	*Carpolobia lutea* Extract Sensitized Photooxygenation of 1-Naphthol at 4 Hours	89
4.43	*Carpolobia lutea* Extract Sensitized Photooxygenation of 1-Naphthol at 9 Hours	91
4.44	Photooxygenation of 1-naphthol using Rose Bengal and *Carpolobia lutea* Extract as Photosensitizers	93
4.45	^{1}H NMR Spectrum of Pure Synthesized 1,4-Naphthoquinone Acquired in $(CD_3)_2CO$	95

4.46	Autoxidation of 1,6-Dihydroxynaphthalene at 0 Hour	95
4.47	Autoxidation of 1,6-Dihydroxynaphthalene at 12 Hours	95
4.48	Rose Bengal Sensitized Photooxygenation of 1,6-Dihydroxynaphthalene at 0 Hours	95
4.49	Rose Bengal Sensitized Photooxygenation of 1,6-Dihydroxynapthalene at 4 Hours	95
4.50	*Carpolobia lutea* Extract Sensitized Photooxygenation of 1,6-Dihydroxynaphthalene at 0 Hours	96
4.51	*Carpolobia lutea* Extract Sensitized Photooxygenation of 1,6-Dihydroxynaphthalene at 12 Hours	96
4.52	*Carpolobia lutea* Extract Sensitized Photooxygenation of 1,6-Dihydroxynaphthalene at 24 Hours	96
4.53	Photooxygenation of 1,6-Dihydroxynaphthalene using Rose Bengal and *Carpolobia lutea* Extract as Photosensitizers	98
4.54	^{1}H NMR Spectrum of Pure Synthesized 6-Hydroxy-1,4-Napthoquinone Acquired in $(CD_3)_2CO$	100
4.55	Chromatogram for Monitoring the Autoxidation of α-Pinene at 0 Hours	102
4.56	Chromatogram for Monitoring the Autoxidation of α-Pinene at 24 hours	102
4.57	Chromatogram for Monitoring the Tetraphenylporphyrin Sensitized Photooxygenation of α-Pinene at 0 Hour	102
4.58	Chromatogram for Monitoring the Tetraphenylporphyrin Sensitized Photooxygenation of α-Pinene After 24 Hour	102
4.59	Chromatogram for Monitoring the *C. lutea* E Extract Sensitized Photooxygenation of α-Pinene at 0 Hour	102
4.60	Chromatogram for Monitoring the *C. lutea* Extract Sensitized Photooxygenation of α-Pinene at 24 Hour	102
4.61	α-Pinene and Pinocarvone Concentrations with Reaction Time in the TPP Sensitized Photooxygenations.	103
4.62	α-Pinene and Pinocarvone Concentrations with Reaction Time in the *C. lutea* sensitized Photooxygenations	103

4.63	^{1}H NMR Spectrum of Synthesized Isolated Pinocarvone	105
4.64	Chromatogram for Monitoring the Autoxidation of β-pinene at 0 Hour	107
4.65	Chromatogram for Monitoring the Autoxidation of β-pinene after 48 Hours	107
4.66	Chromatogram for Monitoring the Tetraphenylporphyrin Sensitized Photooxygenation of β-Pinene at 0 Hour	107
4.67	Chromatogram for Monitoring the Tetraphenylporphyrin Sensitized Photooxygenation of β-pinene at 48 Hour	107
4.68	Chromatogram for Monitoring the *Carpolobia lutea* Extract Sensitized Photooxygenation of α-Pinene at 0 Hour	107
4.69	Chromatogram for Monitoring the *Carpolobia lutea* Extract Sensitized Photooxygenation of β-Pinene After 48 Hour	107
4.70	Photooxygenation of β-pinene using Tetraphynylporphyrin as Photosensitizer	108
4.71	Photooxygenation of β-pinene using *Carpolobia lutea* Extract as Photosensitizer	108
4.72	^{1}H NMR Spectrum of (a) Synthesized Isolated Myrtenal and : (b) Commercially Available Standard Myrtenal(b) Acquired in $CDCl_3$	111
4.73	Absorption Spectrum of Rose Bengal Matched with the Emission Spectrum of the 8 W Cool White Fluorescent Tube	113
4.74	Absorption Spectrum of Methylene Blue Matched with the Emission Spectrum of the 8 W Cool White Fluorescent Tube	113
4.75	Absorption Spectrum of Tetraphenylporphyrin Matched with the Emission Spectrum of the 8 W Cool White Fluorescent Tube	114
4.76	Absorption Spectrum of Three Conventional Dyes (Rose Bengal, Methylene Blue and Tetraphenylporphyrin) Matched with the Emission Spectrum of the 8 W Cool White Fluorescent Tube	114
4.77	Absorption Spectrum of *Hibiscus sabdariffa* Extract Matched with the Emission Spectrum of the 8 W Cool White Fluorescent Tubes.	116
4.78	Absorption Spectrum of *Carpolobia lutea* Extract Matched with the Emission Spectrum of the 8 W Cool White Fluorescent Tube	116

4.79	Absorption Spectrum of *Justicia secunda* Extract Matched with the Emission Spectrum of the 8 W Cool White Fluorescent Tube	118
4.80	Absorption Spectrum of the Three Plant Dyes (*H. sabdariffa Extract, C. lutea* Extract and *J. secunda* Extract) Matched with the Emission Spectrum of the 8 W Cool White Fluorescent Tube	118
4.81	Variation of Absorbance Values of Rose Bengal in Isopropyl Alcohol During 24 Hours of Irradiation	120
4.82	Variation of Absorbance Values of *C. lutea* Extract in Isopropyl Alcohol During 24 Hours of Irradiation	122
4.83	Variation of Absorbance Values of Methylene blue in Acetonitrile During 24 Hours of Irradiation	124
4.84	Variation of Absorbance Values of *C. lutea* in Acetonitrile During 24 Hours of Irradiation	126
4.85	Variation of Absorbance Values of Tetraphenylporphyrin in Dichloromethane During 24 Hours of Irradiation	128
4.86	Variation of Absorbance Values of *C. lutea* in Dichloromethane During 24 Hours of Irradiation	130

LIST OF SCHEMES

Scheme		Page
1.1	Direct Photosensitized Reaction	2
1.2	Indirect Photosensitized Reaction	2
1.3	Type I versus Type II Photosensitization Mechanism	4
1.4	Jablonski Diagram of Photosensitization Processes	4
1.5	Synthesis of Ascaridole	17
1.6	Synthesis of 5-hydroxy-1,4-naphthaquinone	19
1.7	Synthesis of 1,4-Naphthoquinone	20
1.8	Synthesis of 6-hydroxy-1,4-Naphthoquinone	21
1.9	Synthesis of Pinocarvone	22
1.10	Synthesis of Myrtenal	22
1.11	Quantum Yield Determination	23
1.12	Beer Lamberts Law	23
3.1	Fractions from Gradient Eluted VLC of *C.lutea* EtOAc Extract	56
5.1	Reduction of Rose Bengal to its Leuco Form	160
5.2	Reduction of Methylene Blue to its Leuco Form	161
5.3	Reduction of Porphyrin to Chlorin	163

LIST OF PLATES

Plate		Page
3.1	Rayonet Photoreactor (RPR 200, Southern New England Ultraviolet Company, USA) with 8 Watts × 16 Cool White Fluorescent Tubes (1: Pyrex Schlenk Flask, 2: Cold Finger, 3: Oxygen in-let, 4: Air-Outlet)	41
3.2	*Hibiscus sabdariffa* a) Plant b) Calyces	43
3.3	*Carpolobia lutea* Plant	45
3.4	*Justicia secunda* a) Plant b) Extract	47
4.1	TLC Plates (1-7) of Preliminary Extraction Tests	59
4.2	Solvent Extraction of *J.secunda* using a)10→15→20% and b) 25→30→35%Vol of Water/Methanol.	61
4.3	Colour of Isopropyl Alcohol Solution of RB, Before and After 24 Hours of Irradiation	120
4.4	Colour of Isopropyl Alcohol Solution of *C. lutea*, Before and After 24 Hours of Irradiation	122
4.5	Colour of Acetonitrile Solution of Methylene Blue, Before and After 24 Hours of Irradiation	124
4.6	Colour of Acetonitrile Solution of *C. lutea,* Before And After 24 Hours of Irradiation	126
4.7	Tetraphenylporphyrin in Dichloromethane at 0 Hour and After 24 Hours Irradiation	128
4.8	*C. lutea* in Dichloromethane at 0 Hour and After 24 Hours Irradiation	130

LIST OF APPENDICES

Appendix		Page
1	GC Chromatograms for Monitoring the Rose Bengal Sensitized Photooxygenation of α-Terpinene at 90 Minutes Replicates 1 and 2	187
2	GC Chromatograms for Monitoring the Methylene Blue Sensitized Photooxygenation of α-Terpinene at 90 Minutes Replicates 1 and 2	187
3	GC Chromatograms for Monitoring the *Hibiscus sabdariffa* Extract Sensitized Photooxygenation of α-Terpinene at 90 Minutes Replicates 1 and 2	187
4	Chromatograms for Monitoring the *Carpolobia lutea* Extract Sensitized Photooxygenation of α-terpinene at 90 Minutes Replicates 1 and 2	188
5	Chromatograms for Monitoring the *Justicia secunda* Extract Sensitized Photooxygenation of α-terpinene at 90 Minutes Replicates 1 and 2	188
6	Chromatograms for Monitoring the DABCO and *Carpolobia lutea* extract Sensitized Photooxygenation of α-Terpinene at 90mintes Replicates1 and 2	188
7	Chromatograms for Monitoring the ANT-COOH and Carpolobia luteaExtract Sensitized Photooxygenation of α-Terpinene at 90 minutes Replicates1 and 2	189
8	^{1}H NMR Spectra for Monitoring Autoxidation of 1,5-Dihydroxynaphthalene at 8 Hours, Replicates1 and 2	189
9	^{1}H NMR Spectra for Monitoring Rose Bengal Sensitized Photooxygenation of 1,5-Dihydroxynaphthalene at 8 Hours, Replicates1 and 2	189
10	^{1}H NMR Spectra for Monitoring Methylene Blue Sensitized Photooxygenation of 1,5-Dihydroxynaphthalene at 8 Hours, Replicates 1 and 2	190
11	^{1}H NMR Spectra for Monitoring *Hibiscus sabdariffa* Extract Sensitized Photooxygenation of 1,5-Dihydroxynaphthalene at 8 Hours, Replicates 1 and 2	190
12	^{1}H NMR Spectra for Monitoring *Carpolobia lutea* Sensitized Photooxygenation of 1,5-Dihydroxynaphthalene at 8 Hours, Replicates1 and 2	190
13	^{1}H NMR Spectra for Monitoring *Justicia secunda* Sensitized Photooxygenation of 1,5-Dihydroxynaphthalene at 8 hours, Replicates 1 and 2	191
14	^{1}H NMR Spectra for Monitoring Rose Bengal Sensitized Photooxygenation of 1-Naphthol at 2 Hours Replicates1 and 2	191
15	^{1}H NMR Spectra for Monitoring *Carpolobia lutea* Sensitized Photooxygenation of 1-Naphthol at 2 hours Replicates 1 and 2	191

16	^{1}H NMR Spectra for Monitoring Rose Bengal Sensitized Photooxygenation of 1,6-Dihydroxynaphthalene at 8 hours, Replicates 1 and 2	192
17	^{1}H NMR Spectra for Monitoring *Carpolobia lutea* Sensitized Photooxygenation of 1,6-Dihydroxynaphthalene at 12 hours, Replicates1 and 2	192
18	GC Chromatograms for Monitoring the Tetraphenylporphyrin Sensitized Photooxygenation of α-pinene at 24 Hours, Replicates 1 and 2	192
19	GC Chromatograms for Monitoring the Carpolobia lutea Sensitized Photooxygenation of α-pinene at 24 hours, Replicates 1 and 2	193
20	Chromatograms for Monitoring the Tetraphenylporphyrin Sensitized Photooxygenation of β-pinene at 48 hours, Replicates 1 and 2	193
21	GC Chromatograms for monitoring the *Carpolobia lutea* Sensitized Photooxygenation of β-pinene at 48 hours, Replicates 1 and 2	193
22	GC Chromatograms for Monitoring Methylene Blue Sensitized Photooxygenation of Ascaridole at 0 Minutes and 90 Minutes (Standard for Fraction Testing)	194
23	GC Chromatograms for Monitoring *C. lutea* Fraction 1 Sensitized Photooxygenation of Ascaridole at 0 Minutes and 90 Minutes	194
24	GC Chromatograms for Monitoring *C. lutea* Fraction 2a Sensitized Photooxygenation of Ascaridole at 0 Minutes and 90 Minutes	194
25	GC Chromatograms for Monitoring *C. lutea* Fraction 2b Sensitized Photooxygenation of Ascaridole at 0 Minutes and 90 Minutes	195
26	GC Chromatograms for Monitoring *C. lutea* Fraction 2c Sensitized Photooxygenation of Ascaridole at 0 Minutes and 90 Minutes	195
27	GC Chromatograms for Monitoring *C. lutea* Fraction 2d Sensitized Photooxygenation of Ascaridole at 0 Minutes and 90 Minutes	195
28	GC Chromatograms for Monitoring *C. lutea* Fraction 3 Sensitized Photooxygenation of Ascaridole at 0 Minutes and 90 Minutes	196
29	GC Chromatograms for Monitoring *C. lutea* Fraction 4a Sensitized Photooxygenation of Ascaridole at 0 Minutes and 90 Minutes	196
30	GC Chromatograms for Monitoring *C. lutea* Fraction 4b Sensitized Photooxygenation of Ascaridole at 0 Minutes and 90 Minutes	196

31	GC Chromatograms for Monitoring *C. lutea* Fraction 5 Sensitized Photooxygenation of Ascaridole at 0 Minutes and 90 Minutes	197
32	GC Chromatograms for Monitoring *C. lutea* Fraction 6 Sensitized Photooxygenation of Ascaridole at 0 Minutes and 90 Minutes	197
33	GC Chromatograms for Monitoring *C. lutea* Fraction 6 Sensitized Photooxygenation of Ascaridole at 0 Minutes and 90 Minutes	197
34	GC Chromatograms for Monitoring *C. lutea* Fraction 7 Sensitized Photooxygenation of Ascaridole at 0 Minutes and 90 Minutes	198
35	GC Chromatograms for Monitoring *C. lutea* Fraction 8 Sensitized Photooxygenation of Ascaridole at 0 Minutes and 90 Minutes	198
36	GC Chromatograms for Monitoring *C. lutea* Fraction 9 Sensitized Photooxygenation of Ascaridole at 0 Minutes and 90 Minutes	198
37	GC Chromatograms for Monitoring *C. lutea* Fraction 10 Sensitized Photooxygenation of Ascaridole at 0 Minutes and 90 Minutes	199
38	GC Chromatograms for Monitoring *C. lutea* Fraction 11 Sensitized Photooxygenation of Ascaridole at 0 Minutes and 90 Minutes	199
39	GC Chromatograms for Monitoring *C. lutea* Fraction 12 Sensitized Photooxygenation of Ascaridole at 0 Minutes and 90 Minutes	199
40	GC Chromatograms for Monitoring *C. lutea* Fraction 13 Sensitized Photooxygenation of Ascaridole at 0 Minutes and 90 Minutes	200
41	HPLC-MS Chromatogram of *Carpolobia lutea* Extract Fraction 2d	200
42	HPLC-MS Chromatogram of *Carpolobia lutea* Extract Fraction 3	201
43	HPLC-MS Chromatogram of *Carpolobia lutea* Extract Fraction 4	201
44	HPLC-MS Chromatogram of *Carpolobia lutea* Extract Fraction 5	201
45	HPLC-MS Chromatogram of *Carpolobia lutea* Extract Fraction 6	202
46	HPLC-MS Chromatogram of *Carpolobia lutea* Extract Fraction 7	202
47	HPLC-MS Chromatogram of *Carpolobia lutea* Extract Fraction 8	202
48	HPLC-MS Chromatogram of *Carpolobia lutea* Extract Fraction 9	203

49	*Hibiscus sabdariffa* Identification Voucher	204
50	*Carpolobia lutea* Identification Certificate	205
51	*Justicia secunda* Identification Voucher	206

LIST OF ABBREVIATIONS

%	-	Percentage
Abs	-	Absent
ANT-COOH	-	Anthraquinone carboxylic acid
C. lutea	-	*Carpolobia lutea*
Comp.	-	Composition
DABCO	-	1,4 – diazabicyclo[2.2.2]octane
DMAP	-	4-(Dimethylamino) pyridine
DHN	-	Dihydroxynaphthalene
d	-	doublet
dd	-	doublet of doublets
dt	-	doublet of triplets
dq	-	doublet of quartets
et al.	-	and others
EtOAc	-	Ethylacetate
Fr.	-	Fraction
GC-FID	-	Gas Chromatography-Flame Ionization Detector
GC/MSD	-	Gas Chromatography/Mass Selective Detector
g	-	gram
^{1}H-NMR	-	Proton nuclear magnetic resonance
H. sabdariffa	-	*Hibiscus sabdariffa*
hr	-	Hour
LC-MS	-	Liquid Chromatography-Mass Spectrometry

J. secunda	-	*Justicia secunda*
MeOH	-	Methanol
mins	-	Minutes
mL	-	milliliter
mmol	-	millimole
NMR	-	Nuclear Magnetic Resonance
n/a	-	not available
p	-	pentet
q	-	quartet
RT	-	Retention Time
s	-	singlet
sx	-	sextet
t	-	triplet
td	-	triplet of doublets
TLC	-	Thin Layer Chromatography
TPP	-	Tetraphenylporphyrin
UV/Vis	-	Ultraviolet/Visible
VLC	-	Vacuum Liquid Chromatograph

CHAPTER 1
INTRODUCTION

1.1 Background of Study

Natural plant extracts provide endless sources of chemical compounds and thus are constantly being used and researched for various purposes including therapeutics, production of fragrances and aromatherapy, cleaning (detergents and soap making), cosmetics, biofuels, colouring and flavouring agents, textile industry, dye-sensitized solar cells, etc. Moreso, Green Chemistry is becoming increasingly important and concerns about environmental pollution and sustainability have become pressing. Thus, the use of plant extracts favours the principles of green chemistry, which comprise the use of renewable feedstock, products that are non-toxic to the environment and biodegradable chemicals.

On the other hand, photooxygenation is a very important and green synthetic method used for the preparation of valuable commodity chemicals. It allows for easy access to oxygenated products from renewable natural materials in the presence of oxygen, (sun) light and a photocatalyst (Photosensitizer). They solely utilize catalytic amounts of organic dyes as photosensitizers and (sun) light for the activation of oxygen. Importantly, these transformations are used in the fragrance, flavour and pharmaceutical industries, to produce high-value commodity chemicals. Thus, photooxygenations constitute an intriguing application with easy access to natural sunlight and renewable starting materials.

However, a major drawback of photooxygenations as a truly sustainable synthetic method is the use of synthetic dyes as photosensitizers which are commonly not recovered from the reaction mixture and are instead disposed off. These synthetic dyes which include methylene blue, rose bengal, methyl orange, etc, are organic compounds and common environmental pollutants from industries (Hassan *et al.,* 2021; Mittal *et al.*, 2009; Vinuth *et al.,* 2016). Photocatalytic degradation

of dyes using semiconductors, adsorption(by ionic liquids and MOFs), biological treatment, electrocoagulation, reverse osmosis, electrochemical oxidation, ion exchange, Fenton oxidation, and ozonation are some methods currently used for their removal from solution (Hassan *et al.,* 2021; Mittal *et al.*, 2009). However, there are no timely and cost-effective ways to remove both the colour and the harmful qualities of the synthetic dyes released into the environment (Verma and Gupta, 2017). The scientific community is therefore exploring the use of natural dyes in several conventional and recently discovered applications because they are affordable, non-toxic and renewable resources(Verma and Gupta, 2017). This study explores the use of plant dyes as sources of photosensitizers for photooxygenation reactions.

1.2 Photooxygenation Reactions

In photooxygenation reactions, oxygen (O_2) is added to a substrate A in the presence of light (*hv*) to form an addition product AO_2

These reactions may take place via a direct or indirect (or photosensitized) process. In the direct process, (Sun)light is absorbed by the reacting species (A and O_2) which are then transformed into a product (AO_2) (Scheme 1.1).

$$A + O_2 \xrightarrow{hv} AO_2$$

Scheme 1.1: Direct Photosensitized Reaction

In the indirect process, light energy(*hv*) is absorbed by other molecules (a photosensitizer) different from the reactant molecules (A and O_2). The photosensitizer molecules then transfer this energy (*hv*) to the reactant molecules (A and O_2) (Scheme 1.2**)** (Volman *et al.,* 2007).

$$A + O_2 \xrightarrow{\text{Photosensitizer}/hv} AO_2$$

Scheme 1.2: Indirect Photosensitized Reaction

The focus of this study is on dye-photosensitized oxygenation reactions (indirect process) since selected plant extracts are being tested for their photosensitizer ability. Photooxygenation reactions are implicated in the production of many commercial chemicals including flavours, perfumes and other biologically active molecules such as rose oxide, citronellol, 5-hydroxy-1,4-naphthoquinone (**4**), ascaridole (**3**) and artemisinin, hence the interest in finding more efficient photosensitizers for the production of these compounds (Wau *et al.,* 2021).

1.3 Photosensitizers

Most photosensitizers absorb light at wavelengths between 630 nm and 700 nm (Fekrazad *et al.*, 2017). Photosensitizers are also known as photocatalysts because they are not usually used up during photosensitization processes but return to their original state once the process is complete. Photosensitization is important because it is used in the syntheses of natural products and fine chemicals that may not be possible by conventional thermal methods (Oleinick, 2011). When a photosensitizer molecule absorbs a photon, it gets excited and undergoes internal changes that result in the changes in a target molecule (substrate). These changes can occur by two different pathways that is, by Type I and Type II photosensitization reactions (Oleinick, 2011). In Type I photosensitization reactions, the sensitizer reacts with the target molecules by either abstracting a hydrogen atom(s) from them or by transferring an electron to them forming free radicals. In Type II photosensitization reactions, the excited photosensitizer and oxygen molecules exchange energy to create excited singlet oxygen, which is a much more reactive specie than its ground-state triplet (Pouyet and Chapelon, 1987). Type I mechanism requires a direct interaction between the photosensitizer and the substrate; hence they are favored by high substrate concentrations. Considering that oxygen competes with the substrate for contact with the photosensitizers, low oxygen concentration also favours the Type I mechanism. Lower substrate concentrations and

higher oxygen concentrations favour the Type II mechanism (Oleinick, 2011). A summary of Type I and Type II photosensitization mechanisms is shown in Scheme 1.3.

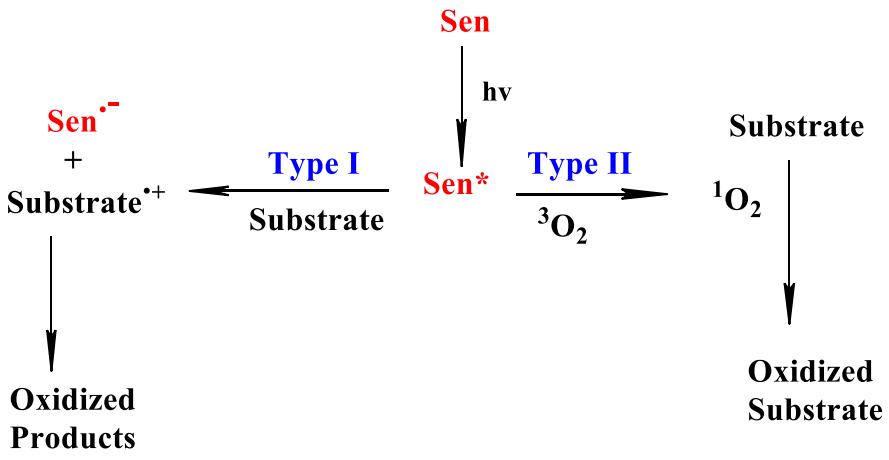

Scheme 1.3: Type I versus Type II Photosensitization Mechanism

The photophysical processes available to photosensitizer molecules may be summarized by the Jablonski diagram in Scheme 1.4.

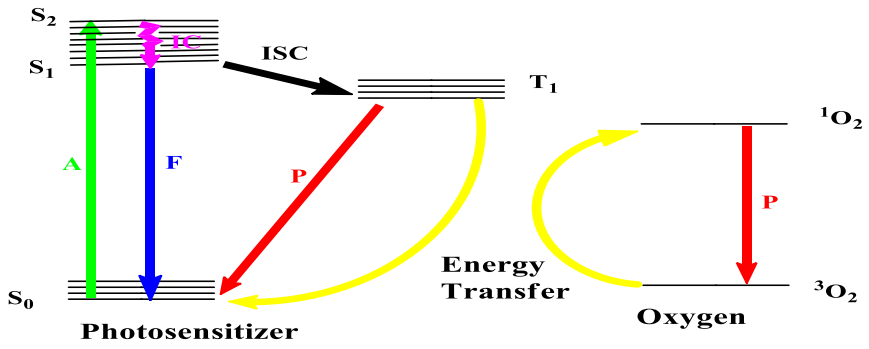

Scheme 1.4: Jablonski Diagram of Photosensitization Processes

Green Arrow(A) shows the absorption of a photon of light by a sensitizer molecule, exciting it. For absorption to take place, the energy of the photon must be equal to the energy difference between the ground state of the sensitizer (S_0) and its excited states (S_1).

Blue Arrow(F) represents fluorescence. This is the emission of energy from an excited molecule in the form of light, which occurs between similar electronic spin states.

Black Arrow (ISC) stands for intersystem crossing**.** This represents a radiationless transition of the sensitizer molecule from a singlet state to a triplet state or vice versa.

Red Arrows(P) stand for phosphorescence. This process, like fluorescence, represents the emission of excitation energy in the form of light but occurs between different electronic spin states (i.e. between triplet and singlet states).

Purple Jagged Arrow (IC) represents internal conversion, showing radiation-less transitions between similar electronic spin states of the sensitizer molecule (i.e. between singlet states or between triplet states).

Yellow Arrows stand for energy transfer. The electronic energy of the photosensitizer is transferred to the molecular ground state oxygen (triplet state) elevating it to the first excited state (singlet state). During this process, the triplet-excited state of the photosensitizer is deactivated to its ground singlet state (Oleinick, 2011).

1.3.1 Properties of Good Photosensitizers

Several molecules which absorb light in the UV/visible region have shown singlet oxygen-generating capacity. According to Crutchley and DeRosa (2002), the properties of good photosensitizers include the following:

1) Ability to absorb light waves effectively at certain spectral regions

2) High quantum yields of triplet state ($Ø_T > 0.4$)

3) Long triplet state lifetime ($^{ŧ}T > 1ʉs$)

4) Triplet state of suitable energy ($E_T \geq 95 KJmol^{-1}$)

5) Have a high photostability

1.3.2 Classification of Photosensitizers

Photosensitizers may be broadly classified as follows: organic dyes, porphyrins, related tetrapyrroles and phthalocyanines, transition metal complexes, and semiconductors.

1.3.2.1 Organic Dyes

Organic dyes are usually efficient photosensitizers because they have chromophores (sets of conjugated double bonds) that absorb light at certain visible wavelengths, thereby exciting their molecules (Hamblin *et al.*, 2019). Methylene blue, rose bengal and eosin are examples of organic dyes with good photosensitizer abilities because they bear triplet states of adequate energies for sensitization of oxygen. Phenothiazinium dyes, e.g. methylene blue, have a strong absorbance in the 550-700 nm range of the spectral region with a good quantum yield of 0.52. Eosin and rose bengal, which are xanthene (1) dyes, have strong absorbance in the 480-550 nm range of the spectral region, with rose bengal giving a high singlet oxygen yield of about 0.76 (Crutchley and DeRosa, 2002).

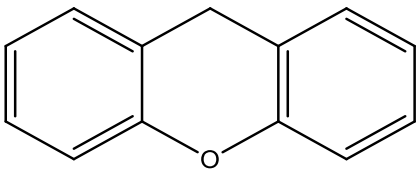

1

1.3.2.2 Porphyrins, Related Tetrapyrroles and Phthalocyanines

Porphyrins are naturally occurring organic photosensitizers, and this makes them good for use in biological singlet oxygen generation; for example, in applications for photodynamic therapy (Berg,

2009; Crutchley and DeRosa, 2002). Porphyrins are made up of four pyrrole subunits linked together by four methane-bridges. Hematoporphyrin (2) is an example of a well-studied porphyrin used in humans for the production of singlet oxygen. Its triplet quantum yield is 0.83 and its singlet oxygen quantum yield is 0.65. It absorbs light at 630 nm (Crutchley and DeRosa, 2002). Other members of the porphyrin family include chlorophyll, tetraphenylporphyrin, chlorins and bacteriochlorins (Berg, 2009; Crutchley and DeRosa, 2002).

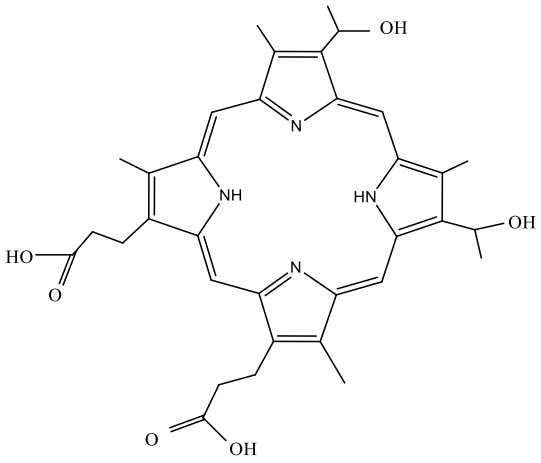

2

1.3.2.3 Transition Metal Complexes

Some inorganic complexes are more efficient singlet oxygen producers than some conventional organic photosensitizers such as methylene blue (Crutchley and DeRosa, 2002). Complexes of Cr(III), Pt(II), Pd(II), Ru(II), Os(II) and Ir(III) have been studied for their sensitization abilities. Ru(II) and Os(II) complexes gave singlet oxygen quantum yields of 0.68-0.86 (Crutchley and DeRosa, 2002).

1.3.2.4 Semiconductors

TiO_2, ZnO, Fe_2O_3, CdS and ZnS are semiconductors that have been used for the production of singlet oxygen. ZnO gives a higher singlet oxygen quantum yield than TiO_2 (Crutchley and

DeRosa, 2002). TiO_2 is the most extensively used for the decontamination of water (Thandu *et al.*, 2015).

1.4 Absorbance Measurement and Photostability Testing of Photosensitizers

Photostability is an important characteristic of good photosensitizers. Photostability can be described as the resistance of a molecule to change on exposure to light (Tonnosen, 2001). Coyle (2010) measured the absorbance of rose bengal, methylene blue and tetraphenylporphyrin. The researcher reported that although tetraphenylporphyrin generates the highest singlet oxygen, amongst the 3 dyes, it is least used because of its solubility challenges. Coyle (2010) also reported that the UV/Visible absorbance measurement and λmax of rose bengal, methylene blue and tetraphenylporphyrin gave the following values: 0.340 at λmax 550nm ($2.456x10^{-4}$ mol), 0.234 at λmax 640nm ($2.5155x10^{-4}$ mol) and 0.977 at λmax 417 nm (2.4073×10^{-4} mol), respectively. Coyle (2010) further measured the stability of rose bengal in organic solvents between the pH range of 3 - 13 using UV/Vis spectrophotometry. The researcher measured the absorbance of rose bengal aqueous solution at a pH range of 2-13 and the absorbance of rose bengal water/methanol solution (1:1) at a pH range of 3-13; and reported that rose bengal is stable under typical photooxygenation settings between a pH range of 4 - 13. However, Linden and Neckers (1988) reviewed the spectral, photochemical properties and photochemical reactivity of rose bengal. The reviewer reported the absorption spectrum of rose bengal in ethanol to have a λmax at 557nm. Linden and Neckers (1988) also reported that rose bengal iodonium salt in methylene chloride solution bleaches in a few seconds in room light by a reduction mechanism forming a leuco rose bengal (a dihydro compound) which has been isolated. Other onium salts of rose bengal bleach more slowly and by the same mechanism.

Shen and Yunus (2002), measured the absorbance of methylene blue molecules doped in a gelatin matrix and observed a λmax at 668 nm and a shoulder at 620 nm. Irradiation with UV/Visible light caused photobleaching of the methylene blue molecules doped in the gelatin matrix and this was attributed to the photoreduction of the methylene blue molecules to its leuco form.

Cavaleiro *et al.* (2001) carried out a photodegradation experiment on meso-tetraphenylporphyrin by irradiation of its solution in benzene using Henovia Xenon-mercury lamp visible range light – 1000W. Photodegradation of tetraphenylporphyrin was observed after 1 hour of irradiation with a decline at the peaks (515 nm and 650 nm, respectively). The peak at 650 nm also had a clear blue shift. When argon-saturated toluene was used as a solvent, the peak at 650 nm increased as the irradiation time increased. This was attributed to the formation of chlorin, a reduction product. The researcher concluded that the presence of oxygen positively influences the photostability of tetraphenylporphyrin.

Chen *et al*. (2018) investigated the photostability of anthocyanin monomers from red cabbage. They kept methanol solutions of the anthocyanins under three different light conditions (darkness, indoor light and artificial light -50-watt xenon lamp) and used HPLC to determine the degradation of anthocyanins by comparing their peak areas. They found anthocyanin monomers with more acyl groups to be more susceptible to photodegradation.

1.5 Immobilization of Photosensitizers

Using photosensitizers in solution poses the problem of removing them from a reaction mixture, hence the increasing popularity of immobilization of photosensitizers on solid support (Thandu *et al.*, 2015). Immobilization of photosensitizers involves adhering them to a suitable solid support. Some benefits of immobilized photosensitizers include the following: easy purification of products in fine chemical synthesis, possible reuse of the immobilized photosensitizer (economically and

environmentally friendly), heterogenous reaction phases allow for the use of various solvents (Crutchley and DeRosa, 2002; Santos *et al.*, 2009). Adhering photosensitizers to solid supports can be carried out by adsorption, conjugation (covalent bond formation), electrostatic interaction and polymerization (Thandu *et al.*, 2015). Much research has been carried out using several materials as sensitizer support. Such materials include polymers, e.g. polystyrene beads, biopolymers, e. g. calcium alginate beads, magnetic nanoparticles, glass, silicones, metal-organic frameworks (MOFs) and resins.

1.6 Applications of Photosensitizers

Some applications of photosensitizers include the following: in wastewater treatment (degradation of chemical pollutants), manufacture of solar cells, photodynamic therapy and the synthesis of fine chemicals. In all of these, photosensitizers are used to generate singlet oxygen, which is then put to different uses.

1.6.1 Wastewater Treatment

Much study has been done on the use of photosensitizers for generating singlet oxygen for the oxidation of toxic compounds in wastewater. Phenol and its derivatives are major toxic compounds found in wastewater of oil refineries, dye manufacturing industries and paper industries. Riboflavin, methylene blue, rose bengal and Zn(II) tetraphenylporphyrin have been studied for this purpose. Also important in wastewater treatment is the oxidation of sulphide salts to sulphates in aqueous solution. Co(II) complexes and all phthalocyanines are good photosensitizers for this application of photoxidation reaction (Crutchley and DeRosa, 2002).

1.6.2 Dye-sensitized Solar Cells (DSSCs)

In 1991, Gratzel and his co-workers developed a dye-sensitized solar cell. The DSSC fabrication was motivated by the energy and electron transfer mechanisms in photosynthesis (Narayan, 2012).

DSSC has since gained amazing attention as an alternative to traditional silicon-based solar cells because of their cheap and easy fabrication, high indoor efficiency, peculiar mechanical and optical properties. A DSSC mainly comprises a semiconductor which has been soaked in a sensitizing dye, a counter electrode and an electrolyte comprising a redox mediator. The dye absorbs light which is transformed into electricity (Arof and Ping, 2017; Carella *et al.*, 2018). Photosensitizers are a major component of DSSC devices. Thousands of dyes have been tested and are now being used as photosensitizers in DSSC. They are broadly divided into 3 main classes namely: metal-free organic dyes, Zn-porphyrin derivatives and ruthenium (II) polypyridyl complexes (Carell *et al*., 2018).

1.6.3 Photodynamic Therapy

The photodynamic effect is the damaging of living cells in the presence of photosensitizers, visible light and oxygen (Berg, 2009; Crutchley and DeRosa, 2002). When the photodynamic effect is applied for its therapeutic result as illustrated in Figure 1.1, it is called photodynamic therapy (Berg, 2009). Photodynamic therapy has been successfully used in blood sterilization, herbicides, insecticides and cancer therapy.

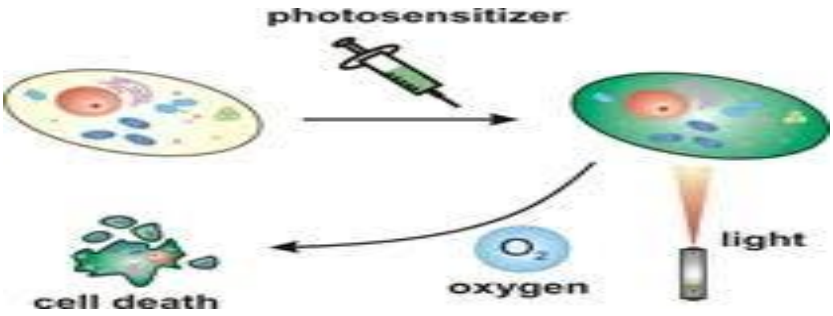

Figure 1.1: **Photodynamic Therapy**

Source: Charles University, Faculty of Pharmacy in Hradec Kralove, 2023. (https://poRTal.faf.cuni.cz/Groups/Azaphthalocyanine-group/Research-Projects/Photodynamic-therapy/)

1.6.3.1 Blood Sterilization

Methylene blue, which has shown a lack of toxicity to humans, was used as a photosensitizer by the Swiss and German Red Cross to destroy extracellular enveloped viruses in blood. Silicon-based phthalocyanines are being studied for their ability to sterilize blood components. Also, there are reports of organic dyes like porphyrins, methylene blue, rose bengal, and phthalocyanines being used for water disinfection (Narayan, 2012).

1.6.3.2 Herbicides

Photodynamic herbicides e.g. δ-Aminolevulinic acid use the lethal effect of singlet oxygen to destroy weeds or unwanted plants. They act by causing the accumulation of chlorophyll and tetrapyrroles in the unwanted plants such that upon exposure to light, these accumulated compounds perform as photosensitizers producing singlet oxygen that destroys the tissue of the treated plants (Duke *et al.,* 1991).

1.6.3.3 Insecticides

Porphyrin-based insecticides and other photosensitizers e.g erythrosine, acridine red, methylene blue, xanthenes, and Phloxin B are administered as baits to insects, which become photosensitive one hour after exposure and this persists for up to 48 hours after administration has stopped (Amor and Jori, 2000; Crutchley and DeRosa, 2002; Luksiene *et al*., 2007).

1.6.3.4 Cancer Therapy

Photosensitizers e.g hematoporphyrin derivatives, benzoporphyrin, mesotetrahydroxyphenyl chlorine, 5 aminolevulinic acid, Sn-etiopurpurin, texaphyrins, chlorin e6, phthalocyanine with visible light and oxygen are now combined to produce deadly species that selectively damage tumor cells (Kudinova and Berezov, 2010). Photosensitizers for cancer treatment, amongst fulfilling the properties of good photosensitizers, should be able to selectively accumulate in

tumour tissue and should have low dark toxicity to the biological tissue (Crutchley and DeRosa, 2002).

1.6.4 Synthesis of Fine Chemicals

The use of photosensitizers for the synthesis of commodity chemicals dates back to 1943 when a scientist named Schenck made use of chlorophyll from the leaves of stinging nettles as a sensitizer. Air and α-terpinene in ethanol were also used for the photochemical synthesis of ascaridole (Esser *et al.*, 1994). Since then, several photochemical transformations leading to the synthesis of fine chemicals have been done. Organic syntheses that make use of photosensitizers are mostly photooxygenation reactions (Type II photosensitized oxidations) (Oelgemoller *et al.*, 2021). The most common photosensitizers used for the synthesis of fine chemicals are rose bengal (as disodium salt), tetraphenylporphyrin and methylene blue. General photooxygenation reactions include [2+4] cycloadditions to alkadienes to form endoperoxides, Schenck-ene-type reactions of alkenes to hydroperoxides and [2+2] cycloadditions to alkenes to produce 1,2-dioxetanes. Examples of some of these photooxygenation reactions include phootoxygenation of α-terpinene to ascaridole (**3**), photooxygenation of citronellol and subsequent transformation to rose oxide, photooxygenation of 1,5-dihydroxynaphthalene to 5-hydroxy-1,4-naphthoquinone (**4**), photooxygenation of β-pinene and further conversion to myrtenol, etc. (Oelgemöller, 2016).

1.7 Plant Extracts as Photosensitizers

Ryberg (2020) used chlorophyll and curcumin extracted from plants as photosensitizers for the disinfection of drinking water. Brar (2013) stated that dissolved organic matter in aquatic systems acted as a photosensitizer to produce singlet oxygen. This observation implies that they have photosensitizer potential for the degradation of pollutants and elimination of pathogens in wastewater.

Literature is replete with studies on the use of natural dyes from plant extracts in the fabrication of dye-sensitized solar cells (DSSCs). Taya *et al*. (2012) studied extracts of pomegranate, walnuts and rhubarb for the fabrication of DSSCs. The walnut extract gave the highest P_{max} (maximum power) of the DSSCs followed by the rhubarb and then the pomegranate extracts. Out of the three selected plants of interest in this study (*Hibiscus sabdariffa, Carpolobia lutea and Justicia Secunda* Vahl), only the use of *Hibiscus sabdariffa* extract as photosensitizer for the production of DSSCs have been reported. Jahn *et al.* (2018) reported the use of *Hibiscus sabdariffa* extract for the production of the photo-electrode in DSSCs. The solar cell produced with this plant extract could generate electricity with an output power of 61µW. Yadav *et al.* (2022) also reported the use of *Hibiscus sabdariffa* extract as an electrolyte in DSSCs. The DSSC produced gave a conversion efficiency (performance) comparable to DSSCs in literature. There is a dearth of literature on the use of magenta (*Justicia Secunda* Vahl) extract in the assembling of DSSCs.

Plant extracts have been proven to have photosensitizing ability for applications in Photodynamic Therapy (PDT). Jong e*t al*. (2013) studied 2,400 plant extracts as new photosensitizers for PDT. Some of these fractions were identified as active photosensitizers, hence they were recommended for further chemical isolation. Villacorta *et al*. (2017) examined three plant extracts (*Lumnitzera racemosa, Albizia procera* and *Cananga odorata*) for their potential as photosensitizers for PDT. Two (*Lumnitzera racemosa* and *Albizia procera*) out of the three plants examined showed that they were cytotoxic against cancer cells, therefore their extracts have the potential to act as good photosensitizers for PDT. Kulkarni *et al*. (2018) investigated the photodynamic antimicrobial effect of henna (*Lawsonia inermis*) extract. They reported that alcoholic henna extract showed photodynamic antimicrobial activity against different types of microorganisms. Ugboaja *et al. (*2022) reported the photo-larvicidal property of *Hibiscus sabdariffa* extract with an 80% mortality

rate and an LC_{50} of 528.44 ppm. There is a scarcity of reports on the use of *Carpolobia lutea* and *Justicia secunda* extract for PDT.

1.8 Use of Plant Extracts for Photochemical Synthesis

There is a dearth of literature reports on the use of plant extracts as photosensitizers for organic synthesis. However, there are a few studies on the use of plant extracts for photochemical syntheses. Triemer *et al*. (2018) synthesized artemisinin (a powerful anti-malaria drug) using crude plant extract, oxygen, acid and light. Dihydroartemisinic acid from the extract of *Artemisia annua* was the biosynthetic precursor and chlorophyll in the plant extract acted as the photosensitizer. Ikram and Ahmed (2015) did a review on the use of plant extracts in the synthesis of gold nanoparticles. The review stated that 24 plant extracts were used for reducing and stabilizing the nanoparticles. Kenny and Fisher (1973) reported the use of natural chlorophyll from kudzu leaves (acetone:water extract, 85:15) for the preparation of *trans*-pinocarveol and myrtenol. 40% conversion of α-pinene to *trans*-pinocarvyl hydroperoxide was achieved and 65% yield of myrtenol was observed.

1.9 Photochemical Synthesis of Selected Chemicals

A brief review on the general methods of synthesis for the selected fine chemicals in this study is as follows:

1.9.1 Ascaridole

Ascaridole (**3**) is a natural peroxide (a bicyclic monoterpene) which has been identified in the essential oils of some plant species namely *Chenopodium ambrosioides L*., *Dysphania ambrosioides* and *Ledum palustre (*Benelli *et al.,* 2020; Dembitsky *et al.,* 2008; Dougnon and Ito, 2020*).* Ascaridole (**3**) was first isolated in 1895 by a German pharmacist. It is majorly mentioned for its anthelmintic properties in the treatment of hookworms and ascarids in humans, pigs, horses,

dogs and cats (Dembitsky *et al.*, 2008). Ascaridole (**3**) has also been reported to have some antimalaria activity, activity against tumour cells, antifungal effect, sedative effects and pain-relieving properties (Dembitsky *et al.*, 2008).

1.9.1.1 Synthesis of Ascaridole

To manufacture ascaridole (**3**), Gunther Otto Schenck built the first solar power facility after World War II (Oelgemöller, 2016). This ascaridole (**3**), due to its anthelminthic properties, was used for the treatment of worm infection in war-torn Germany. 200 glass bottles (10 litres each) were exposed to sunlight and sprayed with water for cooling. These glass bottles were filled with air-saturated ethanol, leaves of stinging nettles (as chlorophyll source) and solutions of α-terpinene. Frequent shaking was ensured to maintain saturation with air. This set-up produced 2kg of ascaridole (**3**) after two sunny summer days (Oelgemöller, 2016). Since then, the synthesis of ascaridole (**3**) has been so common that it has been used for the evaluation of new photochemical setups and photosensitizers (Ronzani *et al.*, 2013; Shvydkiv *et al*., 2018). Shvydkiv *et al*. (2018), synthesized ascaridole (**3**) in a quartz schlenk flask using an external 18 W fluorescent tube to achieve 79% conversion after 15 minutes at a space-time rate of 0.9-1.2 $molL^{-1}h^{-1}$. The complete conversion was achieved in 30 minutes. Ronzani *et al.* (2013), reported 78% composition within 30 minutes of irradiation using 16x8watts fluorescent lamps in an RPR-200 Rayonet Reactor with rose bengal as photosensitizer. Replacing rose bengal with ANT-COOH (a Type I photosensitizer), a negligible 1% yield after 40 minutes was observed. Autoxidation of α-terpinene gave no ascaridole (**3**) peak after 150 minutes but the α-terpinene composition of the starting material dropped from 93% to 44% and p-cymene a side product increased from 4% to 39%. DABCO is a known singlet oxygen quencher. According to a report by Ouannes and Wilson (1968), irrespective of the method of generation of the singlet oxygen (by electric discharge, photochemical method or chemical generation), reactions involving $^1O_2$ are retarded or suppressed by DABCO. In the study

by Ouannes and Wilson (1968), 100% photoxidation of rubrene with 0 M DABCO was achieved within 16 minutes of the reaction. In the presence of 3.4×10^{-3} M DABCO, only 40% photoxidation of rubrene was achieved. An increment in the DABCO concentration to 13×10^{-3} M further suppressed the photoxidation of rubrene to 10% after the same time (16 minutes). Subsequently, DABCO has been known and used as an efficient $^1O_2$ quencher (Li *et al.*, 2022). Scheme 1.5 shows the general equation for the photooxygenation of α-terpinene.

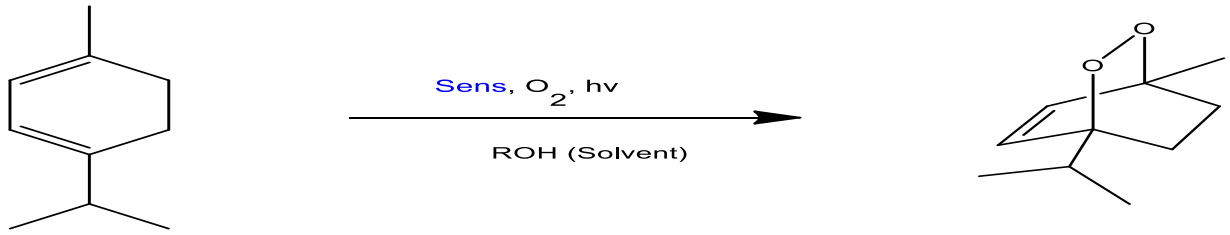

α-terpinene **Ascaridole**

Scheme 1.5: Synthesis of Ascaridole

1.9.2 5-hydroxy-1,4-naphthaquinone

Juglone is a quinoid (5-hydroxy-1,4-naphthaquinone) isolated from the Juglandaceae family and popularly from black walnut - *Juglans nigra L.* (Islam and Widhalm, 2020). 5-hydroxy-1,4-naphthoquinone (**4**) was first synthesized in 1887 and in 1928 it was confirmed to be toxic to plants (Strugstad and Despotovski, 2012). According to Latos *et al.* (2019), 5-hydroxy-1,4-naphthoquinone (**4**) is used for the dyeing of fibres (synthetic and natural). Other applications of 5-hydroxy-1,4-naphthoquinone (**4**) are based on its herbicidal, anti-fungal, anti-bacterial and anti-viral activities. 5-hydroxy-1,4-naphthoquinone (**4**) has been found to have sedative properties, therefore, limiting its use in medicine (Strugstad and Despotovski, 2012). Most importantly, 5-hydroxy-1,4-naphthoquinone (**4**) has proven to be a very important building block chemical for the synthesis of many biologically active quinoid compounds (Oelgemöller *et al.,* 2006).

1.9.2.1 Synthesis of 5-hydroxy-1,4-naphthoquinone

There is ample literature on the photochemical synthesis of 5-hydroxy-1,4-naphthoquinone (**4**). Julio *et al*. (2014) carried out the photooxygenation of 1,5-dihydroxynaphthalene using rose bengal as a photosensitizer in EtOH (solvent media) to yield 75-83% 5-hydroxy-1,4-naphthoquinone (**4**). Oelgemöller *et al*. (2006) investigated the synthesis of 5-hydroxy-1,4-naphthoquinone (**4**) by dye-sensitized photooxygenation of 1,5-dihydroxynaphthalene. The study compared using soluble versus solid-supported sensitizers. Also, moderately concentrated sunlight was compared with halogen lamps (2×50 W Armley Halogen Lamps) as an irradiation source. Good yields of about 79% of 5-hydroxy-1,4-naphthaquinone were achieved after 4 hours of irradiation. Coyle (2010), using rose bengal sensitizer, achieved a 66% isolated yield of 5-hydroxy-1,4-naphthaquinone after 4 hours of solar irradiation of 1,5-dihydroxynaphthalene in a schlenk flask. Lancel *et al.* (2023) under red LEDs (31W) carried out photooxygenation of 1,5-dihydroxynaphthalene at a fixed temperature of 20^0C. Using 0.16 mol of methylene blue, 0.1 M substrate in acetonitrile was irradiated for 4 hours with oxygen bubbling in. The full conversion was observed and 80% isolated 5-hydroxy-1,4-naphthaquinone yield was achieved. Autoxidation of freshly purified 1,5-dihydroxynaphthalene in acetonitrile produced an 82% isolated yield of 5-hydroxy-1,4-naphthaquinone under irradiation with blue light. This yield is higher than almost all other reported isolated 5-hydroxy-1,4-naphthaquinone yields in literature where photosensitizers were used (Lancel *et al*., 2023). Scheme 1.6 shows the general equation of reaction for the synthesis of 5-hydroxy-1,4-naphthaquinone.

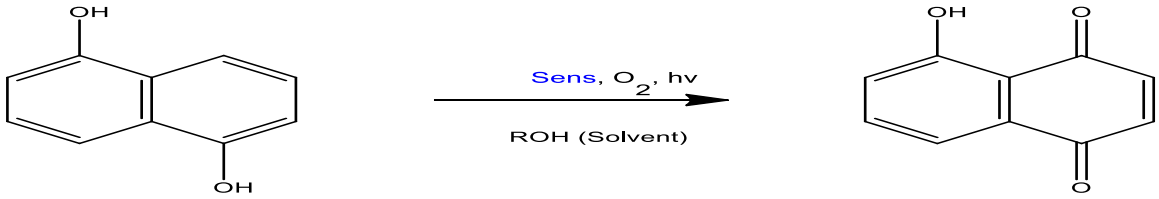

1,5-dyhydroxynaphthalene **5-hydroxy-1,4-naphthaquinone**

Scheme 1.6: Synthesis of 5-hydroxy-1,4-naphthaquinone

1.9.3 1,4-Naphthaquinone

1,4-Naphthaquinones are special molecules because of their numerous biological activities. They are found to occur naturally in plants as substituted compounds. For example, 2-hydroxy-1,4-naphthoquinone (lawsone) is found in *Lawsonia inermis* and 5-hydroxy-1,4-naphthoquinone (juglone) (**4**) is found in black walnut. Other substituted 1,4-naphthoquinones found in plants include α-lapachone and β-lapachone found in the *Bignoniaceae* family (Klotz *et al.,* 2014). 1,4-Naphthaquinones are potent as having cardio-protective/anti-ischemic properties, hepatoprotective properties, anti-inflammatory/analgesic properties, anti-microbial activity, cytotoxic and anti-cancer activity, neuroprotective properties (Klotz *et al*., 2014).

1.9.3.1 Synthesis of 1,4-Naphthoquinone

Coyle (2010) synthesized 1,4-naphthoquinone (**5**) by sonicating a mixture of 1-naphthol (0.144 g, 1 mmol) and rose bengal (0.05 g) in *t*-amyl alcohol (100 mL). This reaction mixture was then irradiated for 24 hours using a 500 W halogen lamp with air bubbling in a reaction vessel. Scheme 1.7 shows the general equation of reaction for the synthesis of 1,4-naphthoquinone (**5**). According to Coyle (2010), 70% conversion of 1-naphthol was achieved after 24 hours. Lancel *et al.,* 2023 reported that autoxidation of 1-naphthol under 460 nm irradiation in a batch reactor showed no

conversion. Suchard *et al.* (2006) reported the photooxygenation of 1-naphthol with rose bengal on Merrifield resin (sensitox), in acetone, irradiating with a mercury lamp and purging with pure oxygen for 5 hours. 53% yield of 1,4-naphthoquinone (**5**) was reported.

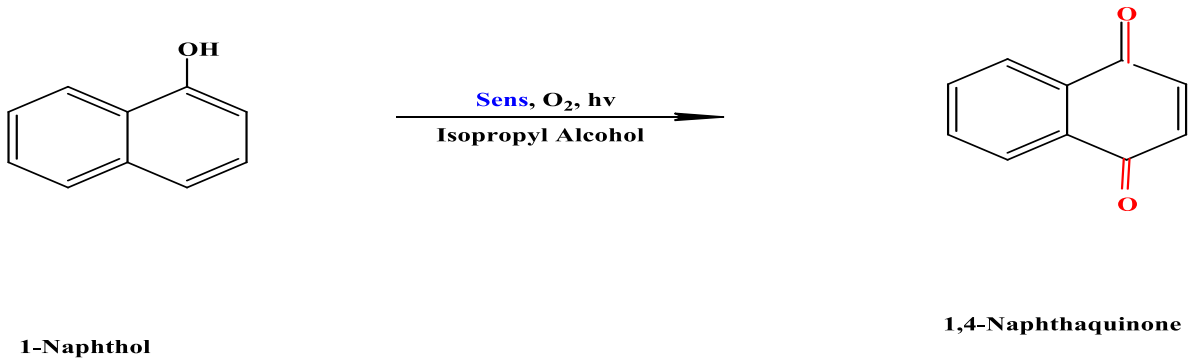

Scheme 1.7: Synthesis of 1,4-Naphthoquinone

1.9.4 6-Hydroxy-1,4-naphthoquinone

6-hydroxy-1,4-naphthoquinone (**6**) is another 1,4-naphthoquinone derivative. 1,4-naphthoquinones are targets for potent therapeutics because of their numerous biological application (Widhalm and Rhodes, 2016).

1.9.4.1 Synthesis of 6-Hydroxy-1,4-naphthoquinone

Coyle (2010) reported to have synthesized 6 - hydroxy-1,4-naphthoquinone by sonicating a mixture of 1,6-dihydroxynaphthalene (0.16 g, 1 mmol) and rose bengal (0.05 g,) in t-amyl alcohol (100 mL). This reaction mixture was then irradiated for 24 hours using a 500 W halogen lamp with air bubbling. Scheme 1.8 shows the general equation of reaction for the synthesis of 6-hydroxy-1,4-naphthoquinone (**6**). Coyle (2010) observed a conversion of 80% after 24 hours. Lancel *et al.* (2023), reported zero conversion after attempting to autoxidize 1,6-dihydroxynaphthalene under 460 nm.

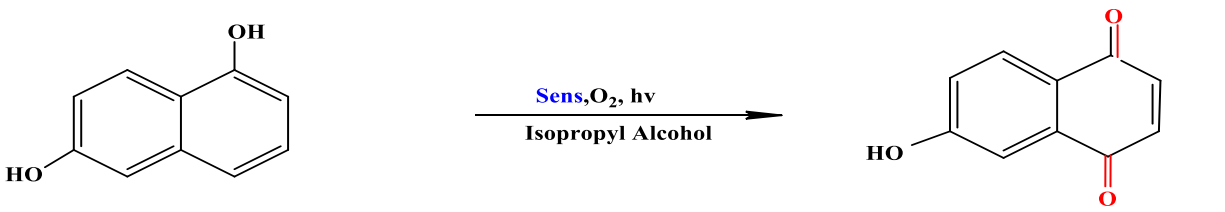

1,6-Dihydroxynaphthalene

6-Hydroxy-1,4-Naphthaquinone

Scheme 1.8: Synthesis of 6-hydroxy-1,4-Naphthoquinone

1.9.5 Pinocarvone and Myrtenal

Essential oils are volatile, oily aromatic liquids which are extracted from plants (Tongnuanchan and Benjakul, 2014). They are important because of their numerous applications, which include anti-viral agents, antimicrobial agents, antioxidants, antidiabetic agents, anti-inflammatory agents, dermal drug delivery and aromatherapy (Edris *et al*., 2007; Svoboda and Hampson, 1999). Pinocarvone (**7**) and myrtenal (**8**) are both essential oils that have been found in plants. Myrtenal (**8**) has been reported to have been found in the essential oils of numerous plants namely: juniper, orange, lemon, ginger, peppermint, parsley, and propolis (Dragmanova *et al.,* 2018). Myrtenal (**8**) is also found in *Schinu polygamus* (14.02%), *Cuminum cyminum* (43.5%) and so many others. Pinocarvone (**7**) has been reported to make up 20% of *Lallemantia royleana* (Benth) essential oil (Sharifi-Rad *et al.,* 2015) and 6.49% composition of *Hyssopus officinalis L.* essential oil (Kizil *et al.*, 2010).

1.9.5.1 Synthesis of Pinocarvone and Myrtenal

Pinocarvone (**7**) and Myrtenal (**8**) aside from being useful essential oils are α,β- unsaturated compounds which are potentially handy in organic synthesis. Mihelich and Eickhoff (1983) reported to have successfully converted α-pinene and β-pinene to pinocarvone (**7**) and myrtenal

(**8**), respectively through a one-pot synthesis. The photooxygenation reactions are shown in Schemes 1.9 and 1.10.

97% yield of pinocarvone (**7**) and 58% yield of myrtenal (**8**) were reported after 1.5 hours and 2 hours, respectively. Park *et al*. (2015) also carried out the photooxygenation of monoterpenes and after 24 hours of irradiation of α-pinene and β-pinene, using methylene photosensitizer in a traditional batch reactor, 20.5% and 2.0% yields of pinocarvone (**7**) and myrtenal (**8**) were respectively reported.

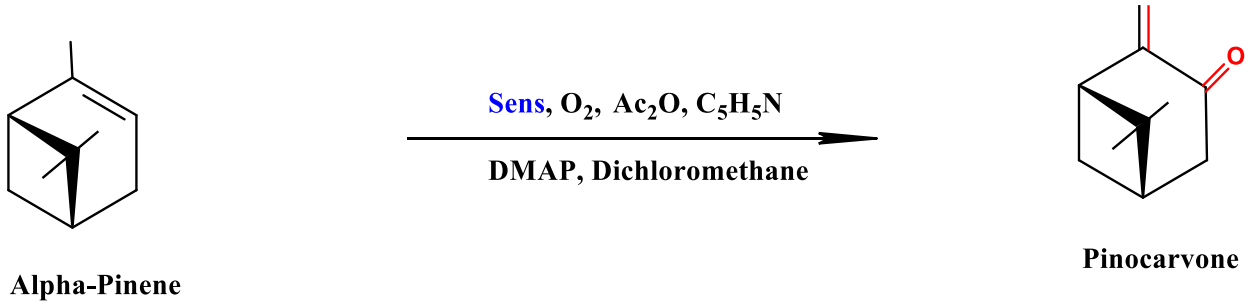

Alpha-Pinene **Pinocarvone**

Scheme 1.9: Synthesis of Pinocarvone

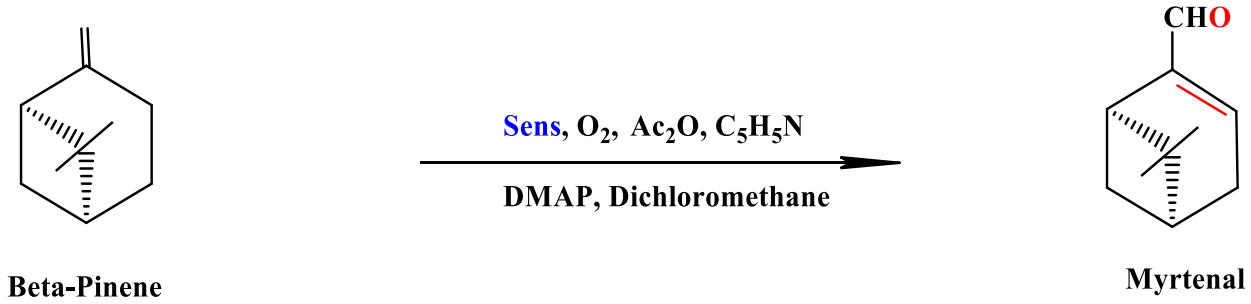

Beta-Pinene **Myrtenal**

Scheme 1.10: Synthesis of Myrtenal

In this study, the syntheses of ascaridole (**3**), 5-hydroxy-1,4-naphthaquinone (**4**), 1,4-naphthoquinone (**5**), 6-hydroxy-1,4-naphthoquinone (**6**), pinocarvone (**7**) and myrtenal (**8**) were used to investigate the photosensitization potentials of the plant extracts.

1.10 Quantum Yield

The efficiency of a photochemical reaction is measured by its quantum yield. It is the ratio of the number of moles of reactant consumed (or product formed) to the number of photons absorbed, measured in photons (Scheme 1.11) (Coyle, 2010; Esser *et al.,* 1994).

$$\Phi\lambda = \frac{Amount\ of\ Reactant\ Consumed\ or\ Product\ Formed}{Amount\ of\ Photons\ Absorbed}$$

Scheme 1.11: Quantum Yield Determination

When quantum yield equals one (Φ_λ 1), it means each photon absorbed by the substrate leads to the formation of a product molecule (Oelgemöller, 2017). In practice, if the quantum yield is greater than 0.3, it is considered an efficient reaction. It is possible to obtain quantum yields greater than one for free radical chain reactions. The Beer-Lambert Law (Scheme 1.12), which expresses how much photons are absorbed by a reaction mixture in direct proportion to its concentration, describes this relationship.

$$A = Log \frac{P_{\lambda o}}{P_\lambda} = \varepsilon c \ell$$

Scheme 1.12: Beer Lamberts Law

Where A is absorbance, P_λ is the observed spectral radiant power, $P_{\lambda o}$ is the spectral radiant power of the incident light, ε is the molar absorption coefficient, c is the concentration and is the path length through the reaction mixture (Coyle, 2010).

Photosensitization, qualities of good photosensitizers, their classification, examples and several applications have been reviewed. Also, the processes for the syntheses of some fine chemicals were reviewed. The search for more efficient, cheap and environmentally friendly photosensitizers is ongoing. Plant extracts, especially the intensely coloured ones, still present the potential to satisfy this demand. The use of natural pigments as photosensitizers reflects current trends in Green Chemistry. Furthermore, there is a dearth of literature on the use of plant extracts as photosensitizers for photochemical syntheses. This research intends to investigate the potential of *Hibiscus sabdariffa*, *Carpolobia lutea* and *Justicia secunda* as photosensitizers in the synthesis of fine chemicals.

1.11 Chemical Composition of Plant Extracts

Plant extracts are characterized to identify and measure the active compounds present in them and correlate these with their activities. For this study, the three plant materials of interest are *Hibiscus sabdariffa, Carpolobia lutea* and *Justicia secunda* Vahl. Tables 1.1 – 1.3 show extraction solvents, extraction methods, extraction time/temperature, extraction yields, chemical compositions, and some uses of these selected plant materials in published literature.

1.11.1 *Hibiscus sabdariffa* (Zobo)

Among the Malvaceae family of plants is the *Hibiscus sabdariffa*. It is a 2-2.5 m tall woody-based shrub. Worldwide, people drink the flowers cup-shaped, purple-red calyces extract, hot (sour tea) or cold (Badreldin *et al.,* 2018). *Hibiscus sabdariffa* calyces is also known as roselle in English speaking countries, 'Zobo' in Nigeria, 'Karkade' in Egypt, Saudi Arabia and Sudan. (Guardiola and Mach, 2014; Riaz and Chopra, 2015).

Generally, good photosensitizer dyes need to possess the basic property of absorbing light in the visible region of the electromagnetic spectrum. *Hibiscus sabdariffa* calyces were selected as a source of photosensitizer for this study because of the deep reddish-purple colour of its extract.

Table 1.1: Summary of Selected Literature Report on *Hibiscus sabdariffa* Calyces' Extract

Author	Extraction Solvent	Extraction Method	Extraction Time/ Temperature	Extraction Yield	Chemical Compositions	Uses of *Hibiscus sabdariffa* Extract
Alarcón-Alonso *et al.* (2011)	Water	-	2hr/55^{0}C	28.3%	Delphinidin-3-O-sambubioside, Cynanidin-3-O-sambubioside, Quercetin, Rutin, Chlorogenic acid	Antihypertensive, Diaphoretic, Diuretic, Cholagogues, Relaxing vascular smooth muscle by calcium antagonism effects, Activation of the endothelial path of nitric oxide
Sekar *et al.* (2015)	Methanol	Maceration	7 days/ 40-50^{o}C	7.46%	Flavonoids, Tannins, Triterpenoids, Fixed oils.	Reduce viscosity of blood, Prevent inflammation of urinary tract and kidney, Filter toxins in the body, Prevent vitamin C deficiency
Akindahunsi and Olaleye, (2003)	Methanol/ Water 4:1	Maceration	96 hr	25.1%	-	Antiseptic, Aphrodisiac, Astringent, Resolvent, Cholagogue, Digestive, Diuretic, Stomachic, Treatment of abscesses, Heart ailment, Hypertension
Banwo *et al.* (2022)	Methanol	Batch with stirring	72 hr	32.21%	Flavonoids, Anthocyanins, Vitamin C, Riboflavin, Carotene, Hiacin, Calcium, Iron, Phenolic-chlorogenic, Caffeic, Cinnamic acid, Gallic acid, Rutin,	Anti-dibetic, Anti-cholesterol, Anti-septic, diuretic, Antioxidant, Anti-mutagenic, Aypercholestermic, Antihypertensive, Antidiabetic, Antimicrobial, Anti-inflammatory

Table 1.1: Summary of Selected Literature Report on *Hibiscus sabdariffa* Calyces' Extract (*Continued*)

Author	Extraction Solvent	Extraction Method	Extraction Time/ Temperature	Extraction Yield	Chemical Compositions	Uses of *Hibiscus sabdariffa* Extract
					Benzoic acid and Catechin	
Alanon *et al.* (2020)	Natural deep eutectic solvents (NADES) based on choline chloride and 25% water	Microwave-assisted extraction	20min/ 65ºC	-	**Antocyanins**-delphinidin-3-sambubioside, cyanidin-3-sambubioside **Phenolic Acids** - Chlorogenic acid quinone, Neochlorgenic acid, chlorogenic acid, cryptochlorogenic acid, coumaroylquinic acid, 5-O-caffeoyl shikimic acid, **Flavonoids**-myricetin-3-arabinogalactoside, quercetin-3-sambubioside, quercetin-3-rutinoside, kaempferol-3-o-sambubioside, quercetin-3-glucoside, methylepigallocatechin, myricetin, quercetin, kaempferol **Other polar compounds** - hydroxy citric acid, hibiscus acid, methyl gallate, N-feruloyl tyramine	Teas, beverages, food and cosmetic products.

1.11.2 *Carpolobia lutea* (Cattle Stick) leaves

Carpolobia lutea G. Don belongs to the Polygalaceae family of plants. It is also known as *Carpolobia lutea* (English). In Nigeria, the plant is known as 'Agba' or 'Angalagala' by the Igbos in eastern Nigeria, 'Oshunshun' by the Yorubas in western Nigeria and 'Ikpafum' by the Ibibios in Southern Nigeria (Yakubu *et al., 2014*). It is a dense evergreen shrub about 5 m high. It is a perennial plant that is indigenous to tropical West and Central Africa (Nwidu *et al.,* 2017). *Carpolobia lutea* leaves extract was chosen for this study because by verbal communication, natives of where the plant was obtained reported that it was used for body painting. Numerous biological activities have also been reported as regards the leaves extract of this plant some of which have been listed in Table 1.2.

Table 1.2 Summary of Selected Literature Report on *Carpolobia lutea* Leaves Extract

Author	Extraction Solvent(s)	Extraction Method	Extraction Time	Extraction Yield	Chemical Composition Reported	Uses
Nwidu *et al.* (2017)	*n*-hexane chloroform EtOAc EtOH	Sequential Extraction by Maceration	72 hr	*n*-hexane fr. 3.7% chloroform 3.0% EtOAc Fr. 3.6% EtOH Fr. 7.8%	Flavonoid, Phenolics, Flavones, Isoflavones	Anti-diarrhoea, Antinociceptive, Gestro-protective,
Nwafor and Bassey (2007)	*n*-hexane chloroform EtOAc EtOH	Sequential Extraction by Maceration	72 hr Room Temp.	*n*-hexane Fr.- 0.93% chloroform Fr. – 1.3% EtOAc Fr. – 11.11% EtOH Fr.– 12.66%	Cinnamoyl 1-deoxy glucosides, Cinnamic acid, Coumaroyl 1-deoxy glucosides	Ulcer treatment, Anti-diarrhoea, aphrodisiac
Akpan *et al*. (2012)	EtOH Chloroform EtOAc MeOH	Sequential Extraction	72 hr	Crude EtOH Extract – 4.74% Chloroform Fr.- 0.50% EtOAc Fr. – 0.30% Me OH Fr.– 1.78%	Tannins Saponins, Cardiac glycosides, Anthraquinones, Flavonoids, steroids, Triterpenes, Cinnamoyl-1-deoxy glucosides, Cinnamic acid, Coumaroyl-1-deoxyglucosides	Malaria, Aphrodisiac, Ulcer, Diarrhoea, Antimicrobial, Analgesic, Contraceptive, Facilitate childbirth, Treat sterility, Vermifuge

Table 1.2 Summary of Selected Literature Report on *Carpolobia lutea* Leaves Extract (*Continued*)

Author	Extraction Solvent(s)	Extraction Method	Extraction Time	Extraction Yield	Chemical Composition Reported	Uses
Ettebong *et al.* (2011)	*n*-hexane chloroform EtOAC MeOH	Sequential Extraction by Maceration	72 hr/ Room Temp.	*n*-hexane – 1.6% chloroform – 1.0% EtOAC - 0.6% MeOH – 2.5%	Saponins, Anthraquinones, Flavonoids, Cardiac glycosides, Terpenes, Simple sugar	Contraceptive, Facilitate Delivery, Aphrodisiac, Helminthiasis, Headache, Anti-arthritic, Anti-inflammatory, Antimicrobial activities, Anti-diarrhoeal, Anti-ulcerogenic

1.11.3 *Justicia secunda* Vahl (Bloodroot) Leaves

Justicia secunda Vahl also known as bloodroot is a member of the Acanthaceae family. Although it grows in tropical and sub-tropical African nations, *Justicia secunda* Vahl is a native of South America (Theiler *et al*., 2014). It is an upright grass with simple leaves and terminal panicles that carry the flowers (Anyasor *et al.,* 2019). It thrives in moist soils and alongside rivers and creeks. In the eastern part of Nigeria, it is called 'Obara Bundu' and 'Sanguinaria' in Venezuela (Anyasor *et al.,* 2019). In Nigeria, it is consumed mainly for its hematinic properties (Onoja *et al.,* 2017). *Justicia Secunda* Vahl extract was selected for this study because of the characteristic red colour of its aqueous extract. Reports show that its leaves extract has been put to different uses most of which are listed in Table 1.3.

Table 1.3 Summary of Selected Literature Report on *Justicia secunda* Vahl Leaves Extract

Author	Solvent	Method	Time/ Temperature	Yield	Chemical Composition Reported	Reported Activity
Onoja *et al.* (2017)	80% MeOH	Maceration	48 Hours/Room Temperature	10.7%	Tannins, Flavonoids, Alkaloids, Quinines, Anthocyanins, Luteolin, Aurantiamide acetate, Auranamide, Quidoline, Pyrrolidone, derivatives (secundarellone A, B, C)	Anti-oxidant, Anti-inflammatory, Anti-nociceptive effects, Anti-Sickling, Haematinic, Anti-Microbial, Anti-Hypertensive, wound healing, abdominal pain treatment
Anyasor *et al.* (2019)	70% MeOH in Water	Maceration	48 Hours	10.2%	Alkaloids, Polyphenols, Flavonoids, Tannins, Leucoanthocyanins, Quinones, Anthocyanins, Luteolin, Auranamide, Aurantiamide acetate, Quindoline, Pyrrolidone derivatives (Secundarellone A, B, C)	Anti-sickling, Anti-microbial, Anti-hypertensive, Hematic, Anti-inflammatory
Theiler *et al.* (2014)	MeOH then Fractionated with $CHCl_2$ and light petroleum	Reflux by Soxhlet	2 Hours /80°C	-	Alkaloids, Polyphenols-Flavonoids, Quinones, Tannins, Anthocyanins, Secundarellone	Treatment of anaemia, Hypertension, Sickle cell, Antibacterial
Oko *et al.* (2022)	EtOH	Soxhlet	-	-	Tannins, Flavonoids, Alkaloids, Phenols, Minerals, Vitamins	Anti-viral, Anti-tumoral, Anti-microbial, Anti-sickling, Anti-inflammatory, Anti-platelet, Aggregation

CHAPTER 2
AIM AND OBJECTIVES

2.1 Aim

This study was generally aimed at investigating the photosensitizer potentials of some plant extracts in selected photooxygenation reactions.

2.2 Objectives

The specific objectives of this research were to

1. collect and prepare *Hibiscus sabdariffa* calyces, *Carpolobia lutea* leaves and *Justicia secunda* leaves and subsequently extract using suitable solvents;
2. test extracts obtained alongside some commercially available photosensitizers for their photoactivity using the following model photooxygenation reactions:
    i. α-terpinene photooxygenation
    ii. 1,5-dihydroxynaphthalene photooxygenation;
3. further test the photoactivity of the photoactive extract using the following photooxygenation reactions:
    i. 1-naphthol photooxygenation
    ii. 1,6-dihydroxynaphthalene photooxygenation
    iii. α-pinene photooxygenation
    iv. β-pinene photooxygenation;
4. measure the absorbance of the commercial dyes and plant dyes in the visible region of the electromagnetic spectrum and match these with the emission spectrum of the light source used for the irradiation;

5. investigate the photostability of the active plant extracts alongside other commercially available photosensitizers in the different solvents used for the photooxygenation reactions;
6. fractionate the photoactive plant extract and test the photoactivity of the fractions via α-terpinene photooxygenation; and
7. analyse of the photoactive VLC fractions by HPLC-MS for identification of compounds present.

CHAPTER 3

MATERIALS AND METHODS

This chapter gives details of the materials, equipment and methods used during the research.

3.1 Materials

The 3 plant materials used for this study were obtained from Nigeria.

All solvents and reagents were obtained from commercial suppliers mainly Sigma Aldrich and Ajax Finechem. They were used without purification.

The reagents used for this study are listed in Table 3.1.

Table 3.1: Reagents

Chemical	CAS Number	Purity (%)	Supplier/Origin
α-terpinene	99-86-5	≥89	Sigma-Aldrich
α-Pinene	80-56-8	98	Sigma Aldrich
(-)-β-Pinene	18172-67-3	99	Sigma Aldrich
(IR)- (-)-Myrtenal	18486-69-6	-	Sigma-Aldrich
1,4-Diazabicyclo (2.2.2) octane	280-57-9	≥99	Sigma-Aldrich
1-Naphthol	99-86-5	≥99	Sigma-Aldrich
1,4-Naphthoquinone	130-15-4	-	Ajax Chemicals
1,5-Dihydroxynaphthalene	83-56-7	97	Sigma Aldrich
1,6-Dihydroxynaphthalene	575-44-0	99	Sigma Aldrich
Acetic anhydride	108-24-7	≥98	Sigma-Aldrich
Acetone-D6	666-52-4	99.9	Cambridge Isotope Laboratories Inc.
Acetonitrile	75-05-8	-	Ajax Fine chem
Chloroform	67-66-3	99.96	Fischer Scientific
Cyclohexane	110-82-7	-	Ajax Finechem
Copper(II)sulphate pentahydrate	7758-99-8	99	Biolab
Chloroform-D	865-49-6	99.8	Cambridge Isotope Laboratories Inc.
Dichloromethane	75-09-2	-	Ajax Finechem
Ethylacetate	141-78-6	-	Ajax Finechem
Hydrochloric acid	7647-01-0	32	Ajax Finechem
Isopropanol	67-63-0	99.5	Chem Supply

Table 3.1: Reagents (*Continued*)

Chemical	CAS Number	Purity (%)	Supplier/Origin
Juglone	481-39-0	97	Fluka Chemika
Magnesium sulphate	7487-88-9	-	Ajax Finechem
Methylene blue	61-73-4	96.0	Ajax Chemicals
Meso-Tetrephenylporphyrin	07-2160		Strem Chemicals
n-hexane	110-54-3	95	Ajax Finechem
Potassium carbonate anhydrous	584-08-7	-	Ajax Finechem
Pyridine	110-86-1	99.5	BDH Laboratories
Rose bengal	632-69-9	-	Alfa Aesar
Sand, acid washed	7631-86-9	-	Ajax finechem
Silica gel 60,0.06-0.2mm (70-230 mesh ASTM)	7631-86-9	-	Scharlab S.L.
Silica Gel 60H (for thin layer chromatography) grain size 5-40µm	7631-86-9	-	Merck
Sodium hydrogen carbonate	144-55-8	99.7	Ajax Finechem
TLC Silica gel 60 F_{254}	7631-86-9	-	Merck

3.2 Equipment

The equipment used for this study is listed in Table 3.2.

Table 3.2: Instrument and Equipment

Equipment	Model	Manufacturer
Analytical weighing balance	NewClassic ML	Mettler Toledo
Bulb-to-bulb distillation apparatus	Glass Oven B-585	Buchi
Cool white fluorescent Tube (8watts x 16)	F8W/T5/33-640 8W Hg	Sylvania
Heating oven	ED 23	Binder
HPLC	1260 infinity	Agilent Technologies
GC-FID	7890A	Agilent Technologies
GC-FID autosampler	7683B series	Agilent Technologies
Microwave oven	MS2021FB/00	LG
Nuclear magnetic resonance Spectrophotometer - 400MHz (Bruker)	Ascend 400	Bruker
Rotary Evaporator	R-210 Rotavapor	Buchi
Rayonet chamber reactor	RPR-200	The Southern New England Ultraviolet Co.
Single quad mass spectrometer	6120	Agilent Technologies
Ultrasonic cleaner	UC S2000H	-
UV/Vis Spectrophotometer	Cary 60 UV-Vis	Agilent Technologies
Traditional grain grinder with high hopper	-	Corona

3.3 Methods

3.3.1 NMR Method

NMR spectrum was recorded using a Bruker 400 AscendTM (^{1}H:400MHz) with MestRenova Software. Data were acquired using Topsin 3.6.2. Samples were prepared in acetone-d_6 (δ 2.05 ppm) and $CDCl_3$ (δ 7.26 ppm). Solvent residual peaks and impurities peaks were compared with literature values in Fulmer *et al.* (2010).

3.3.2 Chromatographic Methods

Column chromatography was carried out in pyrex glass columns using Merck silica gel 60 H (for thin layer chromatography) grain size 5 - 40 µm and Scharlab silica gel, 60, 0.06 - 0.2 mm (70 – 230 mesh ASTM). Cyclohexane, chloroform, ethyl acetate, *n*-hexane and their mixtures were used as mobile phase.

3.3.3 TLC

Thin layer chromatography was performed in glass jars using Merck TLC Silica Gel 60 F_{254} plates. Cyclohexane, chloroform, ethyl acetate, *n*-hexane, and their mixture were used as mobile phases.

3.3.4 GC

GC samples were analyzed using the Agilent 7890A gas chromatograph, the Agilent software and 7683B auto-injector. The columns used during the study include Agilent J &W GC column with 0.25 mm×0.25 µm film thickness (method : run time - 26 minutes, oven temperature - 60°C, injection temperature -100°C, detector temperature - 250°C, pressure - 17.978 psi, flow rate – 24.46 mL/min, septum purge flow - 3.0 mL/min, fuel flow – 30.00 mL/min, make up flow – 25.00 mL/min, signal value 7.4 pA) and Zebron capillary GC column ZB-5 with 0.25 mm×0.25 µm film thickness (method : run time – 22.0 minutes, oven temperature -70.0°C, injection temperature – 280.0°C, detector temperature – 290.0°C, pressure – 9.54 psi, flow rate – 23.67 mL/min, septum

purge flow - 3.0 mL/min, fuel flow – 30.00 mL/min, make up flow – 25.00 mL/min, signal value 8.0 pA).

3.3.5 UV/Vis

Ultraviolet/visible spectroscopy was carried out using a Cary 60 UV/Vis spectrophotometer, Agilent Technologies. Absorbances were measured within a wavelength range of 200 nm - 800 nm.

3.3.6 HPLC-MS

The analysis by liquid chromatography-mass spectrometry (LC-MS) used an Agilent (Santa Clara, CA, USA) 1260 infinity high-performance liquid chromatography (HPLC) system coupled with a 6120 single quad mass spectrometer using Atmospheric Pressure Chemical Ionization (APCI) methods, operated in a positive ion mode, across a mass range of 100 to 1500 amu.

The HPLC system consisted of a diode array detector (DAD), a binary pump, an autosampler, a vacuum degasser, and a column oven. The UV-Vis spectra of peaks were captured by DAD across the range of 190 to 600 nm. The column used was Phenomenex C18 HPLC (5um, 100mm x 4.6 mm). Analysis of data was performed using Agilent Chemstation software with principal peaks identified according to MS and/or UV-Vis spectra and comparison with literature.

3.3.7 Photoreactor

A Rayonet reactor equipped with 16 × 8 W cool white fluorescent tubes was used. All reactions were batch experiments performed in a Pyrex Schlenk flask with oxygen bubbling in. The set-up is shown in Plate 3.1.

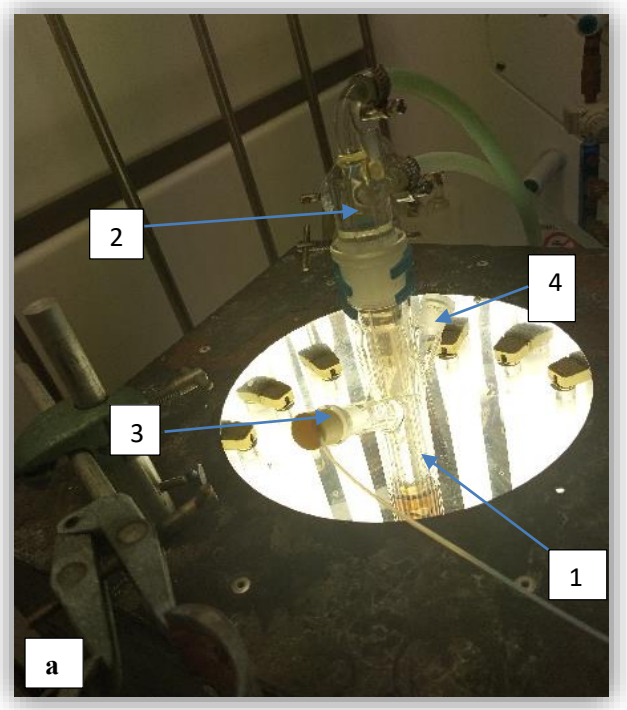

Plate 3.1: Rayonet Photoreactor (RPR 200, Southern New England Ultraviolet Company, USA) with 8 Watts × 16 Cool White Fluorescent Tubes (1: Pyrex Schlenk Flask, 2: Cold Finger, 3: Oxygen in-let, 4: Air-Outlet) (a) Top View (b) Front-side View

3.4 Sample Identification, Preparation and Extraction

3.4.1 *Hibiscus sabdariffa* Calyces (Zobo)

The calyces of the *Hibiscus sabdariffa* (Plates 3.2 a and b) were bought from Mile 3 market in Obio-akpor Local Government Area of Rivers State, Nigeria.

3.4.1.1 Sample Identification and Preparation

The plant was identified with herbarium number UPH/P/245 at the University of Port Harcourt Herbarium (Nigeria). It was cleaned, air dried to constant weight, ground using a hand mill, and extracted as described in section 3.4.1.2.

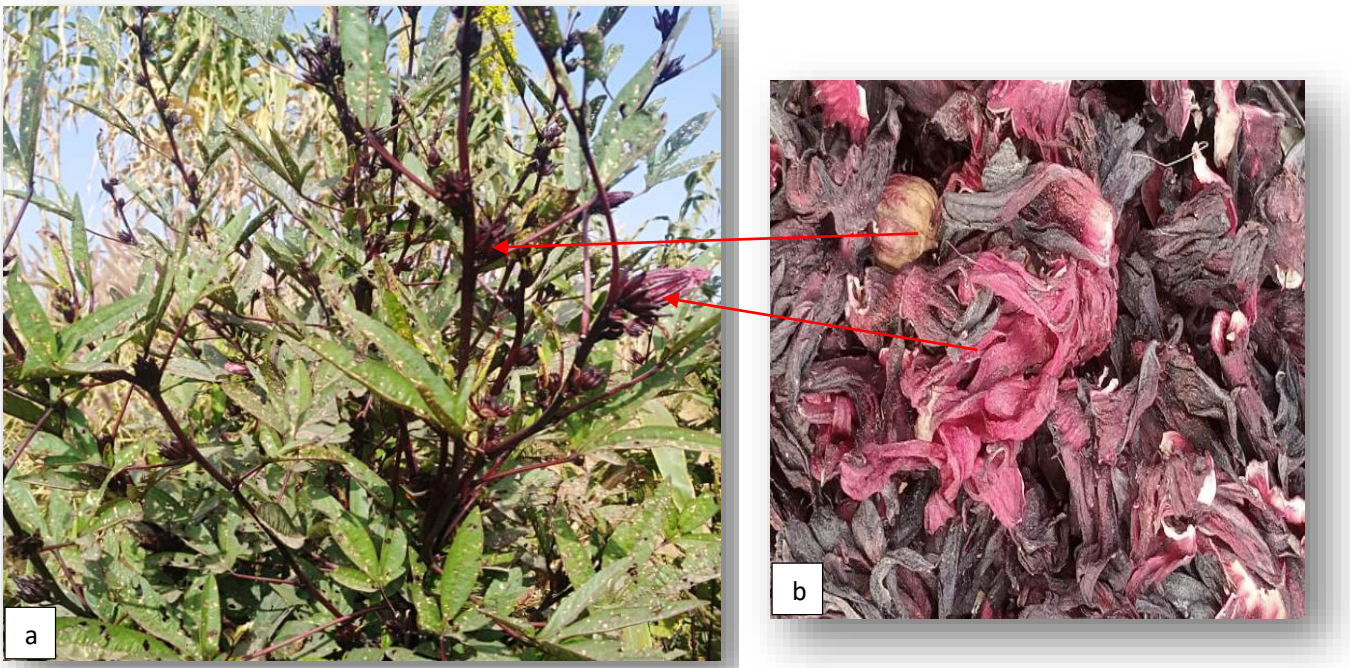

Plate 3.2: *Hibiscus sabdariffa* a) Plant b) Calyces

3.4.1.2 Extraction

A preliminary test by TLC was carried out to determine the solvents to be used for the extraction process. 10 g each of the ground *Hibiscus sabdariffa* calyces was extracted using *n*-hexane, ethyl acetate and ethanol, respectively. The three extracts were each spotted on 7 TLC plates and ran using the following solvent systems as mobile phase: 100% *n*-hexane, 100% dichloromethane, 100% ethyl acetate, 50% *n*-hexane/dichloromethane, 50% *n*-hexane/ethyl acetate, 5% ethanol/dichloromethane, 5% ethanol/ethyl acetate. The solvent which gave the most spots and colours was chosen for the main extraction process after defatting with a less polar solvent.

Sequential extraction was then carried out on the *Hibiscus sabdariffa* plant material using the maceration method. 492 g of the ground plant material was weighed into a glass vessel and defatted twice using ethyl acetate for 24 hours each. Further extraction was carried out twice on the same plant material using methanol for 48 hours each. The methanol extraction solvent was then filtered off through a cotton plug in a funnel and the solvent was removed using a rotary evaporator at 45 ^{o}C to obtain the extract. The extract was stored in a glass container for use.

3.4.2 *Carpolobia lutea* Leaves (Cattle Stick)

The *Carpolobia lutea* leaves (Plate 3.3) were collected from Amaranze in Isiala Mbano Local Government Area in Imo State, Nigeria.

3.4.2.1 Sample Identification and Preparation

The plant was identified with voucher number UNN/04/0355D at the University of Nigeria Nsukka Herbarium. The leaves were cleaned, air dried to constant weight, ground using a hand mill, and extracted as described in section 3.4.2.2.

Plate 3.3: *Carpolobia lutea* Plant

3.4.2.2 Extraction

A preliminary test by TLC was carried out to determine the best solvents for the extraction process. 10 grams each of the ground *Carpolobia lutea* was extracted using *n*-hexane, ethyl acetate and ethanol, respectively. The three extracts were each spotted on 7 TLC plates and ran using the following solvent systems as mobile phase: 100% *n*-hexane, 100% dichloromethane, 100% ethyl acetate, 50% *n*-hexane/dichloromethane, 50% *n*-hexane/ethyl acetate, 5% ethanol/dichloromethane, 5% ethanol/ethyl acetate. The solvent which gave the most spots and colours was chosen for the main extraction process after defatting with a less polar solvent.

Sequential extraction was then carried out on the ground leaves of *Carpolobia lutea (polygalaceae*) using the maceration method. 432 g quantity of the dried leaves in a glass vessel was deffated twice using *n*-hexane for 24 hours each, followed by further extraction (twice) with ethyl acetate for 48 hours each. The ethyl acetate extract was then filtered off through a cotton plug in a funnel and the solvent was removed using a rotary evaporator at 45 ^{o}C. The concentrated extract was stored in a glass container for further use.

3.4.3 *Justicia secunda* Vahl Leaves (Blood root)

The *Justicia secunda* leaves (Plate 3.4 a and b) were collected from Orhuwhorun, Udu Local Government Area in Delta State, Nigeria.

3.4.3.1 Sample Identification and Preparation

The plant was identified with herbarium number UPH/P/244 at the University of Port Harcourt Herbarium (Nigeria). Its leaves were cleaned, air dried to constant weight, ground using a hand mill, and extracted as described in section 3.4.3.2.

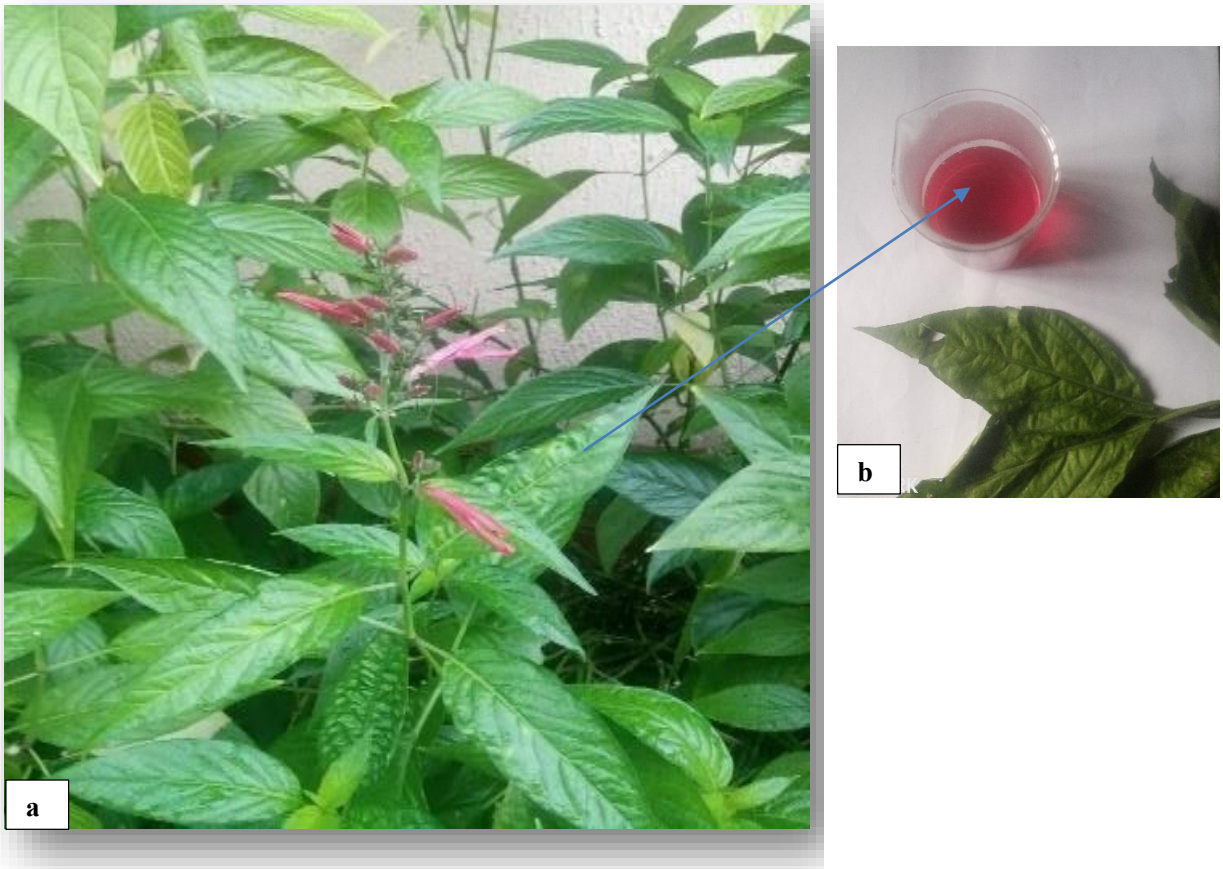

Plate 3.4: *Justicia secunda* a) Plant b) Aqueous Extract

3.4.3.2 Extraction

Heat and water were two conditions necessary for obtaining a red extract from ground *Justicia secunda* leaves. A preliminary extraction test was carried out on *Justicia secunda* leaves to find out the optimal water/methanol ratio, required to obtain the finest red-coloured extract by microwave-assisted extraction method. 10%, 15%, 20%, 25%, 30% and 35% water/methanol solvent mixtures were used for this test.

Microwave-assisted sequential extraction was then carried out on the *Justicia secunda* leaves. 450 g sample of the ground leaves in a glass vessel was defatted twice using *n*-hexane in a microwave oven at med-low setting for 5 minutes and further extracted twice with 35% water/methanol mixture at the same microwave oven setting and duration. The extract was filtered off through a cotton plug in a funnel and concentrated using a rotary evaporator at 45 ^{o}C. The concentrated extract was stored in a glass container.

3.5 General Photooxygenation Reaction Method

The substrate and photosensitizer were dissolved in a suitable solvent with sonication for 5 minutes. The reaction mixture was then poured into a Schlenk flask fitted with a cold finger for cooling, irradiated for a given time in a Rayonet photoreactor (RPR 200, fitted with 16 x 8 W cool white fluorescent tubes) while oxygen bubbling through (Razoni *et al*, 2013). Periodically, samples were taken out with a syringe for monitoring using a GC-FID (Agilent J &W GC column) and/or NMR (Ascend 400) to determine the percentage composition of the reaction mixture or products formed.

All photooxygenation reactions were performed in triplicates to ensure reproducibility.

3.6 Photooxygenation of α-Terpinene using Methylene Blue, Rose Bengal and the Plant Extracts as Photosensitizers

Following the general procedure described in section 3.5, a solution of α-Terpinene ≤ 69% (0.267 g, 2 mmol) and rose bengal (0.033 g, 0.033 mmol) in acetonitrile (50 mL) was photooxygenated for 90 minutes taking 2 mL aliquots for analysis every 30 minutes. In subsequent photooxygenation reactions, rose bengal was replaced severally with methylene blue (0.033 g, 1 mmol, extracts of *Hibiscus sabdariffa* calyces (0.01 g), *Carpolobia lutea* leaves (0.01 g) and *Justicia secunda* leaves (0.01 g). Each photooxygenation reaction was done in triplicates for reproducibility. For the replicates, 0.05 g of each of the plant calyces/leaves extracts and α-terpinene ≤91% (0.267 g, 2 mmol) were used.

After the photooxygenation, the reaction solvent (acetonitrile), any unreacted α-terpinene and p-cymene (a side product) were removed using a rotary evaporator (200 mbar, ≤ 30 ^{o}C) to avoid the decomposition of the ascaridole). The ascaridole (**3**) was isolated from the oily residue by column chromatography on silica gel (particle size 60, 0.06 - 0.2 mm) using a gradient of 0 →2→5vol% ethyl acetate in cyclohexane. The isolated ascaridole (**3**) was analyzed by ^{1}H NMR spectroscopy and the yield was calculated.

0.267 g of α-terpinene was also photooxygenated following the procedure described above but without any sensitizer dye (autoxidation).

3.6.1 Photooxygenation of α-Terpinene with Anthraquinone Carboxylic Acid (ANT-COOH)

α-Terpinene (0.267 g, 2 mmol) was photooxygenated as described in section 3.6 in the presence of ANT-COOH (0.008 g, 0.03 mmol) as type I sensitizer. 2 mL samples were taken every 30 minutes with a syringe for monitoring using a GC-FID (Agilent J &W GC column) to determine

the percentage composition of the product. The experiments were also carried out in triplicates for reproducibility.

3.6.2 Photooxygenation α-Terpinene using *Carpolobia lutea* Extract in the presence of DABCO (1,4-diazabicyclo [2.2.2] octane)

A solution of α-Terpinene (0.267 g, 2 mmol), DABCO (0.033 g, 0.3 mmol) and *Carpolobia lutea* extract (0.01 g) in 50 mL of acetonitrile: chloroform (9:1) solvent was photoxidized in triplicates as described in section 3,6.

3.7 Photooxygenation of 1,5-Dihydroxynaphthalene using Methylene Blue, Rose Bengal and the Plant Extracts as Photosensitizers

For the synthesis of the 1,4-naphthoquinones, a similar method to that of Coyle (2010) was used. 1,5-dihydroxynaphthalene (0.16 g, 1 mmol) and rose bengal (0.033 g, 0.033 mmol) were dissolved in isopropanol (100 mL) with sonication. The reaction mixture was poured into a Schlenk flask fitted with a cold finger for cooling, irradiated for 5 hours in a Rayonet Photoreactor (RPR 200, Southern New England, fitted with 16 x 8 watts cool white fluorescent tubes) and oxygen bubbling in. 2 mL samples were taken every 1 hour with a syringe for monitoring by ^{1}H NMR spectroscopy to determine the percentage conversion of the product. Rose bengal was replaced with methylene blue (0.033 g, 1 mmol). The photooxygenation reactions with the commercial dyes were repeated twice. In subsequent runs, the commercial dyes were replaced with each of the 3 plant extracts(0.01 g each). These plant extract reactions were also run 2 more times using 0.05 g of each, irradiating for 8 hours.

After photooxygenation, the isopropanol solvent was removed from each of the reaction mixtures using a rotary evaporator (100 mbar, 40 ^{o}C) and 5-hydroxy-1,4-naphthaquinone was isolated from the concentrated reaction mix by column chromatography on silica gel (particle size 60,0.06 - 0.2 mm) eluting with chloroform.

0.16 g of 1,5-dihydroxynaphthalene was also photooxygenated following the procedure described but without any sensitizer dye.

3.8 Photooxygenation of 1-Naphthol using Rose Bengal and *Carpolobia lutea* Extract as Photosensitizers

A solution of 1- naphthol (0.14 g, 1 mmol) and rose bengal (0.033 g, 0.033 mmol) dissolved in isopropyl alcohol (100 mL) was prepared and photooxygenated for 12 hours following the procedure described in section 3.7. Aliquots of the reaction mixture were taken periodically in a syringe using ^{1}H NMR spectroscopy to determine the percentage conversion of the product. For the other experiments in this reaction, rose bengal was replaced with *Carpolobia lutea* extract (0.01 g). These experiments were done in triplicates for reproducibility. For the replicates, irradiation in the Rayonet Photoreactor was carried out for only 2 hours and 0.05 g of the plant extract was used. The isopropanol reaction solvent was removed using a rotary evaporator (100 mbar, 40 ^{o}C) and pure(by ^{1}H NMR) 1,4-naphthoquinone was isolated by column chromatography on silica gel (particle size 60, 0.06 - 0.2 mm) using chloroform.

0.14 g of 1-naphthol was also photooxygenated following the procedure described above but without any sensitizer dye (autoxidation).

3.9 Photooxygenation of 1,6-Dihydroxynaphthalene using Rose Bengal and *Carpolobia lutea* Extract as Photosensitizers

1,6-Dihydroxynaphthalene (0.16 g, 1 mmol) and rose bengal (0.033 g, 0.033 mmol) were dissolved in isopropyl alcohol (100 mL) with sonication and photooxygenation for 5 hours as described in section 3.7, taking 2 mL samples every 1 hour for monitoring by ^{1}H NMR spectroscopy to determine the percentage conversion to product. In subsequent photoxidations, rose bengal was replaced with *Carpolobia lutea* extract (0.01 g). The reactions were performed in triplicates for

reproducibility. For the replicate experiments, irradiation was carried out for 8 hours in the rose bengal (0.033 g) sensitized reactions and 12 hours for the *C. lutea* (0.05 g) sensitized reaction.

Solvent stripping by rotary evaporator (100 mbar, 40 ºC) and column chromatography on silica gel (particle size 60,0.06-0.2 mm) using a gradient of 0 →1→2% vol ethyl acetate in chloroform gave pure (by ^{1}H NMR) 6 –hydroxy-1,4-naphthoquinone.

0.16 g of 1,6-dihydroxynaphthalene was also photooxygenated as described above but without any sensitizer dye (autoxidation).

3.10 Photooxygenation of α-Pinene using Tertraphenylporphyrin and *Carpolobia lutea* Extract as Photosensitizers

For the photooxygenation of α-pinene to pinocarvone (**7**) and β-pinene to myrtenal (**8**), the one-pot conversion of olefins to α-β unsaturated carbonyl compound method by Mihelich and Eickhoff, (1983) was used.

α-pinene (6.68 g, 7.66 mL), acetic anhydride (10.209 g, 9.45 mL), pyridine (3.88 g, 3.97 mL), DMAP (0.24 g) and tetraphenylporphyrin (0.007 g) were mixed and made up to 100 mL with dichloromethane and sonicated. The reaction mixture was photoxygenated as described in section 3.5 for 24 hours, taking 2 mL aliquots of the reaction mixtures at regular intervals to monitor the percentage composition of the product by GC-FID (ZB-5 Zebro Capillary GC Column. In a subsequent photooxygenation, tetraphenylporphyrin was replaced with 0.05g of the *C. lutea* extract. The photooxygenation reactions were carried out in triplicates.

Photooxygenation was also carried out as described but in the absence of a photosensitizer (autoxidation).

After the irradiation, each reaction mixture was diluted with 90 mL dichloromethane. It was then extracted with saturated $NaHCO_3$ twice to remove the acetic byproduct. The organic layer was

washed twice with 50 mL 1Nomality HCl until it turned green. Further extraction was carried out with 50 mL saturated $CuSO_4$ followed by drying with 5 g of $MgSO_4$. Another extraction was carried out with 100 mL saturated NaCl, next was drying with 5 g of K_2CO_3 and distillation at 42 ^oC.

3.11 Photooxygenation of β-Pinene using Tetraphenylporphyrin and *Carpolobia lutea* Extract as Photosensitizers

β-pinene (6.68 g, 7.66 mL), acetic anhydride (10.209 g, 9.45 mL), pyridine (3.88 g, 3.97 mL), DMAP (0.24 g and tetraphenylporphyrin (0.007 g) were mixed and made up in DCM (100 mL) and photooxygenated as described in section 3.10. In subsequent photooxygenation reactions, tetraphenylporphyrin was replaced with 0.05 g of the *Carpolobia lutea* extract. The experiments were done in triplicates for reproducibility. Photooxygenation was also carried out as described but in the absence of a photosensitizer (autoxidation).

After 48 hours of photooxygenation, the reaction mixture was worked up as described in section 3.10. The product was dried with K_2CO_3 (5 g) and purified by distillation at 42 ^oC.

3.12 Absorbance Measurements of the Dyes and Plant Extracts

To measure the absorbance of each of the commercial dyes (methylene blue, rose bengal), 0.5 mg of each dye was dissolved in isopropyl alcohol, poured into a 100 mL volumetric flask made up to the mark. Its absorbance peak was measured on UV/Vis spectrophotometer at 400 nm – 800 nm wavelength.

For the absorbance measurement of tetraphenylporphyrin, 0.5 mg of the dye was dissolved in 10 mL of dichloromethane and made up to the mark. Its absorbance was measured in the wavelength range of 400 nm – 800 nm.

To measure the absorbance of the plant extracts, 0.05 g of the plant extracts were dissolved in different solvent systems before making up with isopropyl alcohol because of their different solubilities.

Hibiscus sabdariffa extract was dissolved in 10 mL water, poured into a 100 mL volumetric flask and made up to the 100 mL mark using isopropyl alcohol with shaking.

Carpolobia lutea extract was dissolved in a solvent mixture of 1 mL methanol in 9 mL dichloromethane, poured into a 100 mL volumetric flask and made up to the 100 mL mark using isopropyl alcohol with shaking.

Justicia secunda extract was dissolved in 10 mL water, poured into a 100 mL volumetric flask and made up to the 100 mL mark using isopropyl alcohol with shaking.

3.13 Photostability Testing of Rose Bengal and *Carpolobia lutea* in Isopropyl Alchohol

A 0.5 mg solution of rose bengal in 100 mL of isopropyl alcohol was prepared in a 100 mL volumetric flask. The solution was then transferred into a schlenk flask fitted with a cold finger for cooling and was irradiated in an RPR 200 photoreactor using 16 pieces of cool white 8 watts fluorescent tubes for 24 hours while bubbling oxygen through. 2 mL aliquots of the solution were taken every 2 hours for a UV/Vis spectrophotometer analysis. 5 mg of *C. lutea* extract was similarly made up and its photostability was similarly measured.

3.14 Photostability Testing of Methylene Blue and *Carpolobia lutea* Extract in Acetonitrile

0.5 mg of methylene blue was dissolved in 100 mL of acetonitrile in a 100 mL volumetric flask and irradiated for 24 hours, analyzing as described in section 3.13. The procedure was repeated with 5 mg *C. lutea* extract dissolved in acetonitrile.

3.15 Photostability Testing of Tetraphenylporphyrin and *Carpolobia lutea* Extract In Dichloromethane

0.5 mg of tetraphenylporphyrin dissolved in 100 mL of dichloromethane was irradiated for 24 hours and analysed as described in section 3.13. The procedure was repeated with 5 mg *C. lutea* extract dissolved in dichloromethane using a 100 mL volumetric flask. This solution was then transferred into a Schlenk flask fitted with a cold finger for cooling. This set-up was irradiated in an RPR 200 photoreactor using 16 pieces of 8 W cool white fluorescent tubes for 24 hours. 2 mL samples of the solution were taken every 2 hours for monitoring using a UV/Vapthoquinoneis spectrophotometer. 5 mg of *C. lutea* extract was similarly prepared and irradiated with this set-up for the photostability testing of *C. lutea* extract in isopropyl alcohol.

3.16 Fractionation of *Carpolobia lutea* Extract by Vacuum Liquid Chromatography

Dry ethyl acetate extract of *C. lutea* (1.5 g), obtained as described in section 3.4.2.2 and 3 g of silica gel 60, 0.06 - 0.2 mm, were thoroughly ground together in a mortar and transferred to a sintered glass funnel connected to a vacuum pump for volume liquid chromatography (VLC), that was packed with dry 45 g silica gel (grain size 5 - 40 μm) to a height of 4.5 cm with a layer of treated sand on top.

Gradient elution was carried out with 100% *n*-hexane, *n*-hexane/EtOAc, 100% EtOAc, EtOAc/MeOH and 100% MeOH (Scheme 3.1). The fractions were solvent stripped to dryness in a rotary evaporator and the fractions were tested for their photosensitizer activity in the photooxygenation of α-terpinene to ascaridole (**3**).

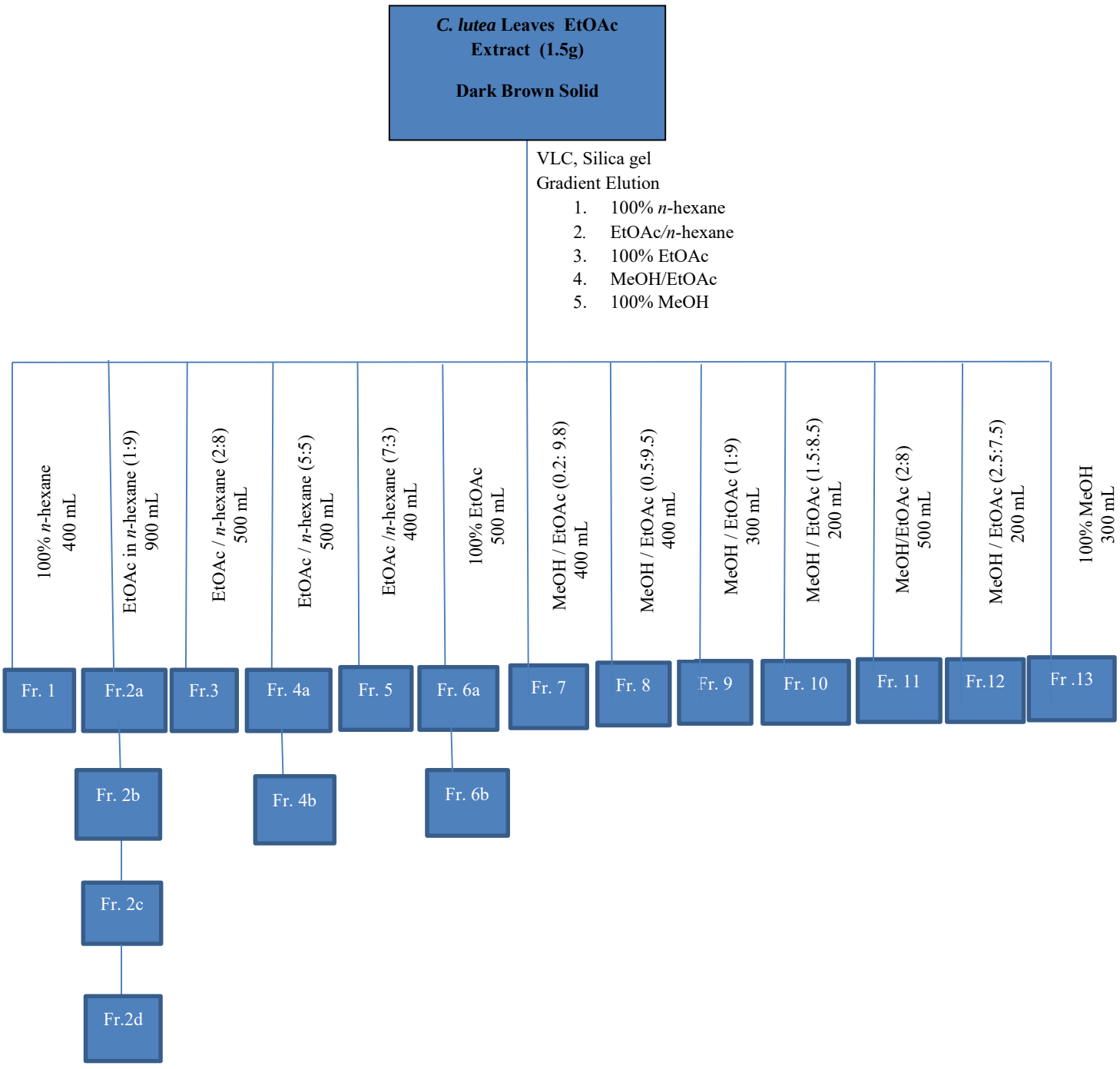

Scheme 3.1: Fractions from Gradient Eluted VLC of *C.lutea* EtOAc Extract

3.17 Photooxygenation of α-Terpinene using VLC Fractions of *C. lutea* Extract as Photosensitizer

A solution of α-terpinene (66%, 0.267 g, 1 mmol) and methylene blue (0.005 g, 0.015 mmol) in acetonitrile (50 mL) was prepared and photooxygenated for 90 minutes as described in section 3.6.

2 mL samples of the reaction mixture were taken every 30 minutes with a syringe for analysis by GC-FID (Agilent J &W GC column) to determine its percentage composition. The procedure was repeated severally replacing methylene blue with 0.01 g of each of the fractions obtained from the VLC of the *C. lutea* extract.

3.18 Analysis of the Photoactive VLC Fractions by HPLC-MS

Active fractions were selected for HPLC-MS analysis. Each fraction was reconstituted in 70% ethanol/water, centrifuged and 5 µL injected into the HPLC machine.

The separation was performed using a solvent gradient of 10% to 95% Water/ACN (HPLC grade) with 0.005% trifluoroacetic acid (TFA) over 18 min, at a flow rate of 0.75 mL/min Column temperature was at 40 ℃.

CHAPTER 4
RESULTS

The three plant materials were identified as *Hibiscus sabdariffa* (appendix 49), *Carpolobia lutea* (appendix 50) and *Justicia Secunda* (appendix 51).

4.1 TLC Result of Preliminary Tests for Suitable Extraction Solvents

Plate 4.1 shows the separations of *n*-hexane, ethylacetate and ethanol extracts of *H. sabdariffa*, *C. lutea* and *J. secunda* in 7 different mobile phases.

The TLC plates $1Z_a$, $2Z_b$ and $5Z_e$, showed no separation for the components of the *H. sabdariffa* extract. Plates $4Z_d$ and $6Z_f$ showed one separation each while plates $3Z_c$, and $7Z_g$ showed at most two separations. With all of these observations, note that the extracts at the origin of these TLC plates (especially ethanol extract c), remained fully loaded and intensely coloured. Also, the mobile phases that showed some separation with the semi-polar to polar solvent systems, that is, 100% ethyl acetate and 5% ethanol/ethyl acetate. These implied that *H. sabdariffa* dye was very polar hence the choice of ethylacetate for defatting and methanol for extraction by maceration method.

TLC Plates $1H_a$ and $5H_e$ showed no separations for the components of the *Carpolobia lutea* extract. Plates $2H_b$ and $6H_f$ which made use of some semi-polar mobile phases (100% dichloromethane and 5% ethanol/dichloromethane), showed some separations running at the centre of the TLC plates while Plates $3H_c$, $4H_d$ and $7H_g$ had the components of the extracts running to the solvent front. These observations implied that the dye components of *C. lutea* extract were semi-polar hence, the plant material was deffated with *n*-hexane and extracted with ethyl acetate by maceration method.

Plate 4.1: TLC Plates (1-7) of Preliminary Extraction Tests

Legend:
Spot a – *n-hexane* extract
Spot b – ethyl acetate extract
Spot c – Ethanol extract
Plate Z - *Hibiscus sabdariffa*
Plate H – *Carpolobia. lutea*
Plate M – *Justicia secunda*

The subscripts on the alphabet at the top right corner of the TLC plates represent the solvent system used as the mobile phase.

Subscript a = 10% *n*-hexane
Subscript b =100% dichloromethane
Subscript c =100% ethyl acetate
Subscript d =50% *n*-hexane/dichloromethane
Subscript e =50% *n*-hexane/ethyl acetate
Subscript f =5% ethanol/dichloromethane
Subscript g =5% ethanol/ethylacetate

The solvent for the extraction of *Justicia secunda* was selected based on its ability to extract the red (by physical inspection) pigment from the plant leaves. The extraction solvent systems with fewer volumes of water (10→15→20 % vol water/methanol) gave green extracts with a red tint (Plate 4.2 a and b). An increase in the volume of water in the solvent system (25→30→35 % vol water/methanol) increased the intensity of the red pigment until an optimal red colour was obtained at 35% water/methanol solvent mixture (Plate 4.2b). *J. secunda* ground leaves were thus defatted using *n*-hexane and extracted using 35% water/methanol as solvent by the microwave-assisted extraction method.

Plates 4.2: Solvent Extraction of *J.secunda* using a)10→15→20% and b) 25→30→35%Vol of Water/Methanol.

4.2 Yield and Physical Properties of Extracts

The extraction yields of the plant materials used in this study are shown in Table 4.1. *Hibiscus sabdariffa* gave the highest yield of 29% followed by *Justicia secunda* which gave a yield of 28% and *Carpolobia lutea* gave the lowest yield of 2%.

Table 4.1: Extraction Yield of Plant

Common Name(s)	Herbarium Number	Botanical Name	Sequential Extraction Solvents	Colour and Texture	Extraction Yield (%)
Zobo	UPH/P/245	*Hibiscus sabdariffa L.*	Ethyl acetate[a] Methanol[b]	Reddish Purple/Sticky	29
Cattle Stick	UNN/04/0355D	*Carpolobia lutea*	*n*-Hexane[a] Ethyl acetate[b]	Dark Brown/Viscous	2
Bloodroot	UPH/P/244	*Justicia secunda* Vahl	*n*-hexane[a] 35% Methanol/ Water[b]	Reddish Brown/Sticky /Deliquincent	28

[a]solvent for first extraction. [b] solvent for second extraction.

4.3 Photooxygenation of α –Terpinene

Photooxygenation of α-terpinene without added photosensitizer was carried out as described in section 3.6 to test if it is autoxidizing. Figures 4.1 and 4.2 show the GC-FID chromatograms of the reaction mixture at 0 minutes and 90 minutes, respectively. Figure 4.1 shows that at 0 minutes, the starting composition of the reaction mixture was 68.96% of α-terpinene (RT 7.09 minutes.) and 16.9% of *p*-cymene (RT 7.23 minutes), no peak corresponding to ascaridole (**3**) was observed. After 90 minutes of photooxygenation, the composition of the starting material, α-terpinene, had decreased slightly to 64.1% and *p*-cymene increased to 19.5% while a peak (0.8%, RT 10.9 minutes) was assigned to the product, ascardiole.

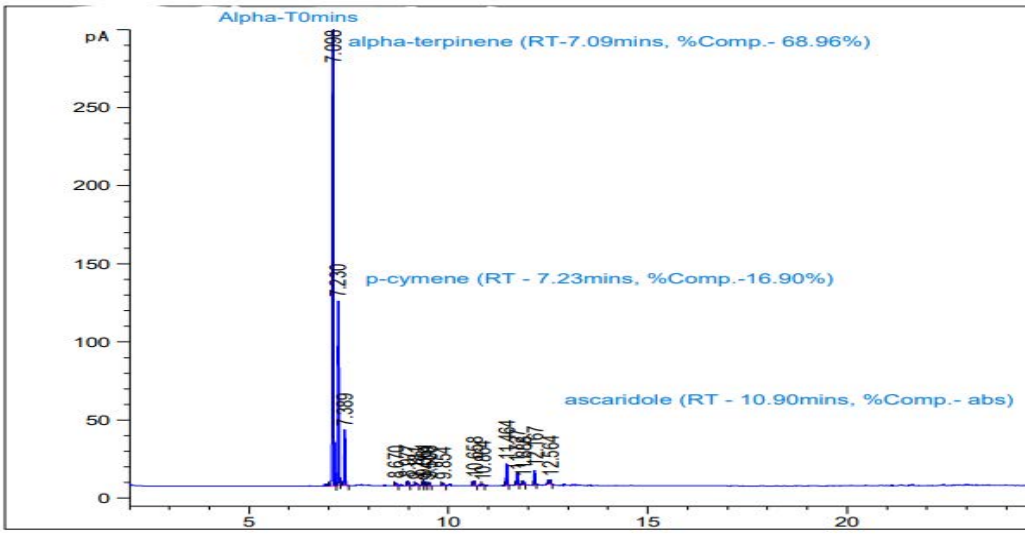

Figure 4.1: Chromatogram of Autoxidation Reaction Mixture of α-Terpinene at 0 Minute

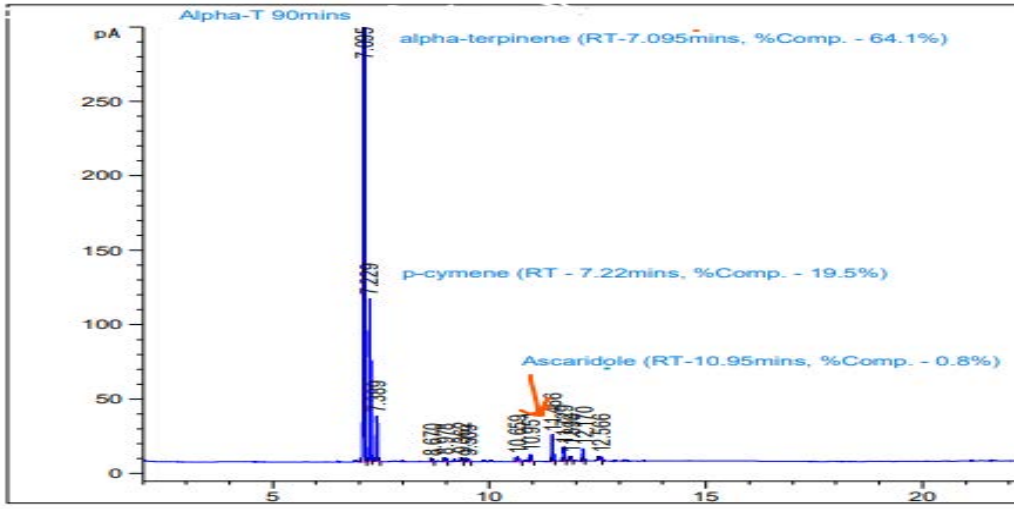

Figure 4.2: Chromatogram of Autoxidation Reaction Mixture of α-Terpinene at 90 Minutes

4.3.1 Photooxygenation of α-Terpinene using Rose Bengal and Methylene Blue as Photosensitizers.

The commercial photosensitizer dyes rose bengal and methylene blue were used severally in the photooxygenation of α-terpinene (see section 3.6). In the rose bengal sensitized reaction, the α-terpinene (RT 7.09 minutes) composition of the reaction mix decreased from 70.0% to 0.6% within 90 minutes while *p*-cymene (RT 7.23 minutes) increased from 15.8% to 19.8% and the ascaridole (**3**) product increased from 0.9% to 60.5% within 90 minutes as indicated by its peak at RT 10.96 minutes (Figures 4.3 and 4.4).

In the methylene blue sensitized reaction, α-terpinene which composed 66.4% (RT 7.09 minutes) of the reaction mixture, decreased from 66.4% to 0.6% after 90 minutes. The side product, *p*-cymene, increased from 13.0% to 15.5% (RT 7.09 minutes) while the major product, ascaridole (**3**) (RT 10.95 minutes), increased from 1.8% to 61.7% after 90 minutes (Figures 4.5 and 4.6).

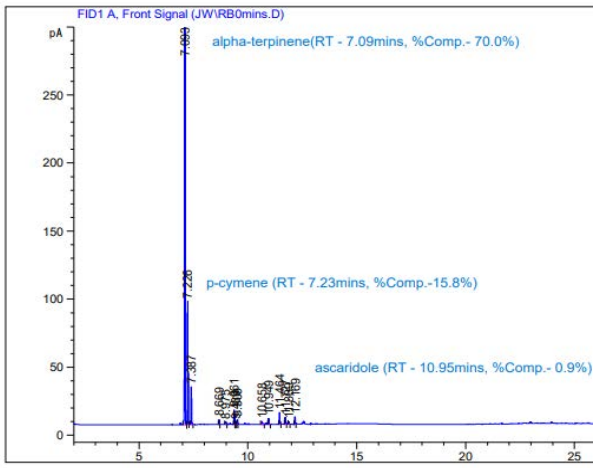

Figure 4.3 Chromatogram of Rose Bengal Sensitized Reaction Mixture of α-Terpinene at 0 Minute

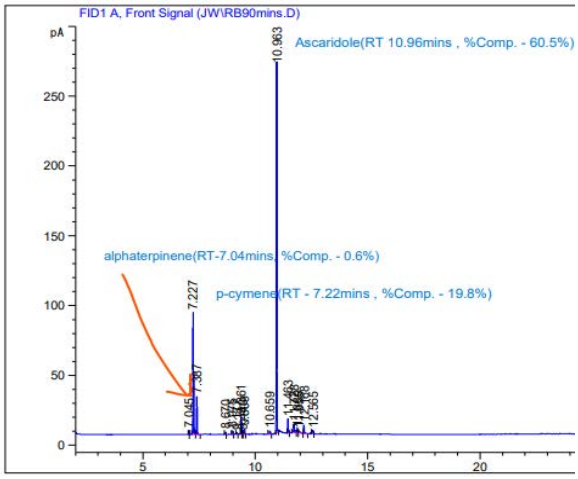

Figure 4.4 Chromatogram of Rose Bengal Sensitized Reaction Mixture of α-Terpinene at 90 Minutes

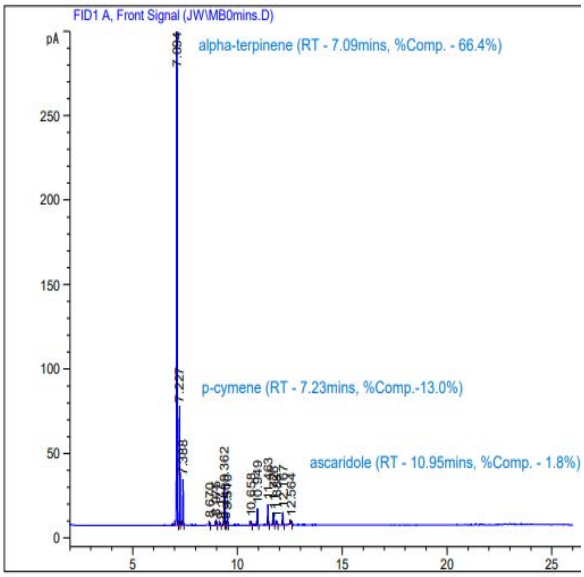

Figure 4.5 Chromatogram of Methylene Blue Sensitized Reaction Mixture of α-%Terpinene at 0 Minute

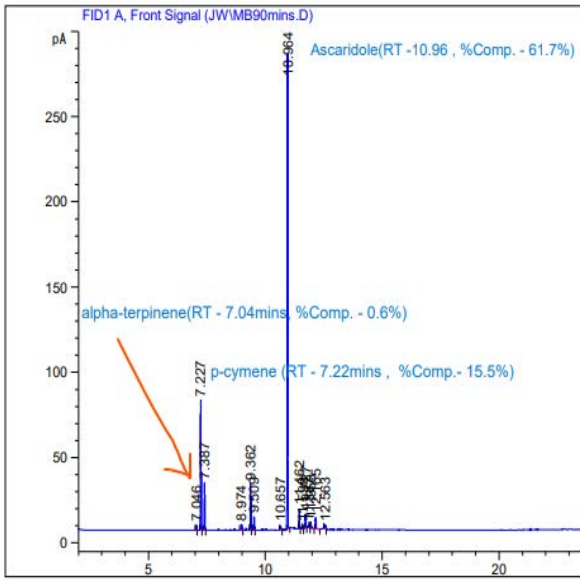

Figure 4.6 Chromatogram of Methylene Blue Sensitized Reaction Mixture of α-Terpinene at 90 Minutes

4.3.2 Photooxygenation of α-Terpinene using *Hibiscus sabdariffa*, *Carpolobia lutea* and *Justicia secunda* Extracts as Photosensitizers

α-Terpinene was photooxygenated as described in section 3.6 using each of the 3 plant extracts severally as photosensitizers. The α-terpinene (RT 7.09 minutes) content in the *Hibiscus sabdariffa* extract sensitized reaction decreased from 67.3% to 64.7% after 90 minutes, while *p*-cymene (RT 7.22 minutes) increased from 15.6% to 16.4% and the ascaridole (**3**) product (RT 10.94 minutes) increased from 0.3% to 3.1% (Figures 4.7 and 4.8).

In the *Carpolobia lutea* sensitized reaction, the α-terpinene (RT 7.09 minutes) content of the reaction mixture reduced from 65.8% to 0.5% after 90minutes, while *p*-cymene (RT 7.23 minutes) increased from 12.8% to 17.1% and the ascaridole (**3**) product (RT 10.95 minutes) increased from 0.5% to 62.8% (Figures 4.9 and 4.10) after 90 minutes.

The α-terpinene (RT 7.09 minutes) content in the *Justicia secunda* extract sensitized reaction decreased from 69.0% to 60.2% after 90 minutes, while *p*-cymene (RT 7.22 minutes) decreased from 15.2% to 15.0% and the ascaridole (**3**) product (RT 10.94 minutes) increased from 0.5% to 5.5% (Figures 4.11 and 4.12).

4.3.3 Summary of the Photooxygenation of α-Terpinene using Different Photosensitizers

Table 4.2 shows a summary of the GC-FID monitoring results for the photooxygenation of α-terpinene without photosensitizer (autoxidation), with commercial dyes (methylene blue and rose bengal) and with the 3 plant extracts (*Hibiscus sabdariffa*, *Carpolobia lutea* and *Justicia secunda* extracts). Autoxidation of α-terpinene gave the least increase in ascaridole (**3**) composition at 0.8% while *Carpolobia lutea* extract gave the highest increase in ascaridole (**3**) composition at 62.3%. *Hibiscus sabdariffa* extract and *Justicia secunda* extracts gave trace increases in the quantity of product at 2.8% and 5.0%, respectively.

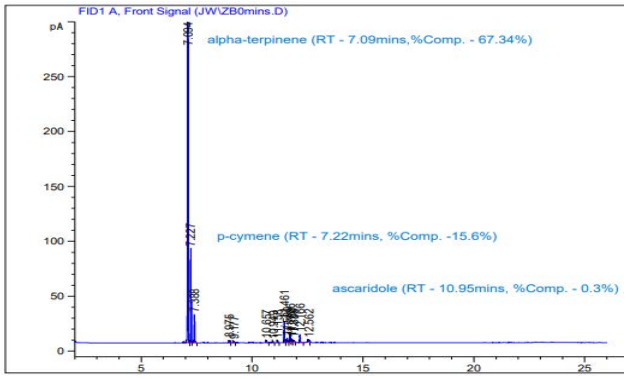

Figure 4.7: Chromatogram of *Hibiscus sabdariffa* Extract Sensitized Reaction Mixture of α-Terpinene at 0 Minute

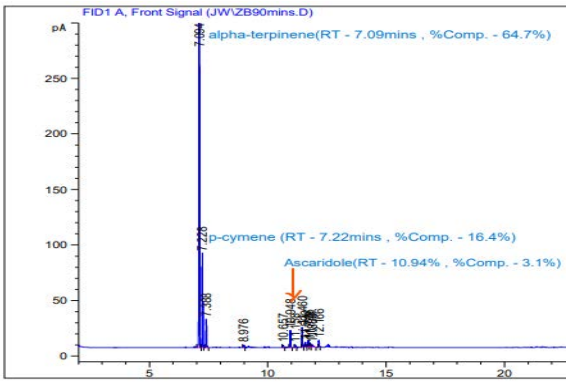

Figure 4.8: Chromatogram of *Hibiscus sabdariffa* Extract Sensitized Reaction Mixture of α-Terpinene at 90 Minutes

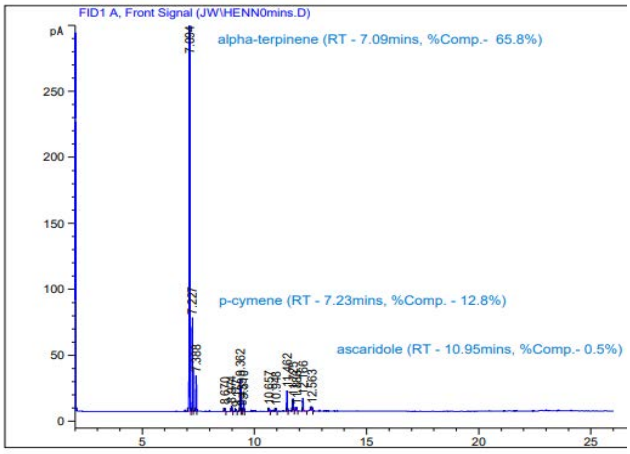

Figure 4.9: Chromatogram of *Carpolobia lutea* Extract Sensitized Reaction Mixture of α-Terpinene at 0 Minute

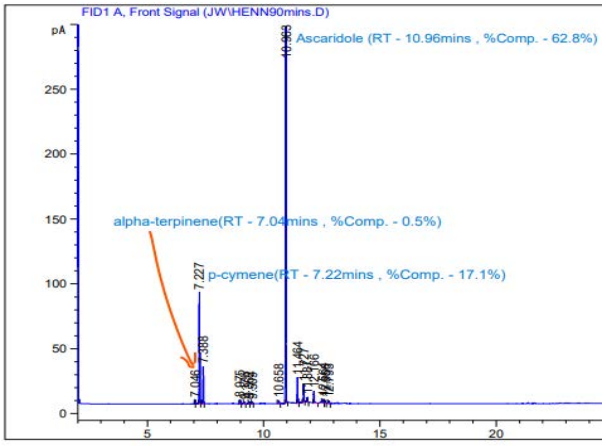

Figure 4.10: Chromatogram of *Carpolobia lutea* Extract Sensitized Reaction Mixture of α-Terpinene at 90 Minutes

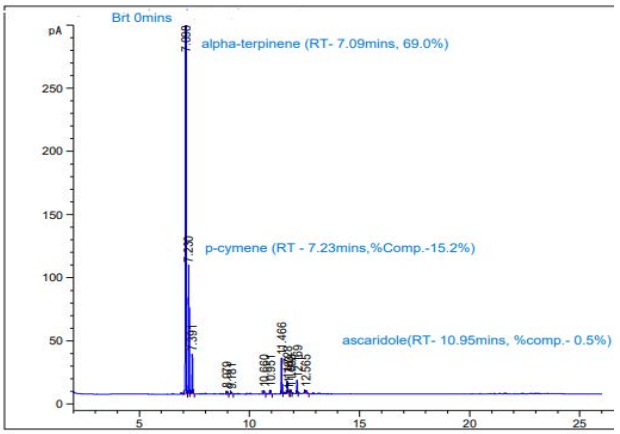

Figure 4.11: Chromatogram of *Justicia secunda* Extract Sensitized Reaction Mixture of α-Terpinene at 0 Minute

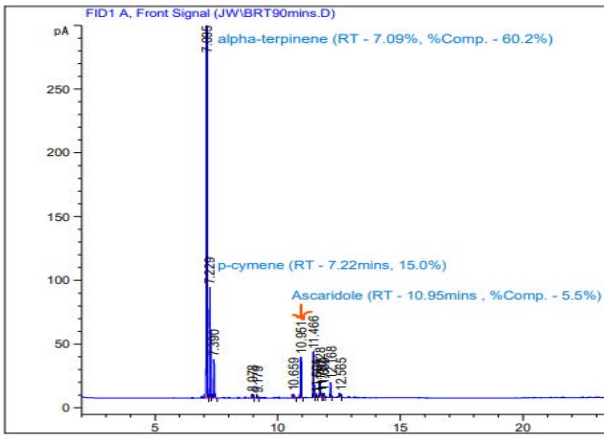

Figure 4.12: Chromatogram of *Justicia secunda* Extract Sensitized Reaction Mixture of α-Terpinene at 90 Minutes

Table 4.2 Summary of Composition of the Photooxygenation of α-Terpinene Reaction Mixtures using Different Photosensitizers

Experiment	Sensitizer	% Composition in Reaction Mixture[a] (0 min – 90 min)		
		α -Terpinene (RT 7.09 mins)	***p*-Cymene (RT 7.24 mins)**	**Ascaridole (RT 10.76 mins)**
1.	No Sensitizer	69.0 - 64.1 (- 4.9)	16.9 - 19.5 (+ 2.6)	0.0 - 0.8 (+ 0.8)
2.	Rose Bengal	70.0 - 0.6 (- 69.4)	15.8 - 19.8 (+ 4.0)	0.9 - 60.5 (+ 59.6)
3.	Methylene Blue	66.4 - 0.6 (- 65.8)	13.0 - 15.5 (+ 2.5)	1.8 - 61.7 (+ 59.9)
4.	*Hibiscus sabdariffa* Extract	67.3 - 64.7 (- 2.6)	15.6 - 16.4 (+ 0.6)	0.3 - 3.1 (+ 2.8)
5.	*Carpolobia lutea* Extract	65.8 - 0.5 (- 65.3)	12.8 - 17.1 (+ 4.3)	0.5 - 62.8 (+ 62.3)
6.	*Justicia secunda* Extract	69.0 - 60.2 (- 8.8)	15.2 - 15.0 (+ 0.2)	0.5 - 5.5 (+ 5.0)

[a] Determined by GC-FID analysis (± 2%).

4.3.4 Photooxygenation of α-Terpinene in the Presence of DABCO and ANT-COOH

Table 4.3, Figures 4.13 and 4.14 show the composition of the reaction mixture in the photooxygenation of α-terpinene using *Carpolobia lutea* extract as a photosensitizer in the presence of 0.07 mmol of DABCO, a singlet oxygen quencher (see section 3.6.4). After 90 minutes of reaction, α-terpinene (RT 7.09 minutes) composition reduced from 65.9% to 3.8%, while *p*-cymene (RT 7.22 minutes) increased from 13.6% to 16.2% and ascaridole (**3**) (RT 10.96 minute) increased from 0.5% to 54.8%. With an increase in the concentration of DABCO to 0.3 mmol, after 90 minutes of reaction, α-terpinene (RT 7.09 minutes) composition reduced from 68.6% to 36.3%, while *p*-cymene (RT 7.22 minutes) slightly decreased from 12.0% to 11.4% and ascaridole (**3**) (RT 10.96 minute) increased from 0.9% to 13.3% (see Figures 4.15 and 4.16)

ANT-COOH, a type 1 photosensitizer, was tested for its ability to sensitize the photooxygenation of α-terpinene (section 3.6.3). Table 4.3, Figures 4.17 and 4.18 show that the composition of α-terpinene (RT 7.08) in the reaction mixture decreased from 65.9% to 28.2%. There was a substantial increase in the composition of the side product *p*-cymene (RT 7.22 minutes), from 14.1% to 33.8% while the expected photooxygenation product, ascaridole (**3**), which was not detectable initially was 3.3% after 90 minutes of reaction.

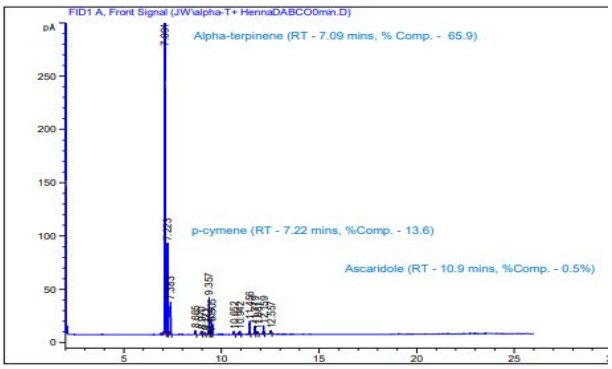

Figure 4.13 GC-FID Chromatogram of Initial Reaction Mixture in the Photooxygenation of α-Terpinene with *C. lutea* Extract as Sensitizer in the Presence of 0.07 mmol DAB CO

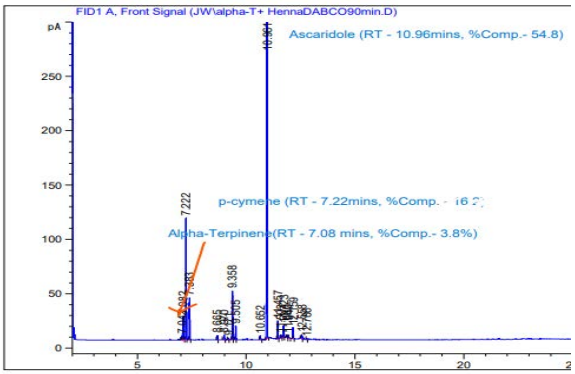

Figure 4.14 GC-FID Chromatogram of Reaction Mixture in the Photooxygenation of α-Terpinene with *C. lutea* Extract as Sensitizer in the Presence of 0.07 mmol DAB CO at 90 Minutes Irradiation

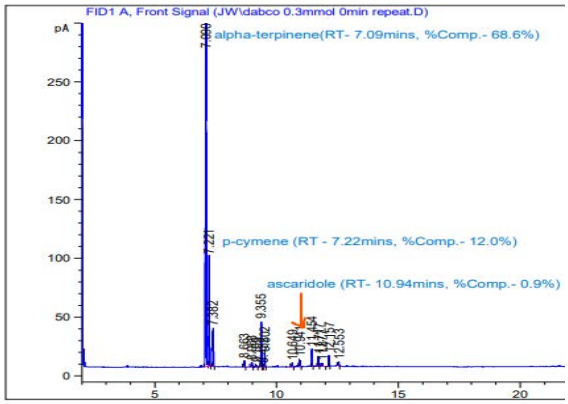

Figure 4.15 GC-FID Chromatogram of Initial Reaction Mixture in the Photooxygenation of α-Terpinene with *C. lutea* Extract as Sensitizer in the Presence of 0.3 mmol DAB CO

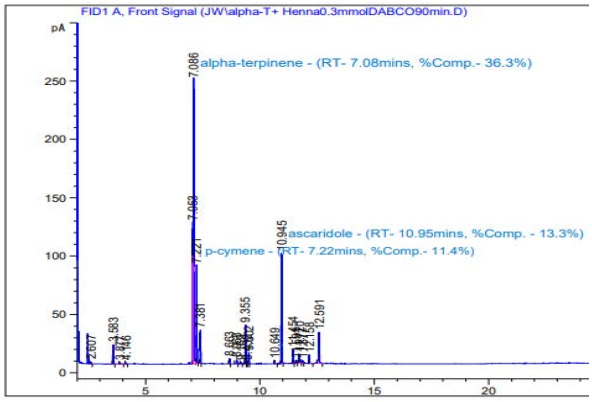

Figure 4.16 GC-FID Chromatogram of Reaction Mixture in the Photooxygenation of α-Terpinene with *C. lutea* Extract as Sensitizer in the Presence of 0.3 mmol DAB CO at 90 Minutes Irradiation

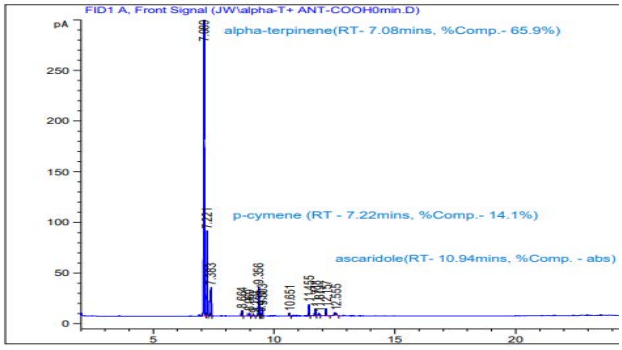

Figure 4.17 GC-FID Chromatogram of Initial Reaction Mixture in the Photooxygenation of α-Terpinene with ANT-COOH as Sensitizer

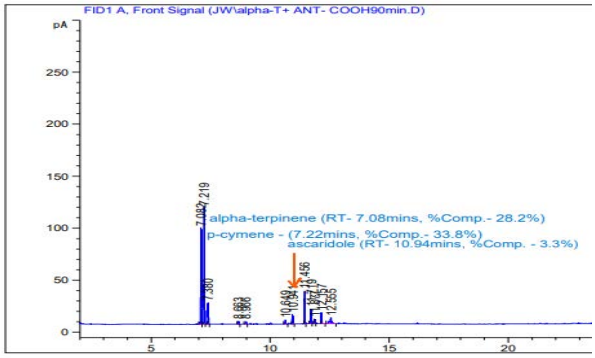

Figure 4.18 GC-FID Chromatogram of Reaction Mixture in the Photooxygenation of α-Terpinene with ANT-COOH as Sensitizer at 90 Minutes Irradiation

Photooxygenation of α-terpinene using *Carpolobia lutea* extract in the presence of 0.3 mmol DABCO gave a small amount of ascaridole (**3**) composition (13.3%) after 90 minutes. Photooxygenation using ANT-COOH as a photosensitizer also gave a product composition of 3.3% as seen in Table 4.3.

Table 4.3 Summary of the Photooxygenation of α-Terpinene with *C. lutea* Extract as Sensitizer in the Presence of DABCO and with ANT- COOH

Reaction Mixture Additive	% Composition in Reaction Mixture[a] (0 min – 90 min)		
	α-Terpinene	***p*-Cymene**	**Ascaridole**
DABCO (0.07 mmol) + *C. lutea* extract (0.01 g)	65.4 - 3.81	13.63 – 16.20	0.5 – 54.8
	(- 61.59)	(+ 2.57)	(+ 54.3)
DABCO (0.3 mmol) + *C. lutea* extract (0.01 g)	68.6 – 36.3	12.0 – 11.4	0.9 – 13.3
	(- 32.3)	(- 0.6)	(+ 12.4)
ANT-COOH	65.9 – 28.2	14.1 - 33.8	0.0 - 3.3
	(- 37.7)	(+ 19.7)	+ 3.3

[a] Determined by GC-FID analysis (± 2%).

4.3.5 α-Terpinene Photooxygenation Replicates Result Summary

On the replication of α-Terpinene photooxygenation for reproducibility purpose, rose bengal gave the highest mean percentage composition value of ascaridole (**3**) as 74.5 ± 4.95 while bloodroot extract gave the lowest mean percentage composition value of ascaridole (**3**) as 2 ± 1.41. DABCO (0.3 M) and *C. lutea* extract (0.008 g) sensitized reaction replicates gave a mean percentage composition of ascaridole (**3**) as 33 ± 2.83 while ANT-COOH sensitized reaction replicates gave a mean percentage composition of ascaridole (**3**) as 5.5 ± 0.71 (Table 4.4). The GC chromatograms are in appendices 1 to 7. Rose bengal gave the highest isolated ascaridole (**3**) yield of 71% , *C. lutea* the second highest isolated ascaridole (**3**) yield of 44% and methylene blue gave the lowest isolated ascaridole (**3**) yield of 31%. For the *Hibiscus sabdariffa*, *Justicia secunda*, DABCO/*C. lutea* and ANT-COOH sensitized reaction replicates, no ascaridole (**3**) product was isolated due to its low percentage composition (see Table 4.4).

Table 4.4: α-Terpinene Photooxygenation Replicate Result Summary

Photosensitizers	%Composition of Ascaridole after 1.5 Hours Irradiation (Mean Value ± SD)	%Yield
Rose Bengal	74.5 ± 4.95	71
Methylene Blue	69.5 ± 0.71	31
H. sabdariffa	4 ± 0.00	n.d.[b]
C. lutea	61.5 ± 2.12	44
J. secunda	2 ± 1.41	n.d.[b]
DABCO (0.3 M) + *C. lutea* Extract (0.008 g)	33 ± 2.83	n.d.[b]
ANT-COOH	5.5 ± 0.71	n.d.[b]

[a] Determined by ^{1}H NMR analysis (± 2%). [b]n.d. = not determined.

The ^{1}H NMR spectrum of ascaridole (**3**) synthesized and isolated is as seen in Figure 4.19 revealing 7 major types of proton signals. The proton signals were at ^{1}H NMR (400 MHz, $CDCl_3$): δ0.92 (6H, d, J = 4 Hz, A), δ1.35 (3H, s, C), δ1.43 (2H, d, J = 8 Hz, D_1 & E_1), δ1.83 (1H, p, J = 8 Hz, B), δ1.93 (2H, m, J = 4 Hz, D_2 & E_2), δ6.32 (1H, d, J = 8 Hz, F), δ6.40 (1H, d, J = 12 Hz, G).

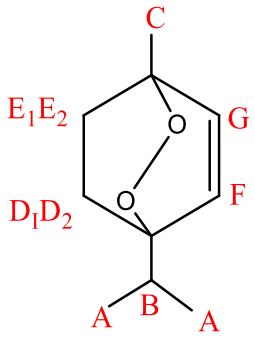

3: Chemical Structure of Ascaridole

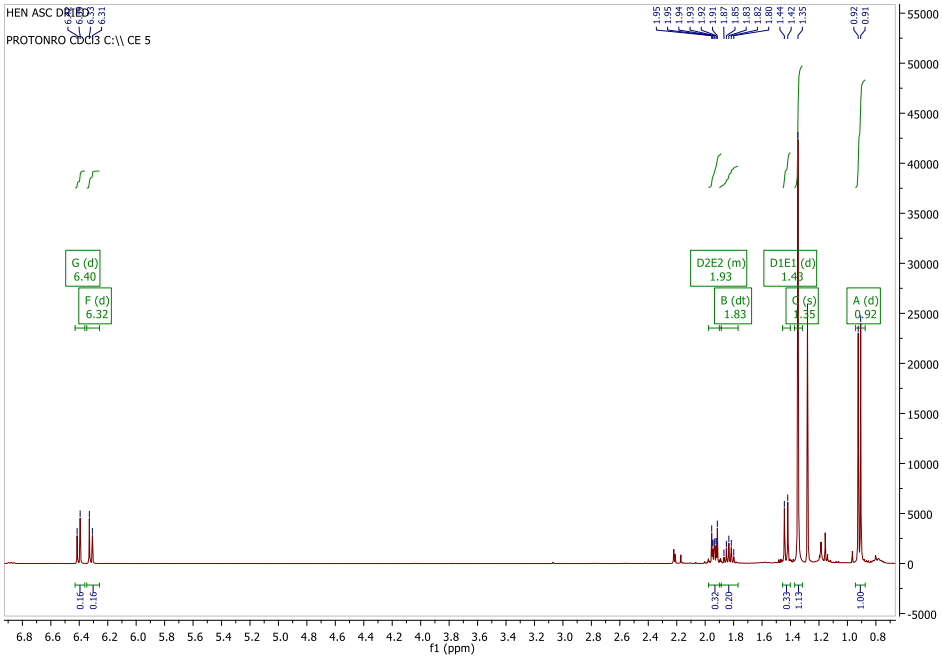

Figure 4.19: ^{1}H NMR Spectrum of Synthesized Isolated Ascaridole Acquired in $CDCl_3$

4.4 Photooxygenation of 1,5-Dihydroxynaphthalene

1,5-dihydroxynaphthalene (**4**) was photooxygenated without sensitizer (ie. autoxidation) see section 3.7. Two doublets at δ6.90 and δ7.73, one triplet at δ7.24 and a singlet at δ8.95 were characteristic peaks of the starting material (Figure 4.20). After 5 hours, the ^{1}H NMR of the reaction mixture showed signals due to the product (5-hydroxy-1,4-naphthaquinone) at δ 7.08 (q), δ7.35 (dd), δ7.60 (dd), δ7.80 (m) and δ11.94 (s) (Figure 4.21). However, the reactant was not completely consumed. ^{1}H NMR peaks due to the reactant (Figure 4.20) were seen in the reaction mixture after 5 hours of photooxygenation (Figure 4.21).

In the rose bengal sensitized reaction, ^{1}H NMR spectra showed that the reactant (Figure 4.22) had been completely converted to the product after 3 hours of photooxygenation (Figure 4.23). Similarly, ^{1}H NMR of the reaction mixture indicated that the reactant (Figure 4.24) was 100% converted to product (Figure 4.25) after 4 hours of reaction, in the methylene blue sensitized photooxygenation. ^{1}H NMR spectra of the *H. sabdariffa* extract-sensitized photooxygenation reaction showed that 48% product conversion was achieved after 5 hours (Figures 4.27 and 4.28). In the *C. lutea* sensitized reaction, 66% product conversion (Figures 4.29 and 4.30) was achieved within 5 hours of photooxygenation. The bloodroot extract sensitized reaction achieved 34% product conversion after 5 hours of photooxygenation (Figure 4.30 and Figure 4.31).

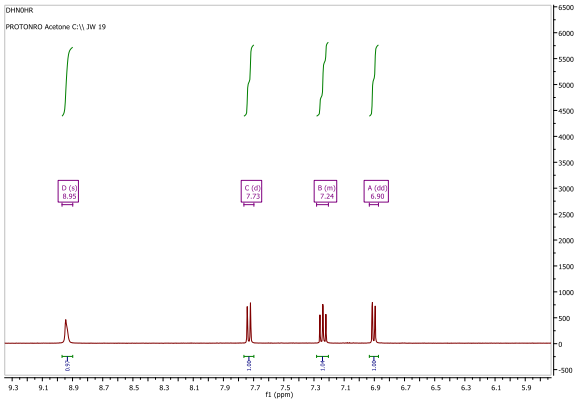

Figure 4.20: Autoxidation 1,5-Dihydroxynaphthalene at 0 Hour Irradiation

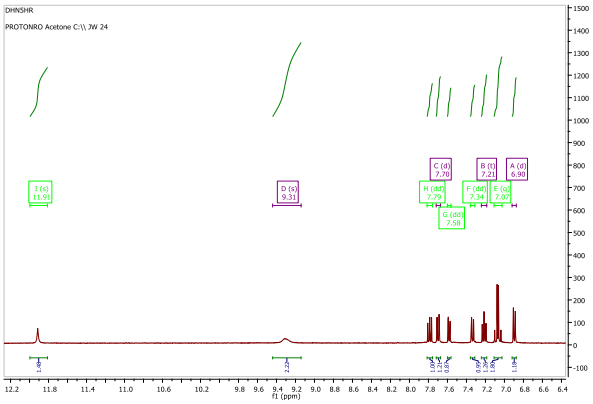

Figure 4.21: Autoxidation of 1,5-Dihydroxynaphthalene at 5 Hours Irradiation

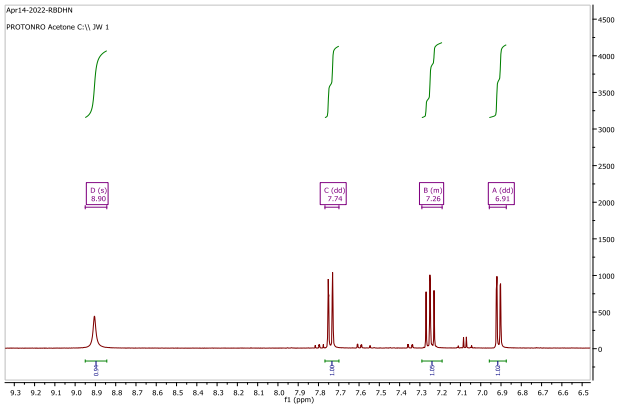

Figure 4.22: Rose Bengal Sensitized Photooxygenation of 1,5-DHN at 0 Hour Irradiation

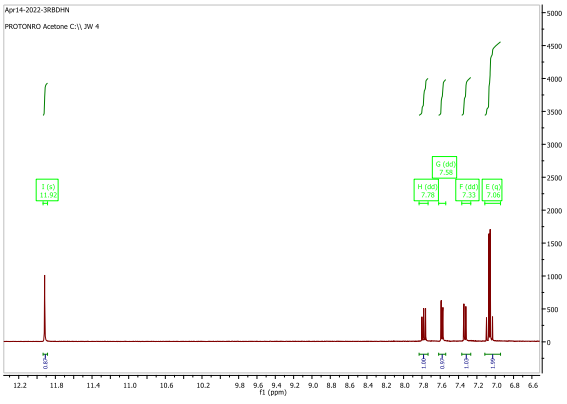

Figure 4.23: Rose Bengal Sensitized Photooxygenation of 1,5-DHN at 5 Hours Irradiation

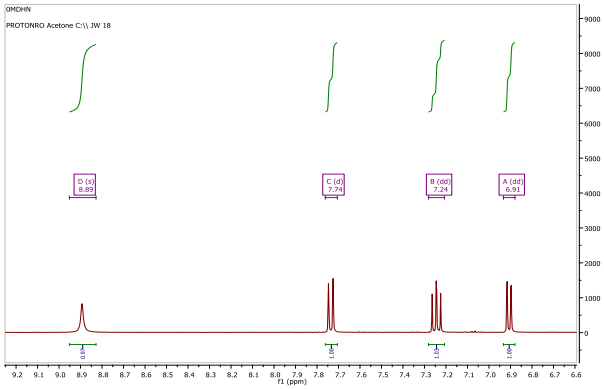

Figure 4.24: Methylene Blue Sensitized Photooxygenation of 1,5-DHN at 0 Hour Irradiation

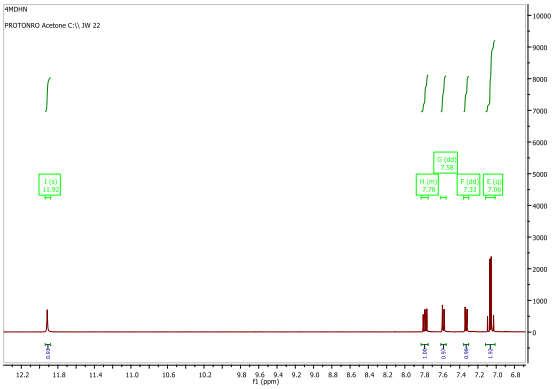

Figure 4.25: Methylene Blue Sensitized Photooxygenation of 1,5-DHN at 5 Hours Irradiation

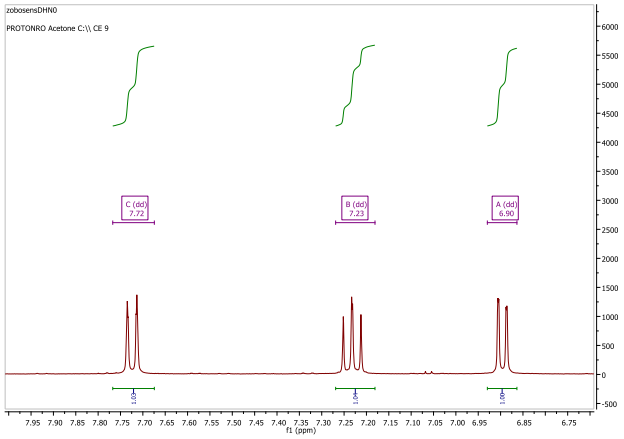

Figure 4.26: *H. sabdariffa* Extract Sensitized Photooxygenation of 1,5-DHN at 0 Hours Irradiation

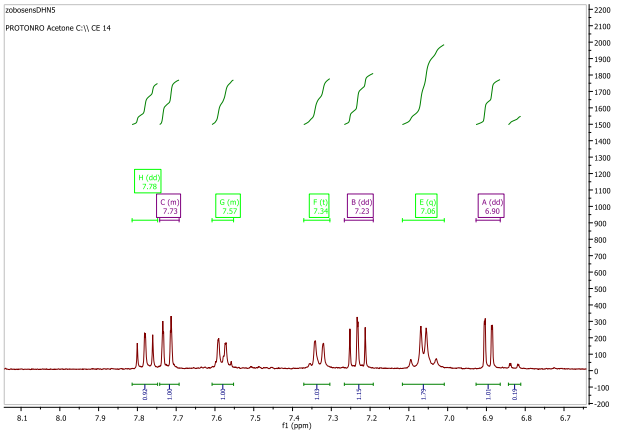

Figure 4.27: *H. sabdariffa* Extract Sensitized Photooxygenation of 1,5-DHN at 5 hours Irradiation

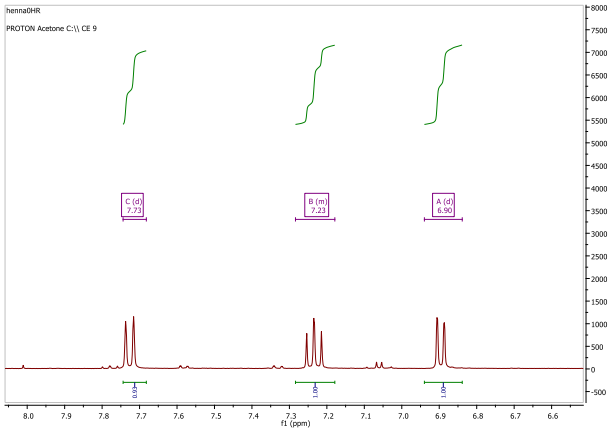

Figure 4.28: *C. lutea* Extract Sensitized Photooxygenation of 1,5-DHN at 0 Hours Irradiation

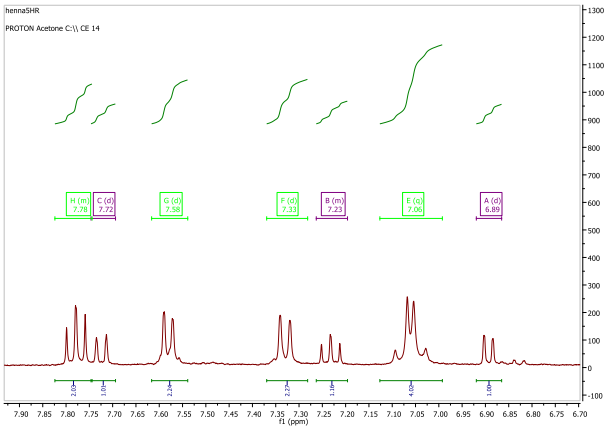

Figure 4.29: *C. lutea* Exract Sensitized Photooxygenation of 1,5-DHN at 5 Hours Exposure

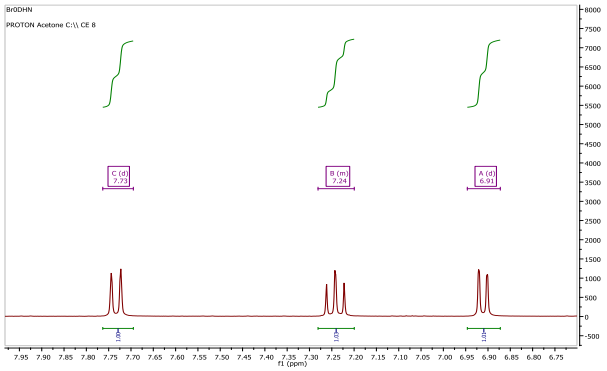

Figure 4.30: *J. secunda* Extract Sensitized Photooxygenation of 1,5-DHN at 0 Hours

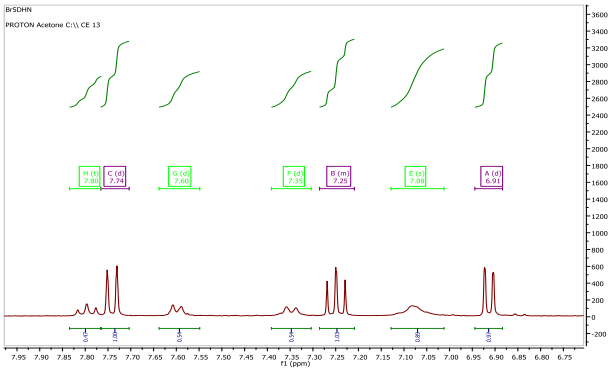

Figure 4.31: *J. secunda* Extract Sensitized Photooxygenation of 1,5-DHN at 5 Hours

4.4.1 Summary of the Photooxygenation of 1,5-Dihydroxynaphthalene

Figure 4.32 shows the hourly conversions (by ^{1}H NMR) of 1,5-dihydroxynaphthalene to 5-hydroxy-1,4-naphthaquinone in the initial photooxygenation reactions using the different photosensitizers. Autoxidation, Rose bengal, methylene blue and *C. lutea* Extract had their highest percentage conversions within the first hour of irradiation at 13%, 52%, 36% and 33%, respectively while *J. secunda* extract gave zero per cent conversion in the first hour of irradiation. Rose bengal achieved 100% conversion within three hours of irradiation while it took methylene blue 4 hours to achieve full conversion. Zero sensitizer, *H. sabdariffa* extract, and *J. secunda* extract sensitized reactions were irradiated for 5 hours but they still did not attain 100% conversion. *C. lutea* extract gave the highest conversion of 67% after 5 hours irradiation (Figure 4.32).

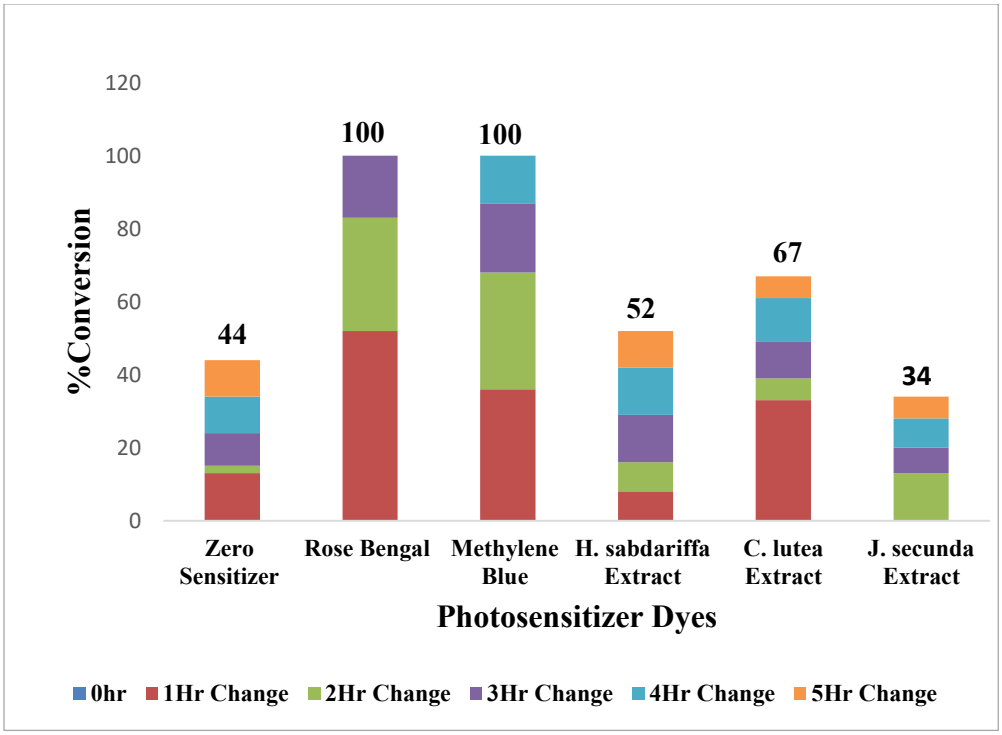

Figure 4.32: Summary of the Hourly Conversion of 1,5-Dihydroxynaphthalene to 5-hydroxy-1,4-naphthaquinone

4.4.2 Percentage Isolated Yields of 5-hydroxy-1,4-naphthaquinone

After solvent evaporation and column chromatography of each of the initial photooxygenation reaction mixtures (section 3.7), the percentage yields of 5-hydroxy-1,4-naphthaquinone were shown in Figure 4.33. Of the plant extract sensitizers, *J. secunda* gave the lowest yield with 29% followed by the autooxidation reaction (39%) while *H. sabdariffa* and *C. lutea* gave moderately higher yields of 44% and 51%, respectively. Of the commercial dyes, the methylene blue sensitized reaction yield (67%) of 5-hydroxy-1,4-naphthoquinone (**4**) was slightly higher than that of the rose bengal sensitized reaction (64%).

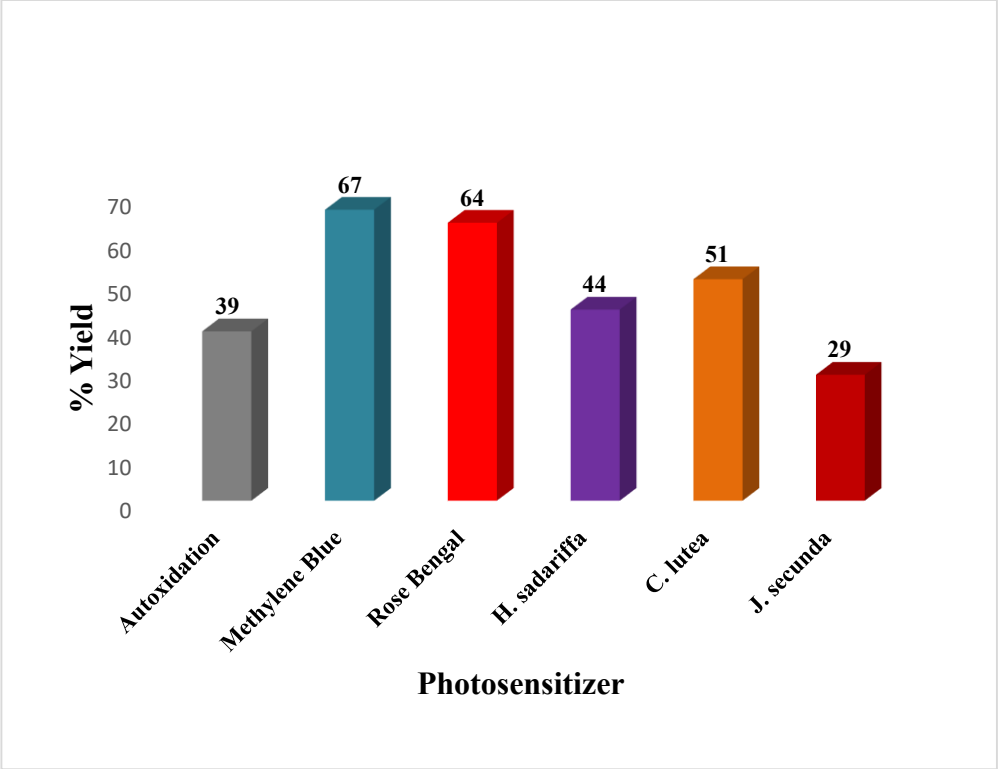

Figure 4.33: Percentage Isolated Yields of 5-hydroxy-1,4-naphthoquinone after Column Chromatography

4.4.3 1,5-Dihydroxynaphthalene Photooxygenation Replicate Result Summary

Table 4.5 shows the mean conversion values and mean yield values of the second and third experiments for 1,5-DHN photooxygenations using zero sensitizers, rose bengal, methylene blue, *Hibiscus sabdariffa* extract, *Carpolobia lutea* extract and *Justicia secunda* extract. Details of the ^{1}H NMR spectra used for monitoring these replicate reactions are in appendices 8 to 13. Rose bengal gave a 100% ± 0.00 mean conversion value and also gave the highest mean yield value of 80.0% ± 0.00 within 8 hours of irradiation. *Justicia secunda* extract sensitized reaction gave the lowest mean conversion value of 45.5% ± 2.12 with a mean yield value of 42.5% ± 3.45. *Hibiscus sabdariffa* sensitized reaction gave a mean conversion value of 51.5% ± 0.71 although its mean yield value of 25.5% ± 0.70 was the lowest.

Table 4.5: 1,5-Dihydroxynaphthalene Photooxygenation Replicate Result Summary

Photosensitizers	%Conversion after 8 Hours Irradiation[a] (Mean Value ± SD)	%Yield[b]
Autoxidation	74 ± 4.24	40.5 ± 4.95
Rose Bengal	100 ± 0.00	80.0 ± 0.00
Methylene Blue	100 ± 0.00	76.5 ± 0.70
H. sabdariffa	51.5 ± 0.71	25.5 ± 0.70
C. lutea	100 ± 0.00	77.0 ± 12.73
J. secunda	45.5 ± 2.12	42.5 ± 3.45

[a] Determined by ^{1}H NMR analysis (± 2%). [b]Isolated yield after column chromatography.

The protons in the ^{1}H NMR spectrum of the isolated 5-hydroxy-1,4-naphthoquinone (**4**) showed the following signals: ^{1}H NMR (400 MHz, $(CD_3)_2CO$) δ 7.08(2H, q, J = 8 Hz, A), δ7.35 (1H, dd, J = 8 Hz, B), δ7.60 (1H, dd, J = 8, 0 Hz, C), 7.80 (1H, m, J = 8 Hz, D), 11.94 (1H, s, E), (Figure 4.34).

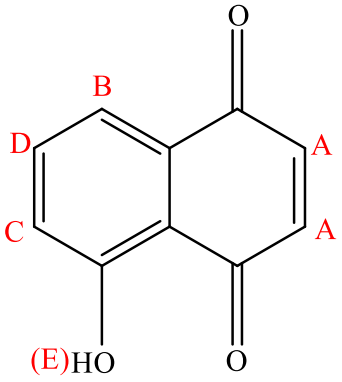

4: Chemical Structure of 5-Hydroxy-1,4-naphthoquinone

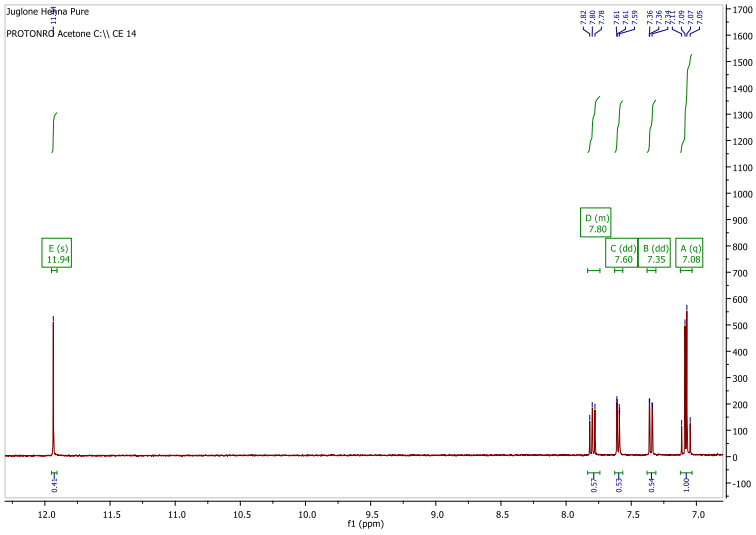

Figure 4.34: ^{1}H NMR Spectrum of Pure Syntheszed 5-Hydroxy-1,4-naphthoquinone Acquired in $(CD_3)_2CO$

4.5 Photooxygenation of 1-Naphthol

1-naphthol was photooxygenated as described in section 3.8. Figures 4.35 and 4.36 show the ^{1}H NMR spectra used for the monitoring of the autoxidation of 1-naphthol. The substrate had the following characteristic peaks: δ6.93(dd), δ7.30(t), δ7.38(d), δ7.47(m), δ7.83(dd), δ8.25(dd), and 9.13(s). The spectra indicate that after 12 hours of irradiation, there was no visible change in the composition of the reaction mixture.

The ^{1}H NMR of the reaction mixture of the rose bengal-sensitized photooxygenation of 1-naphthol after 2 hours of irradiation showed product peak in its spectrum at δ7.04-s, δ7.87- sx and δ8.04-sx, indicating product formation of 59% (Figures 4.37 and 4.38) but after 3 hours, the spectrum became complex with more peaks although the conversion slightly increased to 68% (Figure 4.41). The chemical shifts of product peaks in the ^{1}H NMR spectra of the reaction mixture coincided with peaks in the spectra of authentic 1,4-naphthoquinone (**5**), the expected product. (Figure 4.40). ^{1}H NMR spectra of the *C. lutea* extract-sensitized reaction mixture showed that peaks due to the reactant (Figure 4.41) had reduced and those due to the product (Figure 4.42) had appeared after 4 hours of photooxygenation, representing 68%. After 9 hours, the spectrum became complex (Figure 4.43) and the product conversion slightly decreased to 67%.

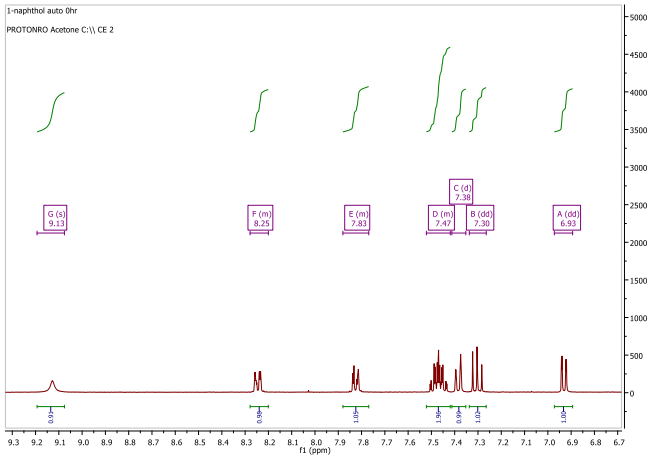

Figure 4.35: Autoxidation of 1-Naphthol at 0 Hours

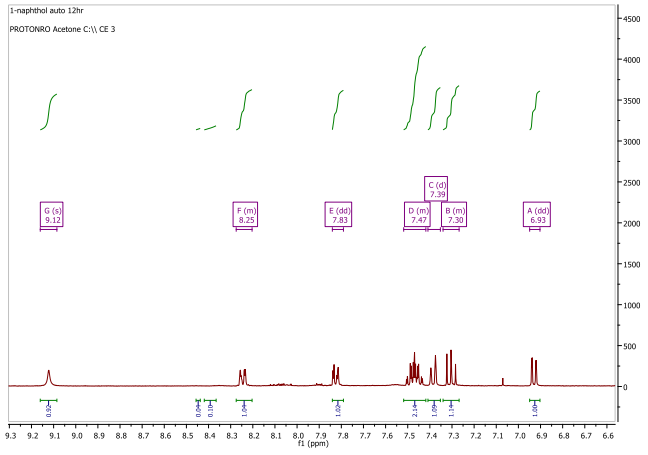

Figure 4.36: Autoxidation of 1-Naphthol at 12 Hours

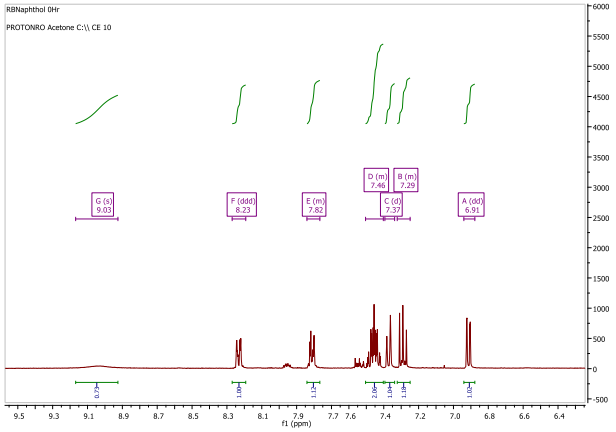

Figure 4.37: Rose Bengal Sensitized Photooxygenation of 1-Naphthol at 0 Hours

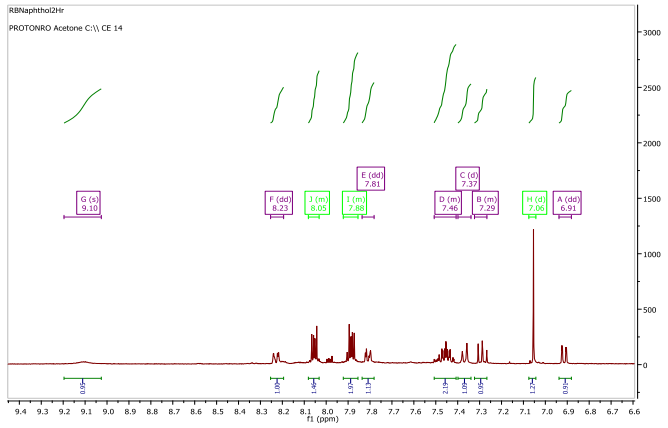

Figure 4.38: Rose Bengal Sensitized Photooxygenation of 1-Naphthol at 2 Hours

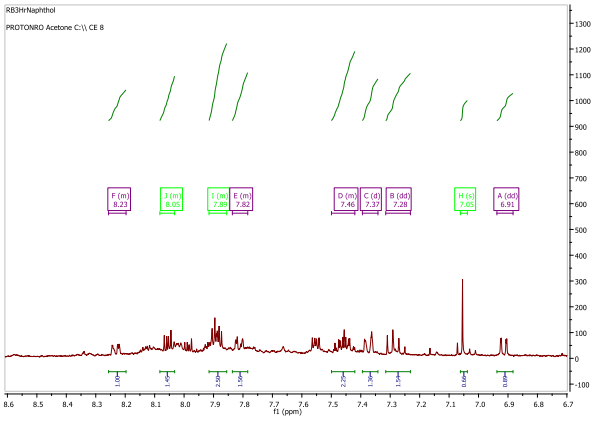

Figure 4.39: Rose Bengal Sensitized Photooxygenation of 1-Naphthol at 3 Hours

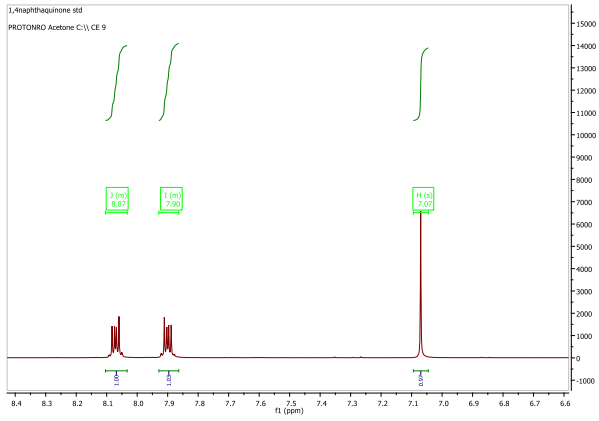

Figure 4.40: 1,4-Naphthaquinone Standard

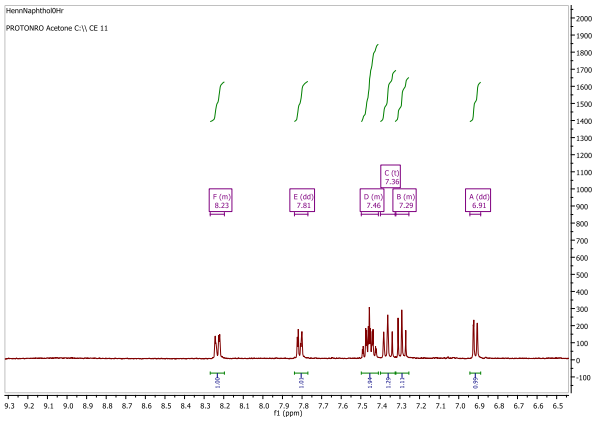

Figure 4.41:*Carpolobia lutea* Extract Sensitized Photooxygenation of 1-Naphthol at 0 Hours

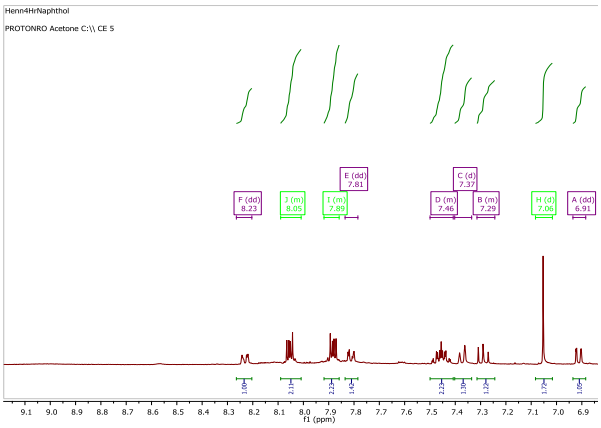

Figure 4.42: *Carpolobia lutea* Extract Sensitized Photooxygenation of 1-Naphthol at 4 Hours

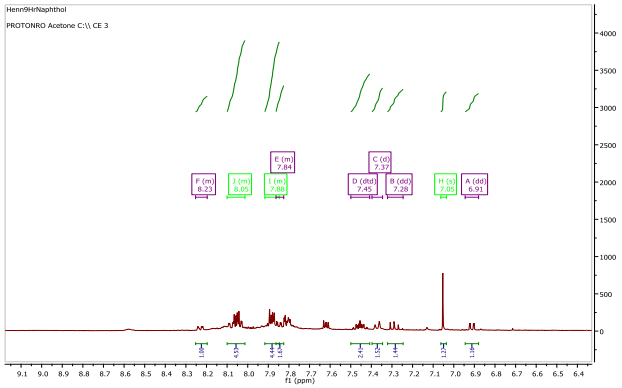

Figure 4.43: *Carpolobia lutea* Extract Sensitized Photooxygenation of 1-Naphthol at 9 Hours

Figure 4.44 is a line graph showing the conversion of 1-naphthol to 1,4-naphthoquinone after four hours irradiation time for the rose bengal sensitized reaction and 9 hours for the *C. lutea* sensitized reaction. In the rose bengal sensitized reaction (red line), the line graph began to flatten out after 2 hours and for the *C. lutea* sensitized reaction (green line), the line graph began to flatten out after 4 hours.

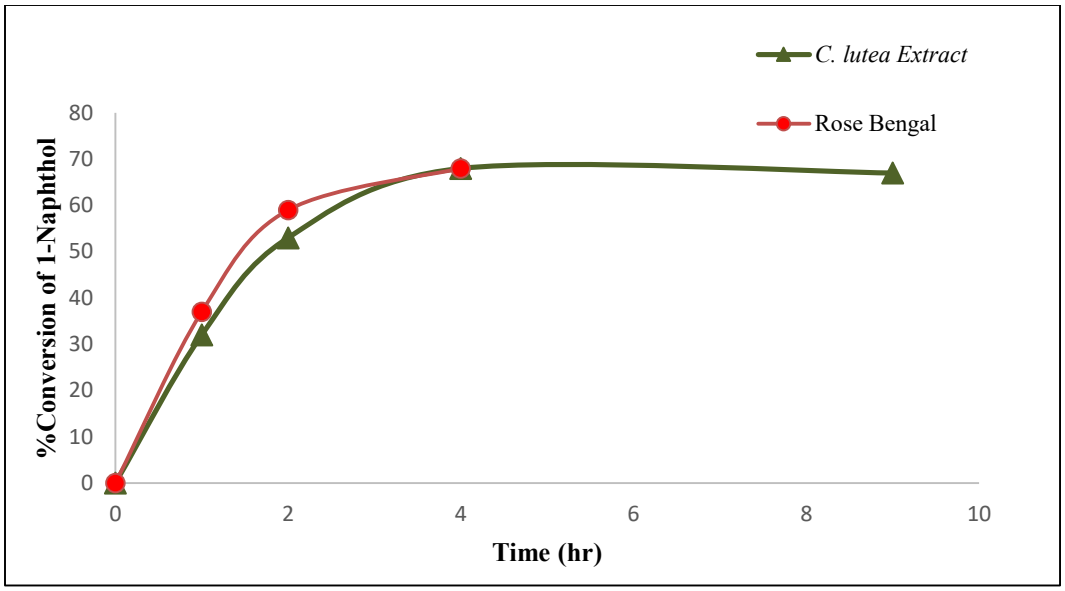

Figure 4.44: Photooxygenation of 1-Naphthol using Rose Bengal and *Carpolobia lutea* Extract as Photosensitizers

Column chromatography of the solvent-stripped rose bengal and *C. lutea* extract-sensitized reaction mixtures gave no isolated yield of 1,4-naphthoquinone, respectively.

4.5.1 1-Naphthol Photooxygenation Replicate Result Summary

Mean conversion values and mean yield values in Table 4.6 were based on the isolation of 1,4-naphthoquinone from the replicate photooxygenation reactions of 1-naphthol by column chromatography. Details of the ^{1}H NMR spectra used for monitoring the replicate reactions are in appendices 14 and 15. Rose bengal gave a higher mean conversion value of 62% ± 1.41 than *Carpolobia lutea* extract (59% ± 11.31) but a lower mean yield of 3.2% ± 2.69 than *Carpolobia lutea* extract (6.6% ± 2.48).

Table 4.6: 1-Naphthol Photooxygenation Replicate Result Summary

Photosensitizers	%Conversion after 2 Hours Irradiation[a] (Mean Value ± SD)	%Yield[b]
Rose bengal	62 ± 1.41	3.2 ± 2.69
C. lutea	59 ± 11.31	6.6 ± 2.48

[a] Determined by ^{1}H NMR analysis (± 2%). [b]Isolated yield after column chromatography.

The protons in the ^{1}H NMR spectrum of the isolated 1,4-naphthaquinone (5) showed the following signals : ^{1}H NMR (400 MHz, $(CD_3)_2CO$) δ7.04 (2H, s, A), δ7.87 (2H, sx, J = 4 Hz, B), δ8.04 (2H, sx, J = 4 Hz, C) (Figure 4.45).

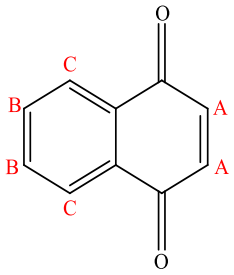

5: Chemical Structure of 1,4-naphthoquinone

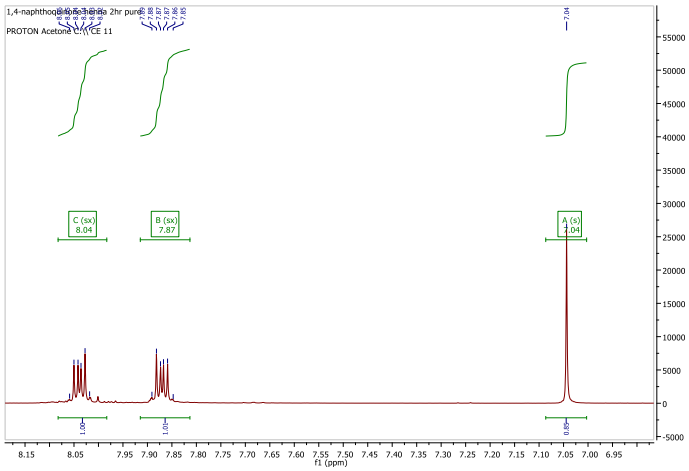

Figure 4.45: ^{1}H NMR Spectrum of Pure Synthesized 1,4-Naphthoquinone Acquired in $(CD_3)_2CO$

4.6 Photooxygenation of 1,6-Dihydroxynaphthalene

Photooxygenation of 1,6-Dihydroxynaphthalene without added photosensitizer was carried out as described in section 3.9 to test if it is autoxidizing. The ^{1}H NMR of the substrate, 1,6-dihydroxynaphthalene, showed 7 prominent peaks at : δ6.70 - dd, δ7.06 - dd, δ7.14 - dd, δ7.18 - m, δ8.11 - d, δ8.66 - s and δ8.94 - s (Figure 4.46). Autoxidation of this starting material (Figure 4.46) for 12 hours resulted in the presence of some new peaks but not the product peaks (Figure 4.47).

In contrast, the rose bengal-sensitized reaction mixture, after 4 hours, gave new peaks in its ^{1}H NMR spectrum at δ6.95 - q, δ7.25 - dd, δ7.41 - d, δ7.94 – d and δ 9.98 – s indicating 100% conversion of reactants to product (Figure 4.48 and 4.52). Similarly, the *C. lutea* extract-sensitized photooxygenation of 1,6-dihydroxynaphthalene, after 12 hours of irradiation showed (by ^{1}H NMR) 92% conversion (Figure 4.50 and 4.51). Combined photooxygenation to 24 hours gave 100% (Figure 4.52).

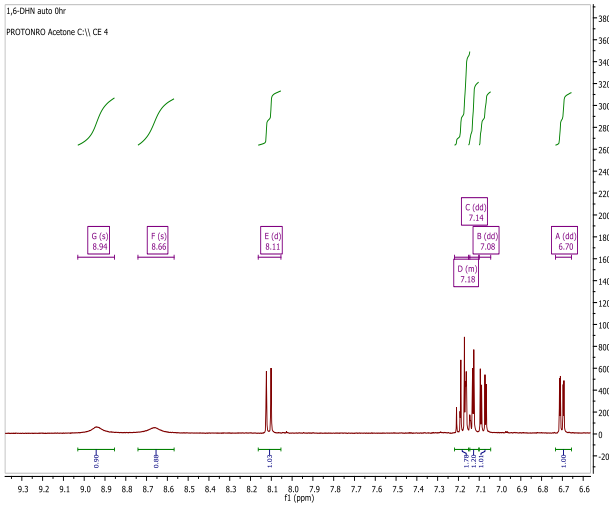

Figure 4.46: Autoxidation of 1,6-Dihydroxynaphthalene at 0 Hour

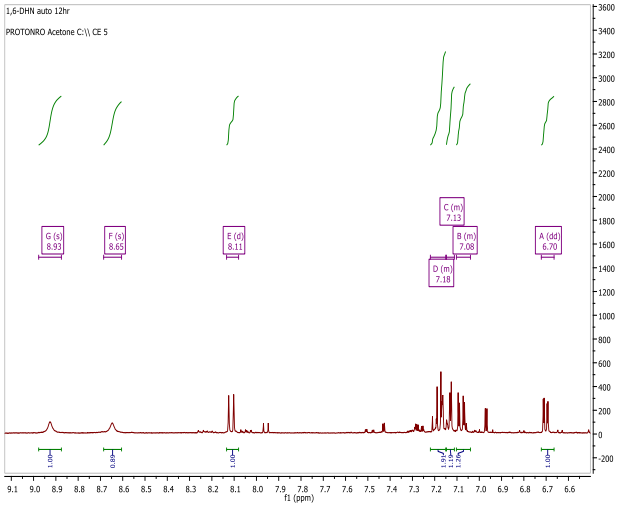

Figure 4.47: Autoxidation of 1,6-Dihydroxynaphthalene at 12 Hours

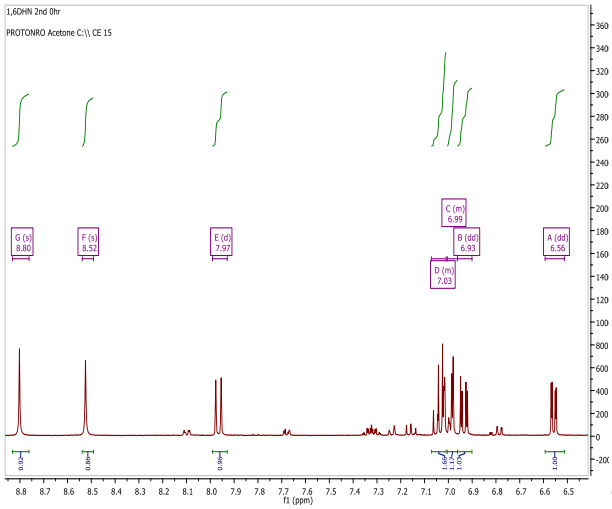

Figure 4.48: Rose Bengal Sensitized Photooxygenation of 1,6-Dihydroxynaphthalene at 0 Hours

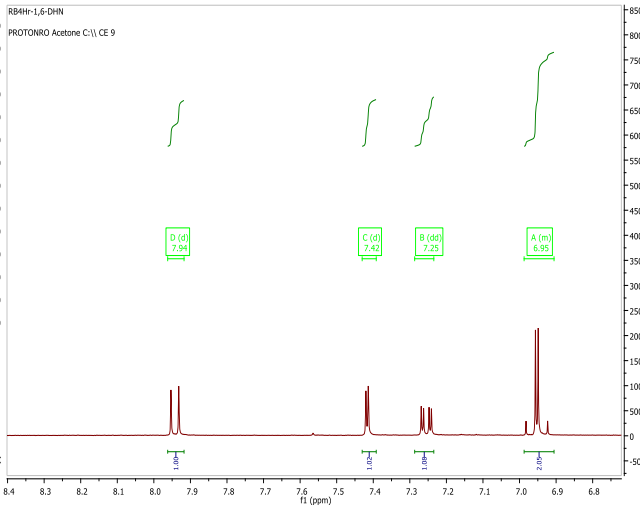

Figure 4.49: Rose Bengal Sensitized Photooxygenation of 1,6-Dihydroxynapthalene at 4 Hours

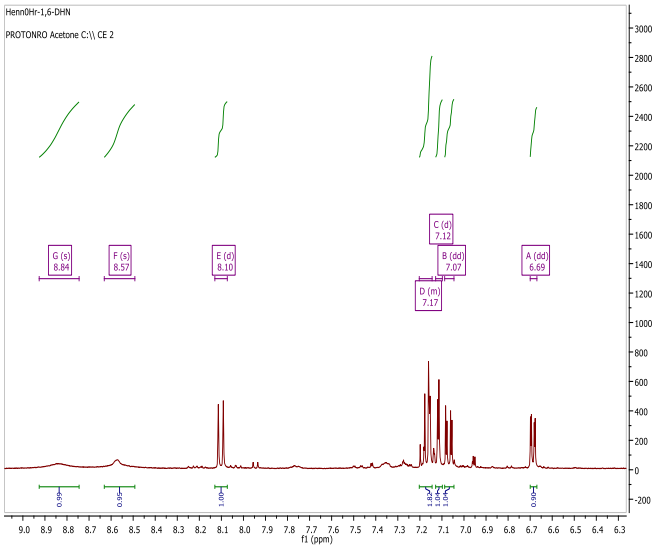

Figure 4.50: *Carpolobia lutea* Extract Sensitized Photooxygenation of 1,6-Dihydroxynaphthalene at 0 Hours

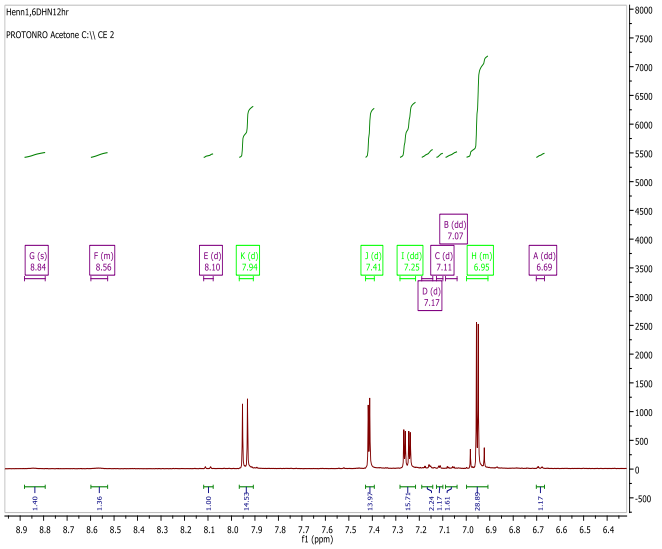

Figure 4.51: *Carpolobia lutea* Extract Sensitized Photooxygenation of 1,6-Dihydroxynaphthalene at 12 Hours

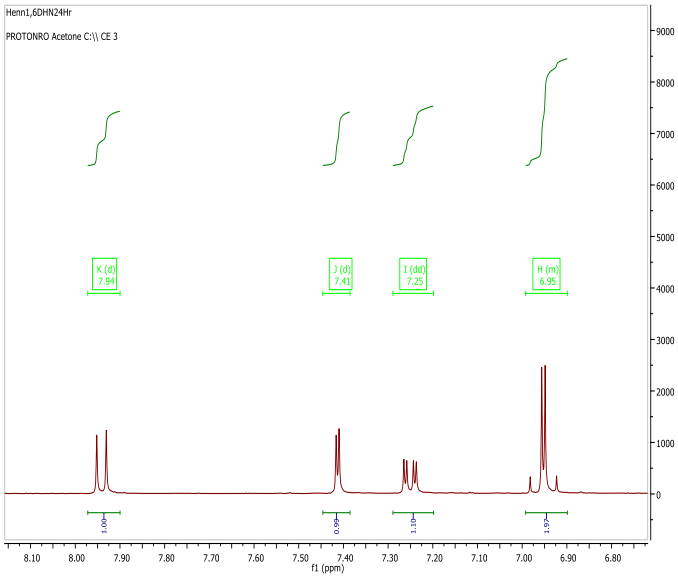

Figure 4.52: *Carpolobia lutea* Extract Sensitized Photooxygenation of 1,6-Dihydroxynaphthalene at 24 Hours

Figure 4.53 is a line graph that summarizes the rose bengal and *Carpolobia lutea* sensitized photooxygenation of 1,6-dihydroxynaphthalene. For the rose bengal sensitized reaction, 100% conversion was observed after 4 hours while *Carpolobia lutea* extract sensitized reaction showed 100% conversion after 24 hours.

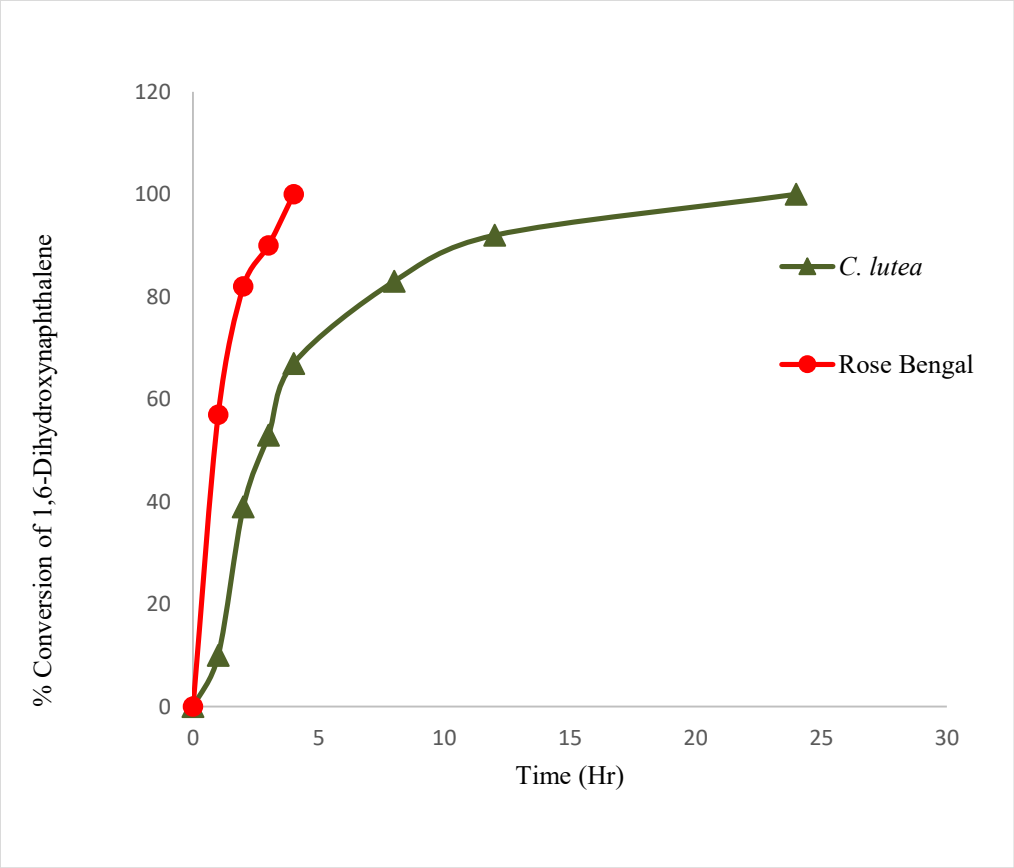

Figure 4.53: Photooxygenation of 1,6-Dihydroxynaphthalene using Rose Bengal and *Carpolobia lutea* Extract as Photosensitizers.

Column chromatography of the solvent-stripped rose bengal and *C. lutea* extract-sensitized reaction mixtures gave 6-hydroxy-1,4-naphthoquinone (**6**) in 47% and 12% yields, respectively.

4.6.1 1,6-Dihydroxynaphthalene Photooxygenation Replicate Result Summary

Table 4.7 shows the mean conversion value and mean yield value for the replicate photooxygenations of 1,6-Dihydroxynaphthalene using rose bengal and *Carpolobia lutea* extract, respectively. Details of the ^{1}H NMR spectra used for monitoring the replicate reactions are in appendices 16 and 17. Rose bengal and *Carpolobia lutea* extract gave 100% conversion each after 12 hours of irradiation but rose bengal gave a lower mean yield of 50.5 ± 1.34 than *Carpolobia lutea* extract which gave a mean yield of 57.9 ± 2.39.

Table 4.7: 1,6-Dihydroxynaphthalene Photooxygenation Replicates Result Summary

Photosensitizers	%Conversion after 12 Hours Iradiation[a] (Mean Value ± SD)	%Yield[b]
Rose bengal	100 ± 0.00	50.5 ± 1.34
C. lutea	100 ± 0.00	57.9 ± 2.39

[a] Determined by ^{1}H NMR analysis (± 2%).[b]Isolated yield after column chromatography.

The ^{1}H NMR spectrum (400MHz, $(CD_3)_2CO$) of 6- Hydroxy-1,4-naphthoquinone (6) had signals at δ6.95 (2H, q, J = 8 Hz, A), δ7.25 (1H, dd, J = 4, 12 Hz, B), δ7.41 (1H, d, J = 0 Hz, C), δ7.94 (1H, d, J = 8Hz, D), δ9.98 (1H, s, E) (Figure 4.54).

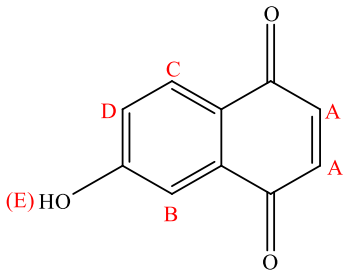

6: Chemical Structure of 6-Hydroxy-1,4-naphthoquinone

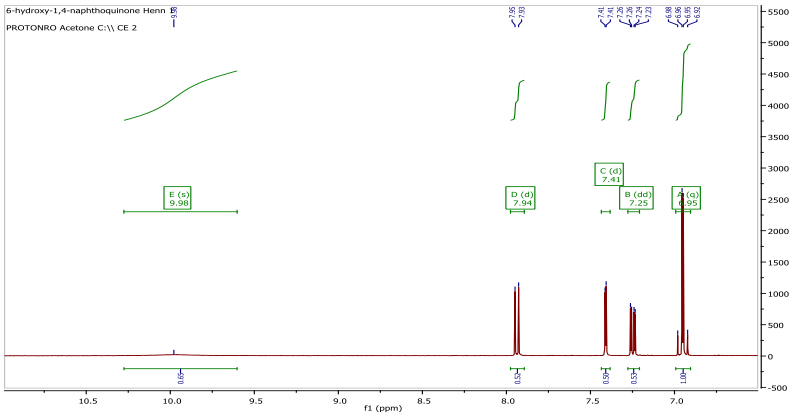

Figure 4.54: ^{1}H NMR Spectrum of Pure Synthesized 6-Hydroxy-1,4-Napthoquinone Acquired in $(CD_3)_2CO$

4.7 Photooxygenation of α-Pinene

In the autoxidation of α-pinene as described in section 3.10, the reactant decreased from 96.7% (RT 8.07 minutes) to 93.8% and the GC-FID of the reaction mixture indicated 1% product (pinocarvone, RT 15.6 minutes) formation after 24 hours of photooxygenation (Figures 4.55 and 4.56). By comparison, in the photooxygenation reaction with Tetraphenyporphyrin as sensitizer, the reactant in the reaction mixture reduced from 95.8% to 3.9% after 24 hours while the pinocarvone (**7**) produced increased from 0.6% to 94.6% (Figures 4.57 and 4.58). In the *C. lutea* extract-sensitized reaction mixture after 24 hours, α-pinene decreased from 92.8% to 3.9% and the product increased from 3.9% to 90.4% (Figures 4.59 and 4.60). Hourly percentage compositions (by GC) of α-pinene and pinocarvone (**7**) products in the TPP and *C. lutea* extract-sensitized photooxygenation reactions are shown in Figures 4.61 and 4.62, respectively.

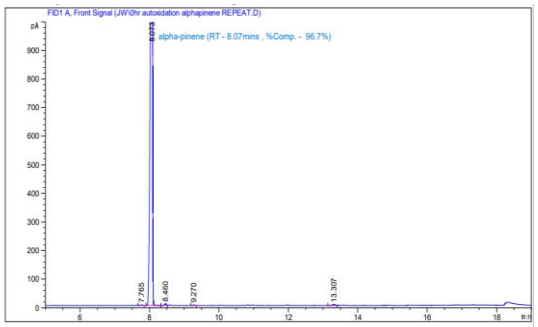

Figure 4.55: Chromatogram for Monitoring the Autoxidation of α-Pinene at 0 Hours

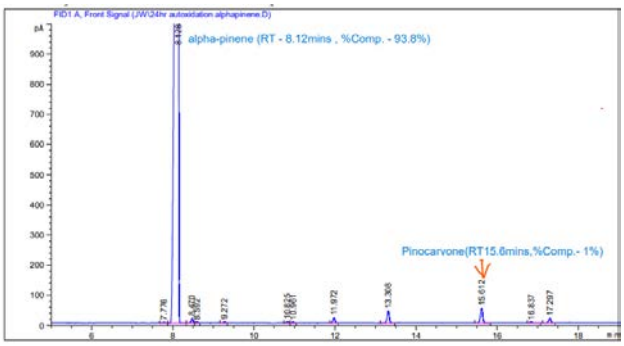

Figure 4.56: Chromatogram for Monitoring the Autoxidation of α-Pinene at 24 Hours

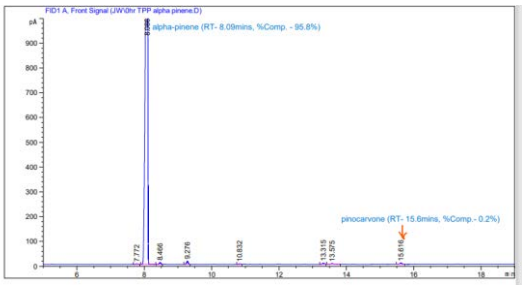

Figure 4.57: Chromatogram for Monitoring the Tetraphenylporphyrin Sensitized Photooxygenation of α-Pinene at 0 Hour

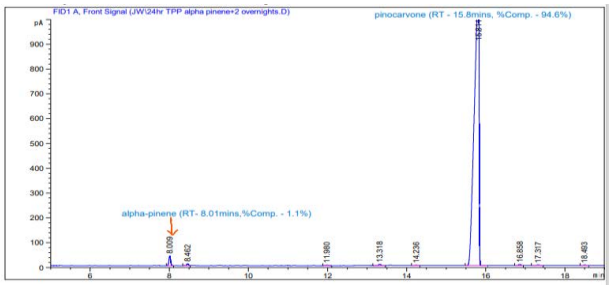

Figure 4.58: Chromatogram for Monitoring the Tetraphenylporphyrin Sensitized Photooxygenation of α-Pinene After 24 Hour

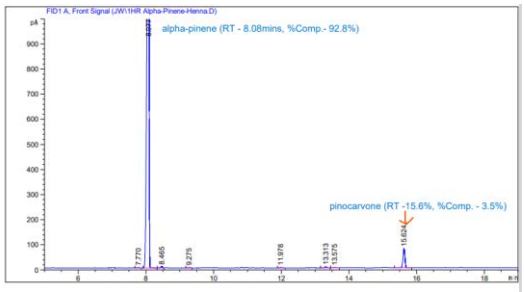

Figure 4.59: Chromatogram for Monitoring the *C. lutea* Extract Sensitized Photooxygenation of α-Pinene at 0 Hour

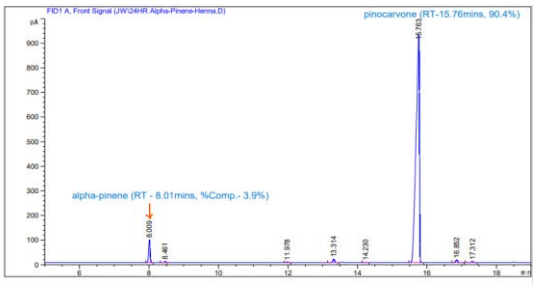

Figure 4.60: Chromatogram for Monitoring the *C. lutea* Extract Sensitized Photooxygenation of α-Pinene at 24 Hour

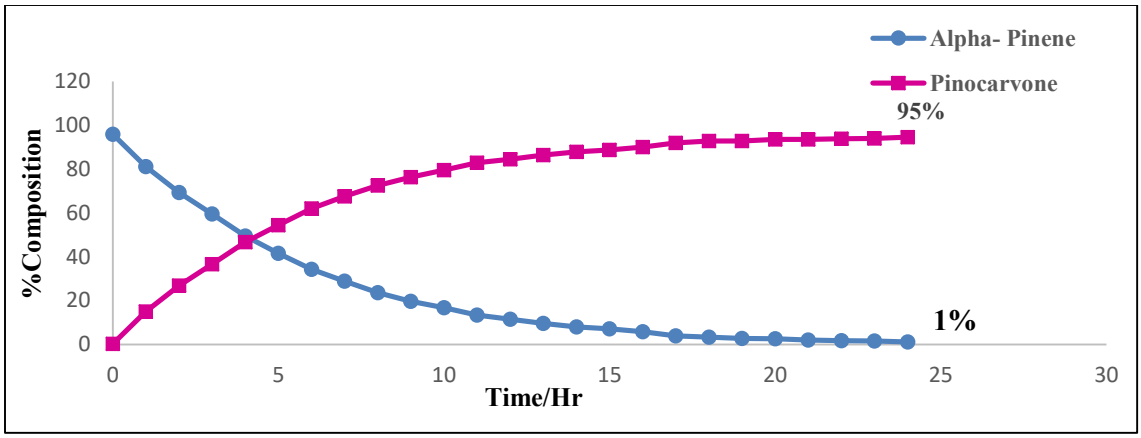

Figure 4.61: α-Pinene and Pinocarvone Concentrations with Reaction Time in the TPP Sensitized Photooxygenations.

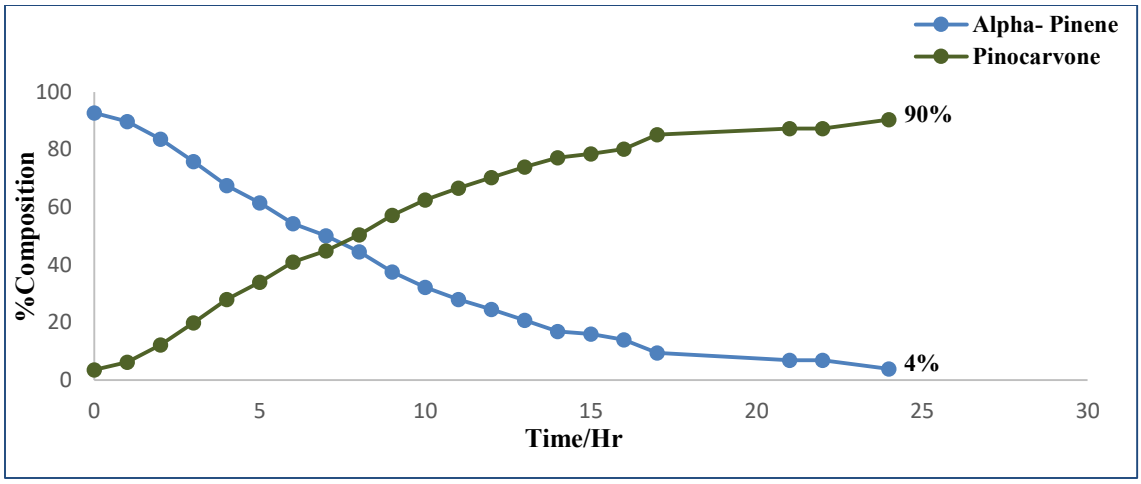

Figure 4.62: α-Pinene and Pinocarvone Concentrations with Reaction Time in the *C. lutea* sensitized Photooxygenations

During the workup as described in section 3.10, synthesized pinocarvone (**7**) was lost. Mean conversions and isolated yields as depicted in Table 4.8 were obtained from replicate photooxygenations of α-pinene.

4.7.1 α-Pinene Photooxygenation Replicate Result Summary

Table 4.8 shows the mean conversion values and yield values for the replicate photooxygenation of α-pinene using tertraphenylporphyrin and *Carpolobia lutea* extract as photosensitizers, respectively. The GC chromatograms are in appendices 18 and 19. Table 4.8 shows that tetraphenylporphyrin (73% ± 5.66) gave a lower mean composition value of pinocarvone (**7**) than *Carpolobia lutea* extract (88.5% ± 2.12). After work-up, rose bengal gave a 0.7% isolated yield while *Carpolobia lutea* extract gave a 3.0% yield.

Table 4.8: α-Pinene Photooxygenation Replicates Result Summary

Photosensitizers	%Composition after 24 Hours Irradiation[a] (Mean Value ± SD)	%Yield[b]
Tetraphenylporphyrin	73 ± 5.66	0.7% (0.05g)
C. lutea	75 ± 0.00	3.0% (0.22g)

[a] Determined by ^{1}H NMR analysis (± 2%). [b]Isolated yield after column chromatography.

Work-up of the reaction mixture as described in section 3.10 gave the product identified as pinocarvone (**7**) with signals of its ^{1}H NMR spectrum (400 MHz, $CDCl_3$) at δ 0.74 (3H, s, A), δ1.22 (1H, d, J = 8Hz, B), δ1.29 (3H, s, C), δ2.00 (1H, s, D), δ2.42 - δ2.46 (1H, d, J = 4Hz, EF), δ2.57 (1H, t, J = 4Hz, G), δ2.62 (1H, tdd, H), δ2.70 (1H, t, J = 4Hz, I), δ4.93 (1H, d, J = 4Hz, J), δ5.86 (1H, d, J = 4Hz, K) (Figure 4.63).

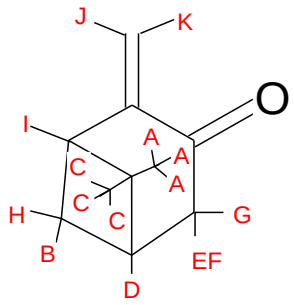

7: Chemical Structure of Pinocarvone

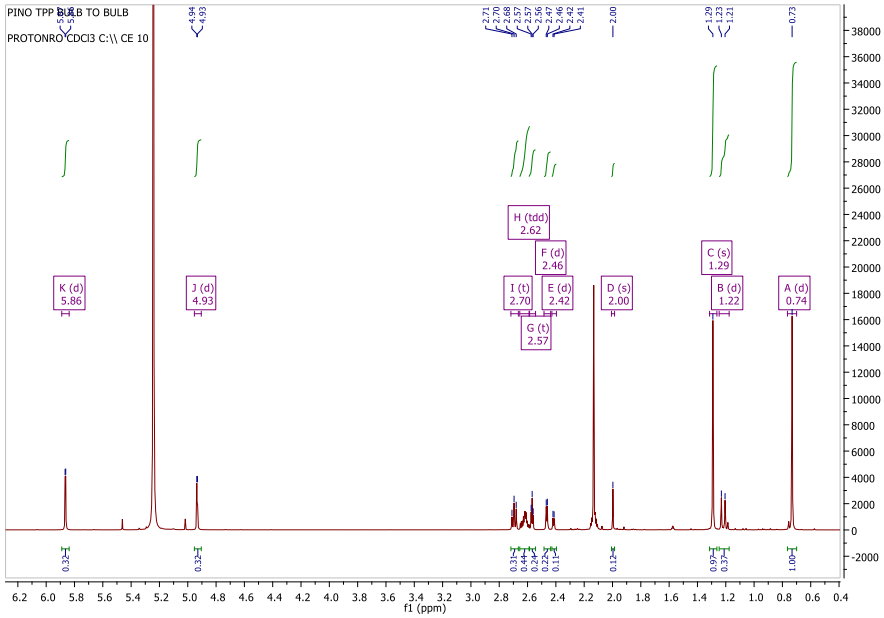

Figure 4.63: ^{1}H NMR Spectrum of Synthesized Isolated Pinocarvone acquired in $CDCl_3$

4.8 Photooxygenation of β-Pinene

β-pinene was photooxygenated as described in section 3.10. In its reaction without sensitizer (i.e. autoxidation), the composition of the substrate by GC (RT 9.35 minutes) in the reaction mixture decreased from 94.2% to 90.7% in 48 hours, and the product (myrtenal RT 16.85 minutes), which was initially undetectable increased to 1.5% (Figure 4.64 and 4.65). Photooxygenations with TPP as a sensitizer reduced the composition of β-pinene from 94.7% to 4.5% (RT 9.41) while the product increased from 0.3% to 82.9% (RT 16.98) after 48 hours of reaction (Figures 4.66 and 4.67)

In the *C. lutea* extract-sensitized reaction mixture, after 48 hours, the composition of β-pinene decreased from 94.9% to 13.0% (RT 9.41 minutes) and the product (RT 17.02 minutes) increased from 0.2% to 76.6% (Figures 4.68 and 4.69). The percentage compositions of the β-pinene substrate and myrtenal (**8**) product using TPP and *C. lutea* extract as sensitizers within 48 hours photoxygenation are represented in Figures 4.70 and 4.71, respectively.

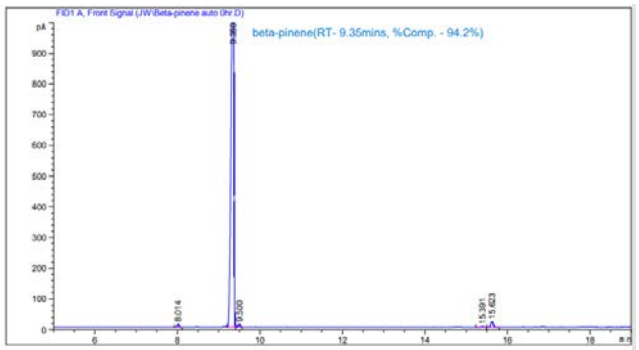

Figure 4.64: Chromatogram for Monitoring the Autoxidation of β-pinene at 0 Hour

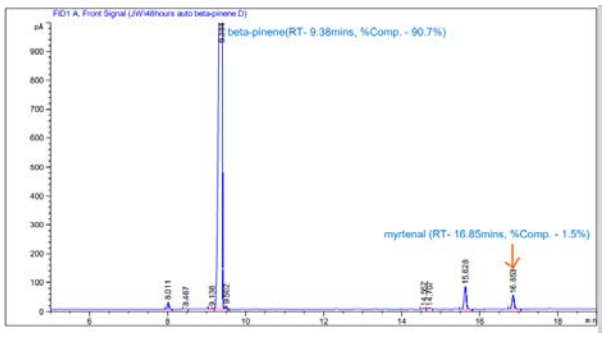

Figure 4.65: Chromatogram for Monitoring the Autoxidation of β-pinene after 48 Hours

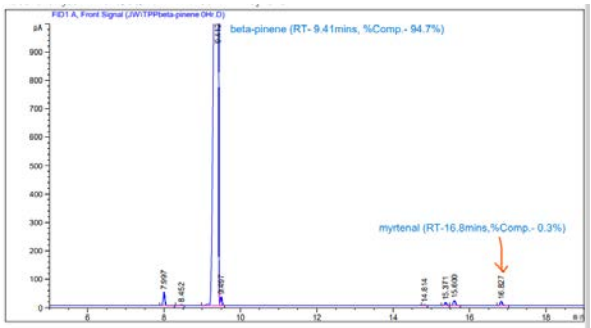

Figure 4.66: Chromatogram for Monitoring the Tetraphenylporphyrin Sensitized Photooxygenation of β-pinene at 0 hour

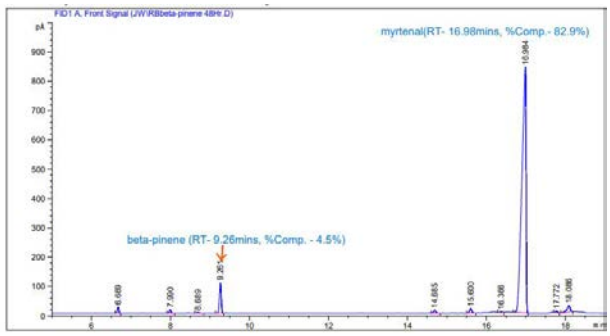

Figure 4.67: Chromatogram for Monitoring the Tetraphenylporphyrin Sensitized Photooxygenation of β-pinene at 48 Hour

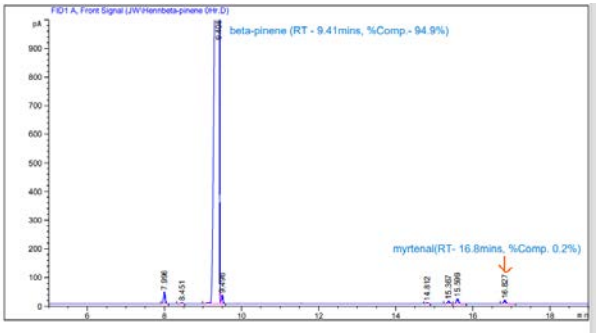

Figure 4.68: Chromatogram for Monitoring the *Carpolobia lutea* Extract Sensitized Photooxygenation of α-Pinene at 0 Hour

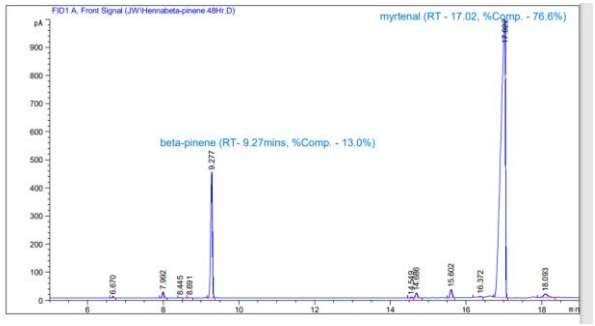

Figure 4.69: Chromatogram for Monitoring the *Carpolobia lutea* Extract Sensitized Photooxygenation of β-Pinene After 48 Hour

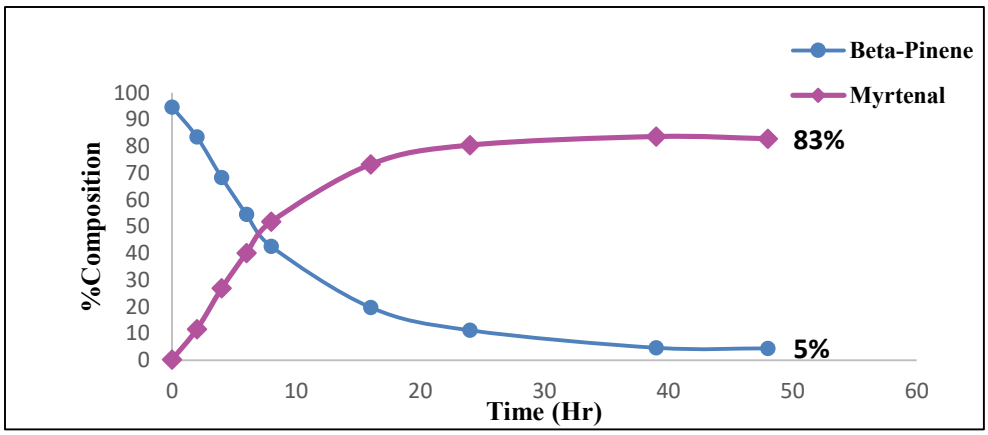

Figure 4.70: Photooxygenation of β-pinene using Tetraphynylporphyrin as Photosensitizer

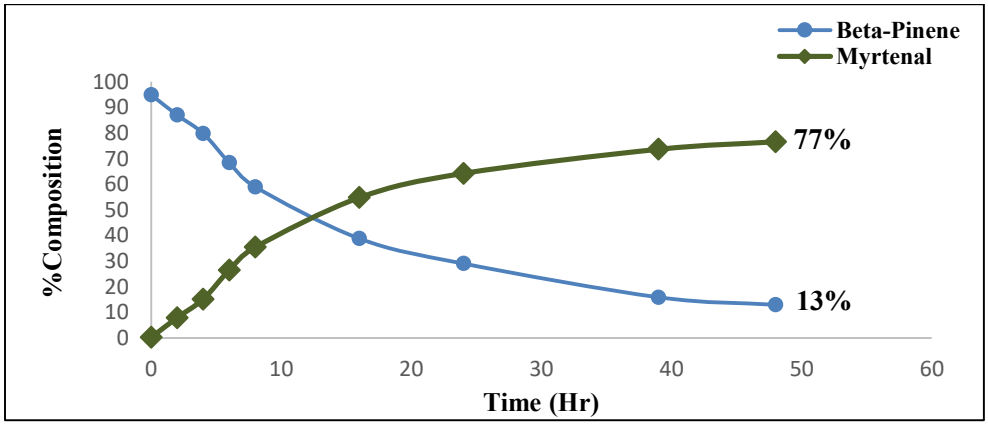

Figure 4.71: Photooxygenation of β-pinene using *Carpolobia lutea* Extract as Photosensitizer

During the workup as described in section 3.10, synthesized myrtenal (**8**) was lost. Mean conversions and isolated yields as shown in Table 4.9 were obtained from replicate photooxygenations of β-pinene.

4.8.1 β-pinene Photooxygenation Replicate Result Summary

Table 4.9 shows mean values of replicate results for the photooxygenation of β-pinene using tetraphenylporphyrin and *Carpolobia lutea* extract. Details of the GC chromatograms are in appendices 20 and 21. Tetraphenylporphyrin gave a higher mean composition value of myrtenal (**8**) (90 ± 4.24) while *Carpolobia lutea* extract gave a lower mean composition value of 88.5 ± 2.12.

The percentage yield of the myrtenal (**8**) product with tetraphenylporphyrin photosensitizer was 5% and that of *Carpolobia lutea* extract was 7%.

Table 4.9: β-pinene Photooxygenation Replicates Result Summary

Photosensitizers	%Composition after 48 Hours Irradiation[a] (Mean Value ± SD)	%Yield[b]
Tetraphenylporphyrin	90 ± 4.24	5.2% (0.38g)
C. lutea	88.5 ± 2.12	7.2% (0.53g)

[a] Determined by ^{1}H NMR analysis (± 2%). [b]Isolated yield after column chromatography.

Work-up as described in section 3.10 gave the isolated product whose ^{1}H NMR (400 MHz, $CDCl_3$) spectrum displayed the following signals (Figure 4.72a) that were comparable to those of authentic myrtenal (**8**) (Figure 4.72b): δ0.73 (3H, s, A), δ1.03 (1H, d, J = 8 Hz, B), δ1.33 (3H, s, C), δ2.17 (1H, m, D), δ2.45 (1H, dt, J = 16 Hz, E), δ2.57 (dt, J = 8 Hz, 4Hz, F), δ2.64 (1H, t, J = 4 Hz, G), δ2.78 (1H, td, J = 4 Hz, H), δ6.76 (1H, s, I), δ9.42 (1H, s, J).

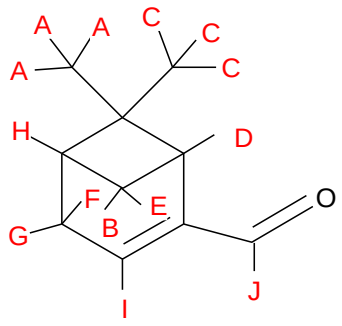

8:
Chemical Structure of Myrtenal

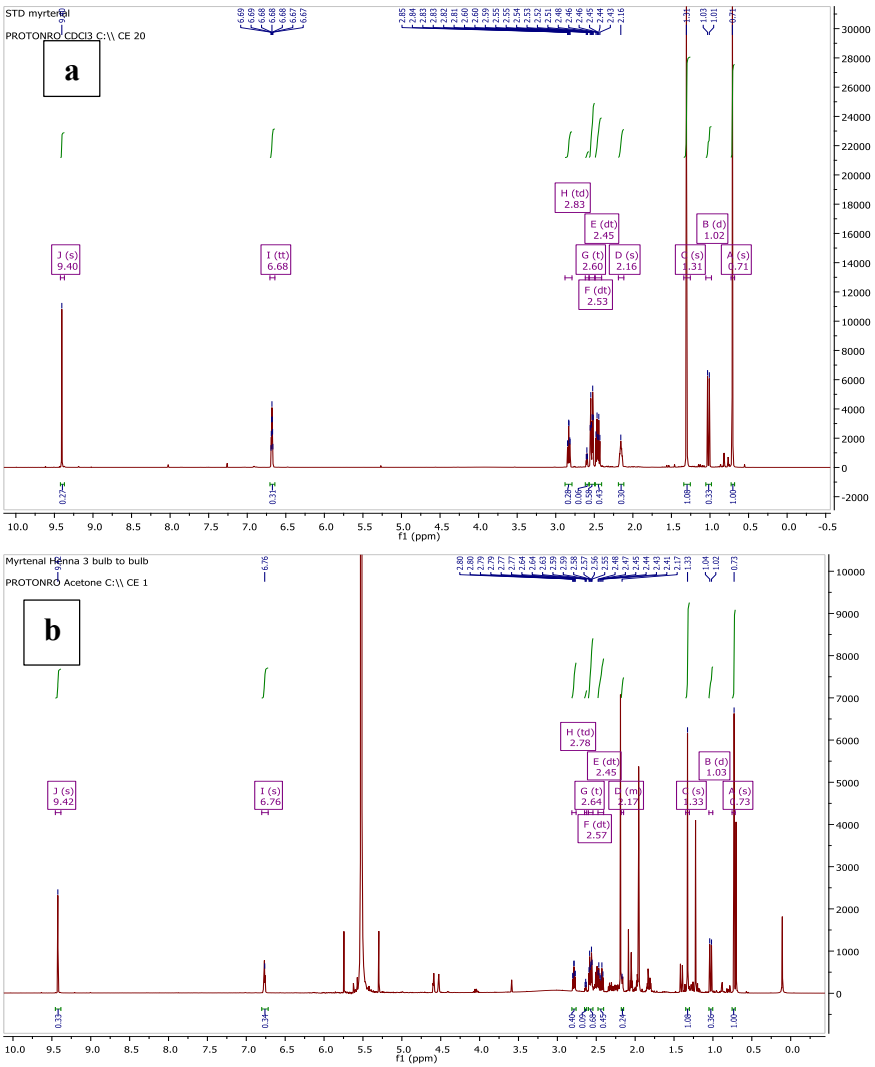

Figure 4.72 ^{1}H NMR Spectrum acquired in $CDCl_3$ (a) Synthesized Isolated Myrtenal and (b) Authentic Myrtenal

4.9 Absorbance of the Dyes and Plant Extract

Figures 4.73 and 4.74 show the absorbance measurements (as described in section 3.12) of the rose bengal and methylene blue plotted against the spectral emission of the 8 W cool white fluorescent tube. Figure 4.73 shows that rose bengal gave a peak absorbance between 482 nm and 587 nm wavelength range with the highest absorbance of 1.50 at 557 nm while methylene blue (Figure 4.74) showed an absorbance peak between 545 nm and 700 nm wavelength range with the highest absorbance value of 1.50 at 658 nm.

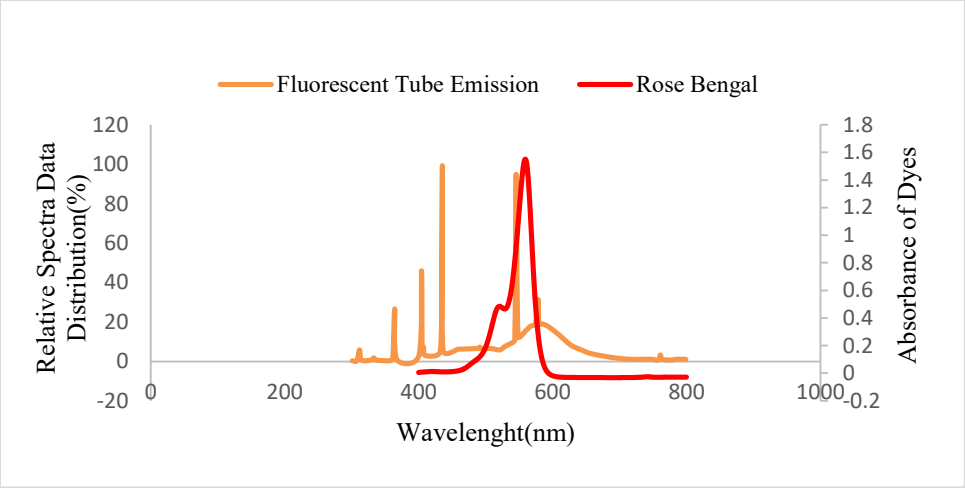

Figure 4.73: Absorption Spectrum of Rose Bengal Matched with the Emission Spectrum of the 8 W Cool White Fluorescent Tube

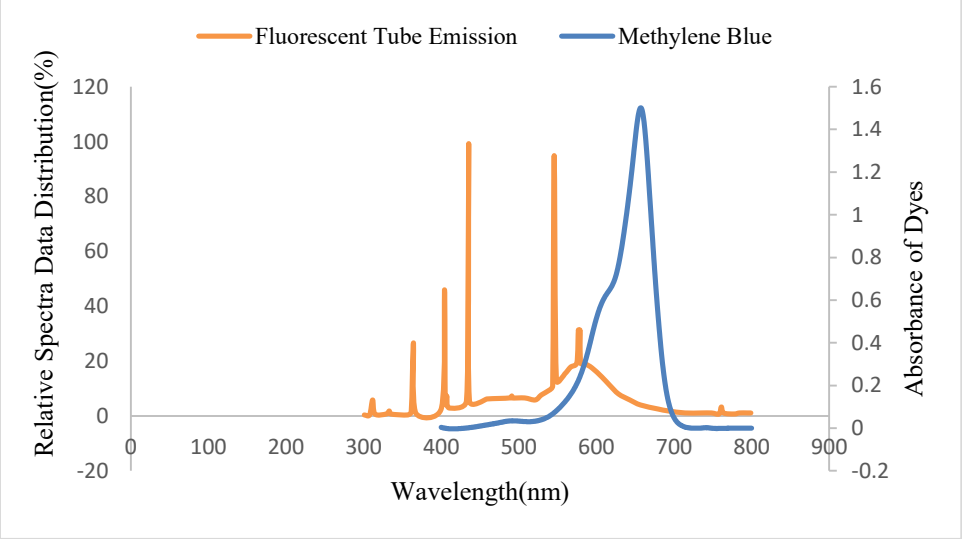

Figure 4.74: Absorption Spectrum of Methylene Blue Matched with the Emission Spectrum of The 8W Cool White Fluorescent Tube

The absorbance measurement for tetraphenylporphyrin (Figure 4.75) showed several peaks between 400 nm and 658 nm, the highest peak occurring at 421 nm with an absorbance value of 2.97 and other smaller peaks at : (513 nm, 0.45), (551 nm, 0.18), (589 nm, 0.14) and (646 nm, 0.12).

The cool white fluorescent tubes had relative spectra emission distribution data (%) occurring from 400 nm to 679 nm. There were several peaks on the broad emission band, the highest of them occurring at 435 nm with a value of 99.27%. All three commercial dyes had their absorbance peaks overlapping with the spectral emission peak of the fluorescent tube (Figure 4.76).

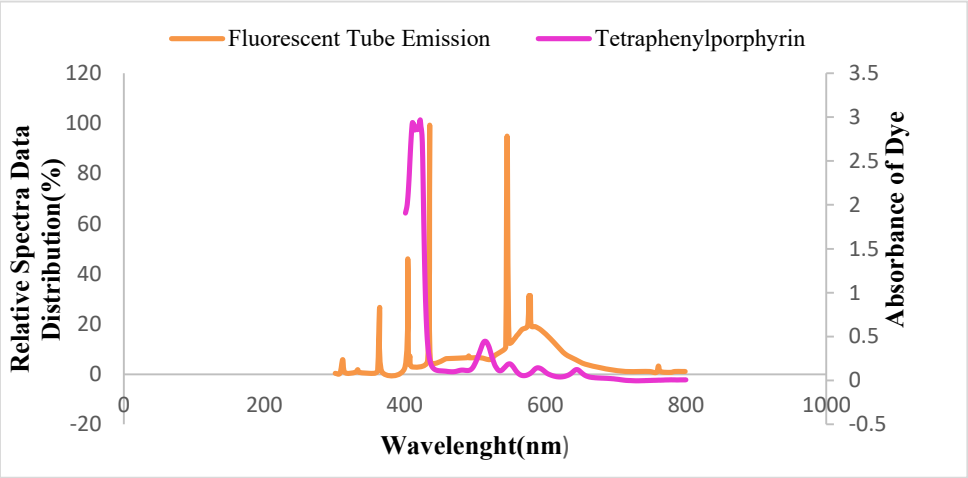

Figure 4.75: Absorption Spectrum of Tetraphenylporphyrin Matched with the Emission Spectrum of the 8 W Cool White Fluorescent Tube

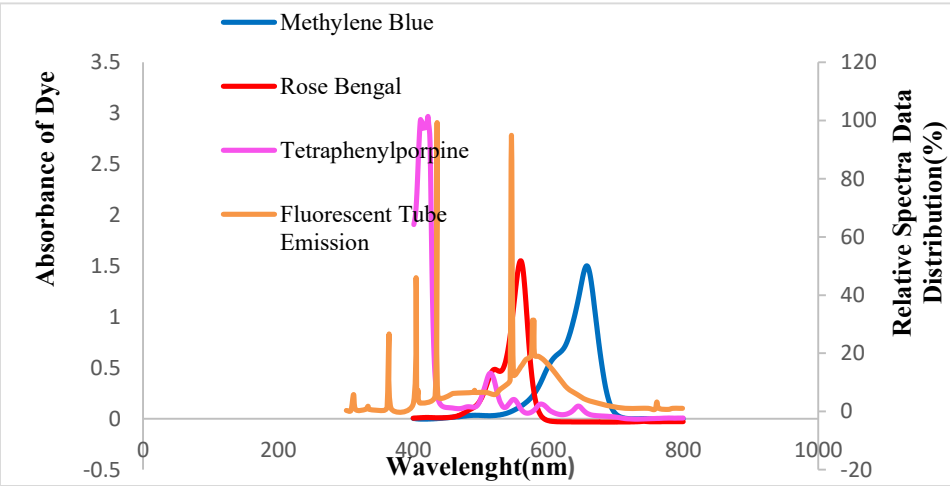

Figure 4.76: Absorption Spectrum of Three Conventional Dyes (Rose Bengal, Methylene Blue and Tetraphenylporphyrin) Matched with the Emission Spectrum of the 8 W Cool White Fluorescent Tube

Figure 4.77 and Figure 4.78 show respectively the absorbance measurements of *H. sabdariffa* extract and *C. lutea* extract each plotted against the spectral emission of the 8 W cool white fluorescent tube. Figure 4.77 shows that *Hibiscus sabdariffa* extract gave an absorbance peak between 440 nm and 676 nm wavelength range with the highest absorbance value of 0.39 occurring at 542 nm while *Carpolobia lutea* extract (Figure 4.78) showed an absorbance peak between 639 nm and 686 nm wavelength range with the highest absorbance value of 1.88 at 665 nm.

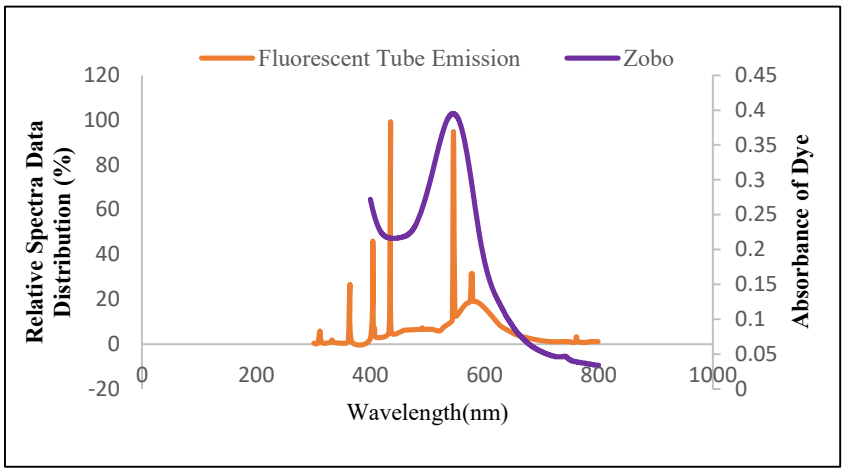

Figure 4.77: Absorption Spectrum of *Hibiscus sabdariffa* Extract Matched with the Emission Spectrum of the 8 W Cool White Fluorescent Tubes.

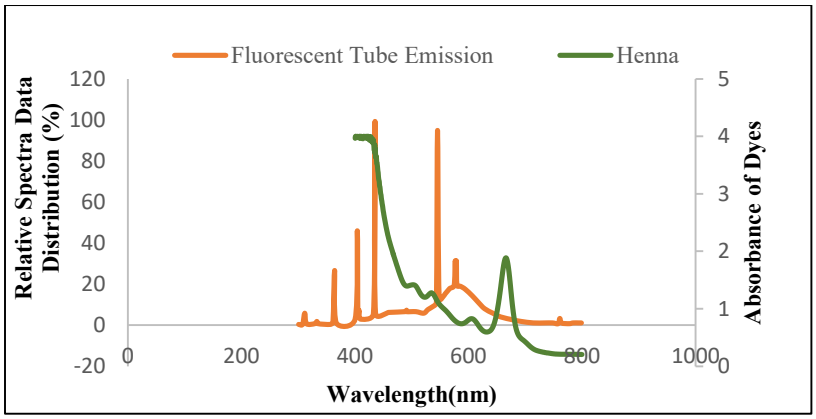

Figure 4.78: Absorption Spectrum of *Carpolobia lutea* Extract Matched with the Emission Spectrum of the 8 W Cool White Fluorescent Tube

The absorbance measurement for *Justicia secunda* (Figure 4.79) showed a broad peak between 521 nm and 645 nm, the highest point on the peak occurring at 602 nm with an absorbance value of 0.15. All three plant extracts had their absorbance peaks occurring within the spectral emission region of the fluorescent tube (Figure 4.80).

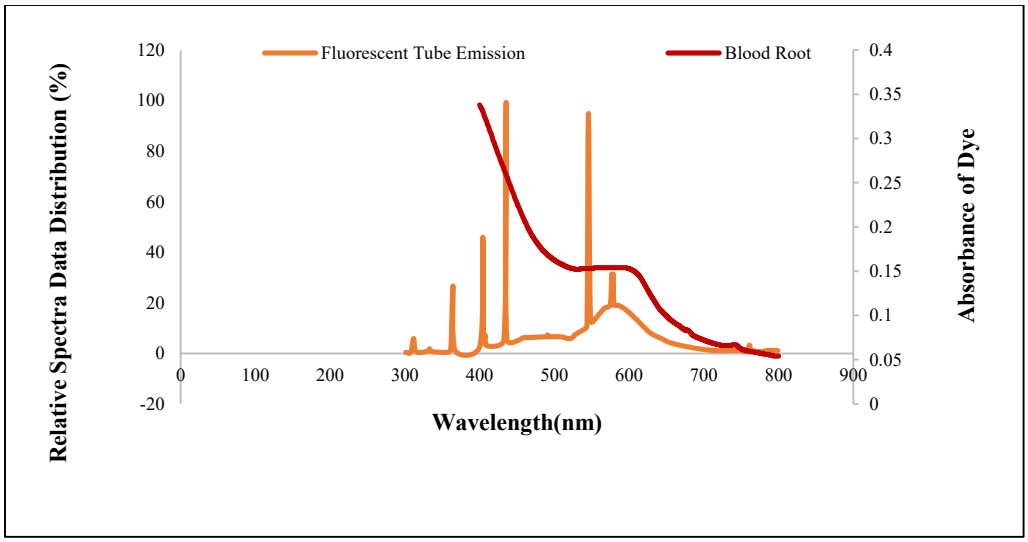

Figure 4.79: Absorption Spectrum of *Justicia secunda* Extract Matched with the Emission Spectrum of the 8 W Cool White Fluorescent Tube

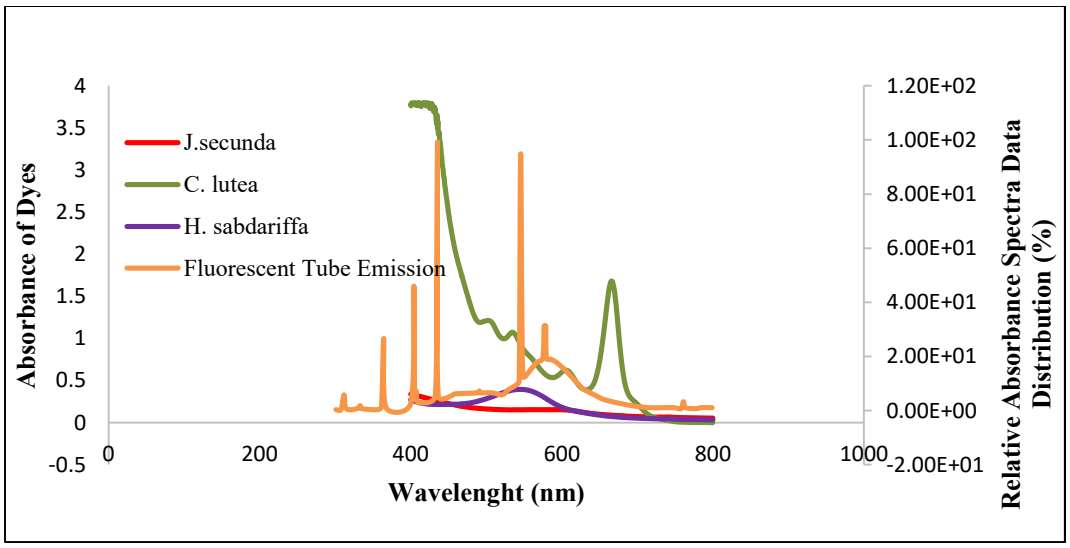

Figure 4.80: Absorption Spectra of *H. sabdariffa Extract, C. lutea* Extract (-0.2) and *J. secunda* Extract Matched with the Emission Spectrum of the 8 W Cool White Fluorescent Tube

4.10 Photostability of Dyes

4.10.1 Photostability of Rose Bengal in Isopropanol

Figure 4.81 shows the UV absorption spectra of rose bengal dissolved in isopropanol and irradiated for 24 hours as set out in section 3.13.

The highest absorbance peak, which occurs at 486 nm – 598 nm was reduced in intensity from 0.34 (561 nm) to 0.12 after 24 hours of irradiation (Figure 4.81) representing a photostability reduction rate of 2.7%/hr. The pink colour of the solution appeared visibly slightly bleached after 24 hours of irradiation (Plate 4.3).

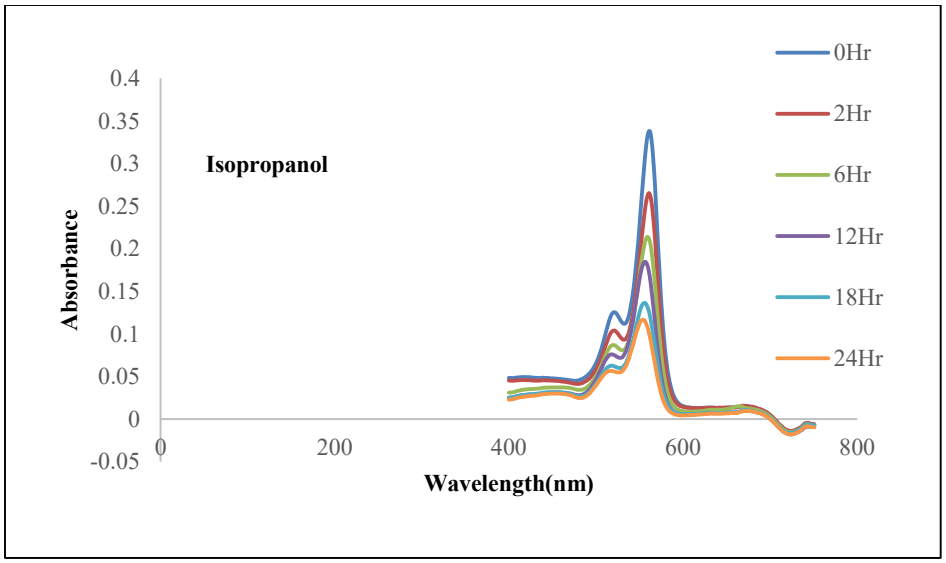

Figure 4.81: Variation of Absorbance Values of Rose Bengal in Isopropyl Alcohol During 24 Hours of Irradiation

before	after

Plate 4.3: Colour of Isopropyl Alcohol Solution of RB, Before and After 24 Hours of Irradiation

4.10.2 Photostability of *Carpolobia lutea* Extract in Isopropanol

In the irradiation of a solution of *C. lutea* extract, as described in section 3.13, the highest absorbance of 0.06 (670 nm) decreased to 0.04 (670 nm) during 24 hours of irradiation (Figure 4.82), representing a photostability reduction rate of 1.4 %/hr. Also, the brown colour of the solution appeared visibly slightly photobleached (see Plate 4.4).

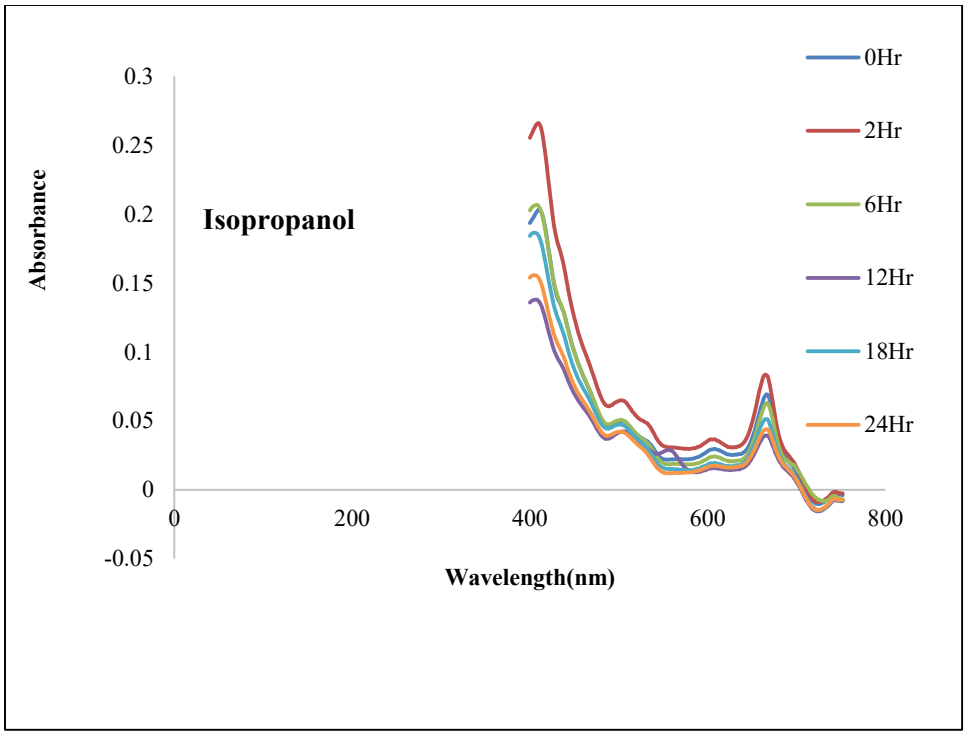

Figure 4.82: Variation of Absorbance Values of *C. lutea* Extract in Isopropyl Alcohol During 24 Hours of Irradiation

before	after

Plate 4.4: Colour of Isopropyl Alcohol Solution of *C. lutea*, Before and After 24 Hours of Irradiation

4.10.3 Photostability of Methylene Blue in Acetonitrile

Figure 4.83 shows the UV absorption spectra of methylene blue dissolved in acetonitrile, irradiated for 24 hours as described in section 3.14. The λ_{max} (1.59) at 654 nm shifted to 650 nm after 24 hours of irradiation and there was virtually no change in absorbance value , although the blue colour was visibly slightly bleached (Plate 4.5).

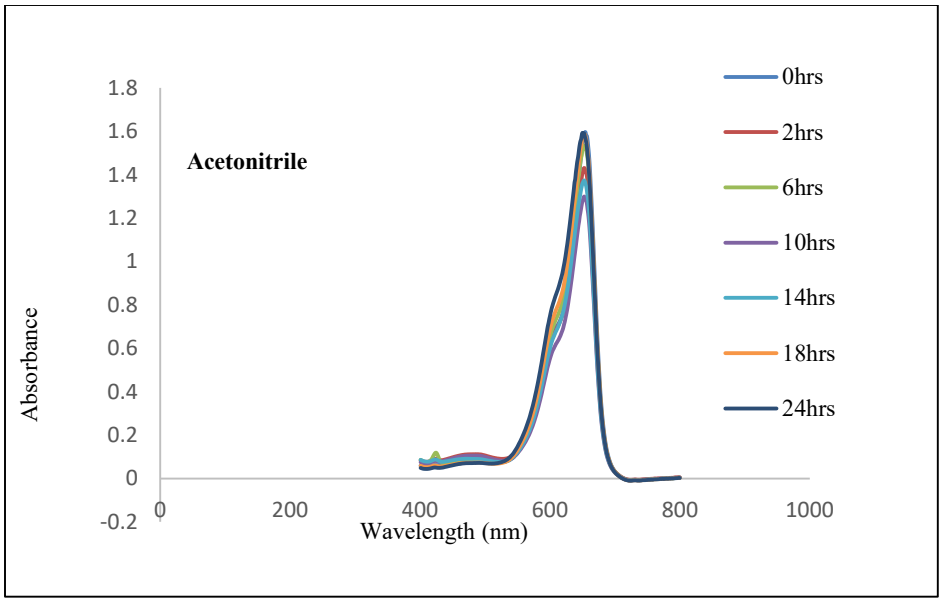

Figure 4.83: Variation of Absorbance Values of Methylene Blue in Acetonitrile During 24 Hours of Irradiation

before	after

Plate 4.5: Colour of Acetonitrile Solution of Methylene blue, Before and After 24 Hours of Irradiation

4.10.4 Photostability of *Carpolobia lutea* Extract in Acetonitrile

Irradiation of acetonitrile solution of *Carpolobia lutea* extract as described in section 3.14 for 24 hours resulted in a slight shift of λ_{max} from 662 nm to 665 nm and a reduction of absorbance value from 0.10 to 0.034 (Figure 4.84) representing a photostability reduction rate of 2.75%/hr. The solution was visibly slightly photobleached going from a green color to a bright gold colour (Plate 4.6).

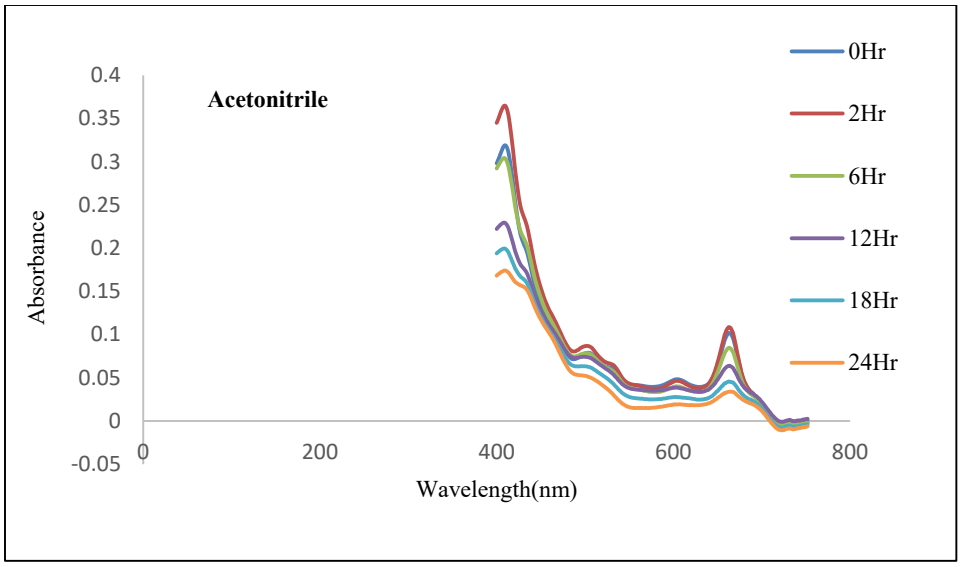

Figure 4.84: Variation of Absorbance Values of *C. lutea* in Acetonitrile During 24 Hours of Irradiation

before	after

Plate 4.6: Colour of Acetonitrile Solution of *C. lutea,* Before and After 24 Hours of Irradiation

4.10.5 Photostability of Tetrraphenylporphyrin in Dichloromethane

A solution of TPP in dichloromethane was irradiated as described in section 3.15. After 24 hours of irradiation, absorbance values of peaks that were at 421 nm (2.97), 513 nm (0.45), 551 nm (0.18), 589 nm (0.14) and 646 nm (0.12) wavelengths initially diminished while new peaks appeared at 417 nm (1.24), 447 nm (2.21) and 662 nm (0.30) (Figure 4.85). The pink colour of TPP in acetonitrile turned lemon green after irradiation for 24 hours (Plate 4.7).

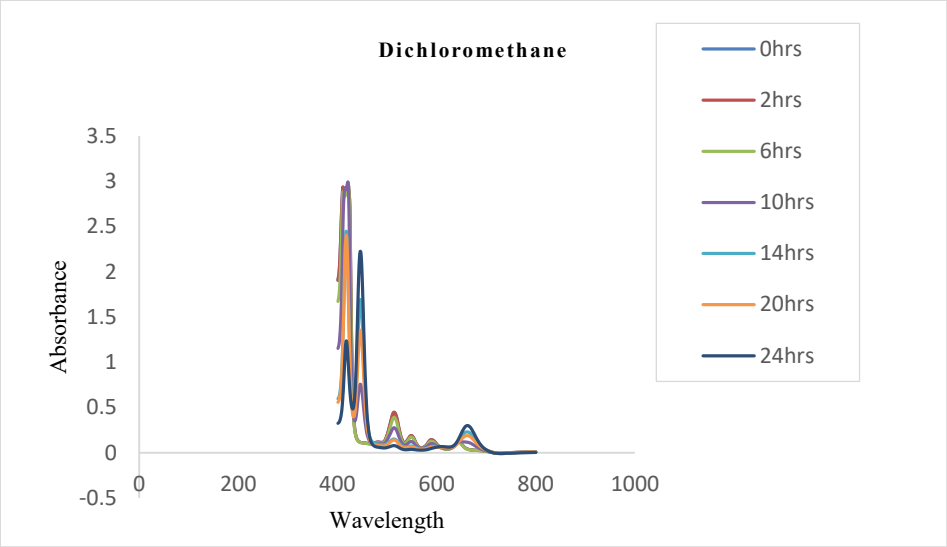

Figure 4.85: Variation of Absorbance Values of Tetraphenylporphyrin in Dichloromethane During 24 Hours of Irradiation

before	after

Plate 4.7: Tetraphenylporphyrin in Dichloromethane at 0 Hour and After 24 Hours Irradiation

4.10.6 Photostability of *C. lutea* Extract in Dichloromethane

On irradiating a solution of *Carpolobia lutea* extract in dichloromethane for 24 hours as described in section 3.15, absorbance of the peak at 670 nm wavelength decreased from 0.15 to 0.02 (Figure 4.86) representing a photostability reduction rate of 3.63%/hr while the colour changed from greenish brown to golden (Plate 4.8).

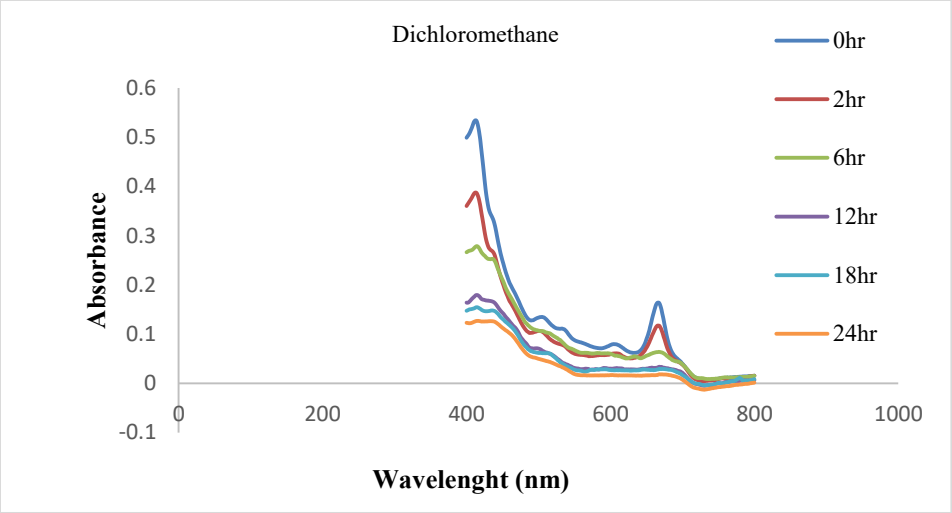

Figure 4.86: Variation of Absorbance Values of *C. lutea* in Dichloromethane During 24 Hours of Irradiation

before	after

Plate 4.8: *C. lutea* in Dichloromethane at 0 Hour and After 24 Hours Irradiation

4.11 Fractions from VLC of *Carpolobia lutea* Extract

Details of VLC fractions of *C. lutea* obtained by the procedure described in section 3.16 are shown in Table 4.10. 18 fractions were obtained from the fractionation of the photoactive *C. lutea* extract with their colours as different shades of yellow, gold and brown. The percentage weight of the fractions showed that fraction 10 had the lowest %weight at 2.0 while fraction 3 had the highest %weight at 16.0.

Table 4.10 Weight of Fractions from VLC of *Carpolobia lutea* Extract

Fraction	%Weight	Colour
1	3.3	Light Yellow
2a	4.7	Yellow
2b	8.0	Golden Yellow
2c	4.0	Old Gold
2d	5.3	Army Green
3	16.0	Army Green
4a	3.3	Army Green
4b	4.7	Army Green
5	5.3	Metallic Gold
6a	5.3	Metallic Gold
6b		Metallic Gold
7	7.3	Metallic Gold
8	2.6	Golden Brown
9	3.3	Metallic Gold
10	2.0	Pecan Brown
11	3.3	Metallic Brown
12	4.7	Brown
13	8.0	Light Gold

4.11.1 Photooxygenation of α-Terpinene using VLC Fractions

Methylene Blue and VLC fractions of *C. lutea* obtained by the procedure described in section 3.16 were used as photosensitizers in the photooxygenation of α-terpinene as described in section 3.17. GC-MS chromatogram of the reaction mixture showed that α-terpinene (RT 7.08 minutes) which was initially 48.5% was converted to ascaridole (**3**) product (RT 10. 97 minutes), which was composed of 49.5% of the reaction mixture in the methylene blue synthesized photooxygenation.

4.11.2 Photoactivity of Methylene Blue and VLC Fractions of *Carpolobia lutea* Extract

A summary of percentage composition (by GC-MS) of α-terpinene, *p*-cymene and ascaridole (**3**) in the reaction mixtures of the photooxygenation reactions using methylene blue and *C. lutea* extract VLC fractions as photosensitizers are shown in Table 4.11. Details of the GC chromatograms of the fractions are in appendices 22 - 40. Of the VLC fractions-sensitized reactions, fraction 1 gave the lowest composition (2.38%) of ascaridole (**3**) product after 90 minutes of photooxygenations while fraction 6 gave the highest product composition (50.2%). Fractions 2d – 9 gave product compositions higher than 40%.

Table 4.11: % Composition of Reaction Mixtures in the Photooxygenation of α-Terpinene using Methylene Blue and VLC fractions of *C. lutea* Extract as Photosensitizers

Fraction	α-Terpinene %Composition at 90 minutes[a]	*p*-Cymene %Composition at 90 minutes[a]	Ascaridole %Composition at 90 minutes[a]
Methylene Blue	0.35	16.93	49.47
1	45	17.19	2.38
2a	13.17	21.20	21.70
2b	2.93	26.89	33.00
2c	1.99	18.59	39.90
2d	1.85	19.10	46.03
3	3.75	15.61	41.87
4a	2.88	17.73	49.18
4b	0.39	16.84	45.24
5	3.47	6.71	42.70
6a	3.01	16.64	50.20
6b	3.90	17.09	47.34
7	0.3	16.77	48.21
8	5.75	5.59	46.33
9	0.23	16.90	49.57
10	25.25	17.47	21.74
11	16.99	16.78	32.23
12	30.65	15.76	16.12
13	43.12	16.66	11.08

[a] Determined by GC-FID analysis (± 2%).

4.12 HPLC-MS Result of *C. lutea* Extract VLC Fractions Active as Photosensitizers

Due to their capabilities to sensitize the formation of >40% ascaridole (**3**) production, fractions 2d, 3, 4, 5, 6, 7, 8 and 9 were selected for tentative identification of their components by HPLC-MS. The results obtained in the HPLC-MS of fractions 2d-5 are summarized in Table 4.12 and their corresponding chromatograms are summarized in appendices 41- 44. Similarly, the summary of HPLC-MS results for fractions 6 - 9 and their corresponding chromatograms are summarised in Table 4.13. See appendices 45 - 48 for the actual chromatograms.

Table 4.12: Summary of Fractions 2d, Fraction 3, Fraction 4 and Fraction 5 HPLC-MS Results

Fraction No.	Fraction 2d			Fraction 3			Fraction 4			Fraction 5		
Peak No.	RT (Minutes)	Fragment ions [M+H]	Tentative ID (MW)	RT (Minutes)	Fragment ions [M+H]	Tentative ID (MW)	RT (Minutes)	Fragment ions [M+H]	Tentative ID (MW)	RT (Minutes)	Fragment ions [M+H]	Tentative ID (MW)
1.	5.3	575, 592	Phenolic Derivatives - Phloroglucinol Derivative	2.4	-	Protocatechuic Acid	2.4	-	Protocatechuic acid	2.4	-	Protocatechuic acid
2.	6.5	289	Flavanone Derivative	4.1	-	Phenolic derivative	4.8	301	Flavanone Derivative	4.8	303	Flavanone derivative
3.	7.9, 8.1, 8.3	213, 243, 273	Phenolic derivative, Xanthone Derivatives	4.8	-	Flavanone Derivative	6.5	289	Flavanone Derivative	5.3, 5.5, 5.6, 5.8	289	Phenolic Derivative, Flavanone Derivatives
4.	9.6, 9.8	238, 257, 403, 289	Xanthone Derivatives	5.3, 5.8	179	Phenolic-Phloroglucinol Derivative	6.8, 7.2	287,105, 238, 256	Flavone, Terpenoid	6.2, 6.5, 6.8	289, 287	Flavanone, Flavonone Derivatives
5.	11.4	445, 423	Anthraquinone	6.5, 6.8	289, 287	Flavanone Derivative, Flavone	8.8, 7.2	301, 385, 403	Flavonoid Derivative, Triterpene Derivative	7.2 - 7.9	407, 377, 419	Phenolic and Phenolic Acid Derivatives

Table 4.12: Summary of Fractions 2d, Fraction 3, Fraction 4 and Fraction 5 HPLC-MS Results (*Continued)*

Fraction No.	Fraction 2d			Fraction 3			Fraction 4			Fraction 5		
Peak No.	RT (Minutes)	Fragment ions [M+H]	Tentative ID (MW)	RT (Minutes)	Fragment ions [M+H]	Tentative ID (MW)	RT (Minutes)	Fragment ions [M+H]	Tentative ID (MW)	RT (Minutes)	Fragment ions [M+H]	Tentative ID (MW)
6.	12.3, 12.6	403, 421, 439	Anthraquinone or Dianthrone Derivatives	7.5, 7.8, 8.2	275, 243, 273, 303	Xanthone, flavonone, Chromone Derivatives	11.2, 11.4	445, 423	Xanthone derivative, Anthraquinone	8.7, 9.5	385, 403	Phenolic Derivatives, Triterpene Derivative
7.	12.9, 13.2	507, 421,437	Triterpene, Dianthrone Derivatives	11.2 ,11. 4	423, 445	Xanthone or Chromone, Anthraquino ne Derivatives	12.6, 12.8	105, 238, 256, 507	Dianthrone, Triterpene derivatives	13.3	-	Phenolic derivative
8.	14.4, 14.8, 15.0	421, 439	Anthraquinone or Dianthrone Derivatives	12.9	507	Triterpene Derivative	13.5, 14.2	599, 629	Anthraquinone, Dianthrone Derivatives	17.6, 17.9	593	Chlorophyll Derivatives
9.	15.6	390, 421	Anthraquinone or Dianthrone Derivatives	14.5 ,14. 8,15 .0	405, 423	Dianthrone, Anthraquino ne Derivatives						
10.	16.0	390, 407, 424	Mixed peak – Anthraquinone and methoxy or prenyl flavone derivatives	15.6, 16.0	405, 421, 423, 651	Dianthrone, Anthraquino ne derivatives						

Table 4.13: Summary of Fractions 6, Fraction 7, Fraction 8 and Fraction 9 LCMS Results

Fraction No.	Fraction 6			Fraction 7			Fraction 8			Fraction 9		
Peak No.	RT (min)	Fragment ions [M+H]	Tentative ID (MW)	RT (min)	Fragment ions [M+H]	Tentative ID (MW)	RT (Min)	Fragment ions [M+H]	Tentative ID (MW)	RT (min)	Fragment [M+H]	Tentative ID (MW)
1	1.8	-	Gallic Acid Derivative	1.8	-	Gallic Acid Derivative	1.8	-	Gallic acid Derivative	1.8	-	Gallic Acid Derivative
2.	2.5	-	Protocatechuic Acid	2.5	-	Protocatechuic Acid	2.5	-	Protocatechuic Acid	2.5	-	Protocatechuic Acid
3.	3.8, 4.2	449, 433	Flavonoid C-glycosides orientin, Vitexin	3.8, 4.2	449, 433	Flavonoid C - glycosides orientin, Vitexin	3.8, 4.2	449, 433	Flavonoid C-glycosides orientin, Vitexin	3.6, 3.8	449	Flavonoid C - glycoside – orientins
4.	4.8, 5.0	359, 417, 491	Flavanone, Flavonoid Glycoside	4.8, 5.0	359, 417, 491	Flavanone, Flavonoid Glycoside	4.8, 5.0	359, 417, 491	Flavanone, Flavonoid Glycoside	4.2, 4.3	433	Flavonoid C-Glycosides – Vitexins
5.	5.5	475	Flavonoid C-glycoside	5.5	475	Flavanone C - Glycoside	5.5	475	Flavanone C – Glycoside	4.8, 5.0	359, 417, 491	Flavanone, Flavonoid Glycoside
6.	6.5, 6.8	287	Flavanone, Flavonoid-Tetrahydroxy Flavone	6.5, 6.8	287	Flavanone, Flavonoid-Tetrahydroxy Flavone	6.5, 6.8	287	Flavanone, Flavonoid – Tetrahydroxy Flavone	6.5, 6.8	287	Flavanone, Flavonoid – Tetrahydroxy Flavone

Table 4.13: Summary of Fractions 6, Fraction 7, Fraction 8 and Fraction 9 LCMS Results (*Continued*)

Fraction No.	Fraction 6			Fraction 7			Fraction 8			Fraction 9		
Peak No.	RT (min)	Fragment ions [M+H]	Tentative ID (MW)	RT (min)	Fragment ions [M+H]	Tentative ID (MW)	RT (Min)	Fragment ions [M+H]	Tentative ID (MW)	RT (min)	Fragment [M+H]	Tentative ID (MW)
7.	9.3	349, 362, 380	Terpenoid or Amine Derivative	12.1	447, 629	Phenolic Derivative	7.8	270, 275	Phenolic Derivative	7.8	270, 275	Phenolic Derivative
8.	14.3	-	Phenolic Derivative	14.3		Phenolic Derivative	12.1	447, 629	Phenolic Derivative	8.7	301, 318	Phenolic Derivative – Lignan
9.	16.7, 17.1	609	Chlorophyll Derivatives	16.7 – 17.7	593, 609	Chlorophyll Derivatives	14.3	-	Phenolic Derivative	12.7	507, 573	Methoxy Flavone Derivative
10.	17.4 - 18.4	535, 593	Chlorophyll Derivatives, Terpenoid				16.7-17.7	593, 609	Chlorophyll Derivatives	14.3	-	Phenolic Derivative
11.										16.7-17.7	593, 609	Chlorophyll Derivatives

CHAPTER 5
DISCUSSION

5.1 Identification and Extraction of Plant Materials

Preliminary extraction of the respectively identified plant materials with *n*-hexane, ethyl acetate and methanol indicated (by TLC) the choice of solvent that gave the highest number and intensity of their coloured components (Plate 4.1).

Defattening of the three plant materials with *n*-hexane or ethylacetate and subsequent extraction with selected solvents gave the yields reported in Table 4.1. The higher yields of 29% and 28% obtained for *H. sabdariffa* and *J. secunda*, respectively, may be attributed to the high polarity of the MeOH used solvent, extracting both polar and semi-polar components. Alarcón-Alonso *et al.* (2011) and Banwo *et al.* (2022) reported yields of 28.3% and 32.2% in the extraction of *H. sabdariffa* with water and methanol, respectively.

The low yield of 2% in the ethylacetate extract of *C.lutea* may be explained by the semi-polar nature of the solvent, extracting semi-polar components only. The low yield is comparable to the values of 3.5% and 0.3% reported for ethyl acetate extraction of *C. lutea* leaves by Nwidu *et al*. (2017) and Akpan *et al*. (2012), respectively.

The extraction yield of *J. secunda* may have been assisted by the use of a microwave in the procedure, which has been reported to give an improved yield over traditional methods such as maceration, soxhlet, etc (Kaufman and Christen, 2002; Mandal *et al*., 2007). The extraction yield obtained in the current study for *J. secunda* (28%) was higher than the 10.7% reported by Onoja *et al*. (2016) in the extraction by maceration of the same plant leaves for 48 hours in 80% MeOH/H_2O. Anyasor *et al.* (2019) also reported a yield of 10.2% obtained when extraction by maceration of *J. secunda* was carried out using 70% MeOH/H_2O The higher yield of 28%

observed in the current study may be attributed to the greater polarity of the 35% MeOH/H_2O solvent and the microwave-assisted extraction method used.

5.2 α-Terpinene Photooxygenation

Prior to the photooxygenation of α-terpinene with the commercial dyes and plant extracts as sensitizers, the substrate was photooxidized without dye to determine its readiness to undergo autoxidation under the reaction conditions in this study. The results show that the α-terpinene content of the reaction mixture decreased from 69% to 64% after 90 minutes of photooxygenation while the product (ascaridole) only formed 0.8% of the mixture. The side product of the reaction increased from 16.9% to 19.5%. This is similar to the observation by Ronzani *et al.* (2013) that α-terpinene decreased from 93% to 44% after 150 minutes of photooxygenation without dye, no ascaridole (**3**) was present, while *p*-cymene increased from 4% to 39%. The differences in the values may have arisen from variations in the reaction conditions.

p-Cymene is formed as a side reaction during the photooxygenation of α-terpinene for any of the following reasons; electron transfer involving the sensitizer, thermal autoxidation of α-terpinene, intermediate hydroperoxide breakdown or decomposition of ascaridole (**3**) (Shvydkiv *et al*., 2018). The current results support the observation that α-terpinene does not undergo autoxidation in its photooxygenation reaction in the absence of a dye sensitizer.

5.3 Rose Bengal and Methylene Blue Sensitized Photooxygenation of α-Terpinene

Rose bengal and methylene blue are commercially available photosensitizers commonly used in the photooxygenation of α-terpinene (Park *et al*., 2015; Shvydkiv *et al.*, 2018). In this study, rose bengal and methylene blue as sensitizers were used in the photooxygenation of α-terpinene for 90 minutes, the ascaridole (**3**) produced in the reaction mixture were 60.5% and 61.7%, respectively (Table 4.2). The *p*-cymene content of the rose bengal and methylene blue sensitized reactions

increased by 4% and 2.5%, respectively. Razoni *et al*. (2013) reported higher compositions of ascaridole (**3**) (78%) and *p*-cymene (14%) in the photooxygenation of α-terpinene in acetonitrile within a shorter irradiation time of 30 minutes using 16×8 W cool white lamps in an RPR 200 photoreactor and rose bengal (0.03 mmol) as a sensitizer. In another study by Park *et al.* (2015), photooxygenation of α-terpinene by batch reaction with a 16 W LED lamp using methylene blue as photosensitizer gave 92% composition of ascaridole (**3**) in the reaction mixture after 180 minutes. The higher product yield may be a result of the higher percentage composition of α-terpinene (93%) in the starting solution and longer reaction duration than used in the current study. The current results quantitatively support the conclusion that α-terpinene forms products and side products in its photooxygenation reaction with rose bengal and methylene blue as sensitizers under the reaction conditions in this study.

5.4 *Hibiscus sabdariffa* Extract, *Carpolobia lutea* Extract and *Justicia secunda* Extract Sensitized Photooxygenation of α-Terpinene

To determine the extent to which *Hibiscus sabdariffa* Extract, *Carpolobia lutea* Extract and *Justicia secunda* Extract can act as photosensitizers, α-terpinene was photoxygenated for (90 minutes), in the presence of each of the 3 plant extracts. The results obtained are in Table 4.2. Using the *H. sabdariffa* extract as a sensitizer, the α-terpinene composition was reduced by 2.6%, the *p*-cymene by-product increased by 0.6% and the ascaridole (**3**) product increased by 2.8%. The values indicate that only a very small quantity of the substrate reacted and that the free radical pathway and e-transfer between sensitizer and reactant/product are not viable processes in the reaction using *H. sabdariffa* extract as a sensitizer (Karapire *et al.,* 2002). Although *H. sabdariffa* extracts have been reported to be photoactive in dye-sensitized solar cells (Jahng *et al.,* 2017; Yadav *et al,* 2022) and in photodynamic therapy (Al-fawwaz and Al-Khaza'leh, 2016), the

performance of its components in the photooxygenation of α-terpinene, as observed in this study, is negligible.

The use of *C. lutea* as a sensitizer resulted in the reduction of α-terpinene reactant by 65.3%, an increase in *p*-cymene by 4.3% with a corresponding increase in ascaridole (**3**) product by 62.3%. These values are slightly better than the corresponding ones in the reactions where rose bengal and methylene blue were used as sensitizers. There is a scarcity of reports on the use of *Carpolobia lutea* extract as a photosensitizer for its application in photooxygenation reactions or photodynamic therapy.

Similar to that of the *Hibiscus sabdariffa* extract, the *Justicia secunda* extract had negligible photoactivity. The α-terpinene composition in the *J. secunda* sensitized reaction mixture decreased by 8.8%, its *p*-cymene composition increased by 0.2% while its ascaridole (**3**) product composition increased by 5.0% after 90 minutes of photooxygenation (Figure 4.11 and 4.12). This accounts for the lowest increase in the value of *p*-cymene among all the photosensitizer dyes (commercial and plant extracts) tested. This suggests that *J. secunda* extract does not generate singlet oxygen nor any free radicals and electrons that would have led to more *p*-cymene side product. There are no identified reports on the use of *Justicia secunda* extract as a photosensitizer.

H. sabdariffa and *J. secunda* extracts were not very successful in the phootoxygenation of α-terpinene since their reaction mixtures showed negligible compositions (3.1% and 5.1%, respectively) of ascaridole (**3**) after 90 minutes. However, rose bengal, methylene blue and *Carpolobia lutea* extract-sensitized reaction mixtures showed full consumption of the substrate after 90 minutes giving 60.5%, 61.7% and 62.8% compositions of ascaridole (**3**), respectively (Table 4.2).

5.5 The Photooxygenation of α-Terpinene in the Presence of DABCO and ANT-COOH

DABCO is a known singlet oxygen quencher (Li *et al.,* 2022). The purpose of this experiment was to test if *Carpolobia lutea* extract acts through the Type I or Type II photosensitization mechanism. Since DABCO quenches singlet oxygen, its presence should eliminate or reduce the quantity of singlet oxygen generated by any photosensitizer operating through the Type II photosensitization mechanism described in Chapter 1, Scheme 1.3. The addition of 0.3 M DABCO to *Carpolobia lutea* extract sensitized photooxygenation of α-terpinene, led to a decrease in ascaridole (**3**) product after 90 minutes to 13.3% (Table 4.3) contrary to the 62.8% ascaridole (**3**) product initially obtained in the absence of DABCO (Table 4.2). The increase in the composition of *p*-cymene was equally low (0.6%). The addition of DABCO to the *Carpolobia lutea-sensitized* photooxygenation of α-terpinene confirmed that *Carpolobia lutea* extract generates $^1O_2$. Ouannes and Wilson (1968), reported that an increase in the concentration of DABCO suppressed to a high percentage, in the photooxygenation of rubrene. Their study reported that within 16 minutes irradiation, 100% conversion of rebrene was achieved in the absence of DABCO, this decreased to 40% conversion when 3.4×10^3 M DABCO was added and this further decreased to 10% conversion when DABCO concentration was increased to 13×10^3 M.

Similarly, in the current study, an increase in the concentration of DABCO added to the *Carpolobia lutea* sensitized photooxygenation of α-terpinene increasingly suppressed the photooxygenation of α-terpinene. In the absence of DABCO, after 90 minutes of *Carpolobia lutea* sensitized photooxygenation α-terpinene, 62.8% ascaridole (**3**) product composition was achieved (approximately 100% conversion) (Table 4.2). The addition of 0.07 mmol DABCO to a *C. lutea* extract sensitized reaction mixture gave 54.8% ascaridole (**3**) (95% conversion of α-terpinene), increase in the concentration of DABCO to 0.3mmol, further decreased the composition of ascaridole (**3**) to 13.3% (48% conversion of α-terpinene) after the same time (Table 4.3). This

result confirms that *Carpolobia lutea* extract acts more through the Type II photosensitization mechanism and less through the Type I mechanism.

ANT-COOH is known to be a Type I photosensitizer. It was used to determine if α-terpinene photooxygenation takes place predominantly through the Type I or Type II photooxygenation pathway. After 90 minutes of irradiation using 0.03 mmol ANT-COOH as a photosensitizer, the α-terpinene composition of the reaction mixture decreased from 65.9% to 28.2%, its *p*-cymene composition increased from 14.1% to 33.8% and ascaridole (**3**) which was initially absent increased to 3.3%. The use of ANT-COOH photosensitizer which operates through a free radical pathway (Type 1 mechanism), directed the selectivity of this reaction towards *p*-cymene production. A study by Ronzani *et al.* (2013) made use of a similar photooxygenation set-up for the ANT-COOH (0.03 mmol) sensitized photooxygenation of α-terpinene and observed a complete consumption of α-terpinene (initial composition = 93%) within 40 minutes irradiation time. *p*-Cymene increased from 4% to 64% while ascaridole (**3**) increased from 0% to 1% within the same time. Other side products, cuminaldehyde (8%) and isoascaridole (27%) were equally detected. This result varies greatly with that of the current study despite the similarity in the photoreactor used. This variation may be attributed to other reaction conditions such as compositions of the substrates, the irradiation lamps, etc.

The ^{1}H NMR spectrum of synthesized and isolated ascaridole (**3**) is seen in Figure 4.19 revealing 7 major types of proton signals. The proton signals were at ^{1}H NMR (400 MHz, $CDCl_3$): δ 0.92 (6H, d, J = 4 Hz, A), δ 1.35 (3H, s, C), δ1.43 (2H, d, J = 8 Hz, D_1 & E_1), δ1.83 (1H, p, J = 8 Hz, B), δ1.93 (2H, m, J = 4 Hz, D_2 & E_2), δ 6.32 (1H, d, J = 8 Hz, F), δ6.40 (1H, d, J = 12 Hz, G).

Monzote *et al.* (2009) reported the following similar ascaridole ^{1}H NMR peaks - (400.13MHz, $CDCl_3$): δ1.00 (6H, d, 6.9 Hz isopropyl CH_3), 1.38 (3H, s, 4-CH_3), 1.52 (2H,m,^{5}CHH, ^{6}CHH), 1.92 (1H, sept, 6.9 Hz, isopropyl CH), 2.03 (2H, m,^{5}CHH, ^{6}CHH), 6.41 (1H, d, 8.5 Hz, olefinic 8-CH), 6.50 (1H, d, 8.5 Hz, olefinic 7 – CH).

5.6 1,5-Dihydroxynaphthalene Photooxygenation

Photooxygenation of 1,5-DHN is a model reaction popular for its use in trying new photocatalysts (Huang *et al.,* 2013; Lancel *et al.,* 2023). However, a major drawback of this reaction is that the compound is highly self-sensitizing so when it is irradiated in the absence of any photosensitizer, the product (5-hydroxy-1,4-naphthoquinone) (**4**) yield is reasonably high.

In this study, autoxidation of 1,5 DHN for 5 hours resulted in 44% product conversion (Figure 4.32) and 39% isolated yield (Figure 4.33). Two more replicates of this experiment gave a mean conversion value of 74% ± 4.24 and a mean isolation yield value of 40.5% ± 4.95 (Table 4.5). However, a study by Lancel *et al*. (2023) reported an 82% isolated yield of 5-hydroxy-1,4-naphthoquinone (**4**) after autoxidation of 1,5-DHN dissolved in acetonitrile and irradiated under 12 blue LEDs for 4 hours. This difference in the autoxidation yields may be a result of the phootoxygenation conditions such as solvent, irradiation light source, photoreactor type, amount of substrate or amount of photosensitizers used. The study by Lancel *et al*. (2023), reported one of the highest yields in literature and further stated that 1, 5-DHN does not need any photosensitizer to achieve full conversion within 4 hours of irradiation giving better yields in the absence of photosensitizers. In the current study, photooxygenation of 1,5-DHN was further carried out using methylene blue, rose bengal, *Hibiscus sabdariffa* extract, *Carpolobia lutea* extract and *Justicia secunda* extract as photosensitizers.

Rose bengal sensitized photooxygenation of 1,5-DHN gave 100% conversion after 3 hours of irradiation and a 64% isolated 5-hydroxy-1,4-naphthoquinone (**4**) yield. The replicate experiments in the current study gave 100% ± 0.00 mean conversion values and a higher mean isolated yield of 5-hydroxy-1,4-naphthoquinone (**4**) (80.0% ± 0.00) although it took a longer irradiation time of 8 hours to achieve full 1,5-DHN conversion (Table 4.5). The longer time it took for full conversion in the replicate experiments may be a result of the dwindling emission of the fluorescent tube due to use. Coyle (2010) reported a similar 66% yield of 5-hydroxy-1,4-naphthoquinone (**4**) after 4 hours direct sunlight irradiation of 1,5-DHN (0.48 g, 3.0 mmol) and rose bengal (100 mg, 98 µmol) dissolved in 300 mL of t-amyl alcohol.

Methylene blue sensitized reaction gave 100% conversion within 4 hours with an isolated yield of 67%. This difference between the percentage conversion (100%) and yield (67%) may be a result of loss of the product during the purification process. Two replicates of this experiment achieved a mean conversion value of 100% ± 0.00 within a longer time (8 hours) and a higher mean isolated yield of 76.5% ± 0.70. The mean yield value of the replicate experiments is similar to a study by Lancel *et al.* (2023) which reported an 80% yield in a methylene blue sensitized photooxygenation of 1,5-DHN using 31 W red light as a light source.

Hibiscus sabdariffa and *Justicia secunda* extracts sensitized photooxygenation of 1,5-DHN gave poor percentage conversions and isolated yields comparable to the autoxidation reaction results but lower than those of the conventional dyes (methylene blue and rose bengal). In the first experiment, *Hibiscus sabdariffa* extract sensitized reaction gave 48% conversion which is higher by a negligible 4% than the autoxidation value of 44% after 5 hours irradiation. The isolated yield of the *Hibiscus sabdariffa* extract sensitized reaction (44%) was also higher by a trace of 5% than the isolated yield of the autoxidation reaction (39%). The mean conversion value and mean isolated

yield of the replicates experiments in the *Hibiscus sabdariffa* extract sensitized reaction mixture were 51.5% ± 0.71 and 25.5% ± 0.70, respectively which were lower than the mean values of the replicate autoxidation reactions (%conversion – 74 ± 4.24 and %isolated yield - 40.5 ± 4.95). Going with these mean values of the replicate experiments, it can be said that the autoxidation reactions produced better results than the *Hibiscus sabdariffa* extract-sensitized reaction mixtures. A possible explanation for this is that the *Hibiscus sabdariffa* extract competed for absorbance of light with 1,5-DHN which did not lead to the generation of singlet oxygen in its photooxygenation reaction thereby resulting in a lesser yield than its self-sensitized reaction.

Carpolobia lutea extract-sensitized photooxygenation of 1,5-dihydroxynaphthalene gave the highest conversions and yields among the three plant extracts being tested for their photoactivity. In its first reaction, a conversion of 66% and an isolated yield of 51% were observed after 5 hours of irradiation. For the replicate reactions, 100% ± 0.00 conversion was attained (Table 4.4) with 77.0% ± 12.73 isolation yield within 8 hours. This showed that *Carpolobia lutea* extract had a good singlet oxygen-generating ability, comparable to the commercial dyes (rose bengal and methylene blue)

Justicia secunda extract sensitized photooxygenation of 1, 5-dihydroxynaphthalene gave lower conversions (34%) and isolated yields (29%) than the autoxidation reactions. Replicate experiments which were irradiated for 8 hours, showed a similar trend of a lower mean conversion value of 45.5% ± 2.12 and a mean isolated yield of 42.5% ± 3.45 to the autoxidation reactions. The explanations given for the observed low conversion and yield in the *Hibiscus sabdariffa* extract sensitized reaction, applies in the case of *Justicia secunda*. Generally, it can be said that *Hibiscus sabdariffa* and *Justicia secunda* extracts are not efficient in generating singlet oxygen although Yadav *et al.* (2022) and Jahng *et al.* (2018) reported the use of *Hibiscus sabdariffa* extract

as a photosensitizer in the production of performing dye-sensitized solar cells. Ugboaja *et al.* (2022) also reported its photoactivity as a photo-larvicide, in a photodynamic therapy application.

The ^{1}H NMR spectrum of synthesized and isolated 5-hydroxy-1,4-naphthoquinone (**4**) is seen in Figure 4.34 revealing 5 types of proton signals. The proton signals were: δ7.08 (2H, q, J = 8 Hz, A), δ7.35 (1H, dd, J = 8.0 Hz, B), δ7.60 (1H, dd, J = 8, 0 Hz, C), 7.80 (1H, m, J = 8 Hz, D), 11.94 (1H, s, E), (Figure 4.34). Suchard *et al*. (2006) reported four but similar ^{1}H NMR peaks for 1,5-DHN as follows: ^{1}H NMR (400MHz, $CDCl_3$) : δ6.94 (s, 2H), 7.27 (dd, H, J = 2.2, 7.5Hz), 7.60-7.65 (m, 2H), 11.90 ppm (s, H, OH). The slight variations observed between these two NMR spectra may be a result of the different deuterated solvents used for NMR analysis (Current study-$(CD_3)_2CO$, Suchard *et al*., 2006 - $CDCl_3$).

5.7 1-Naphthol Photooxygenation

Autoxidation of 1-naphthol was carried out to see if 1-naphthol is self-sensitizing. After 12 hours of irradiation with monitoring by ^{1}H NMR (Figure 4.35 and Figure 4.36), no product peaks (1,4 – naphthoquinone peaks) were observed. This shows that 1-naphthol is not self-sensitizing. This observation is supported by the study of Lancel *et al.* (2023) who reported that in the absence of a photosensitizer using a 460 nm light source, photooxygenation of 1-naphthol shows no conversion.

Rose bengal sensitized photooxygenation of 1-naphthol (Figure 4.37) gave 61% conversion after 2 hours of irradiation time (Figure 4.38) but these peaks became blurry at 3 hours of irradiation (Figure 4.39). According to Sortino *et al*. (2002), 1, 4-napthoquinone is highly photolabile and this may have been responsible for the blurry peaks observed at 3 hours and the absence of any isolated yield after irradiation for a total of 12 hours. However, for the replicate experiments, after irradiating for only 2 hours, the mean conversion value (62% ± 1.41) and mean isolated yield (3.2% ± 2.69) were obtained for the rose bengal sensitized reactions (Table 4.6).

In the photooxygenation of 1-naphthol using *Carpolobia lutea* extract, the photolabile 1,4 - naphthoquinone being produced seemed to be somewhat protected by the plant dye so that after 4 hours of irradiation (Figure 4.42), the ^{1}H NMR spectrum of the reaction mixture still showed sharp reactant and product peaks. However, at 9 hours of monitoring, the peaks had become blurry (Figure 4.43). Similar to the observation in its rose bengal sensitized reaction, no product was isolated despite the 64% conversion observed after 4 hours. The replicate experiments showed 59% ± 11.31 mean conversion value and 6.6% ± 2.48 mean yield values after 2 hours of irradiation. These results show that *Carpolobia lutea* extract sensitized photooxygenation of 1-naphthol gave similar conversions and yields as the rose bengal sensitized photooxyganation of 1,4 - naphthoquinone.

Suchard *et al.* (2006) reported that photooxygenation of 1-naphthol using rose bengal immobilized on Merrifield resin-RB_{MF} (sensitox) in acetone, irradiated with mercury lamp for 5 hours and purging with pure oxygen gave 53% yield of 1,4-naphthoquinone. This isolated yield by Suchard *et al.* in 2006 (53%) was way much more than what was achieved in this study (rose bengal - 3.5% ± 3.54 and *Carpolobia lutea* extract - 7.5% ± 3.54). This difference in isolated yield may be as a result of the type of lamp used for these reactions. While Suchard *et al.* (2006) used mercury lamp (UV light), the current study made use of cool white fluorescent tubes (visible light). Coyle (2010), reported 70% conversion to 1,4 - naphthoquinone after 24 hours irradiation using halogen lamps. The current study achieved lesser conversions (rose bengal - 62% and *Carpolobia lutea* extract – 59%) although within a shorter time (2 hours).

The ^{1}H NMR spectrum of the purified 1,4-naphthoquinone showed similar peaks : δ7.04 (2H, s, A), δ7.87 (2H, sx, J = 4 Hz, B), δ8.04 (2H, sx, J = 4 Hz, C) to that of Suchard *et al.* (2006) at:

(400MHz, $CDCl_3$): δ 6.96 (2H, m), δ7.74 (2H, m), δ8.06 (2H, m).

5.8 1,6-Dihidroxynaphthalene Photooxygenation

Autoxidation of 1,6-DHN was carried out to see if 1,6-DHN is self-sensitizing. After 12 hours of irradiation and monitoring with ^{1}H NMR (Figure 4.46 and Figure 4.47), no product peaks of 6-Hydroxy-1,4-naphthoquinone peaks were observed. This observation is supported by the study of Lancel *et al.* (2023) who reported that in the absence of a photosensitizer using a 460 nm light source, photooxygenation of 1,6-DHN showed no conversion.

In the rose bengal sensitized photooxygenation of 1,6-DHN, 4 hours of irradiation produced 100% conversion of 1,6-DHN to 6-hydroxy-1,4-naphthoquinone (**6**) (Figure 4.49) with a 47% isolated yield. In a similar study reported by Coyle (2010), rose bengal sensitized photooxygenation of 1,6-DHN gave 80% conversion in 24 hours. The light source used by Coyle, (2010) was a halogen lamp and the reaction solvent was t-amyl. This might have been responsible for the poorer conversion and longer reaction time observed by Coyle (2010). The *Carpolobia lutea*-sensitized photooxygenation of 1,6-DHN took a longer time to achieve full conversion. After 12 hours of irradiation, 92% conversion was achieved (Figure 4.51). The reaction mixture was further irradiated for 24 hours after which 100% conversion (Figure 4.52) and 12% isolated yield were observed . In the replicate reactions, a 100% ± 0.00 mean conversion value was achieved within 12 hours for the rose bengal and *Carpolobia lutea* extract-sensitized reactions and the mean value of the isolated yield was 50.5% ± 1.34 and 57.9% ± 2.39, respectively. The ^{1}H NMR spectrum of the purified 6-hydroxy-1,4-naphthoquinone (**6**) showed peaks at : δ 6.95 (2H, q, J = 8 Hz, A), δ7.25 (1H, dd, J = 4,12 Hz, B), δ7.41 (1H, d, J = 0 Hz, C), δ7.94 (1H, d, J = 8 Hz, D), δ 9.98 (1H, s, E) which are not similar to that of Sortino *et al.* (2002) at: (500 MHz, $CDCl_3$): δ 5.39 (1H, s), δ6.96 (1H, d), δ6.98 (1H, d), δ7.18 (1H, dd), δ7.40 (1H, dd), δ8.51 (1H, dd). This may be as a result of the difference in solvent used for the ^{1}H NMR analysis. While Sortino *et al.* (2002) reported use of the $CDCl_3$, the current study made use of $(CD_3)_2CO$ for ^{1}H NMR analysis.

5.9 α-Pinene Photooxygenation

Autoxidation of α-pinene showed that α-pinene is not self sensitzing. After 24 hours of irradiation in the absence of tetraphenylporphyrin (or any photosensitizer), no product peak was observed on GC at the characteristic retention time (15.6 minutes) of the expected photooxygenation product (pinocarvone). The composition of the starting material reduced from 96.7% (Figure 4.55) to 93.8% (Figure 4.56). This reduction in the composition of the starting material by a negligible 2.9% may be a result of the formation of some unidentified autoxidation products other than pinocarvone (**7**). This can be seen as 6 new unidentified peaks in Figure 4.56 (RT 8.59, 10.83, 10.96, 11.97, 16.8, 17.30) which were not present in the starting material (Figure 4.55).

Tetraphenylporphyrin sensitized photooxygenation of α-pinene (98.5% starting composition), showed 94.6% composition of pinocarvone (**7**) after 24 hours irradiation (Figure 4.58). This is approximately 96% reactant conversion. In the replicate experiments, tetraphenylporphyrin sensitized reaction gave 73% ± 5.66 mean composition value of pinocarvone (**7**) (Table 4.8).

Carpolobia lutea extract similarly showed good conversion of α-pinene (starting composition 92.8%) giving a 90.4% composition of pinocarvone (**7**) after 24 hours of irradiation (Figure 4.60). This is also approximately 96% conversion, the same as in tetraphenylporphyrin sensitized reaction. Figures 4.61 and 4.62 show that the conversion was evenly spread through the 24 hours for both sensitizers. In the replicate experiments, *C. lutea* extract gave a 75% ± 0.00 mean composition value of pinocarvone (**7**) (Table 4.8) . This confirms that *Carpolobia lutea* extract is equally as good as tetraphenylporphyrin in the photooxygenation of α-pinene.

After workup, the isolated yields of tetraphenylporphyrin and *Carpolobia lutea* extract photosensitizers were quite poor (0.7% and 3.0%, respectively – Table 4.8). This may be attributed to the loss of the product due to the rigorous workup process.

Mihelich and Eickhoff (1983), achieved a 97% yield of pinocarvone (**7**) within a much shorter irradiation time (1.5 hours) using a similar procedure. However, the major difference between the two procedures is the light source. While 16 x 8 Watts cool white fluorescent tubes were used as irradiation source in the current study, Mihelich and Eickhoff, 1983 made use of a 400 W sodium vapor lamp (Lu-400W). This may have been responsible for the shorter irradiation time.

The proton signals of the purified pinocarvone (**7**) were: δ0.74 (3H, s, A), δ1.22 (1H, d, J = 8 Hz, B), δ1.29 (3H, s, C), δ2.00 (1H, s, D), δ2.42 - δ2.46 (1H, d, J = 4 Hz, EF), δ2.57 (1H, t, J = 4 Hz, G), δ2.62 (1H, tdd, H), δ2.70 (1H, t, J = 4 Hz, I), δ4.93 (1H, d, J = 4 Hz, J), δ5.86 (1H, d, J = 4 Hz, K), similar to that of Ganji *et al.* (2020) of (-)-pinocarvone given as: ^{1}H NMR ($CDCl_3$, 500 MHz) δ (in ppm): δ0.78 (3H, s,), δ1.27 (1H, d, J = 10.5 Hz), δ1.33 (3H, s), δ2.24 -2.17 (1H, m), δ 2.52 (1H, dd, J = 19.3 and 2.7 Hz), δ 2.63 (1H, d, J = 2.6 Hz), δ2.69 – δ2.64 (1H, m), δ 2.74 (1H, t, J = 5.9 Hz), δ4.99 (1H, s), δ5.94 (1H, s).

5.10 β-Pinene Photooxygenation

Autoxidation of β-pinene equally showed a trace composition (1.5%) of the expected photooxygenation product (myrtenal) at RT 16.85 minutes after 48 hours of irradiation. The composition of the starting material (β-pinene) also decreased by a negligible amount, from 94.2% (Figure 4.64) to 90.7% (Figure 4.65). The decrease in the starting material may be a result of the formation of some other autoxidation product other than myrtenal (**8**). Four unidentified new peaks appeared on the chromatograms used for monitoring this reaction at RT 8.47, 9.14, 14.57 and 14.71 minutes after 48 hours of irradiation although at trace amounts. An unidentified peak at RT 15.6 minutes, which was initially present in the starting material, increased in composition from 1.14% (Figure 4.64) to 2.55% (Figure 4.65).

Tetraphenylporphyrin-sensitized photooxygenation of β-pinene at RT 9. 41 minutes (94.7% starting composition), showed 82.9% composition of myrtenal (**8**) at RT 16. 9 minutes after 48 hours of irradiation (Figure 4.67). This is approximately 95% reactant conversion. In the replicate experiments, tetraphenylporphyrin sensitized reaction gave a 90 ± 4.24 mean composition value of myrtenal (**8**) (Table 4.9).

Carpolobia lutea extract similarly showed good conversion of β-pinene at 9.41 minutes (starting composition - 94.9%) giving a 76.6% composition of myrtenal (**8**) at RT 17.0 minutes after 48 hours of irradiation (Figure 4.69). This is approximately 86% conversion, which is slightly lower by 11% when compared to what was observed in the tetraphenylporphyrin sensitized reaction. The conversion rate peaked within the first 20 hours of the reactions after which it flattened out over the remaining hours for both sensitizers (Figures 4.70 and 4.71).

In the replicate experiments, *C. lutea* extract gave 88.5% ± 2.12 mean composition value of myrtenal (**8**) (Table 4.9). The replicate experiment conversion values measure up to that tetraphenylporphyrin sensitized reaction conversion values (90 ± 4.24 mean composition value) confirming that *Carpolobia lutea* extract is a relatively good photosensitizer for the photooxygenation of β-pinene.

The tetraphenylporphyrin and *Carpolobia lutea* extract photosensitizers also gave poor yields of pure myrtenal (**8**) (5.2% and 7.2%, respectively – Table 4.9) after the work-up. This may be attributed to the loss of the product due to the rigorous workup process.

Mihelich and Eickhoff (1983), achieved a 58% yield of myrtenal (**8**) within a much shorter irradiation time (2.5 hours) using a similar procedure. The light source (400 W sodium vapour lamp -Lu-400W) used by Mihelich and Eickhoff (1983) may have been responsible for the shorter irradiation time they reported. This study however achieved higher conversions (90 ± 4.24 -

tetraphynyl porphyrin and 88.5 ± 2.12 - *Carpolobia lutea* extract), than that reported by Mihelich and Eickhoff (58% yield).

The ^{1}H NMR spectrum of the synthesized and purified myrtenal (**8**) is seen in Figure 4.72a revealing 10 types of proton signals. The proton signals were at δ0.71 (3H, s, A), δ1.02 (1H, d, 8 Hz, B), δ1.31 (3H, s, C), δ2.16 (1H, s, D), δ2.45 (1H, dt, J = 16 Hz, E), δ2.53 (dt, J = 8 Hz, F), δ2.60 (1H, t, 4 Hz, G), δ2.83 (1H, td, J = 4 Hz, H), δ6.68 (1H, tt, I), δ9.40 (1H, s, J).

The ^{1}H NMR spectrum of commercially available myrtenal (**8**) (as a standard) shows 10 types of proton signals with similar peaks as those identified in the synthesized myrtenal (**8**). The proton signals were at δ 0.73 (3H, s, A), δ1.03 (1H, d, 8Hz, B), δ1.33 (3H, s, C), δ2.17 (1H, m, D), δ2.45 (1H, dt, J = 16Hz, E), δ2.57 (dt, J = 8Hz, 4Hz, F), δ2.64 (1H, t, 4Hz, G), δ2.78 (1H, td, J = 4Hz, H), δ6.76 (1H, s, I), δ9.42(1H, s, J). These proton signals were also to that of Mills (1996).

5.11 Absorbance of Dyes

Figures 4.73 and 4.74 show the absorbance measurements of the rose bengal (5 ppm, 0.0005/100 mL, 5.1×10^{-6} M) and methylene blue (5 ppm, 0.0005/100 mL, 1.6×10^{-5} M) matched with the emission spectrum of the 8 W cool white fluorescent tube. Figure 4.73 shows that rose bengal gave a peak absorbance between 482 nm to 587 nm wavelength range with the highest absorbance of 1.50 at 557 nm. It can be said that the absorbance spectrum of rose bengal adequately coincides with the emission spectrum of the fluorescent tubes. The rose bangal wavelength of maximum absorption (λmax) at 557 nm and the absorbance peak range (482 nm - 587 nm), falls within the broad emission spectrum of the cool white fluorescent tubes (400 nm – 679 nm). Coyle (2010) reported 550 nm as the λmax of rose bengal in acetone. This is lower than the λmax of rose bengal isopropyl alcohol solution, observed in the current study (557 nm). Freire *et al*. (2014) also reported 550 nm as λmax of rose bengal dissolved in phosphate-buffered saline (PBS). However,

Linden and Neckers (1988) stated that the λmax of rose bengal depends on the solvent used and reported rose bengal disodium salt to have a λmax of 557 nm in dimethyl ether, 553 nm in ethanol and 549 nm in dilute aqueous solution. Also, Coyle (2010) reported the absorbance of rose bengal at λmax as 0.34 which is lower than that observed in the current study (1.5). The difference between the absorbance values observed by Coyle (2010) and that observed in the current study may be attributed to the difference in concentrations of rose bengal which was higher in the current study (5.1×10^{-6} M) than that used by Coyle (2.46×10^{-6} M). Better solubility in the solvent used is another factor that can affect the absorbance value of rose bengal. Acetone and isopropyl alcohol are both polar solvents but with different polarities, therefore it can be said that the solubility of rose bengal in the different solvents may have also affected its absorbance values at λmax.

Methylene blue (Figure 4.74) showed an absorbance peak between 545 nm to 700 nm wavelength range with the highest absorbance value of 1.50 at λmax of 658 nm. The methylene blue wavelength of maximum absorption at 658 nm and a good part of its absorbance spectrum (545 nm to 679 nm), falls within the broad emission spectrum of the cool white fluorescent tubes (400 nm – 679 nm). It was observed that rose bengal and methylene blue had the same absorbance values of 1.50 at their corresponding λmax despite their different concentrations of 5.1×10^{-6} M and 1.6×10^{-5} M, respectively. This can be attributed to the solubility of the dyes in the solvents used. Coyle (2010) reported an absorbance of 0.23 at a λmax of 640 nm for 2.51×10^{-6} M methylene blue dissolved in acetone. Sheng and Yunus (2005) also reported a well-resolved characteristic peak by methylene blue doped gelatin sample at 668 nm with a shoulder at 620 nm. The pure gelatin matrix was transparent between 450 nm and 800 nm of the spectrum so it can be assumed that the absorption of the doped gelatin sample was that of the methylene blue alone. The methylene blue λmax observed at 658 nm in the current study was longer than that reported by Coyle (2010) (640 nm) but shorter than that reported by Sheng and Yunus (2005) (668 nm). The difference in λmax

can be attributed to the solvents used for absorbance measurement. Rauf *et al.* (2019) reported that fluorescent dyes undergo solvatochromic shift (show variation in absorption λmax with change in solvent).

The absorbance value of methylene blue observed in the current study (1.50 at 1.6×10^{-5} M) was higher than that reported by Coyle (2010) (0.23 at 2.51×10^{-6} M). This can be explained by the difference in the concentration of methylene blue used for the absorbance measurements(that of the current study being higher than Coyle's) and the solubilities of methylene blue in the different solvents used. Isopropyl alcohol has a higher polarity than acetone so it can be said that the solubility of methylene blue in isopropyl alcohol was higher than its solubility in acetone and may have contributed to the higher absorbance value observed for the isopropyl alcohol solution.

The absorbance measurement (5 ppm, 0.0005/100 mL, 8.1×10^{-6} M) of tetraphenylporphyrin (Figure 4.75) showed several peaks between 400nm – 658 nm, the highest peak occurring at 421 nm with an absorbance value of 2.97. Tetraphenylporphyrin had other smaller peaks at (513 nm, 0.45), (551 nm, 0.18), (589 nm, 0.14) and (646 nm, 0.12). These smaller peaks are similar to the four absorbance peaks reported by Taniguchi *et al.* (2021) for the UV/Vis absorption measurement of tetraphenylporphyrin between 450 nm – 700 nm.

The tetraphenylporphyrin wavelength of maximum absorption at 421 nm and its other absorbance peaks occurring between 400 nm to 658 nm, fall within the broad emission spectrum of the cool white fluorescent tubes (400 nm – 679 nm).

The λmax observed for tetraphenylporphyrin (421 nm) is closest to that reported by Coyle (2010) (417 nm) despite the difference in the solvent used for the absorbance measurement. In the current study, a λmax absorbance value (2.97 at 8.1×10^{-6} M) different from that reported by Coyle (2010) (0.98 at 2.4×10^{-5} M) was observed. Despite the lower concentration of tetraphenylporphyrin used

for the current study, a higher absorbance (2.97) at λmax was observed than that reported by Coyle (2010) (0.98). This can be attributed to solubility. Tetraphenylporphyrin was not soluble in isopropyl alcohol so dichloromethane was used for its absorbance measurement. Dichloromethane is a semi-polar solvent so it was a good solvent for the dissolution of tetraphenylporphyrin, better than acetone used by Coyle (2010). This explains the higher absorbance value observed in this study.

All three commercial dyes had their absorbance peaks overlapping with the spectral emission peak of the fluorescent tube (Figure 4.76).

Figures 4.77 and 4.78 show respectively the absorbance measurements of *Hibiscus sabdariffa* extract and *Carpolobia lutea* extract matched with the spectral emission of the 8 W cool white fluorescent tube. Figure 4.77 shows that *Hibiscus sabdariffa* extract gave an absorbance peak between 440 nm to 676 nm wavelength range with the highest absorbance value of 0.39 occurring at 542 nm. Alshehri and Abdulmohsen (2017) measured the absorbance of *Hibiscus sabdariffa* extract and reported peaks at 287 nm, 322 nm and 519 nm. The last peak reported by Alshehri and Abdulmohsen (2017) (519 nm) had the closest wavelength to that observed in this study (542 nm). *Carpolobia lutea* extract (Figure 4.78) showed an absorbance peak between 639 nm and 686 nm wavelength range with the highest absorbance value of 1.88 occurring at 665 nm (λmax).

The absorbance measurement for *Justicia secunda* (Figure 4.79) showed a broad peak between 521 nm and 645 nm with a λmax at 602 nm and an absorbance value of 0.15. All three plant extracts had their absorbance peaks matching the spectral emission region of the fluorescent tube -Table 4.86 and the visible region of the electromagnetic spectrum (400 nm - 800 nm). However, despite their higher concentration (500 ppm, 0.05 g in 100 mL) than that of the conventional dyes (5 ppm), they had low absorbance values (*Hibiscus sabdariffa* extract - 0.39, *Carpolobia lutea*

extract - 1.88, *Justicia secunda* extract - 0.15) relative to those of the conventional dyes (rose bengal – 1.50, methylene blue – 1.50, tetraphenylporphyrin – 2.97). Amongst the three plant extracts, *Carpolobia lutea* extract stood out with a λmax absorbance value of 1.88 which is also higher than the λmax absorbance of two of the commercial dyes (1.50). This explains the high photoactivity shown by *Carpolobia lutea* extract. The lower absorbance values shown by these plant extracts, despite their higher concentrations, may be explained by the fact that they are not pure compounds but a mixture of some plant dyes and other numerous natural products.

5.12 Photostability of Rose Bengal in Isopropanol

Figure 4.81 shows the UV/Vis absorption spectra of rose bengal dissolved in isopropanol and irradiated for 24 hours. Rose bengal absorbance peak which occurs between 486 nm-598 nm did not disappear throughout the 24 hours irradiation time although there was a drop in its absorbance value from 0.34 at 0 hour to 0.12 at 24 hours (Figure 4.81) and a slight hypsochromic shift from 561 nm at 0 hour to 555 nm at 24 hours. This blue shift and decrease in absorption intensity might be a result of photobleaching. By physical examination, a slight bleaching in the pink colour of the rose bengal in the isopropanol solution was observed between the 0 hour solution and 24 hour solution (Plate 4.3). Linden and Neckers (1988) reported that rose bengal bleaches slowly by a reduction mechanism in protic solvents to give a leuco rose bengal product (a dihydro compound) which has been previously isolated (see Scheme 5.1). Triplet oxygen in the dark can oxidize the leuco rose bengal (colourless) back to the normal rose bengal (pink). It was observed in the current study that rose bengal was slightly photobleached in protic isopropyl alcohol. The photobleaching of the rose bengal may have been reduced by the presence of oxygen preventing the reduction of the rose bengal to its leuco form.

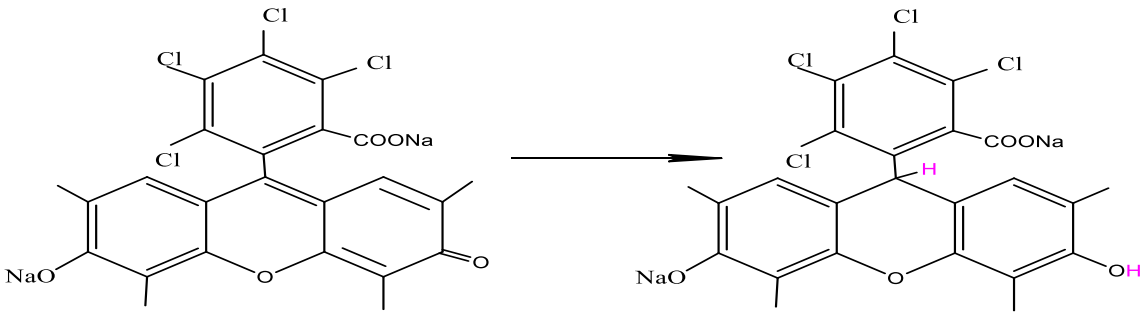

Rose Bengal

Leuco form of Rose Bengal

Scheme 5.1: Reduction of Rose Bengal to its Leuco Form

Terra *et al.*(2023) however stated that photobleaching is an irreversible light-induced transformation of a photocatalyst into a new molecule that is less photoactive or is not photoactive at all. A photosensitizer can be degraded or photobleached by light or singlet oxygen.

5.13 Photostability of *Carpolobia lutea* Extract in Isopropanol

The isopropanol solution of *Carpolobia lutea* extract in Figure 4.82 showed little change in the absorption peak occurring between 568 nm and 708 nm with time. The highest point on the peak (λmax) was at 670 nm with an absorbance value of 0.06 which was reduced to 0.04 after 24 hours. The photostability reduction rate observed was 1.4%/hr being the least among the 3 plant extracts. Plate 4.4 confirms that the photobleaching of *Carpolobia lutea* extract in isopropyl solution is minimal as the solution went from greenish brown to a gold colour. The *Carpolobia lutea* extract dye was most stable in isopropyl alcohol, a protic solvent although its solubility was poor in this solvent (absorbance at λmax = 0.06). An explanation for this might be that the presence of oxygen in the irradiation system suppressed its bleaching or that the bleaching of the *Carpolobia lutea* dye does not occur by reduction mechanism due to the protic solvent as in the case of rose bengal.

5.14 Photostability of Methylene Blue in Acetonitrile

Figure 4.83 shows the UV absorption spectra of methylene blue dissolved in acetonitrile, irradiated for 24 hours in the presence of oxygen.

The methylene blue absorbance peak which occurred between 534 nm and 712 nm remained the same throughout the 24 hours irradiation time. There was no change in the λmax at 1.59 although there was a slight blue shift in λmax from 654 nm at 0 hours to 650 nm at 24 hours (Figure 4.83). Plate 4.5 also shows that there was slight bleaching in the blue colour of the methylene blue in acetonitrile solution. According to Sheng and Yungs (2005), methylene blue molecules doped in a gelated matrix were photobleached by UV/Vis irradiation. With the increase in irradiation time, its λmax at 668 nm weakened and broadened. This was also attributed to the production of the leuco form of methylene blue caused by photoreduction of the dye as seen in Scheme 5.2. Like rose bengal, re-oxidation of the leuco methylene blue back to the dye molecules was observed after storage in a dark room for 12 hours and exposure to atmospheric air.

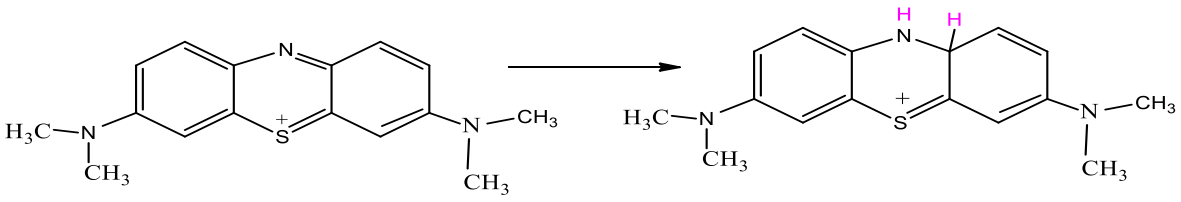

Methylene Blue

Leuco form of Methylene Blue

Scheme 5.2: Reduction of Methylene Blue to its Leuco Form

Methylene blue in the current study did not show appreciable bleaching and this can be attributed to the absence of a reducing agent (acetone which as an aprotic solvent was used) and the additional presence of oxygen reduced any reduction reactions.

5.15 Photostability of *Carpolobia lutea* Extract in Acetonitrile

The acetonitrile solution of *Carpolobia lutea* extract in Figure 4.84 showed an absorption peak occurring between 625 nm and 724 nm with a λmax of 662 nm and an absorbance of 0.10. After 24 hours, absorbance decreased to 0.034 at a new λmax of 665 nm (a bathochromic shift). A photostablity reduction rate of 2.75% which was higher than that of *C. lutea* in isopropyl alcohol (1.4%/hr) was observed. Plate 4.6 shows the solution was slightly photobleached going from green to a light gold color. Unlike methylene blue, the bleaching mechanism of *Carpolobia lutea* extract may not be by reduction so even in the absence of a protic solvent, bleaching was still observed in the *Carpolobia lutea* extract dye. The presence of oxygen during irradiation did not quite protect the *Carpolobia lutea* extract dye.

5.16 Photostability of Tetrraphenylporphyrin in Dichloromethane

The solution of TPP in dichloromethane showed 5 absorption peaks which disappeared/reduced with irradiation over time while some three new absorption peaks were formed (Figure 4.85). The 5 peaks that occurred before irradiation (at 0 hours) include (421 nm, 2.97), (513 nm, 0.45), (551 nm, 0.18), (589 nm, 0.14) and (646 nm, 0.12). These peaks diminished over the 24 hours of irradiation leading to the development of a new peak at 447 nm with an absorbance value of 2.21. The peak at 421nm underwent a hypsochromic (blue) shift to 417 nm with a decreased absorbance value of 1.24. The Peaks at 513 nm and 551 nm remained present but their absorbance values decreased to 0.07 and 0.03, respectively. The peak at 589 nm disappeared. The peak at 646 nm underwent a bathochromic (red) shift to 662 nm and its absorbance increased to 0.30 (Figure 4.85). These peaks and observations are consistent with the report of Cavaleiro *et al*. (2001) who studied the photostability of meso-tetraphenylporphyrins(e.g meso-tetrakispentafluorophenylporphyrins) on irradiation with 1000 W xenon lamp in an aerated vessel using toluene or dichloromethane as solvents. Cavaleiro *et al*. (2001) reported peaks at near 650 nm, 589 nm, 540 nm, 515 nm and 400

nm which all decreased with an increase in irradiation time. The peak at 515 nm was used to monitor the irreversible degrading of the dyes. The current study observed similar peaks at 646 nm, 589 nm, 551 nm, 513 nm and 421 nm. According to Cavaleiro *et al*. (2001), the increase in the absorbance band near 650 nm with irradiation time similarly observed in the current study, can be explained to be due to the reduction of the porphyrin to the corresponding chlorin (Scheme 5.3).

Although the presence of oxygen is said to have a protective effect on tetraphenylporphyrin by deexciting its triplet state, the degradation of tetraphenylporphyrin was still observed in the current study. In the absence of the quenching of the triplet tetraphenylporphyrin dye by oxygen, porphyrin abstracts hydrogen from any donor (ground state porphyrin molecules, solvent, solvent impurities or reactive addictives, etc) through a photoreduction mechanism leading to chlorin.

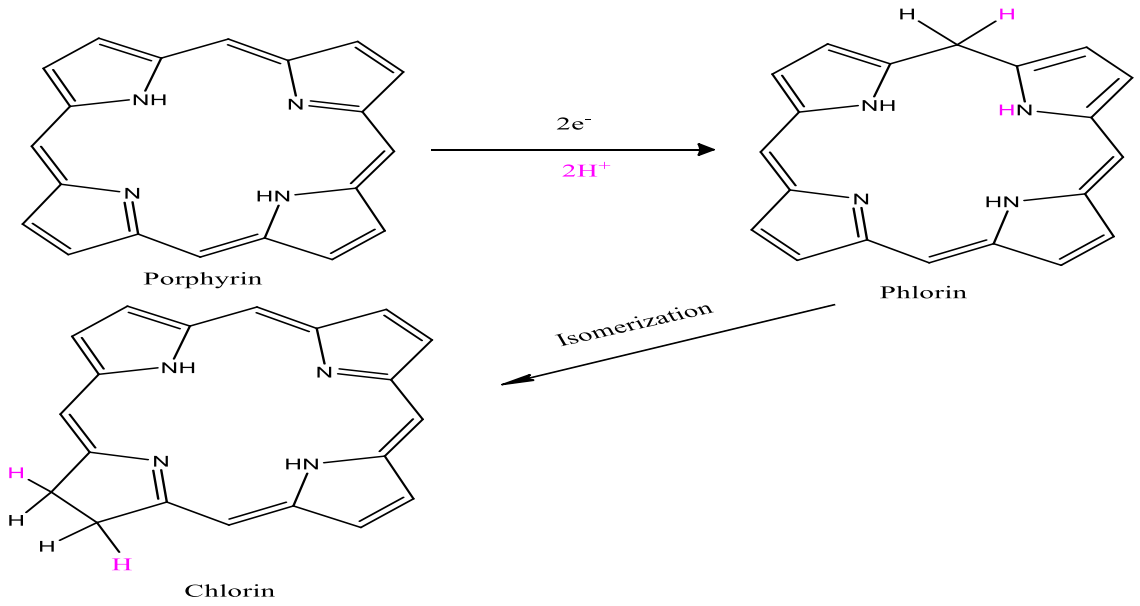

Scheme 5.3: Reduction of Porphyrin to Chlorin

Cavaleiro *et al*. (2001) also stated that the photobleaching of tetraphenylporphyrins has been observed to be accelerated by chlorinated solvents. This may have contributed to the degradation

tetraphenylporphyrin in this study (since the solvent used was dichloromethane), despite the presence of oxygen during irradiation.

Plate 4.7 shows the colour change that was physically observed in the solution between 0 hour and 24 hour irradiation. The pink colour of TPP in acetonitrile turned lemon green after irradiation for 24 hours. Based on the changes in the absorbance measurement of the solution, this colour change observed can be attributed to the photobleaching of TPP.

5.17 Photostability of *C. lutea* in Dichloromethane

A solution of *Carpolobia lutea* extract in dichloromethane showed a λmax of 670 nm with an absorbance value of 0.15 before irradiation. The *Carpolobia lutea* extract which is a semi-polar dye was most soluble in dichloromethane and this is the reason for the high absorbance value (0.15) of its dichloromethane solution relative to its absorbance value in the other solvents, that is, 0.06 in isopropyl alcohol and 0.10 in acetonitrile (0.10). The peak flattened out as its absorbance value decreased from 0.15 to 0.02 at λmax of 670 nm after 24 hours of irradiation (Figure 4.86). With the highest photostability reduction rate of 3.635/hr, *Carpolobia lutea* extract can be said to be least stable in dichloromethane when compared to its stability in isopropyl alcohol (1.45/hr) and acetonitrile (2.75%/hr). No blue or red shifts were observed just bleaching leading to a decrease in absorbance value at λmax. The colour of the solution bleached from greenish brown to a bright gold colour (Plate 4.8). The colour change and observations for tetraphenylporphyrin in dichloromethane were not similar to that of the *Carpolobia lutea* extract presumably because the chemical composition of the *Carpolobia lutea* extract is quite different from the tetraphenylporphyrin ring. Despite the presence of oxygen in the irradiation system, bleaching of the natural dye was still observed. An explanation for this may be that the compounds that make up the plant dye are bleached by singlet oxygen and not by a reduction mechanism.

5.18 Photoactivity of C*arpolobia lutea* VLC Fractions

The active *Carpolobia lutea* extract was separated into fractions with fewer chemical components based on gradient polarity using VLC. The fractions were further tested for their photoactivity by the photooxygenation of 48.5% α-terpinene solution to ascaridole (**3**). Methylene blue was used as a control photosensitizer. 49.5% composition of ascaridole (**3**) (RT 10.97 minutes) was achieved after 90 minutes of irradiation using methylene blue as photosensitizer (Appendix 22, Table 4.11). The first 4 fractions (fractions 1, 2a, 2b and 2c) and the last four fractions (fractions 10, 11, 12 and 13) gave the least product compositions (< 40%) of the expected product (ascaridole), after 90 minutes irradiation so they were not characterized for their chemical composition. The middle fractions 2d -9 seemed to be the most photoactive (Table 4.11). An explanation for this may be that since the *Carpolobia lutea* extract was obtained using a semi-polar solvent (ethyl acetate) after defatting with *n*-hexane, the non-polar component of the extract is expected to be negligible. Similarly, the polar composition of the plant was not extracted so its polar composition is expected to be minimal too. Amongst the active fractions, there was no trend to the photoactivity observed (fraction 2d - 46.0%, fraction 3 - 41.9%, fraction 4a - 49.2%, fraction 4b - 45.2%, fraction 5 - 42.7%, fraction 6a - 50.20%, fraction 6b - 47.3%, fraction 7 - 48.2%, fraction 8 - 46.3%, fraction 9 – 49.57%). Fractions 2d - 9 gave good ascaridole (**3**) product conversions (above 40%) thus the need to find out the chemical compositions responsible for their excellent photoactivity using the HPLC-MS.

5.19 Components of the Photoactive Fractions of *Carpolobia lutea* Extract

Looking at the HPLC chromatograms of the selected photoactive fractions (Appendices 41 - 48), compounds which had prominent peaks (highest mass area) were identified and compared with literature if they were already known photosensitizer molecules. The following were the tentative compounds associated with the prominent HPLC peaks in the chromatograms of the 8 photoactive

fractions: fraction 2d – Anthraquinone, fraction 3- triterpene derivatives and flavone derivatives, fraction 4 – flavanone derivatives and protocatechuic acid, fraction 5 – protocatechuic acid, fraction 6 – flavonoid c-glycoside, protocatechuic acid, terpenoid amine derivative, chlorophyll derivatives, fraction 7 – flavonoid C-glycosides, gallic acid derivative, orientin and vitexin, fraction 8 – flavonoid C-glycosides, gallic acid derivatives, fraction 9 – protocatechuic acid, flavanone, flavonoids. In summary, there were 9 compounds which had prominent peaks in the 8 photoactive *Carpolobia lutea* fractions. These compounds will be broadly discussed as 4 major classes of compounds namely: anthraquinones, flavonoids, polyphenols and chlorophyll derivatives.

Aside from these prominent peaks, there are some compounds which showed up repeatedly in various fractions such as phenolic derivatives (fractions 2d, 3, 5), xanthone derivatives (fractions 2, 3, 4) and dianthrone derivatives (fractions 2d, 3 and 4). The phloroglucinol and chromone derivatives showed up sparingly and scarcely.

There are no reports in literature on the HPLC-MS of *Carpolobia lutea* leaves extract although 5 compounds have been previously isolated (18) and some qualitative/quantative phytochemical analysis has been carried out on the plant extracts (Table 1.2). The following compounds tentatively identified by HPLC-MS in the current study, agree with literature reports on the compounds previously identified in the plant extracts: anthraquinones (Akpan *et al.,* 2012; Ettebong *et al.,* 2011), flavonoids - flavanones and flavones (Akpan *et al.,* 2012; Ettebong *et al*., 2011; Nwidu *et al.,* 2017), Phenolics (Akpan *et al.,* 2012; Nwidu *et al*., 2017), triterpenes (Akpan *et al.,* 2012; Ettebong *et al*., 2011).

Anthraquinones have been reported as the largest group of plant dyes with impressive photostability making them useful photocatalysts (Cervantes-Gonzalez *et al.,* 2020). Montoya *et*

al. (2005) studied the photosensitization properties of 6 natural anthraquinones (soranjidiol, damnacanthal, soranjidiol-1-methyl ether, rubiadin-1-methyl ether, rubiadin, damnacanthol) isolated from *Heterophyllaea pustulata Hook*. F. (Rubiaceae) leaves and stems. It was observed that aside from rubiadin-1-methyl ether which operated through the Type I photosensitization mechanism, the remaining five compounds operated through both Type I and II photosensitization mechanisms and damnacanthal gave the highest quantum yield of singlet oxygen. *Carpolobia lutea* extract was confirmed by the current study to operate through both Type I and Type II photosensitization mechanisms although it was shown to operate more through the Type II mechanism than the Type 1 mechanism. This was confirmed by the addition of DABCO (a singlet oxygen quencher) to *Carpolobia lutea* extract during the photooxygenation of α-terpinene (Table 4.3). Mugas *et al*. (2021) also showed that parietin, a natural anthraquinone, showed promising photocatalytic ability for photodynamic treatment of leukemic cells. These reports from literature confirm that natural anthraquinones (present in fractions 2d, 3 and 4) are good photosensitizers and must have contributed to the photoactivity of *Carolobia lutea* extract.

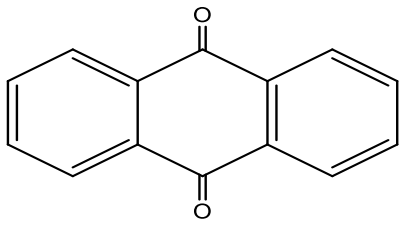

9

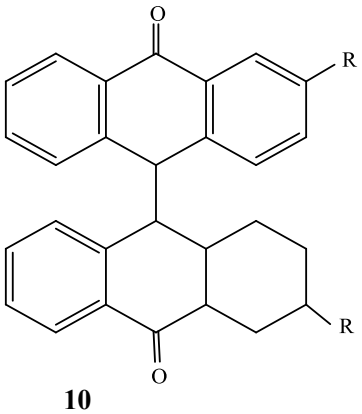

10

Dianthrones (10) are dimeric moleclues of anthraquinones (9) having hypericin elsinochrome, duclauxin, sennoside A as some members of its family (Kirakosyan *et al.,* 2008; Schwarting, 1977). Hypericin has been reported to have an outstanding singlet oxygen-generating ability and

is one of the best photosensitizers in nature (Waser and Falk., 2011). The limitations of its applications are attributed to its limited solubility, expensive isolation cost and its absorption maximum. The exact dianthrones tentatively identified in *Carpolobia lutea*, have not been isolated and identified. However, based on the reports on hypericin, a dianthrone, it can be inferred that the presence of dianthrones in fractions 2d, 3 and 4 may have contributed to the photoactivity of these fractions.

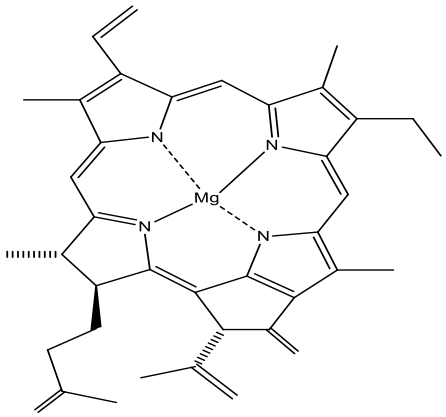

11

Chlorophyll (11) is a known effective photosensitizer from plant extract. It contains the porphyrin structure and belongs to the porphyrin class of compounds as tetraphenylporphyrin, chlorins and bacteriochlorins. One of the first mention of its use as a photosensitizer was when chlorophyll from spinach leaves was used for the synthesis of ascaridole (**3**) just after the Second World War (Oelgemöller, 2016). Kenney and Fisher (1973), also reported to have used chlorophyll alongside an acetone: water extract from kudzu leaves as photosensitizer for the photooxygenation of α-pinene and β-pinene. Triemer *et al. (*2018) reported the use of chlorophyll from the extract of *Artemisia annua* as a photosensitizer for artemisinin synthesis. Mejica *et al.* (2022) reported the use of chlorophyll A as a good catalyst in dye-sensitized solar cells. In the HPLC-MS analysis of *Carpolobia lutea*, chlorophyll occurred in fractions 6, 7, 8 and 9 and must have contributed to the photoactivity of these fractions.

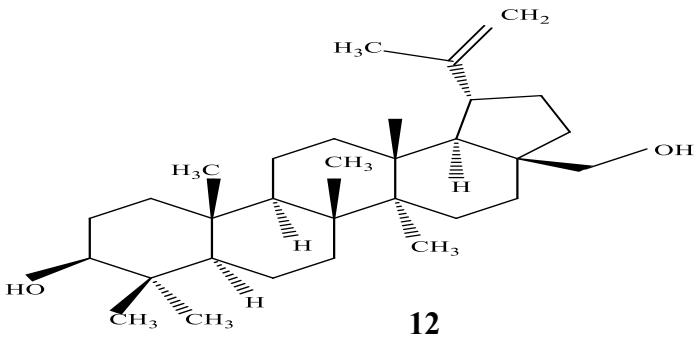

12

In triterpenes, there is the absence of a conjugated pi-electron system which is requisite for a molecule to absorb light in the visible portion of the electromagnetic spectrum. Also, betulin (12) which is a known triterpene has no reports of any photoactivity. There is a dearth of literature on the photoactivity of triterpenes rather, there are reports on its photosensitization in animals. Bezerra, (2021) reported that triterpenes saponins isolated from *Enterolobium contortisiliquum*(Vell.) Morong(Fabaceae) caused photosensitization poisoning in animals that ingested the pods of the plants. According to Gasparetto *et al.* (2010), triterpenes, steroids and flavonoids present in extracts of *Alternanthera maritime*, gave promising results when used as photosensitizers in photodynamic antimicrobial therapy. Based on these literature reports, it can be said that the presence of terpinene may have contributed to the photoactivity of fractions 2d, 3, 4, and 5.

Flavonoids are a group of naturally occurring phenolics with the general backbone of chromone (Cotelle*,* 2001). Flavones (13), flavonols (13), flavanones (14), flavanols (14) all belong to these class of compounds. A review by Cotelle (2001) reported that flavonoids have been shown to have both antioxidant and prooxidant effects. Chromone (15) has the core structure of flavonoids, . Xanthones (16) have structural similarities to flavonoids. 5,7,3^{1},4^{1}-tetrahydroxyflavanone (17) is a flavanone. All of these tentatively identified compounds will be discussed as flavanones.

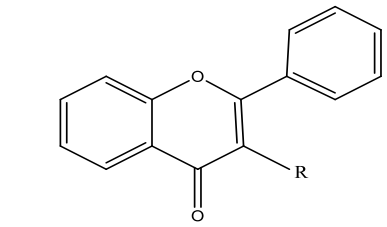

R = H Flavones
R = OH Flav

13

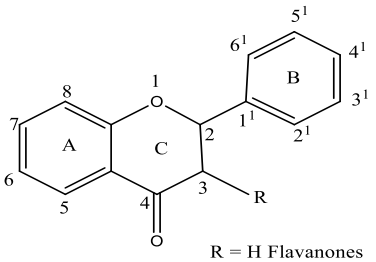

R = H Flavanones
R = OH Flavanols

14

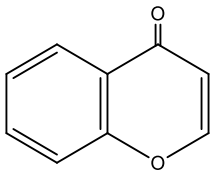

15

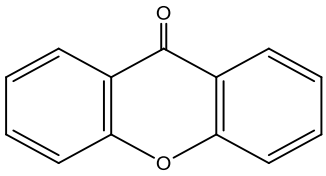

16

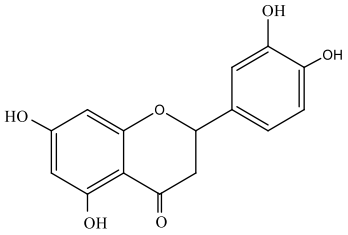

17

Nwidu *et al.* (2012), reported the isolation of cis/trans cinnanoyl glucoside (12) and cis/trans coumaroyl (18) glucoside and cinnamic acid (18) from ethyl acetate leaf fraction of *Carpolobia lutea*. Vitexin and oretin (13 and 14) which are C-glucoside flavones were tentatively identified by HPLC-MS and are the closest compounds in chemical structure to these compounds previously isolated from *C. lutea* extract.

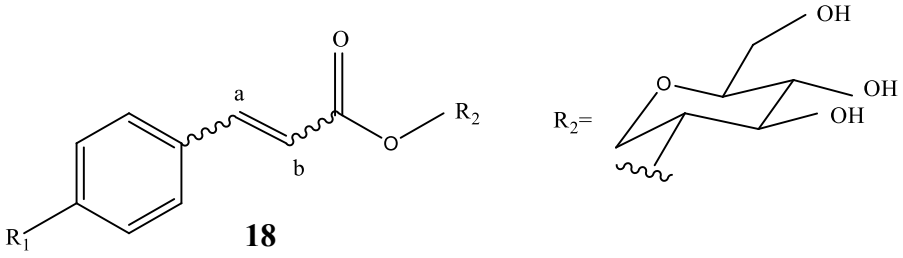

18

1. a,b - Cis, R_1 = H, R_2 = 1- deoxyglucopyranose
2. a,b - Trans, R_1 = H, R_2 = 1- deoxyglucopyranose
3. a,b - Trans, R_1 = H, R_2 = H
4. a,b - Cis, R_1 = OH, R_2 = 1- deoxyglucopyranose
5. a,b - Trans, R_1 = OH, R_2 = 1- deoxyglucopyranose

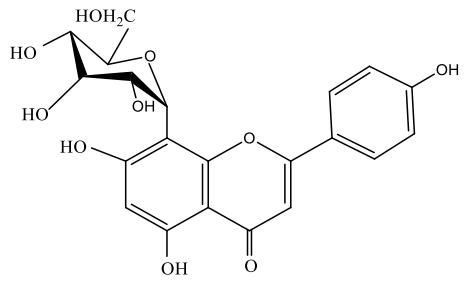

19

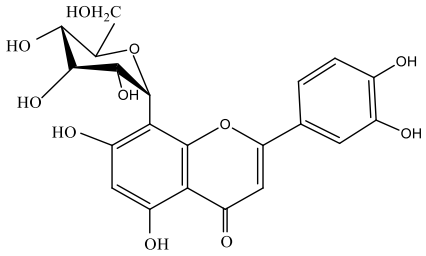

20

Flavonoids are known for their antioxidant effects which they achieve by scavenging for free radicals and suppression of the production of reactive oxygen species. However, these processes can be accompanied by the formation of reactive oxygen species or secondary flavonoid radicals (Cotelle, 2001). Narayan and Raturi (2011) reported that coreopsin - a flavonoid, extracted from *Cosmos sulphureus* gave the highest photoelectric behavior compared to betalains extracted from *Bougainvillea spectabilis* and lutein extracted from *Allamanda cathartica* when used as photosensitizers in the fabrication of DSSCs. Lv *et al.* (2020) also studied the photosensitization effect of flavonoids in the photolysis of chlorothalonil. All six flavonoids (cyaniding, morin, kaempferol, quercetin, galangin and luteolin sensitized the photolysis of chlorothalonil using sunlight or mercury lamps with a higher photosensitization effect under sunlight. Cyanidin showed the highest photosensitization effect. The presence of the aromatic C-ring or the hydroxyl group at the C-3 position enhanced the photosensitization effect of the flavonoids (14). The study by Lv *et al.* (2020) further suggested the presence of $OH^{\cdot}$ or $H^{\cdot}$ radicals play a significant role in the photolysis system.

It is important to note that photosensitization reports on flavonoids did not require the presence of oxygen so we can say that while some of the flavonoid molecules in *Carpolobia lutea* extract acted

as singlet oxygen quenchers, other flavonoids may have generated reactive oxygen species contributing to the photosensitization effect of the plant extract by Type I photosensitization mechanism.

Gallic acid (21), protocatechuic (22) acid and phloroglucinol (23) acid are all phenolic derivatives as seen in Figure 5.7 and will be discussed as such. Lagunes *et al.* (2017) investigated 12 red wine extracts and 10 out of of these extracts were able to act as weak photosensitizers. Lagunes *et al.* (2017) reported that resveratrol and quercetin are among the most important antioxidants reported in red wine, they can generate singlet oxygen while gallic acid remains a singlet oxygen quencher. However, there is a report on the use of a gallic acid derivative (octyl gallate) as a photosensitizer in photodynamic therapy (Shi *et al.*, 2021). So like flavonoids which are also polyphenolic compounds, while some phenolic compounds are oxygen scavengers, others can generate singlet oxygen.

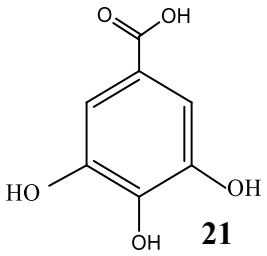

21

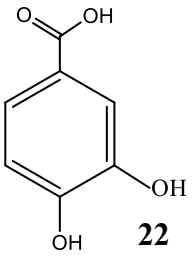

22

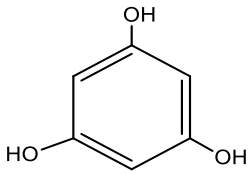

23

There are no reports on any of the photosensitizing effects of phloroglucinols. According to Kakkar and Souravh (2014), protocatechuic acid is a phenolic acid which occurs in nature and is structurally similar to gallic acid. It is a potent antioxidant and there are no reports on any photosensitization ability. It may be safe to say that the phenolics which are gallic acid, protocatechuic acid and phloroglucinol may have contributed minimally to the photoactivity of the fractions rather they may have acted as singlet oxygen quenchers.

CHAPTER 6
CONCLUSION AND RECOMMENDATION

6.1 Conclusion

Hibiscus *sabdariffa* calyces methanol extract gave the highest yield (29%) followed by *Justicia secunda* water/methanol extract (28%) and *Carpolobia lutea* ethyl acetate extract gave the lowest yield (2%).

Carpolobia lutea ethyl acetate extract gave interesting results with comparable conversions to that of rose bengal, methylene blue and tetraphenylporphyrin in the photooxygenations of α-terpinene, 1,5-DHN, 1-naphthol, 1,6-DHN, α-pinene and β-pinene. The yields after work-up were equally good and similar to those obtained using the commercial photosensitizers. Replicate experiments confirmed these observed conversions and yields. *Hibiscus sabdariffa* and *Justicia secunda* showed negligible photoactivity in the photooxygenations of α-terpinene and 1,5- DHN.

Although all three plant extracts investigated had some absorbance in the visible region of the electromagnetic spectrum, *Carpolobia lutea* extract stood out as it had the highest absorbance value of 1.88 at a λmax of 665nm.

Carpolobia lutea extract was observed to be most stable in isopropyl alcohol, stable only for a few hours in acetonitrile but least stable in dichloromethane, its solubility in the various solvents seem to be in the same order.

HPLC-MS analysis of *Carpolobia lutea* extract has shown that it contains some known singlet oxygen-generating compounds (anthraquinones, dianthrones, flavonoids and chlorophyll), some oxygen-scavenging phenolics (gallic acid, phloroglucinol and procatechuic acid) and other compounds such as triterpene.

While the presence of the photosensitizer molecules may have accounted for its success as a photosensitizer, the presence of the singlet oxygen quenchers may have been responsible for the

somewhat photostability of the extract as observed. Also, the presence of these singlet oxygen quenchers may have given a protective effect to some of the unstable photooxygenation products (such as 1,4 – naphthoquinone) which is highly photolabile. These singlet oxygen quenchers may have also increased the time required for the complete conversion of some of the substrates such as 6-Hydroxy-1,4-naphthoquinone **(6)** which took 4 hours for complete conversion using rose bengal but more than12 hours using *Carpolobia lutea* as a photosensitizer.

6.2 Recommendations

1. Isolation of these identified photoactive compounds should be carried out and the photosensitizer activity of these pure compounds tested to see if they are more efficient photosensitizers as pure compounds. This would also help clarify if the high photoactivity of the photoactive fractions is a result of a synergy between the different photosensitizer compounds identified in each fraction.
2. The photoactivity of *Carpolobia lutea* extract in other applications of photosensitizers such as photodynamic therapy and dye-sensitized solar cells should be investigated to see if it gives excellent outcomes as in photooxygenations.
3. The search for natural photosensitizers which have comparable or even better photoactivity than synthetic dyes should continue as this would provide non-toxic and renewable alternatives for the many applications of photosensitizers.

6.3 Contribution To Knowledge

1) *Carpolobia lutea* leaves extract has been identified and proven to be an efficient, green, photosensitizer for photooxygenation reactions comparable to commercially available photosensitizers.

2) Compounds identified which may have been responsible for the effective photoactivity of the *Carpolobia lutea* extract include anthraquinones, dianthrones, chlorophyll, and flavonoids. These compounds contain conjugated double-bond systems and other chromophores and have been reported to be good plant photosensitizers before now.
3) This study also provides some data on the HPLC of *Carpolobia lutea* extract which is scarcely present in literature before now.

REFERENCES

Al-fawwaz, A. T. & Al-Khaza'leh, K. A. (2016). Antibacterial and antifungal effect of some natural extracts and their potential use as photosensitizers. *European Scientific Journal*, *12*(147), 10-19044.

Alañón, M. E., Ivanović, M., Pimentel-Mora, S., Borrás-Linares, I., Arráez-Román, D. & Segura-Carretero, A. (2020). A Novel Sustainable Approach for the Extraction of Value-added Compounds from *Hibiscus sabdariffa L. calyces* by Natural Deep Eutectic Solvents. *Food Research International*, *137*, 109646.

Alarcón-Alonso, J., Zamilpa, A., Aguilar, F. A., Herrera-Ruiz, M., Tortoriello, J. & Jimenez-Ferrer, E. (2012). Pharmacological Characterization of the Diuretic Effect of *Hibiscus sabdariffa* Linn (Malvaceae) Extract. *Journal of Ethnopharmacology*, *139*(3), 751-756.

Ali, B. H., Wabel, N. A. & Blunden, G. (2005). Phytochemical, Pharmacological and Toxicological Aspects of *Hibiscus sabdariffa* L.: a Review. *Phytotherapy Research: An International Journal Devoted to Pharmacological and Toxicological Evaluation of Natural Product Derivatives*, *19*(5), 369-375.

Alshehri, A., Malik, M. A., Khan, Z., Al-Thabaiti, S. A. & Hasan, N. (2017). Biofabrication of Fe Nanoparticles in Aqueous Extract of *Hibiscus sabdariffa* with enhanced photocatalytic activities. *RSC Advances*, *7*(40), 25149-25159.

Akpan, M. M., Okokon, J. E. & Akpan, E. J. (2012). Antidiabetic and Hypolipidemic Activities of Ethanolic Leaf Extract and Fractions of *Carpolobia lutea. Molecular and Clinical Pharmacology*, *3*, 100-7.

Akindahunsi, A. A. & Olaleye, M. T. (2003). Toxicological Investigation of aqueous-Methanolic Extract of the Calyces of *Hibiscus sabdariffa L. Journal of Ethnopharmacology*, *89*(1), 161-164.

Amor, T. B. & Jori, G. (2000). Sunlight-activated Insecticides: Historical Background and Mechanisms of Phototoxic Activity. *Insect Biochemistry and Molecular Biology*, *30*(10), 915-925.

Anyasor, G. N., Okanlawon, A. A. & Ogunbiyi, B. (2019). Evaluation of Anti-inflammatory Activity of *Justicia secunda* Vahl Leaf Extract using in Vitro and In vivo Inflammation Models. *Clinical Phytoscience*, *5*, 1-13.

Banwo, K., Sanni, A., Sarkar, D., Ale, O. & Shetty, K. (2022). Phenolics-Linked Antioxidant and Anti-hyperglycemic Properties of Edible Roselle *(Hibiscus sabdariffa Linn.)* Calyces Targeting Type 2 diabetes Nutraceutical Benefits in Vitro.*Frontiers in Sustainable Food Systems*,*6*, 6.

Benelli, G., Pavela, R., Cianfaglione, K., Sender, J., Danuta, U., Maślanko, W. & Maggi, F. (2020). Ascaridole-rich Essential Oil from Marsh Rosemary (*Ledum palustre*) Growing in Poland Exerts Insecticidal Activity on Mosquitoes, Moths and Flies Without Serious Effects on Non-target Organisms and Human Cells. *Food and Chemical Toxicology*, *138*, 111184.

Benites, J., Cortes, M., Miranda, L., Estela, C., Rios, D., Arenas, J. & Valderrama, J.A. (2014).Green Synthetic Approaches to Furoylnaphthohydroquinone and Juglone. *Journal of the Chilean Chemical Society, 59*(2), 2455–2457.

Berg, K. (2009, November 11). Photosensitizers in Medicine. *Photobiological Sciences Online*. http://photobiology.info/Berg.html

Bezerra, J. J. L., Pinheiro, A. A. V. & Lucena, R. B. (2021). Phytochemistry and Poisoning in Ruminants by *Enterolobium contortisiliquum* (Vell.) Morong (Fabaceae): A Systematic Review. *Toxicon*, *201*, 46-53.

Brar, K. S., Sarma, S. J. & Das, R. K. (2013). Singlet Oxygen Production by Organic Matter and Disintegration of Pathogens and Pollutants During Wastewater Treatment: How Important? *Hydrology Current Research*. *4*(3).

Cavaleiro, J. A., Görner, H., Lacerda, P. S., MacDonald, J. G., Mark, G., Neves, M. G., Nohr, R. S., Schuchmann, H., Sonntag, C. V. & Tomé, A. C. (2001). Singlet oxygen formation and photostability of meso-tetraarylporphyrin derivatives and their copper complexes. *Journal of Photochemistry and Photobiology A: Chemistry*, *144*(2-3), 131-140.

Carella, A., Borbone, F. & Centore, R. (2018). Research Progress on Photosensitizers for DSSC. *Frontiers in Chemistry*, 6.

Cervantes-González, J., Vosburg, D. A., Mora-Rodriguez, S. E., Vázquez, M. A., Zepeda, L. G., Villegas Gomez, C. & Lagunas-Rivera, S. (2020). Anthraquinones: Versatile Organic Photocatalysts. *ChemCatChem*, *12*(15), 3811-3827.

Charles University, Faculty of Pharmacy in Hradec Kralove. (2023). Photodynamic Therapy. https://portal.faf.cuni.cz/Groups/Azaphthalocyanine-group/Research-Projects/Photodynamic-therapy/

Chen, Y., Wang, Z., Zhang, H., Liu, Y., Zhang, S., Meng, Q. & Liu, W. (2018). Isolation of High Purity Anthocyanin Monomers from Red Cabbage with Recycling Preparative Liquid Chromatography and Their Photostability. *Molecules, 23*(5), 991.

Cotelle, N. (2001). Role of Flavonoids in Oxidative Stress. *Current Topics in Medicinal Chemistry*, *1*(6), 569-590.

Coyle, E. (2010). Green Photochemistry: The Synthesis of Fine Chemicals with Sunlight. [Doctoral Thesis, School of Chemical Science, Dublin City University].

Crutchley, R. J. & DeRosa, M. C. (2002). Photosensitized Singlet Oxygen and Its Applications. *Coordination Chemistry Reviews*, 233-234, 351-371.

Dembitsky, V., Shkrob, I. & Hanus, L. O. (2008). Ascaridole and Related Peroxides from the genus Chenopodium. *Biomedical Papers of the Medical Faculty of Palacky University in Olomouc*, *152*(2).

Dhanemozhi, C., Sathyajothi, S. & Jayavel, R. (2017). The Fabrication of Natural Dye-Sensitized Solar Cell (DSSCS) Based on TiO_2. Using Henna and Beetroot Dye Extracts. *Materials Today: Proceedings*. *4*(2), 668-676.

Dougnon, G. & Ito, M. (2020). Role of Ascaridole and P-cymene in the Sleep-promoting Effects of *Dysphania ambrosioides* Essential Oil via the GABAergic System in a ddY Mouse Inhalation Model. *Journal of Natural Products*, *84*(1), 91-100.

Dragomanova, S., Tancheva, L. & Georgieva, M. (2018). A Review: Biological Activity of Myrtenal and Some Myrtenal-containing Medicinal Plant Essential Oils. *Scripta Scientifica Pharmaceutica*, *5*(2), 22-33.

Duke, S. O., Becerril, J. M., Sherman, T. D. & Matsumoto, H. (1991). Photosensitizing Porphyrins as Herbicides In *Naturally Occurring Pest Bioregulators (pp. 31 –39)*, Washington, DC: American Chemical Society. doi:10.1021/bk-1991-0449.ch026

Edris, A. E., Jirovetz, L., Buchbauer, G., Denkova, Z., Stoyanova, A. & Slavchev, A. (2007). Chemical Composition, Antimicrobial Activities and Olfactive Evaluation of a *Salvia officinalis* L.(sage) Essential Oil from Egypt. *Journal of Essential Oil Research*, *19*(2), 186-189.

Ettebong, E. O., Nwafor, P. A., Ekpo, M. & Ajibesin, K. K. (2011). Contraceptive, Estrogenic and Anti-Estrogenic Potentials of Methanolic Root Extract of *Carpolobia lutea* in Rodents. *Pakistan Journal of Pharmaceutical Science*, *24*, 445-449.

Esser, P., Pohlmann, B. & Scharf, H.-D. (1994). The Photochemical Synthesis of Fine Chemicals with Sunlight. *Angewandte Chemie International Edition in English, 33*(20), 2009–2023.

Fekrazad, R., Nejat, A. H. & Kalhori, K. A. M. (2017). Micro & Nano Technologies. In A. Ficai and A. M. Grumezescu (EDs.), *Antimicrobial Photodynamic Therapy with Nanoparticles Versus Conventional Photosensitizers in Oral Diseases*. (pp. 237-259). Elsevier.

Freire, F., Costa, A. C. B. P., Pereira, C. A., Beltrame-Junior, M., Junqueira, J. C. & Jorge, A. O. C. (2014). Comparison of the Effect of Rose Bengal-and Eosin Y-mediated Photodynamic Inactivation on Planktonic Cells and Biofilms of Candida albicans. *Lasers in Medical Science*, *29*, 949-955.

Fulmer, G. R., Miller, A. J., Sherden, N. H., Gottlieb, H. E., Nudelman, A., Stoltz, B. M. & Goldberg, K. I. (2010). NMR Chemical Shifts of Trace Impurities: Common Laboratory Solvents, Organics, and Gases in Deuterated Solvents Relevant to the Organometallic Chemist. *Organometallics*, *29*(9), 2176-2179.

Gassama, A., Ernenwein, Cã©. & Hoffmann, N. (2009). Photochemical Key Steps in the Synthesis of Surfactants from Furfural-Derived Intermediates. *Chemistry Sustainability Energy Materials, 2*(12), 1130–1137.

Gasparetto, A., Lapinski, T. F., Zamuner, S. R., Khouri, S., Alves, L. P., Munin, E. & Salvador, M. J. (2010). Extracts from *Alternanthera maritima* as Natural Photosensitizers in Photodynamic Antimicrobial Chemotherapy (PACT). *Journal of Photochemistry and Photobiology B: Biology*, *99*(1), 15-20.

Guardiola, S. & Mach, N. (2014). Therapeutic Potential of *Hibiscus sabdariffa*: A Review of the Scientific Evidence. *Endocrinología y Nutrición (English Edition)*, *61*(5), 274-295.

Hamblin, M. R., Mansoori, B., Mohammadi, A., Doustvandi, M.A, Mohammadnejad, F., Kamari, F., Gjerstorff, M.F & Baradaran, B. (2019). Photodynamic Therapy for Cancer: Role of Natural Products. *Photodiagnosis Photodynamic Therapy*, *26*, 395-404.

Hassan, A. A., Sajid, M., Tanimu, A., Abdulazeez, I., & Alhooshani, K. (2021). Removal of methylene blue and rose bengal dyes from aqueous solutions using 1-naphthylammonium tetrachloroferrate (III). *Journal of Molecular Liquids*, *322*, 114966.

Huang, L., Cui, X., Therrien, B. & Zhao, J. (2013). Energy-funnelling-based Broadband Visible-light-absorbing Bodipy–C60 triads and Tetrads as Dual Functional Heavy-atom-free Organic Triplet Photosensitizers for Photocatalytic Organic Reactions. *Chemistry–A European Journal*, *19*(51), 17472-17482.

Ikram, S. & Ahmed, S. (2015). Synthesis of Gold Nanoparticles using Plant Extracts: An Overview. *Nano Research and Application*. 1(1).

Islam, A. M. & Widhalm, J. R. (2020). Agricultural uses of Juglone: Opportunities and Challenges. *Agronomy*, *10*(10), 1500.

Ismail, B., Suriani, D., Misrun, M. I. & Nair, G. (2018). Natural Dyes from Roselle Flower as a Sensitizer in Dye-Sensitized Solar Cell. *Indonesian Journal of Electrical Engineering and Computer Science*. *9*(1), 191-197. http://doi.org/10.11591/ijeecs.v9.i1.pp191-197

Jahng, W. J., Tajudeen, H. K., Onuigbo, I. O., Isaac, S. O., Moses, P., Ifekauche, C., Uwiringiyimana, E., Sylvester, O., Kane, M., Neksumi, M., Adams, V. F., Agboola, B. O., Okoro, L. N., & Uche, O. (2017). Synthesis of Dye-Sensitized Solar Cells Using Chromophores from West African Plants. *International Journal of Scientific and Engineering Research*. *8*(6).

Jasim, K. E. (2012). Natural Dye-Sensitized Solar Cell Based On Nanocrystalline TiO_2. *Sains Malaysiana*, *41*(8), 1011-1016.

Jong, W. W., Tan, P. J., Kamarulzaman, F. A., Mejin, M., Lim, D., Ang, I., Naming, M., Yeo,T. C., Ho, A. S., Teo, S. H. & Lee, H. B. (2013). Photodynamic activity of plant extracts from Sarawak, Borneo. *Chemistry & biodiversity*, *10*(8), 1475-1486. doi:10.1002/cbdv.201200303

Julio, B., Michael, C., Luis, M., Cynthia, E., David, R., Jorge, A. & Jaime A. V. (2014). Green Synthetic Approaches to Furoylnaphthohydroquinone and Juglone. *Journal of the Chilean Chemical Society*, *59*(2), 2455-2457.

Kakkar, S. & Bais, S. (2014). A Review on Protocatechuic Acid and Its Pharmacological Potential. *International Scholarly Research Notices*, *2014*.

Karapire, C., Kolancilar, H., Oyman, Ü. & Icli, S. (2002). Fluorescence Emission and Photooxidation Studies with 5, 6-And 6, 7-Benzocoumarins and a 5, 6-Benzochromone Under Direct and Concentrated SunLight. *Journal of Photochemistry and Photobiology A: Chemistry*, *153*(1-3), 173-184.

Kaufmann, B. & Christen, P. (2002). Recent Extraction Techniques For Natural Products: Microwave-Assisted Extraction and Pressurised Solvent Extraction. *Phytochemical Analysis: An International Journal of Plant Chemical and Biochemical Techniques*, *13*(2), 105-113.

Kenney, R. L. & Fisher, G. S. (1973). Preparation of Trans-Pinocarveol and Myrtenol. *Industrial & Engineering Chemistry Product Research and Development*, *12*(4), 317-319.

Kirakosyan, A., Gibson, D. M. & Kaufman, P. B. (2008). The production of dianthrones and phloroglucinol derivatives in St. John's Wort. In *Bioactive molecules and medicinal plants* (pp. 149-164). Berlin, Heidelberg: Springer Berlin Heidelberg.

Kizil, S., Hasimi, N., Tolan, V., Kilinc, E. & Karatas, H. (2010). Chemical Composition, Antimicrobial, and Antioxidant Activities of Hyssop (*Hyssopus officinalis L.*) Essential Oil. *Notulae Botanicae Horti Agrobotanici Cluj-Napoca*, *38*(3), 99-103.

Klotz, L. O., Hou, X. & Jacob, C. (2014). 1, 4-Naphthoquinones: from Oxidative Damage to Cellular and Inter-cellular Signaling. *Molecules*, *19*(9), 14902-14918.

Kudinova, N. V. & Berezov, T. T. (2010). Photodynamic therapy of cancer: Search for ideal photosensitizer.*Biochemistry (Moscow) Supplement Series B: Biomedical Chemistry*,*4*(1), 95-103.

Kulkarni, S., Kale, V. & Valenkar, K. (2018). To Study the Photodynamic Antimicrobial Activity of Henna Extract and Preparation of Topical Gel Formation. *The Journal of Phytopharmacology*. *7*(3), 242-252.

Lagunes, I., Vázquez-Ortega, F. & Trigos, Á. (2017). Singlet Oxygen Detection Using Red Wine Extracts as Photosensitizers. *Journal of Food Science*, *82*(9), 2051-2055.

Lancel, M., Zimberlin, P., Gomez, C., Port, M., Khrouz, L., Monnereau, C. & Amara, Z. (2023). Self-Sensitized Photooxidation of Naphthols to Naphthoquinones and the Use of Naphthoquinones as Visible Light Photocatalysts in Batch and Continuous Flow Reactors. *The Journal of Organic Chemistry*, *88*(10), 6498-6508.

Latos, M., Masek, A. & Zaborski, M. (2019). The Potential of Juglone as Natural Dye and Indicator for Biodegradable Polyesters. *Proceedings of the Institution of Mechanical Engineers, Part L: Journal of Materials: Design and Applications*, *233*(3), 276-285.

Li, J., Wang, L., Li, J., Shao, Y., Liu, Z., Li, G. & Akkaya, E. U. (2022). Taming of Singlet Oxygen: Towards Artificial Oxygen Carriers Based on 1, 4-Dialkylnaphthalenes. *Chemistry–A European Journal*, *28*(34), e202200506.

Linden, S. M. & Neckers, D. C. (1988). Type I and Type II Sensitizers Based on Rose Bengal Onium Salts. *Photochemistry and Photobiology*, *47*(4), 543-550.

Lukšienė, Ž., Kurilčik, N., Juršėnas, S., Radžiutė, S. & Būda, V. (2007). Towards Environmentally and Human-Friendly Insect Pest Control Technologies: Photosensitization of leaf Miner Flies *Liriomyza bryoniae*. *Journal of Photochemistry and Photobiology B: Biology*, *89*(1), 15-21.

Lv, P., Min, S., Wang, Y., Zheng, X., Wu, X., Li, Q. X. & Hua, R. (2020). Flavonoid-sensitized Photolysis of Chlorothalonil in Water. *Pest Management Science*, *76*(9), 2972-2977.

Mandal, V., Mohan, Y. & Hemalatha, S. J. P. R. (2007). Microwave Assisted Extraction—an Innovative and Promising Extraction Tool for Medicinal Plant Research. *Pharmacognosy Reviews*, *1*(1), 7-18.

Mejica, G. F. C., Ramaraj, R. & Unpaprom, Y. (2022). Natural dye (Chlorophyll, Anthocyanin, Carotenoid, Flavonoid) Photosensitizer for Dye-sensitized Solar Cell: A Review. *Maejo International Journal of Energy and Environmental Communication*, *4*(1), 12-22.

Mihelich, E. D. & Eickhoff, D. J. (1983). A One-pot Conversion of Olefins to. Alpha., Beta.-unsaturated Carbonyl Compounds. An Easy Synthesis of 2-cyclopentenone and Related Compounds. *The Journal of Organic Chemistry*, *48*(22), 4135-4137.

Mills, N. S. (1996). Complete Assignment of Proton Chemical Shifts in Terpenes: An Experiment Combining 2D NMR Spectroscopy with Molecular Modeling. *Journal of Chemical Education*, *73*(12), 1190.

Mittal, N., Shah, A., Punjabi, P. B. & Sharma, V. K. (2009). Photodegradation of Rose Bengal using MnO_2 (manganese dioxide). *Rasayan Journal of Chemistry*, *2*(2), 516-520

Montoya, S. C. N., Comini, L. R., Sarmiento, M., Becerra, C., Albesa, I., Argüello, G. A. & Cabrera, J. L. (2005). Natural Anthraquinones Probed as Type I and Type II Photosensitizers: Singlet Oxygen and Superoxide Anion Production. *Journal of Photochemistry and Photobiology B: Biology*, *78*(1), 77-83.

Monzote, L., Stamberg, W., Staniek, K. & Gille, L. (2009). Toxic effects of carvacrol, caryophyllene oxide, and ascaridole from the essential oil of Chenopodium ambrosioides on mitochondria. *Toxicology and Applied Pharmacology*, *240*(3), 337-347.

Mugas, M. L., Calvo, G., Marioni, J., Céspedes, M., Martinez, F., Vanzulli, S., Saenz, D., Di Venosa., G. & Casas, A. (2021). Photosensitization of a subcutaneous tumour by the natural anthraquinone parietin and blue light. *Scientific Reports*, *11*(1), 23820.

Narayan, M. R. (2012). Dye sensitized solar cells based on natural photosensitizers. *Renewable and sustainable energy reviews*, *16*(1), 208-215.

Nsubuga, H., Basheer, C., Al-Muallem, H. A. S. & Kalanthoden, A. N. (2016). Isolation, Characterization and Evaluation of Photochemical Potential of Rice Husk-Based Furfural via Continuous Flow Reactor. *Journal of Environmental Chemical Engineering, 4*(1), 857–863.

Nwafor, P. A. & Bassey, A. I. (2007). Evaluation of Anti-diarrhoeal and Anti-ulcerogenic Potential of Ethanol Extract of *Carpolobia lutea* Leaves in Rodents. *Journal of Ethnopharmacology*, *111*(3), 619-624.

Nwidu, L. L., Elmorsy, E., Thornton, J., Wijamunige, B., Wijesekara, A., Tarbox, R. & Carter, W. G. (2017). Anti-acetylcholinesterase Activity and Antioxidant Properties of Extracts and Fractions of *Carpolobia lutea. Pharmaceutical biology*, *55*(1), 1875-1883.

Nwidu, L. L., Nwafor, P. A. & Vilegas, W. (2012). Neuropharmacological Screening and Isolation of Cinnamoyl and Coumaroyl-Glucosides From Leaf Fraction of *Carpolobia lutea G. Don (Polygalaceae). Indian Journal of Novel Drug Delivery*, *4*(1), 28-37.

Oelgemöeller, M., Robertson, J. M. & Wau, S. J. (2021). Solar Photooxygenations for the Manufacturing of Fine Chemicals-Technologies and Applications. *Molecules*, *26*(6), 1685.

Oelgemöller, M., Goodine, T. & Malakar, P. (2017). Flow Photochemistry - a Green Technology with a Bright Future. *Sustainable Flow Chemistry,* 1–24. https:// org/10.1002/9783527689118.ch1

Oelgemöller, M. (2016). Solar Photochemical Synthesis: From the Beginnings of Organic Photochemistry to the Solar Manufacturing of Commodity Chemicals. *Chemical Reviews, 116*(17), 9664–9682. https://doi.org/10.1021/acs.chemrev.5b00720

Oelgemöller, M., Healy, N., de Oliveira, L., Jung, C. & Mattay, J. (2006). Green Photochemistry: Solar-Chemical Synthesis of Juglone with Medium Concentrated Sunlight. *Green Chemistry*, *8*(9), 831–834.

Oko, A. O., Ekuma, E. T. & Eluu, S. C. (2022). *Justicia Secunda*: a Poultry Phytogenic Growth Promoter. Pre-print at *Justicia secunda*: a Poultry Phytogenic Growth Promoter | Research Square (2022)

Oleinick, N. L. (2011, September 9). Photosensitization: Basic Photosensitization. *Photobiological Sciences Online*. http://photobiology.info/Oleinick.html

Onoja, S. O., Ezeja, M. I., Omeh, Y. N. & Onwukwe, B. C. (2017). Antioxidant, Anti-inflammatory and Antinociceptive Activities of Methanolic Extract of *Justicia secunda* Vahl leaf. *Alexandria Journal of Medicine*, *53*(3), 207-213.

Ouannes, C. & Wilson, T. (1968). Quenching of Singlet Oxygen by Tertiary Aliphatic Amines. Effect of DABCO (1, 4-diazabicyclo [2.2. 2] octane). *Journal of the American Chemical Society*, *90*(23), 6527-6528.

Park, C. Y., Kim, Y. J., Lim, H. J. Park, J. H., Kim, M. J., Seo, S. W. & Park, C. P. (2015). *Continuous Flow Photooxygenation of Monoterpenes. RSC Advances., 5*(6), 4233–4237.

Pouyet, B. & Chapelon, R. (1987). Photochemical Mechanisms in Photosensitization. *Journal de Physique*, *48*(C7), 247-251.

Protti, S., & Fagnoni, M. (2009). The Sunny Side of Chemistry: Green Synthesis by Solar Light. *Photochemical & Photobiological Sciences*, *8*(11), 1499-1516.

Rauf, M. A., Graham, J. P., Bukallah, S. B. & Al-Saedi, M. A. (2009). Solvatochromic Behavior on the Absorption and Fluorescence Spectra of Rose Bengal Dye in Various Solvents.*Spectrochimica Acta Part A: Molecular and Biomolecular Spectroscopy*,*72*(1), 133-137.

Riaz, G. & Chopra, R. (2018). A Review on Phytochemistry and Therapeutic Uses of *Hibiscus sabdariffa L*. *Biomedicine & Pharmacotherapy*, *102*, 575-586.

Ronzani, F., Costarramone, N., Blanc, S., Benabbou, A. K., Le Bechec, M., Pigot, T., Oelgemöller, M. & Lacombe, S. (2013). Visible-light photosensitized oxidation of α-terpinene using novel silica-supported sensitizers: Photooxygenation vs. Photodehydrogenation. *Journal of Catalysis*, *303*, 164-174.

Ryberg, E. C., Knight, J. & Kim, J.-H. (2020). Farm-to-Tap Water Treatment: Naturally-Sourced Photosensitizers for Enhanced Solar Disinfection of Drinking Water. *ACS ES&T Engineering.*

Santos, D.T, Albarelli, J. Q., Joyce, K. & Oelgemoller, M.(2009). Sensitizer Immobilization in Photochemistry: Evaluation of a Novel Green Support. *Journal of Chemical Technology Biotechnology*. *84*: 1026-1030.

Schwarting, A. E. (1977). Dimeric natural compounds with pharmacological activity. In *New Natural Products and Plant Drugs with Pharmacological, Biological or Therapeutical Activity: Proceedings of the First International Congress on Medicinal Plant Research, Section A, held at the University of Munich, Germany, September 6–10, 1976* (pp. 197-211). Springer Berlin Heidelberg.

Sekar, M., Hashim, H. N. M., Fadzil, F. S. A., Sukaini, S. S. M., Zukhi, N. N. M., Nadzri, M. N. & Abdullah, M. S. (2015). Antibacterial Activity of the Methanolic Extract of *Hibiscus sabdariffa* Leaves and Fruits. *British Microbiology Research Journal*, *10*(5), 1-6.

Simon, M. I. (1967). *Photosensitization*. In M. Florkin and E. H. Stotz (Eds.), Comprehensive Colloques Biochemistry (pp. 137-156). https://doi.org/10.1016/B978-1-4831-9716-6.50012-4.

Sharifi-Rad, J., Hoseini-Alfatemi, S. M., Sharifi-Rad, M. & Setzer, W. N. (2015). Chemical Composition, Antifungal and Antibacterial Activities of Essential Oil from L allemantia Royleana (B enth. in W all.) B enth. *Journal of Food Safety*, *35*(1), 19-25.

Sheng, C. K. & Yunus, W. M. M. (2005). Study of Photobleaching Mechanism in Methylene Blue Sensitized Gelatin Using a Single Beam UV-Vis. Fibre Optics Spectrophotometer. *Journal Science & Technol*ogy, *13*(1), 23-30.

Shi, Y. G., Zhu, C. M., Li, D. H., Shi, Z. Y., Gu, Q., Chen, Y. W., Wang, J-Q, Ettelaie, R. & Chen, J. S. (2021). New Horizons in Microbiological Food Safety: Ultraefficient Photodynamic Inactivation Based on a Gallic Acid Derivative and UV-A Light and Its Application with Electrospun Cyclodextrin Nanofibers.*Journal of Agricultural and Food Chemistry*,*69*(49), 14961-14974.

Shvydkiv, O., Jähnisch, K., Steinfeldt, N., Yavorskyy, A. & Oelgemöller, M. (2018). Visible-Light Photooxygenation of Alpha-Terpinene in a Falling Film Microreactor. Catalysis Today, *308*, 102–118.

Sortino, S., Petralia, S., Boscà, F. & Miranda, M. A. (2002). Irreversible photo-oxidation of propranolol triggered by self-photogenerated singlet molecular oxygen. *Photochemical & Photobiological Sciences*, *1*(2), 136-140.

Strugstad, M. & Despotovski, S. (2012). A Summary of Extraction, Synthesis, Properties, and Potential Uses of Juglone: A Literature Review. *Journal of Ecosystems and Management*, *13*(3).

Suchard, O., Kane, R., Roe, B. J., Zimmermann, E., Jung, C., Waske, P. A., Mattay, J. & Oelgemöller, M. (2006). Photooxygenations of 1-Naphthols: an Environmentally Friendly Access to 1, 4-Naphthoquinones. *Tetrahedron*, *62*(7), 1467-1473.

Svoboda, K. P. & Hampson, J. B. (1999). Bioactivity of Essential Oils of Selected Temperate Aromatic Plants: Anti-bacterial, Anti-oxidant, Anti-inflammatory and Other Related

Pharmacological Activities. *Plant Biology Department, SAC Auchincruive, Ayr, Scotland, UK., KA6 5HW*, *16*, 1-7.

Taniguchi, M., Lindsey, J. S., Bocian, D. F. & Holten, D. (2021). Comprehensive Review of Photophysical Parameters (E, Φf, Ts) of Tetraphenylporphyrin (H_2TPP) and Zinc Tetraphenylporphyrin (ZnTPP)–Critical Benchmark Molecules In Photochemistry And Photosynthesis. *Journal of Photochemistry and Photobiology C: Photochemistry Reviews*, *46*, 100401.

Taya, S.A., El-Agez, T.M., Al-Kahlout, A. & Abdel-latif, M.S. (2012). Dye-Sensitized Solar Cells Based on ZnO Films and Natural Dyes. *International Journal of Material and Chemistry*, *2*(3), 105-110. doi: 10.5923/j.ijmc.20120203.04

Thandu, M., Comuzzi, C. & Goi, D. (2015). Phototreatment of Water by Organic Photosensitizers and Comparison with Inorganic Semiconductors. *International Journal of Photoenergy*, 1-22.

Terra, J. C., Desgranges, A., Amara, Z. & Moores, A. (2023). Photocatalysis on Magnetic Supports for Singlet Oxygen Generation: Role of Immobilization and Photobleaching. *Catalysis Today*, *407*, 52-58.

Theiler, B. A., Revoltella, S., Zehl, M., Dangl, C., Caisa, L. O. E., König, J. & Glasl, S. (2014). Secundarellone A, B, and C from the Leaves of *Justicia secunda* Vahl. *Phytochemistry Letters*, *10*, cxxix-cxxxii.

Tongnuanchan, P. & Benjakul, S. (2014). Essential Oils: Extraction, Bioactivities, and their uses for food preservation. *Journal of Food Science*, *79*(7), R1231-R1249.

Tønnesen, H. H. (2001). Formulation and Stability Testing of Photolabile Drugs. *International Journal of Pharmaceutics, 225*(1-2), 1-14.

Triemer, S., Gilmore, K., Vu, G. T., Seeberger, P. H. & Seidel-Morgenstern, A. (2018). Literally Green Chemical Synthesis of Artemisinin from Plant Extracts. *Angewandte Chemie International Edition, 57*(19), 5525–5528.

Ugboaja, T. A., Ndukwe, G. I. & Fekerurhobo, G. K. (2022). Investigation of *Hibiscus sabdariffa* as a New Eco-friendly Photo-larvicidal Natural Product for the Control of Mosquitoes. *Scientia Africana*, *21*(1), 245-252.

Verma, S. & Gupta, G. (2017). Natural Dyes and its Applications: A Brief Review. *International Journal of Research and Analytical Reviews*, *4*(4), 57-60.

Villacorta, R. B., Roque, K. F. J., Tapang, G. A. & Jacinto, S. D. (2017). Plant Extracts as Natural Photosensitizers in Photodynamic Therapy: In Vitro Activity Against Human Mammary Adenocarcinoma MCF-7 Cells. *Asian Pacific Journal of Tropical Biomedicine, 7*(4), 358–366.

Vinuth, M., Naik, H. B., Vinoda, B. M., Pradeepa, S. M., Kumar, G. A. & Sekhar, K. C. (2016). Rapid removal of hazardous Rose Bengal dye using Fe (III)–Montmorillonite as an effective adsorbent in aqueous solution. *Journal of. Environmental and Analytical. Toxicology*, *6*(2), 1000355.

Volman, D. H., Hammond, G. S. & Gollnick, K. (Ed.). (2007*). Advances in Chemistry*. John Wiley and Sons.

Wagner, H. K., & Wolff, P. M. (Eds.). (2012). *New Natural Products and Plant Drugs with Pharmacological, Biological or Therapeutical Activity: Proceedings of the First International Congress on Medicinal Plant Research, Section A, Held at the University of Munich, Germany, September 6–10, 1976*. Springer Science & Business Media.

Waser, M., & Falk, H. (2011). Progress in the Chemistry of Second Generation Hypericin Based Photosensitizers. *Current Organic Chemistry*, *15*(23), 3894-3907.

Wau, J. S., Robertson, M. J. & Oelgemöller, M. (2021). Solar photooxygenations for the manufacturing of fine chemicals—technologies and applications. *Molecules*, *26*(6), 1685.

Widhalm, J. R. & Rhodes, D. (2016). Biosynthesis and Molecular Actions of Specialized 1, 4-Naphthoquinone Natural Products Produced by Horticultural Plants. *Horticulture Research*, *3*.

Yadav, S. C., Sharma, A., Devan, R. S. & Shirage, P. M. (2022). Role of Different Counter Electrodes on Performance of TiO2 Based Dye-sensitized Solar Cell (DSSC) Fabricated with Dye Extracted from *Hibiscus sabdariffa* as Sensitizer. *Optical Materials*, *124*, 112066.

Yakubu, M. T. & Jimoh, R. O. (2015). Aqueous Extract of *Carpolobia lutea* Root Ameliorates Paroxetine-induced Anti-androgenic Activity in Male Rats. *Middle East Fertility Society Journal*, *20*(3), 192-197.

APPENDICES

Appendix 1: GC Chromatograms for Monitoring the Rose Bengal Sensitized Photooxygenation of α-Terpinene at 90 Minutes Replicates 1 and 2

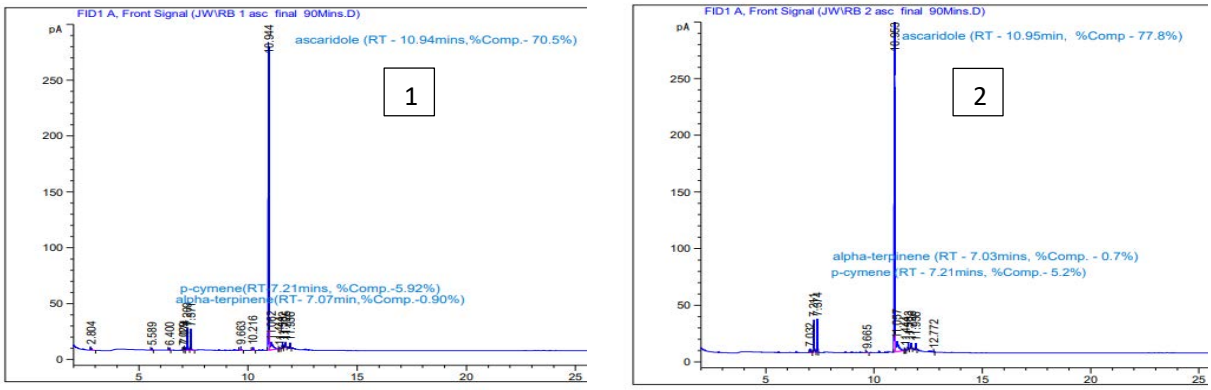

Appendix 2: GC Chromatograms for Monitoring the Methylene Blue Sensitized Photooxygenation of α-Terpinene at 90 Minutes Replicates 1 and 2

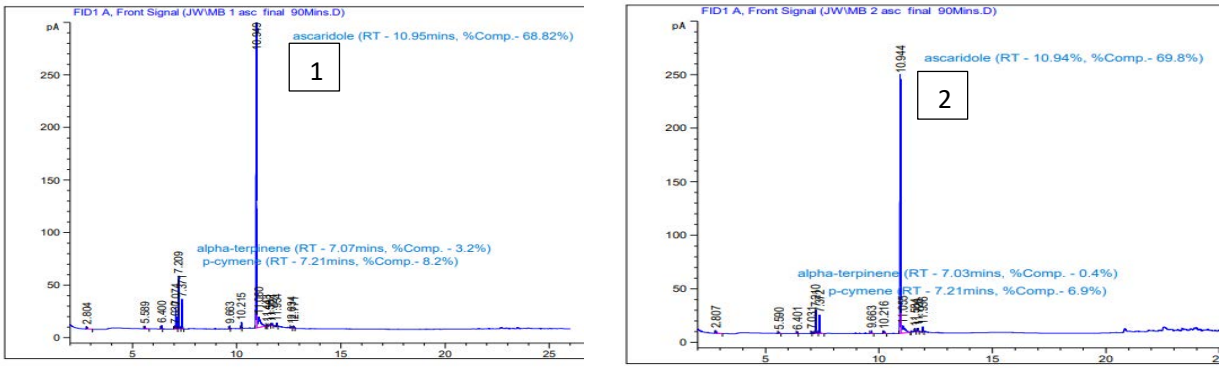

Appendix 3: GC Chromatograms for Monitoring the *Hibiscus sabdariffa* Extract Sensitized Photooxygenation of α-Terpinene at 90 Minutes Replicates 1 and 2

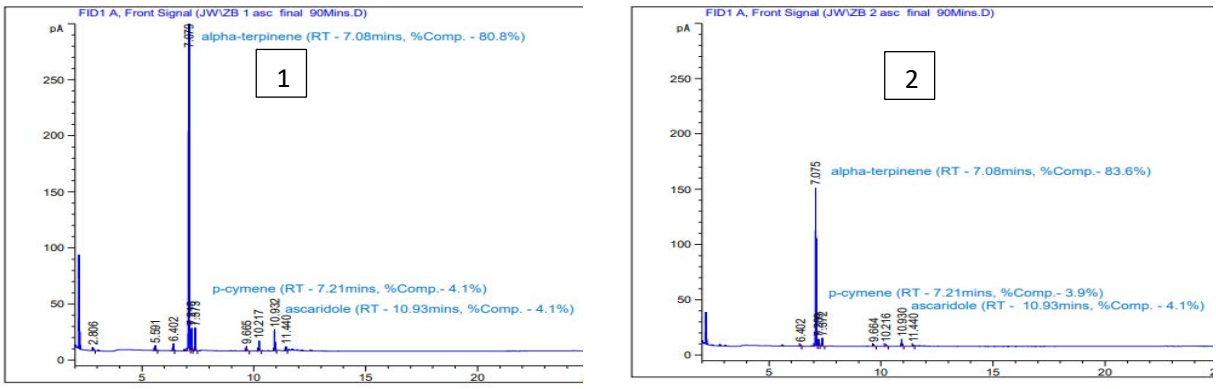

Appendix 4: Chromatograms for Monitoring the *Carpolobia lutea* Extract Sensitized Photooxygenation of α-Terpinene at 90 Minutes Replicates 1 and 2

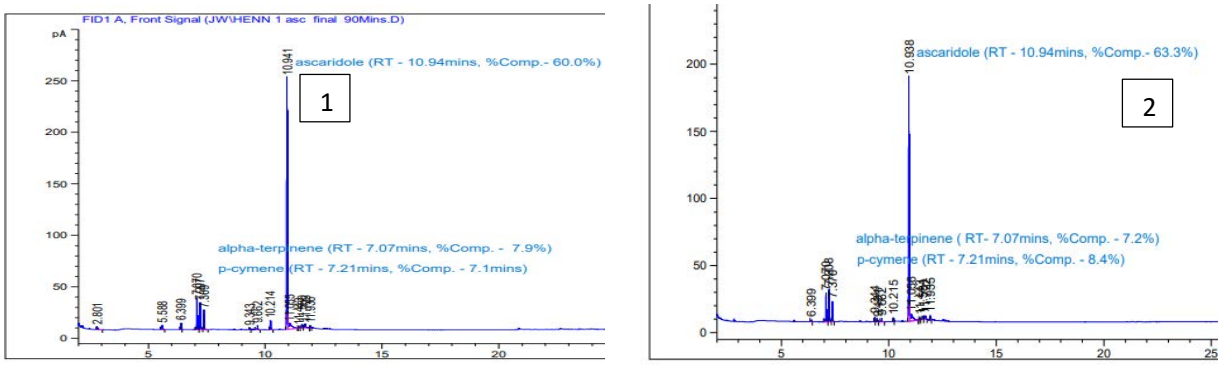

Appendix 5: Chromatograms for Monitoring the *Justicia secunda* Extract Sensitized Photooxygenation of α-Terpinene at 90 Minutes Replicates 1 and 2

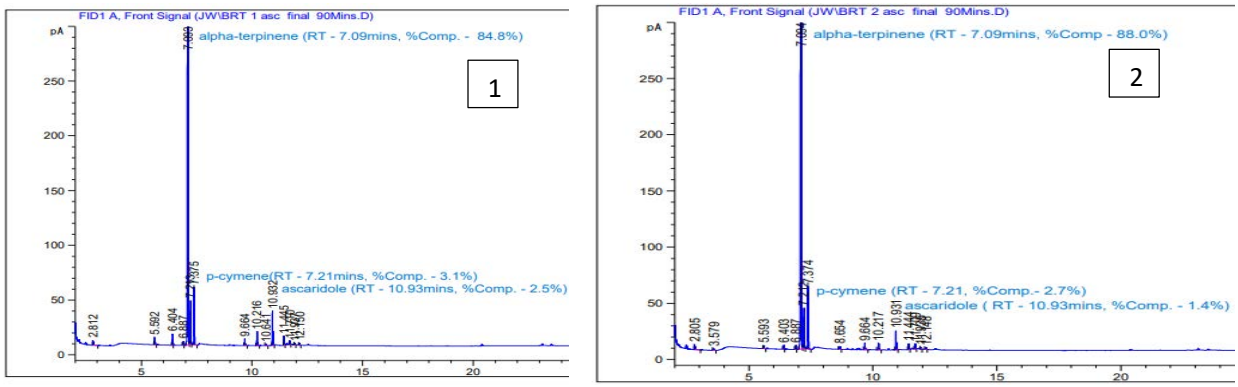

Appendix 6: Chromatograms for Monitoring the DABCO and *Carpolobia lutea* Extract Sensitized Photooxygenation of α-Terpinene at 90 Minutes Replicates1 and 2

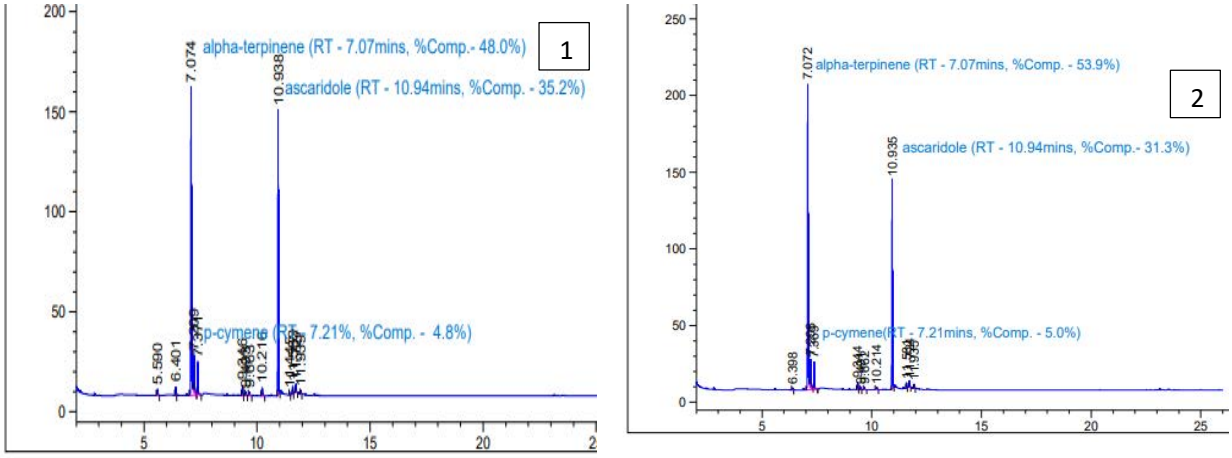

Appendix 7: Chromatograms for Monitoring the ANT-COOH and *Carpolobia lutea* Extract Sensitized Photooxygenation of α-Terpinene at 90 Minutes Replicates1 and 2

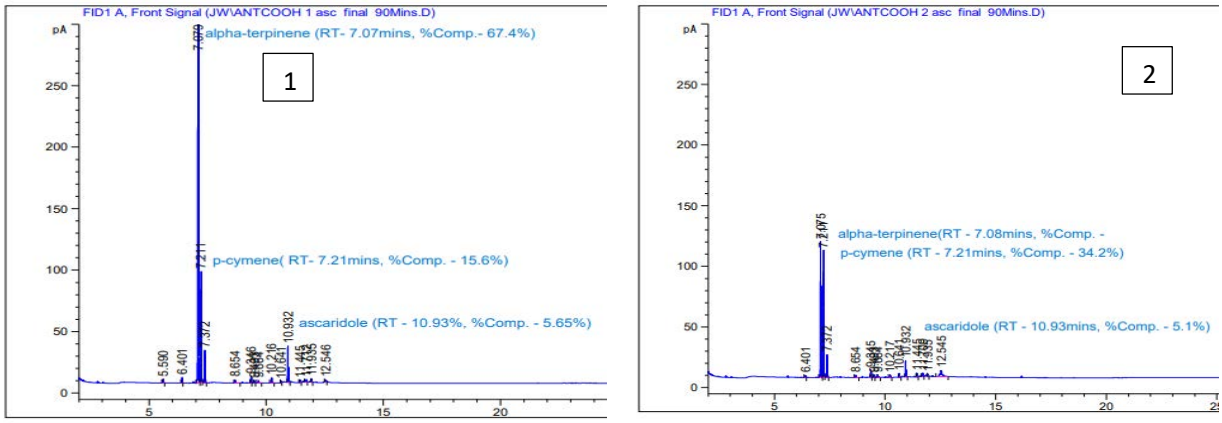

Appendix 8: **^{1}H NMR Spectra for Monitoring Autoxidation of 1,5-Dihydroxynaphthalene at 8 Hours, Replicates1 and 2**

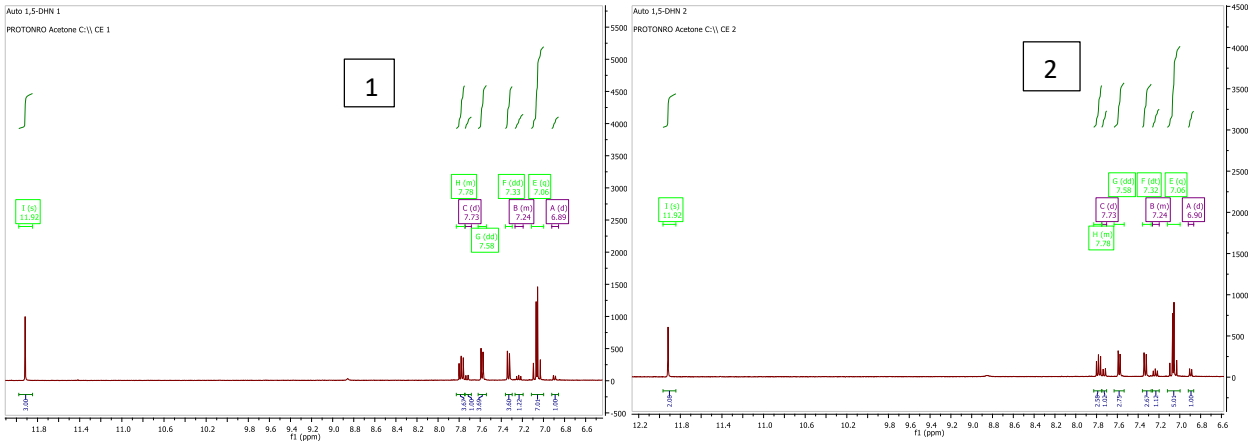

Appendix 9: ^{1}H NMR Spectra for Monitoring Rose Bengal Sensitized Photooxygenation of 1,5-Dihydroxynaphthalene at 8 Hours, Replicates1 and 2

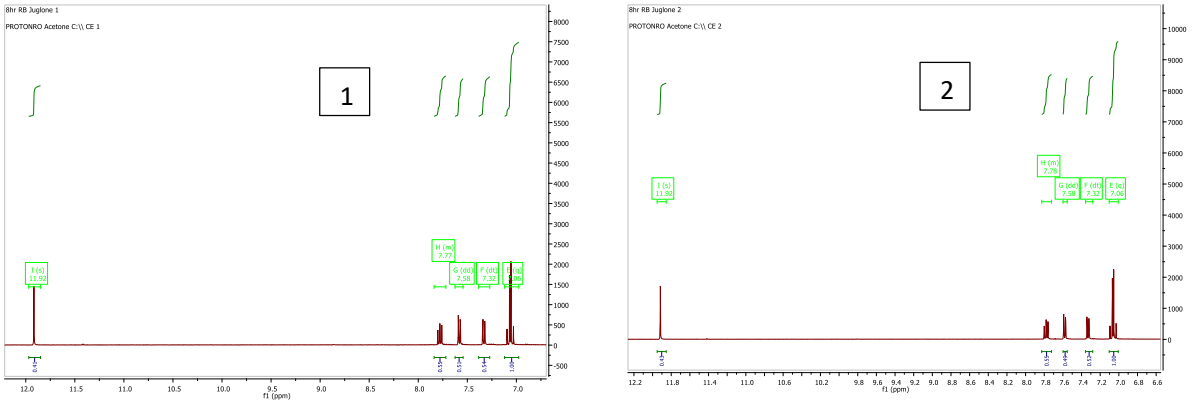

Appendix 10: ^{1}H NMR Spectra for Monitoring Methylene Blue Sensitized Photooxygenation of 1,5-Dihydroxynaphthalene at 8 Hours, Replicates 1 and 2

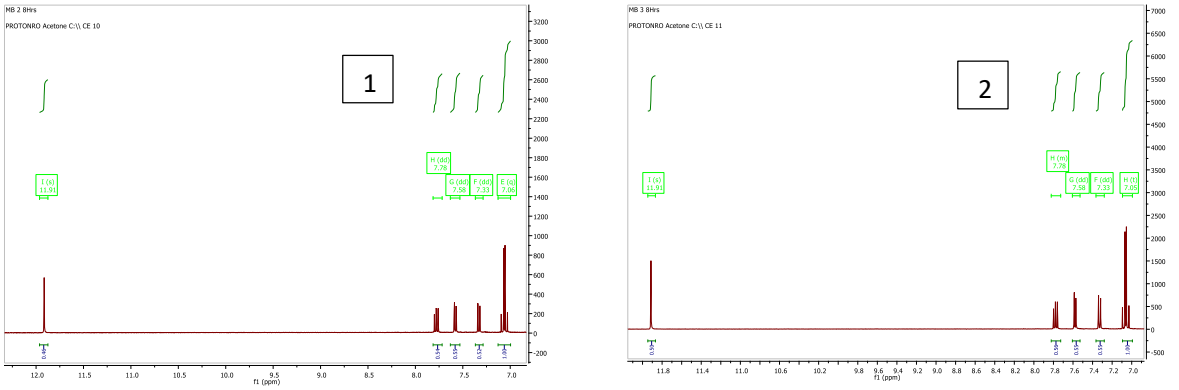

Appendix 11: ^{1}H NMR Spectra for Monitoring *Hibiscus sabdariffa* Extract Sensitized Photooxygenation of 1,5-Dihydroxynaphthalene at 8 Hours, Replicates1 and 2

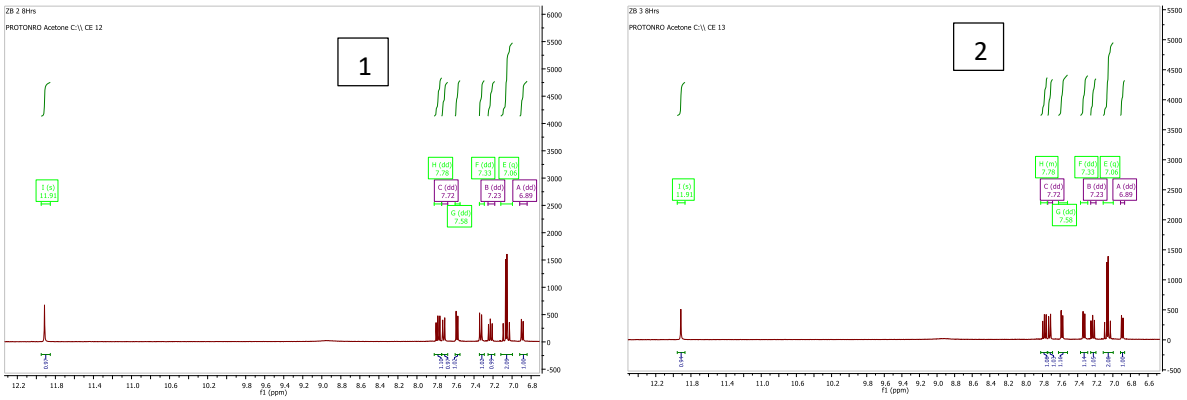

Appendix 12: ^{1}H NMR Spectra for Monitoring *Carpolobia lutea* Sensitized Photooxygenation of 1,5-Dihydroxynaphthalene at 8 Hours, Replicates1 and 2

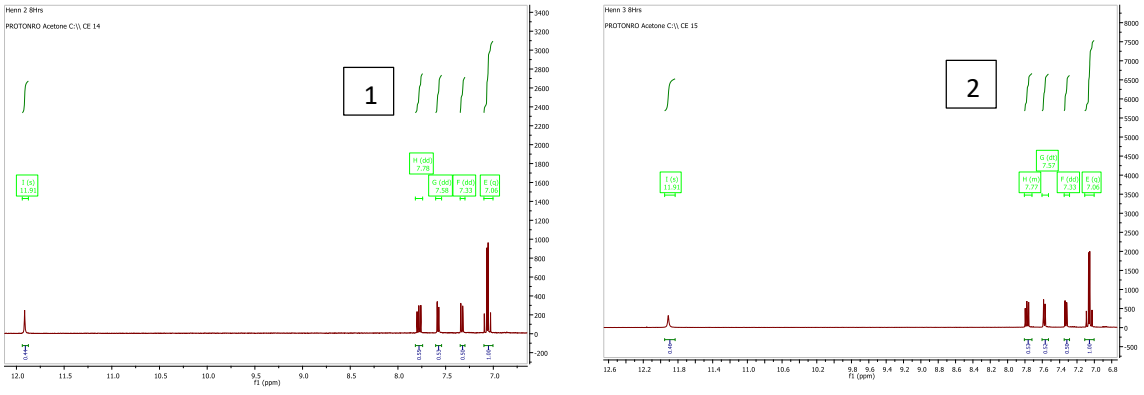

Appendix 13: **^{1}H NMR Spectra for Monitoring *Justicia secunda* Sensitized Photooxygenation of 1,5-Dihydroxynaphthalene at 8 Hours, Replicates 1 and 2**

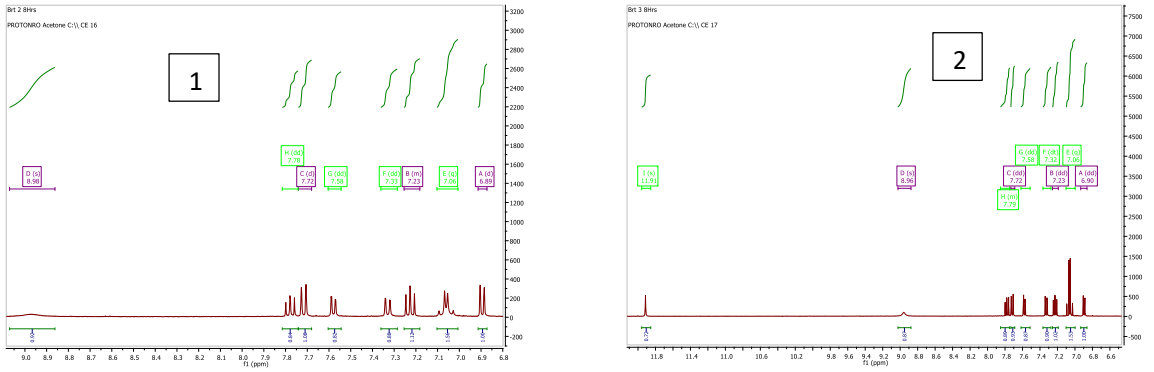

Appendix 14: **^{1}H NMR Spectra for Monitoring Rose Bengal Sensitized Photooxygenation of 1-Naphthol at 2 Hours Replicates1 and 2**

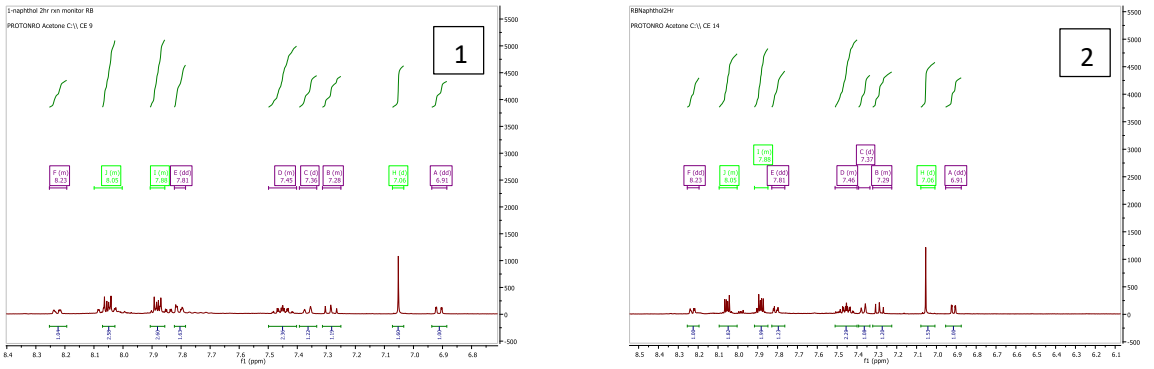

Appendix 15: ^{1}H NMR Spectra for Monitoring *Carpolobia lutea* Sensitized Photooxygenation of 1-Naphthol at 2 Hours Replicates 1 and 2

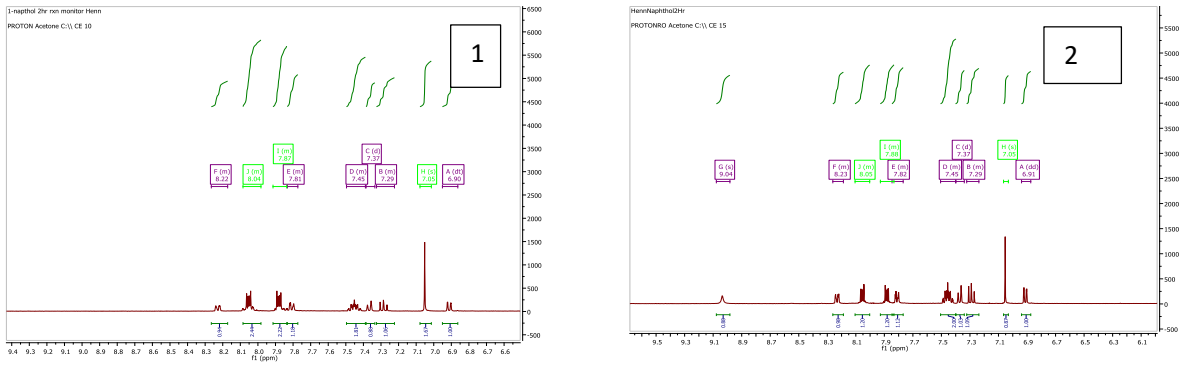

Appendix 16: **^{1}H NMR Spectra for Monitoring Rose Bengal Sensitized Photooxygenation of 1,6-Dihydroxynaphthalene at 8 Hours, Replicates 1 and 2**

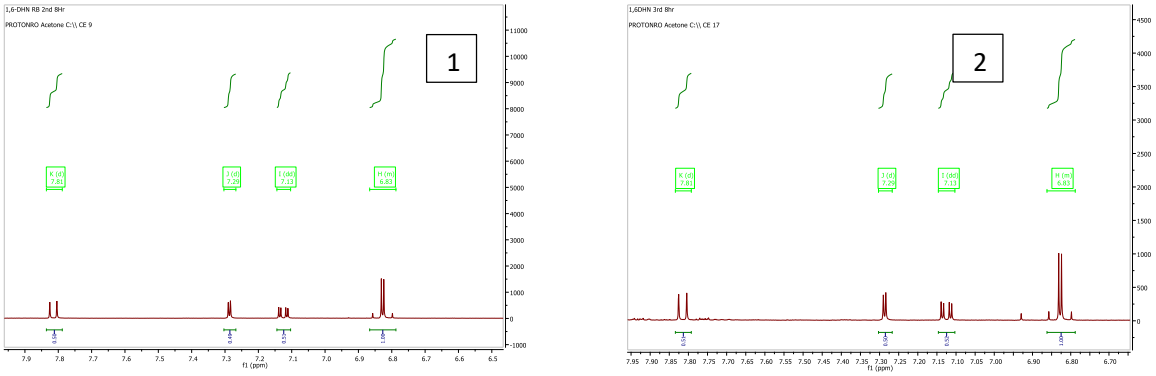

Appendix 17: ^{1}H NMR Spectra for Monitoring *Carpolobia lutea* Sensitized Photooxygenation of 1,6-Dihydroxynaphthalene at 12 Hours, Replicates1 and 2

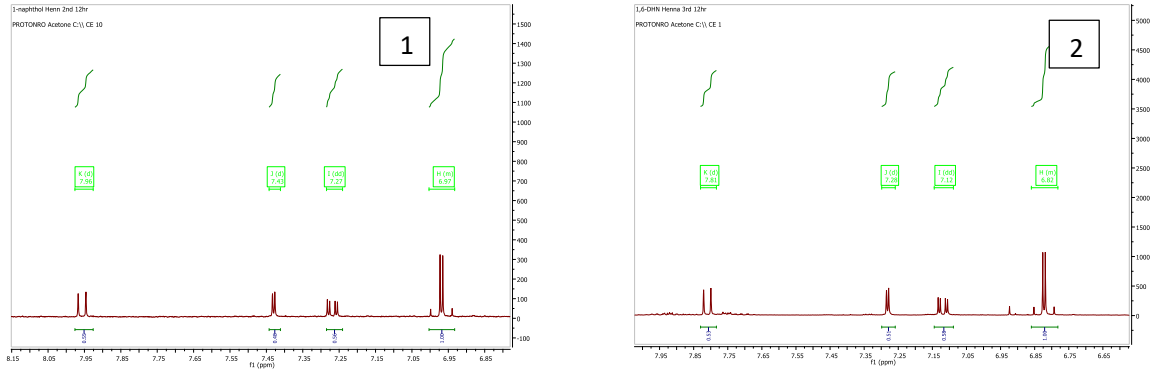

Appendix 18: GC Chromatograms for Monitoring the Tetraphenylporphyrin Sensitized Photooxygenation of α-pinene at 24 Hours, Replicates 1 and 2

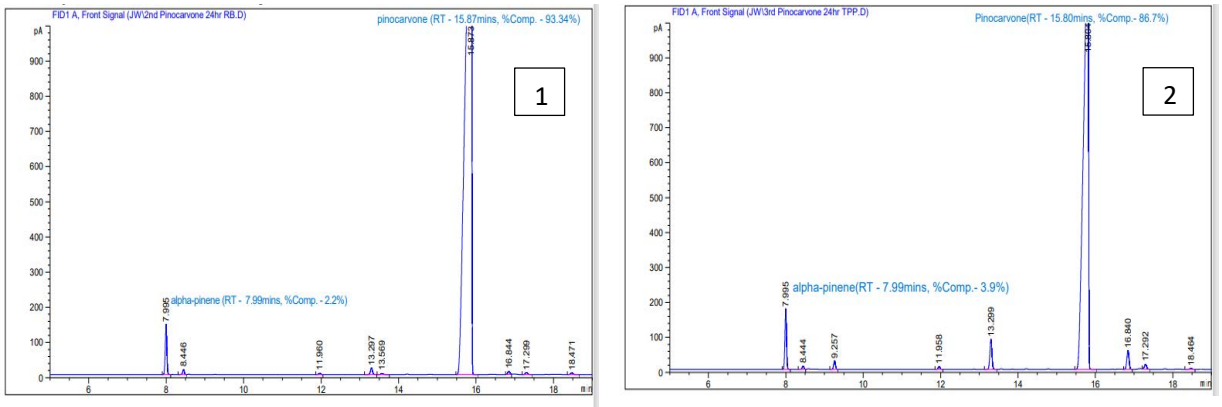

Appendix 19: GC Chromatograms for Monitoring the *Carpolobia lutea* Sensitized Photooxygenation of α-Pinene at 24 Hours, Replicates 1 and 2

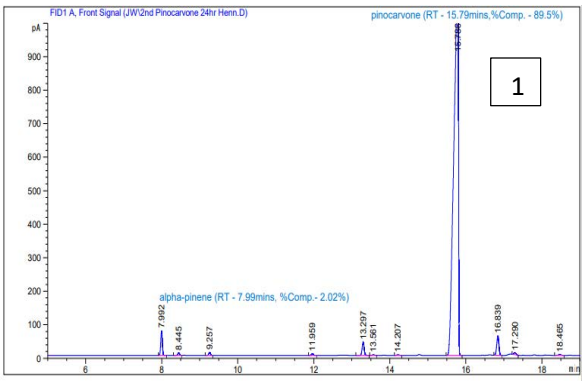

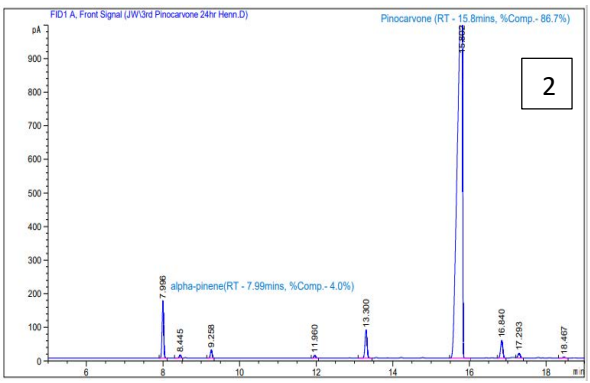

Appendix 20: Chromatograms for Monitoring the Tetraphenylporphyrin Sensitized Photooxygenation of β-pinene at 48 Hours, Replicates 1 and 2

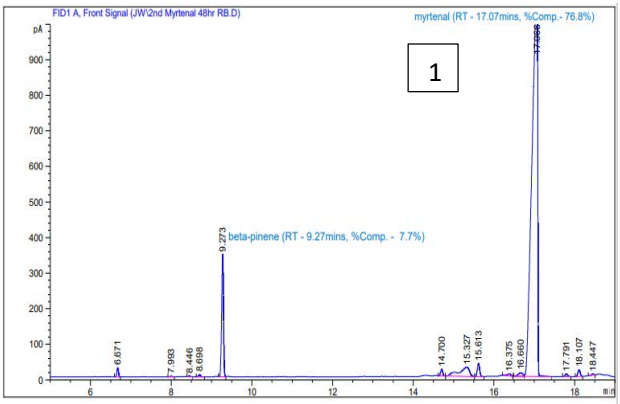

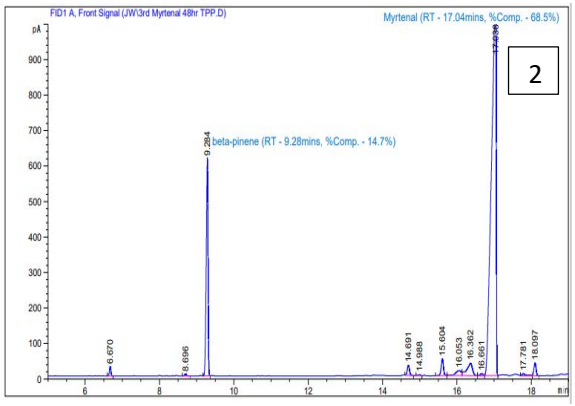

Appendix 21: GC Chromatograms for Monitoring the *Carpolobia lutea* Sensitized Photooxygenation of β-pinene at 48 Hours, Replicates 1 and 2

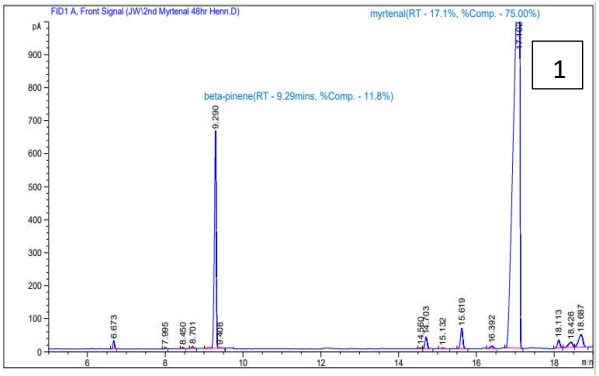

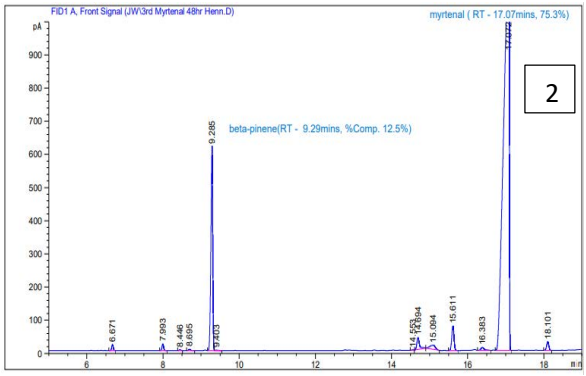

Appendix 22: GC Chromatograms for Monitoring Methylene Blue Sensitized Photooxygenation of Ascaridole at 0 Minutes and 90 Minutes (Standard for Fraction Testing)

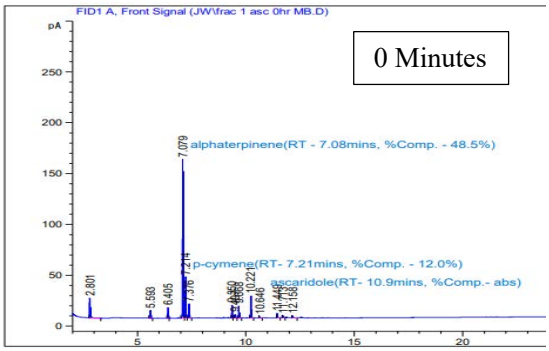

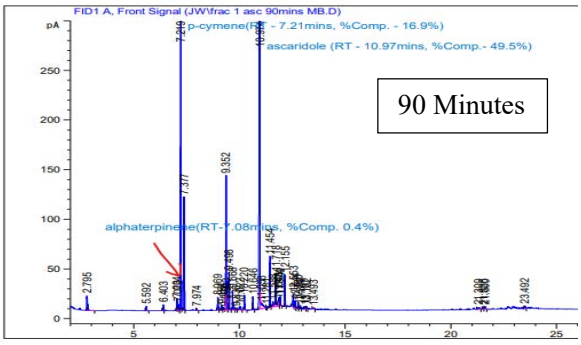

Appendix 23: GC Chromatograms for Monitoring *C. lutea* Fraction 1 Sensitized Photooxygenation of Ascaridole at 0 Minutes and 90 Minutes

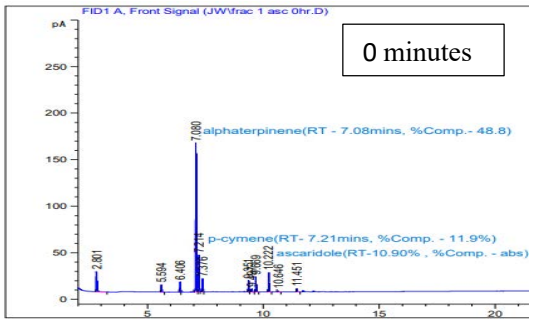

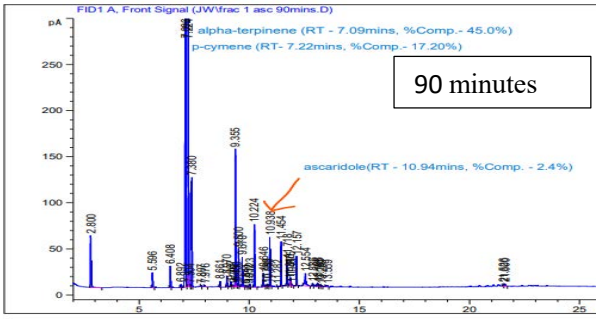

Appendix 24: GC Chromatograms for Monitoring *C. lutea* Fraction 2a Sensitized Photooxygenation of Ascaridole at 0 Minutes and 90 Minutes

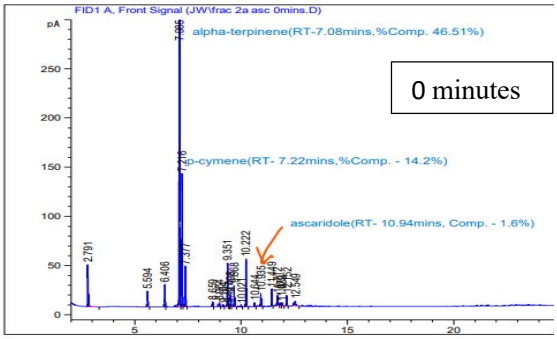

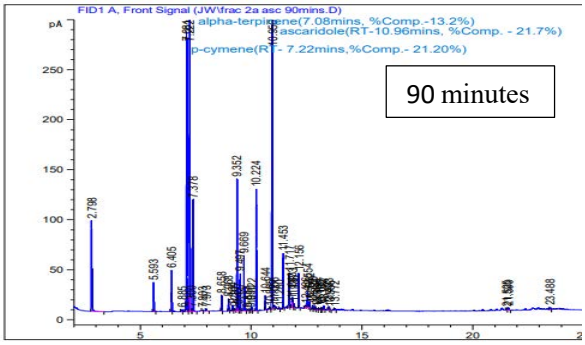

Appendix 25: GC Chromatograms for Monitoring *C. lutea* Fraction 2b Sensitized Photooxygenation of Ascaridole at 0 Minutes and 90 Minutes

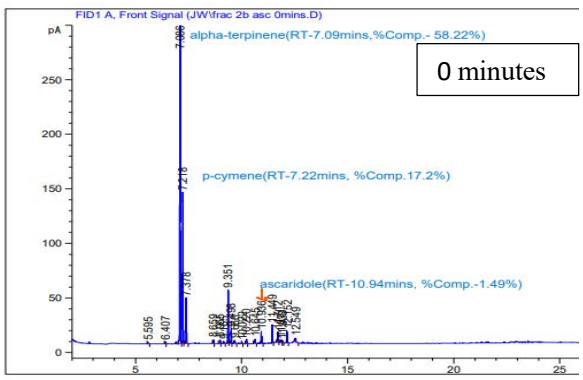

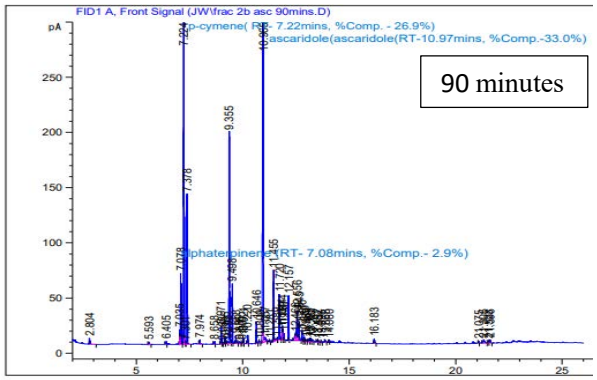

Appendix 26: GC Chromatograms for Monitoring *C. lutea* Fraction 2c Sensitized Photooxygenation of Ascaridole at 0 Minutes and 90 Minutes

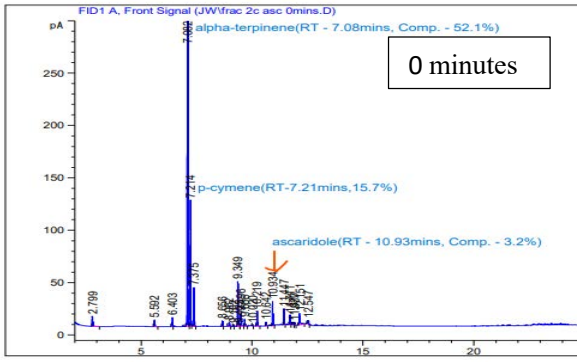

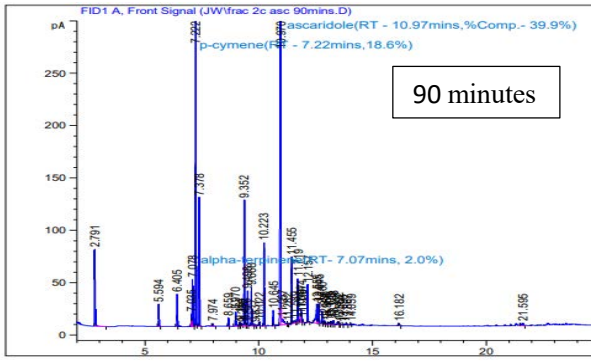

Appendix 27: GC Chromatograms for Monitoring *C. lutea* Fraction 2d Sensitized Photooxygenation of Ascaridole at 0 Minutes and 90 Minutes

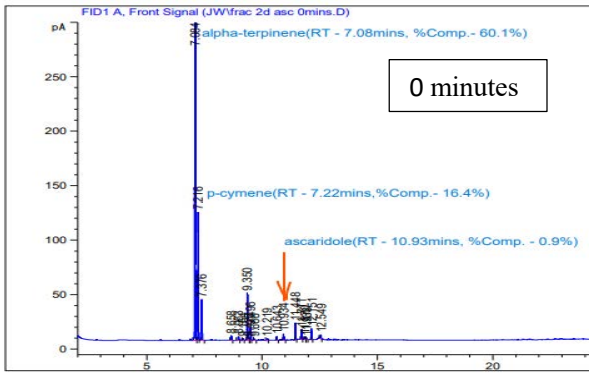

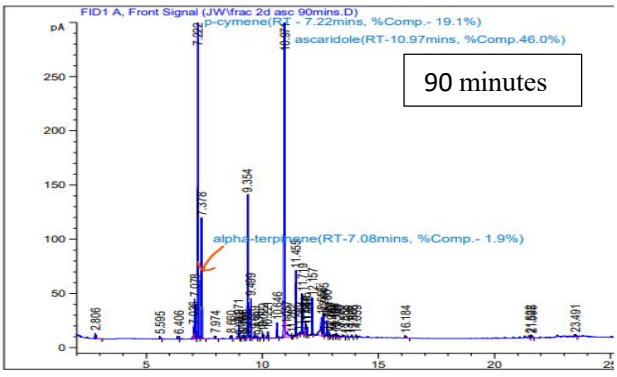

Appendix 28: GC Chromatograms for Monitoring *C. lutea* Fraction 3 Sensitized Photooxygenation of Ascaridole at 0 Minutes and 90 Minutes

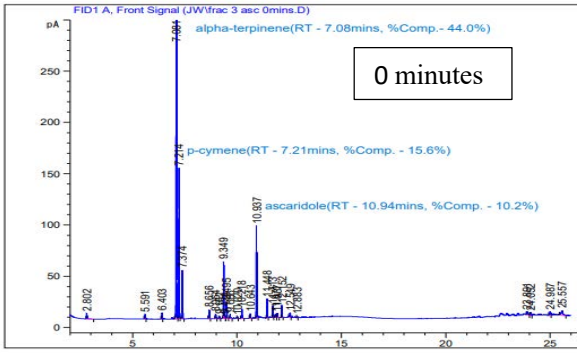

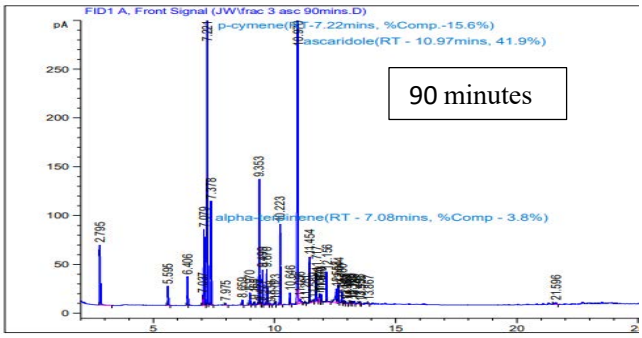

Appendix 29: GC Chromatograms for Monitoring *C. lutea* Fraction 4a Sensitized Photooxygenation of Ascaridole at 0 Minutes and 90 Minutes

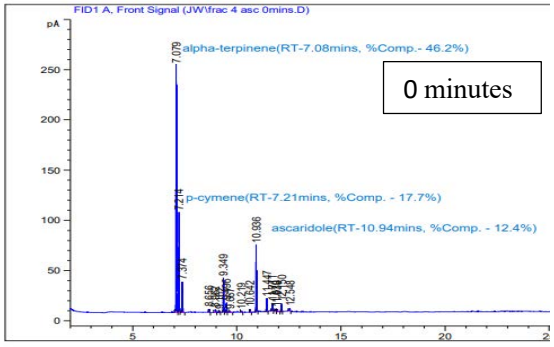

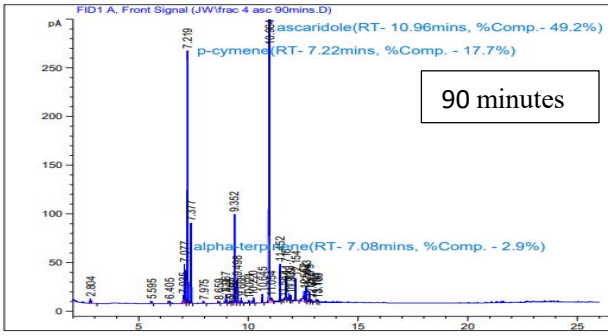

Appendix 30: GC Chromatograms for Monitoring *C. lutea* Fraction 4b Sensitized Photooxygenation of Ascaridole at 0 Minutes and 90 Minutes

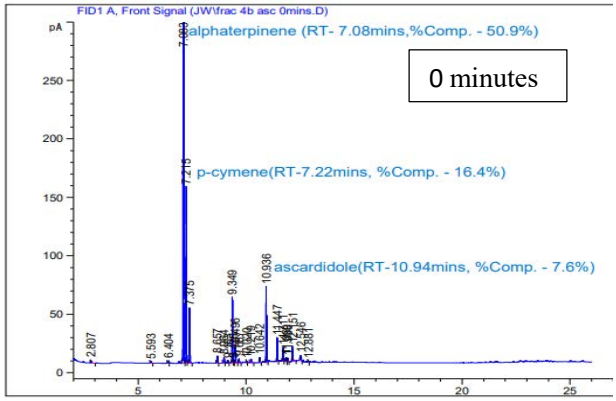

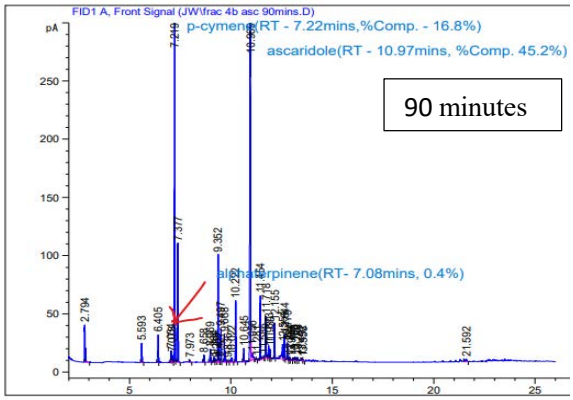

Appendix 31: GC Chromatograms for Monitoring *C. lutea* Fraction 5 Sensitized Photooxygenation of Ascaridole at 0 Minutes and 90 Minutes

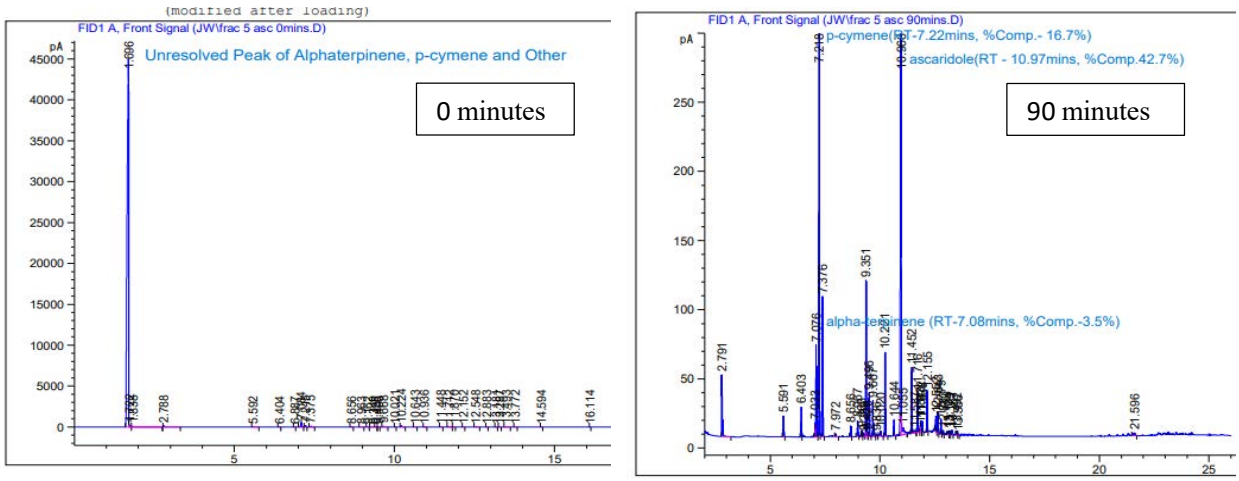

Appendix 32: GC Chromatograms for Monitoring *C. lutea* Fraction 6a Sensitized Photooxygenation of Ascaridole at 0 Minutes and 90 Minutes

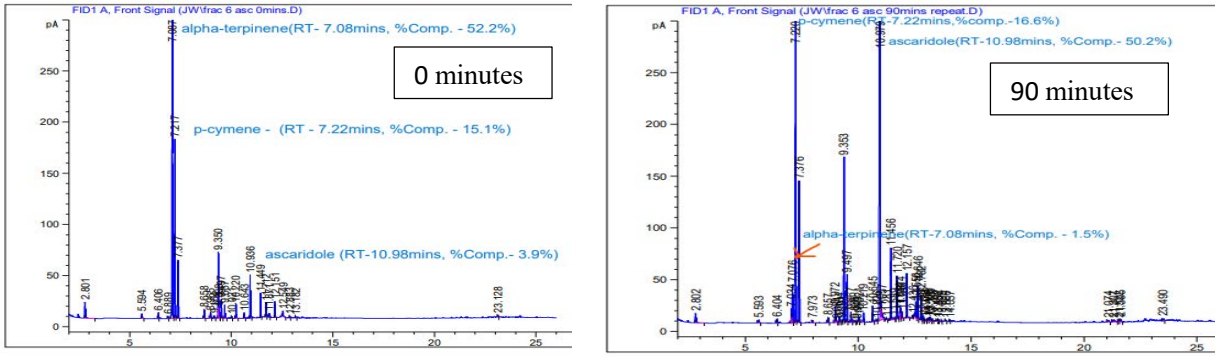

Appendix 33: GC Chromatograms for Monitoring *C. lutea* Fraction 6b Sensitized Photooxygenation of Ascaridole at 0 Minutes and 90 Minutes

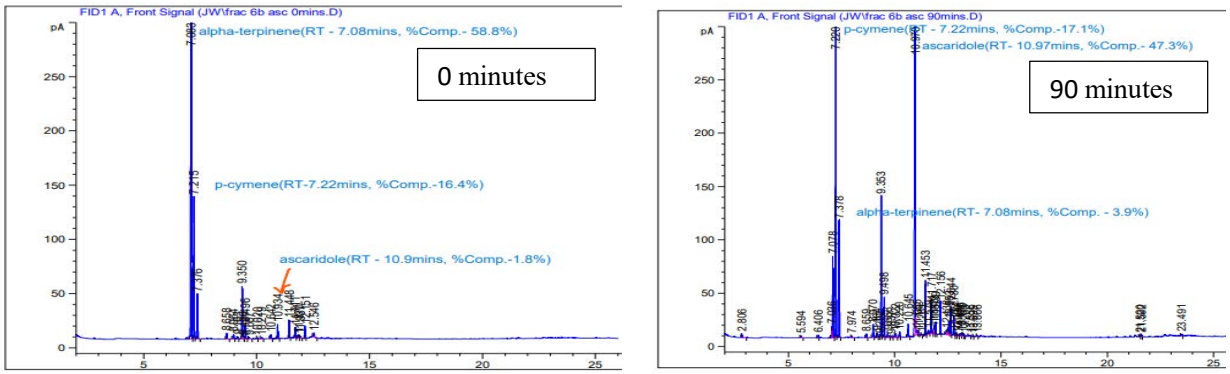

Appendix 34: GC Chromatograms for Monitoring *C. lutea* Fraction 7 Sensitized Photooxygenation of Ascaridole at 0 Minutes and 90 Minutes

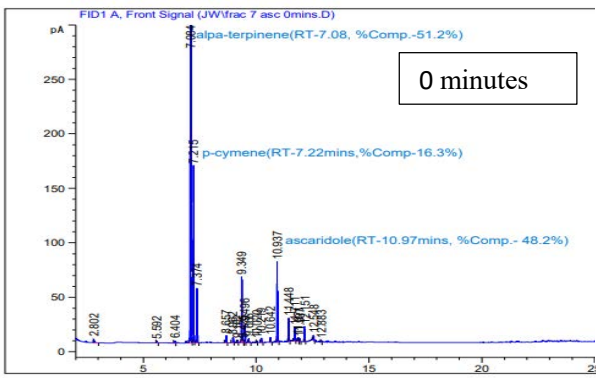

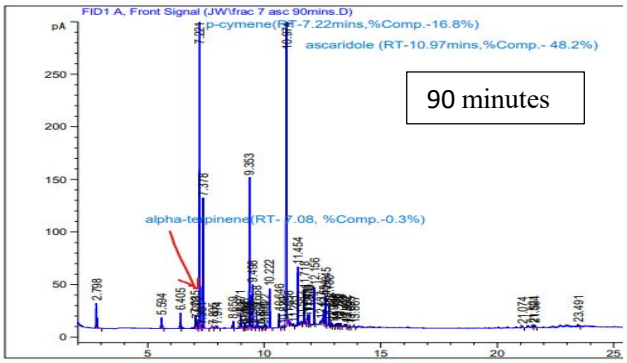

Appendix 35: GC Chromatograms for Monitoring *C. lutea* Fraction 8 Sensitized Photooxygenation of Ascaridole at 0 Minutes and 90 Minutes

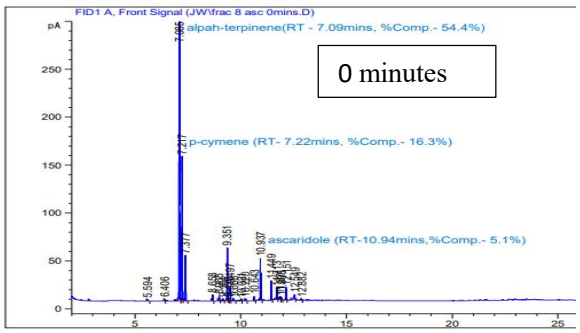

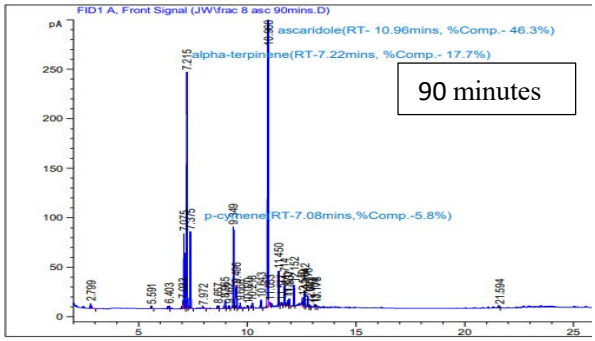

Appendix 36: GC Chromatograms for Monitoring *C. lutea* Fraction 9 Sensitized Photooxygenation of Ascaridole at 0 Minutes and 90 Minutes

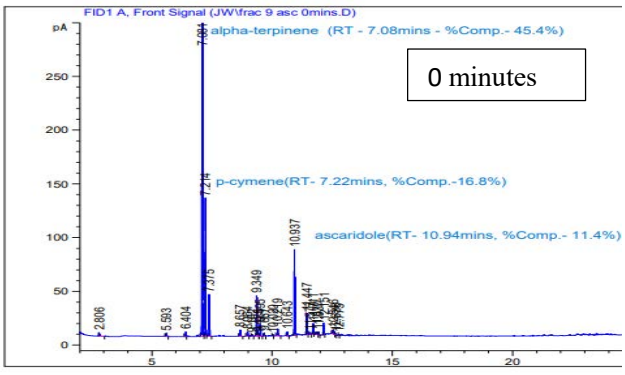

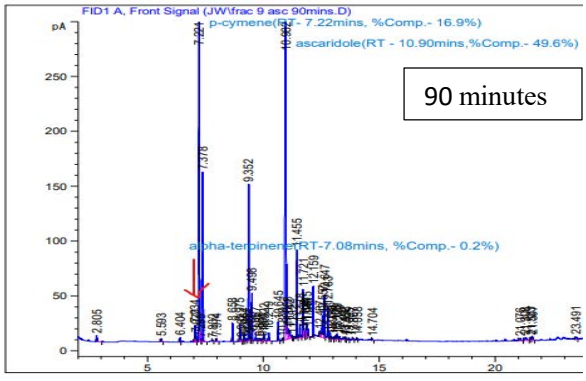

Appendix 37: GC Chromatograms for Monitoring *C. lutea* Fraction 10 Sensitized Photooxygenation of Ascaridole at 0 Minutes and 90 Minutes

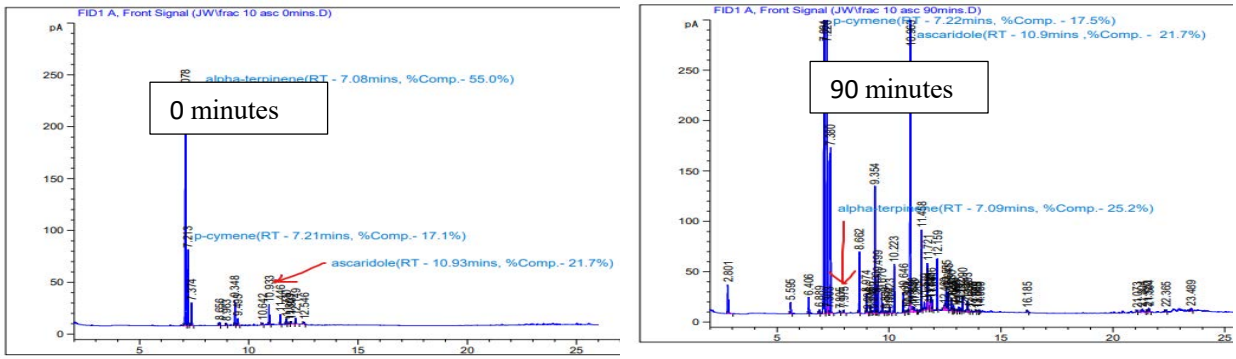

Appendix 38: GC Chromatograms for Monitoring *C. lutea* Fraction 11 Sensitized Photooxygenation of Ascaridole at 0 Minutes and 90 Minutes

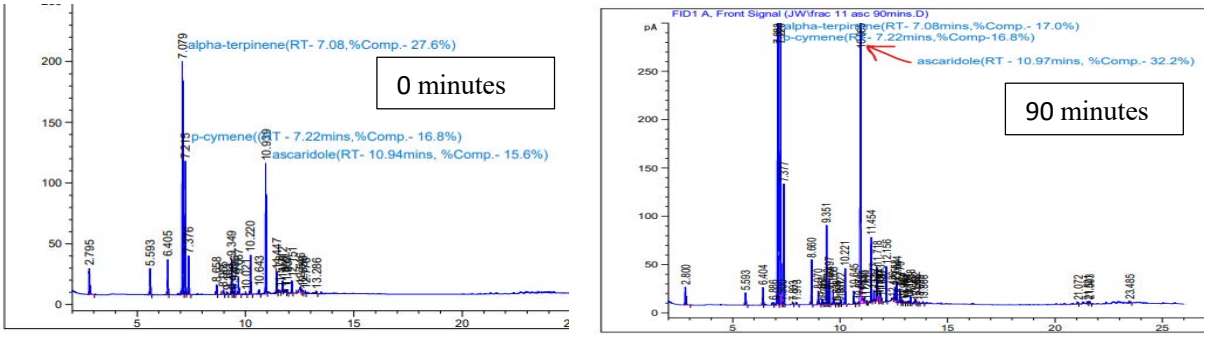

Appendix 39: GC Chromatograms for Monitoring *C. lutea* Fraction 12 Sensitized Photooxygenation of Ascaridole at 0 Minutes and 90 Minutes

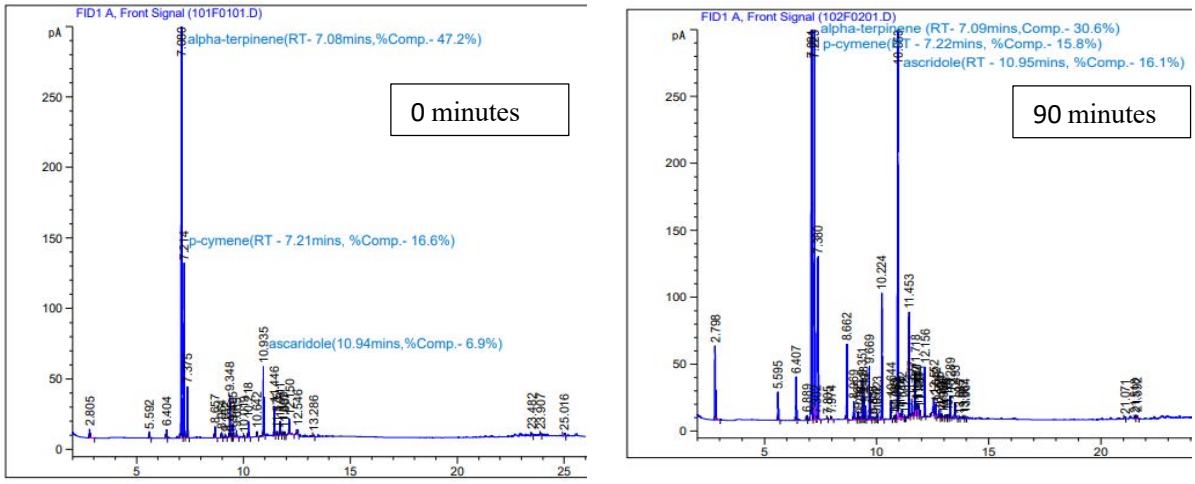

Appendix 40: GC Chromatograms for Monitoring *C. lutea* Fraction 13 Sensitized Photooxygenation of Ascaridole at 0 Minutes and 90 Minutes

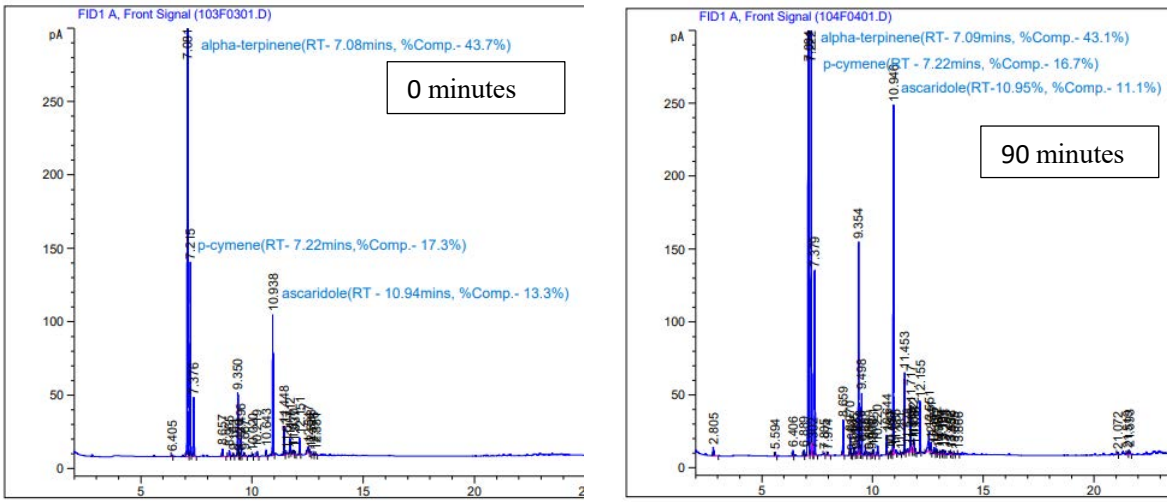

Appendix 41: HPLC-MS Chromatogram of *Carpolobia lutea* Extract Fraction 2d

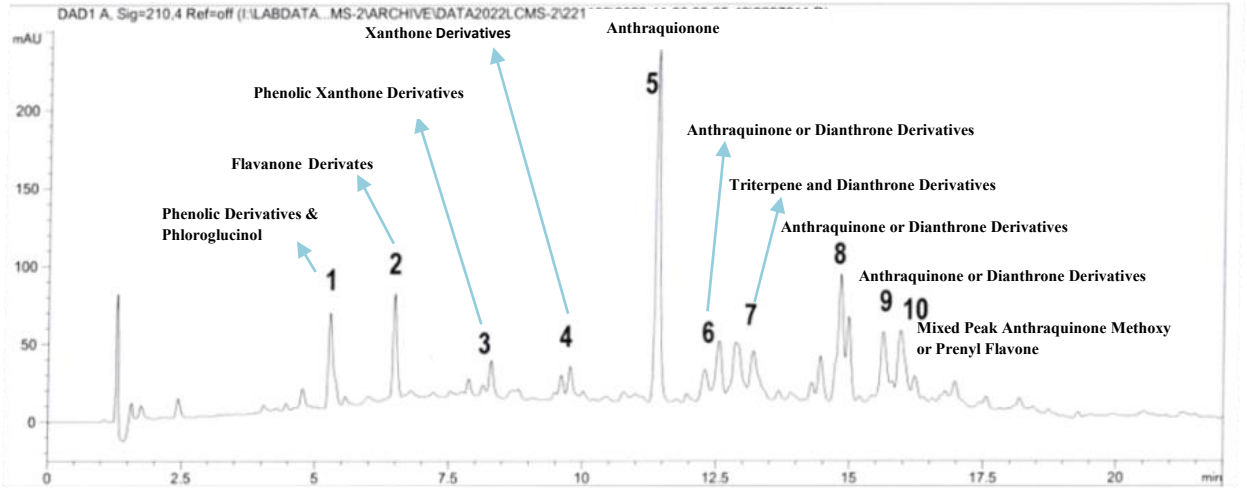

Appendix 42: HPLC-MS Chromatogram of *Carpolobia lutea* Extract Fraction 3

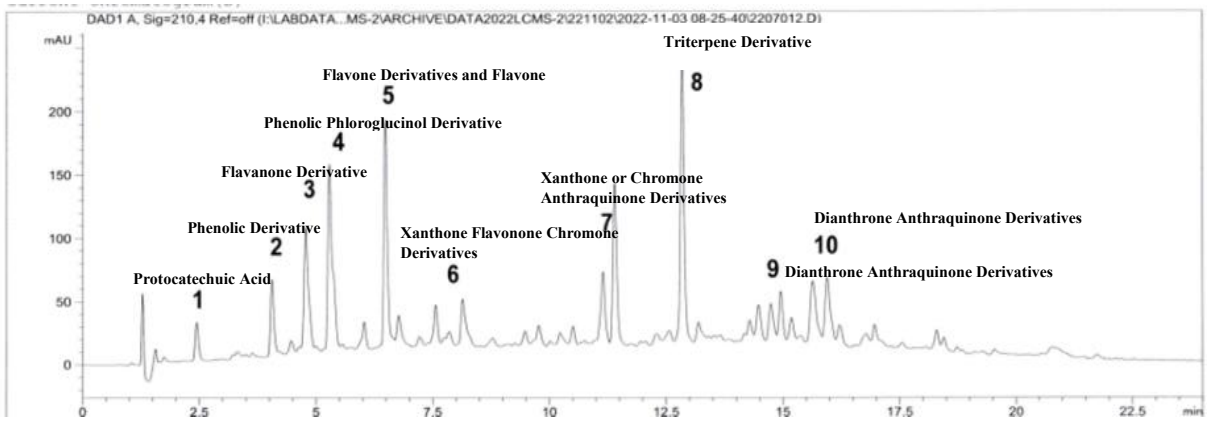

Appendix 43: HPLC-MS Chromatogram of *Carpolobia lutea* Extract Fraction 4

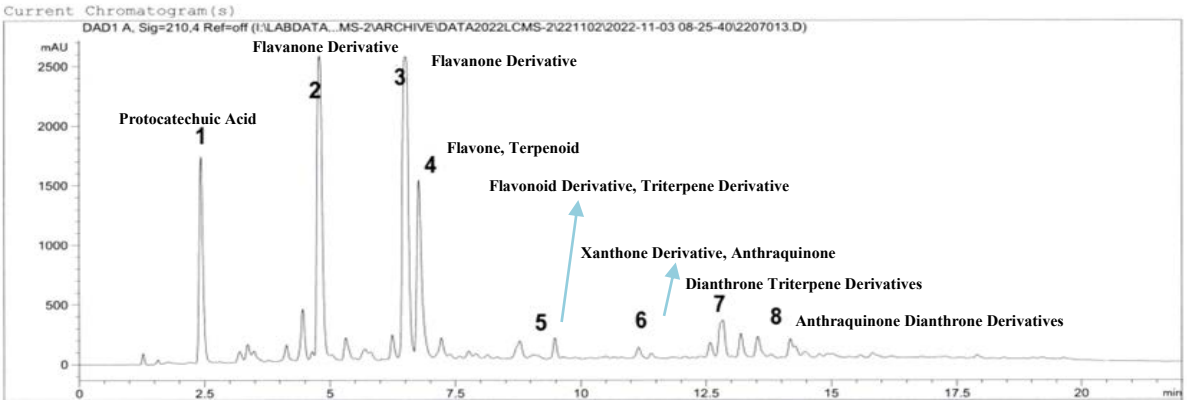

Appendix 44: HPLC-MS Chromatogram of *Carpolobia lutea* Extract Fraction 5

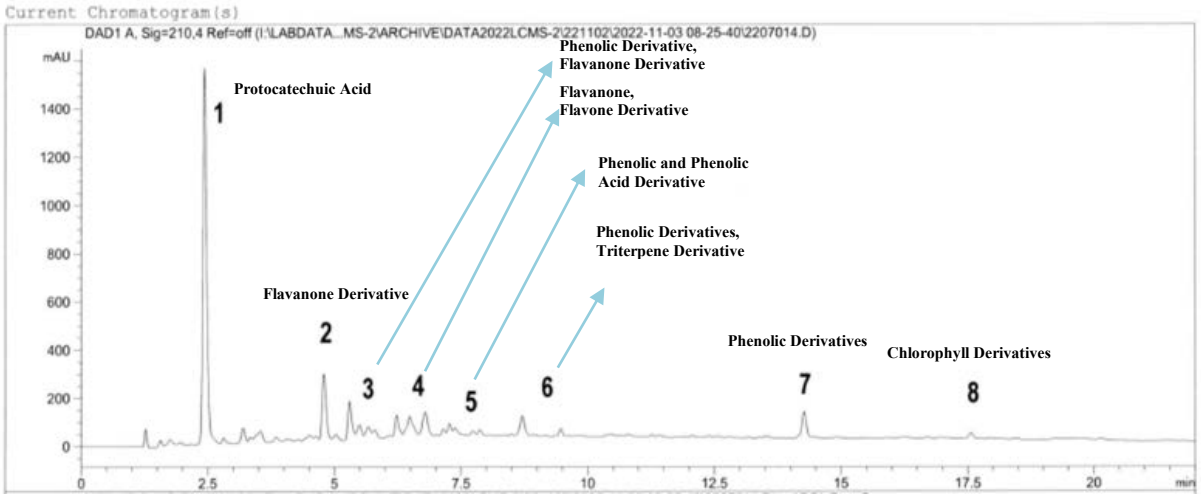

Appendix 45: HPLC-MS Chromatogram of *Carpolobia lutea* Extract Fraction 6

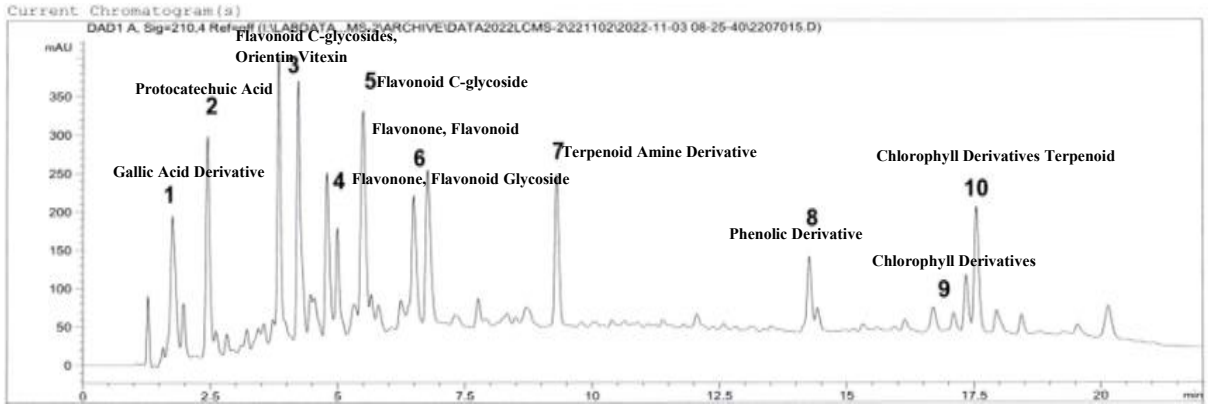

Appendix 46: HPLC-MS Chromatogram of *Carpolobia lutea* Extract Fraction 7

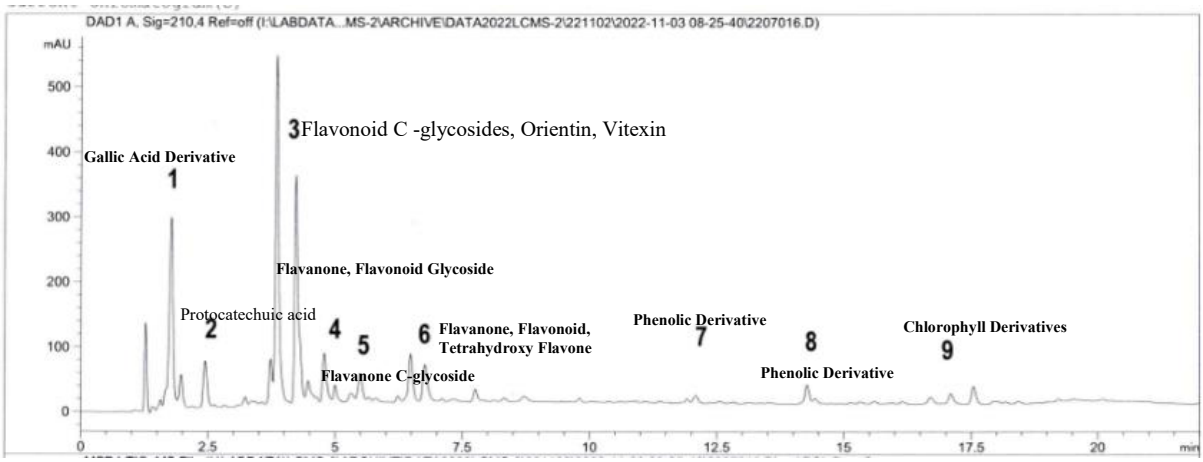

Appendix 47: HPLC-MS Chromatogram of *Carpolobia lutea* Extract Fraction 8

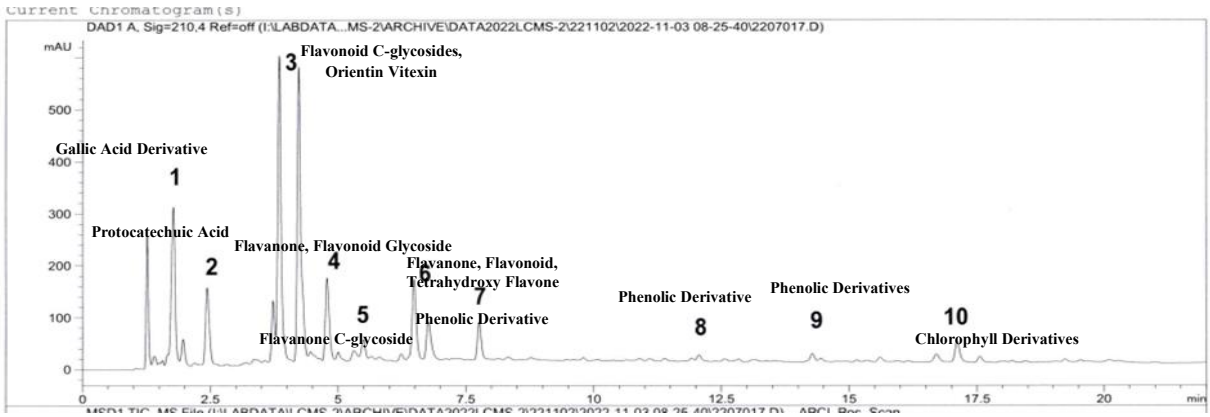

Appendix 48: HPLC-MS Chromatogram of *Carpolobia lutea* Extract Fraction 9

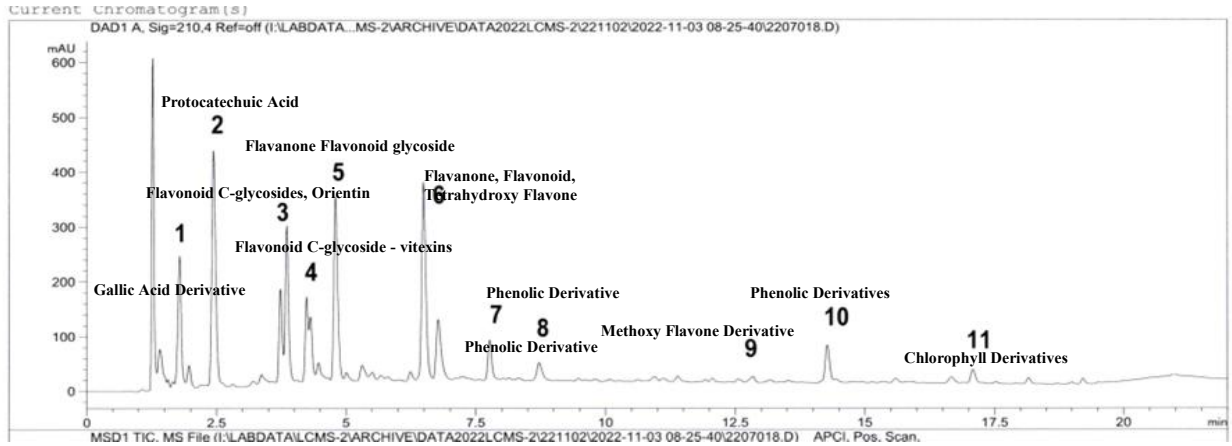

Appendix 49: *Hibiscus sabdariffa* Identification Voucher

University of Port Harcourt

Faculty of Science

Department of Plant Science and Biotechnology

UPH REFERENCE HERBARIUM FOR RESEARCH AND GERMPLASM CONVERVATION

FROM: THE HERBARIUM
Ref. No.: UPH/PSB/2021/29
DATE: 26th May, 2021

TO: Enyi Chinyere Chidimma
Dept. of Chemistry
Rivers State University.

TAXONOMIC CLASSIFICATION

Accession number	001
Kingdom	Plantae- Plant
Division/Phylum	Magnoliophyta Flowering plant
Class	Magnoliopsida Dicotyledons
Order	Malvales
Family	Malvaceae
Tribe	------
Genus	*Hibiscus*
Specific epithet	*sabdariffa*
Species	*Hibiscus sabdariffa* L.
Synonym(s) i.e. **Old name(s)	
Herbarium Number	UPH/P/245

Thanks.

Ekeke, Chimezie (*Ph.D.*)
08038718783
For The Herbarium

Appendix 50: *Carpolobia lutea* Identification Certificate

UNIVERSITY OF NIGERIA, NSUKKA

FACULTY OF BIOLOGICAL SCIENCES

DEPARTMENT OF PLANT SCIENCE AND BIOTECHNNOLOGY

HERBARIUM UNIT

December 05, 2023

To Whom It May Concern,

PLANT IDENTIFICATION/AUTHENTICATION CERTIFICATE

Issued to: Enyi, Chinyere Chidimma

Contact Address: Chemistry Dept., Rivers State University, Nkpolu-Oroworukwo

This is to certify that the following plant was identified/authenticated and voucher specimens deposited at the University of Nigeria Herbarium (UNN), which is domiciled in the Department of Plant Science and Biotechnology, Faculty of Biological Sciences, University of Nigeria, Nsukka as follows:

Scientific Name / Author	Family	Voucher N0
***Carpolobia lutea* G. Don**	POLYGALACEAE	UNN/04/0355D

Authenticated by

Mr Felix 1. Nwafor
Curator/Taxonomist
University of Nigeria Herbarium (UNN)
Contact: felix.nwafor@unn.edu.ng; 08036062242

Appendix 51: *Justicia secunda* Identification Voucher

University of Port Harcourt

Faculty of Science

Department of Plant Science and Biotechnology

UPH REFERENCE HERBARIUM FOR RESEARCH AND GERMPLASM CONVERVATION

FROM: THE HERBARIUM **Ref. No. :** UPH/PSB/2021/30 **DATE:** 26th May, 2021	**TO:** Enyi Chinyere Chidimma Dept. of Chemistry Rivers State University.

TAXONOMIC CLASSIFICATION

Accession number	001
Kingdom	Plantae
Phylum/Division	Tracheophyta
Class	Magnoliopsida
Order	Lamiales
Family	Acanthaceae
Subfamily	---------
Tribe	Justicieae
Genus	*Justicia* Hooker
Specific epithet	*secunda*
Species	*Justicia secunda* Vahl
Synonym(s) i.e. **Old name(s)	*Dianthera secunda* (Vahl) Griseb., *Echolium secundum* (Vahl) Kuntze, *Justicia caracasana* Willd. ex Nees, *Justicia caripensis* Kunth, *Justicia geniculata* Sims, *Justicia moricandiana* (Nees) Lemee, *Rhacodiscus moricandianus* (Nees) Bremek., *Rhacodiscus secundus* (Vahl) Bremek., *Rhytiglossa moricandiana* Nees, *Rhytiglossa secunda* (Vahl) Nees and *Sericographis caripensis* (Kunth) Nees.
Herbarium Number	UPH/P/244

Thanks.

Ekeke, Chimezie (*Ph.D.*)
08038718783
For The Herbarium